การศึกษาเชิงเปรียบเทียบของมรกตที่ได้จากสภาพการเกิดทางธรณีวิทยาต่าง ๆ

นางสาวฐิตินทรีย์ ปวโร

วิทยานิพนธ์นี้เป็นส่วนหนึ่งของการศึกษาตามหลักสูตรปริญญาวิทยาศาสตรมหาบัณฑิต
สาขาวิชาโลกศาสตร์   ภาควิชาธรณีวิทยา
คณะวิทยาศาสตร์   จุฬาลงกรณ์มหาวิทยาลัย
ปีการศึกษา 2547

ISBN : 974-17-7069-3

COMPARATIVE STUDY OF EMERALDS FROM DIFFERENT GEOLOGICAL OCCURRENCES

Miss Thitintharee Pavaro

A Thesis Submitted in Partial Fulfillment of the Requirements
for the Degree of Master of Science in Earth Science
Department of Geology
Faculty of Science
Chulalongkorn University
Academic Year 2004
ISBN : 974-17-7069-3

Thesis Title	Comparative Study of Emeralds from Different Geological Occurrences
By	Miss Thitintharee Pavaro
Field of Study	Earth Science
Thesis Advisor	Associate Professor Visut Pisutha-Arnond, Ph.D.
Thesis Co-advisor	Mrs. Wilawan Atichat

Accepted by the Faculty of Science, Chulalongkorn University in Partial Fulfillment of the Requirements for the Master's Degree

…………………………………………….Dean of Faculty of Science
(Professor Piamsak Menasveta, Ph.D.)

THESIS COMMITTEE

…… ……………………………………………………….Chairman
(Assistant Professor Veerote Daorerk, M.Sc.)

………………………………………………………….Thesis Advisor
(Associate Professor Visut Pisutha-Arnond, Ph.D.)

……………………………………………………..Thesis Co-advisor
(Mrs. Wilawan Atichat, M.Sc.)

…………………………………………………………………Member
(Assistant Professor Pornsawat Watanakul, Ph.D.)

…………………………………………………………………Member
(Assistant Professor Somchai Nakaphadungrat, Ph.D.)

ฐิตินทรีย์ ปวโร : การศึกษาเชิงเปรียบเทียบของมรกตที่ได้จากสภาพการเกิดทาง ธรณีวิทยาต่าง ๆ อ. ที่ปรึกษา : รองศาสตราจารย์ ดร. วิสุทธ์ พิสุทธอานนท์, อ. ที่ปรึกษาร่วม : นางวิลาวัณย์ อติชาติ จำนวนหน้า 196 หน้า ISBN : 974-17-7069-3

ประเทศไทยเป็นศูนย์กลางการเจียระไนอัญมณี การผลิตเครื่องประดับและส่งออกสินค้าอัญมณีที่สำคัญแห่งหนึ่งของโลก ประเทศไทยได้มีการนำเข้ามรกตก้อนหรือแบบที่เจียระไนแล้วจากแหล่งต่าง ๆ ที่สำคัญ อาทิ โคลัมเบีย บราซิล แซมเบีย มาดากัสการ์ และไนจีเรีย การทราบแหล่งที่มาของมรกตจะมีผลต่อราคาและเป็นประโยชน์ต่อวงการตลาดอัญมณี ดังนั้นจุดประสงค์ของการศึกษาครั้งนี้ เพื่อเปรียบเทียบสมบัติต่าง ๆ ลักษณะภายใน การดูดกลืนรังสี และองค์ประกอบทางเคมีของมรกตที่ได้จากสภาพการเกิดทางธรณีวิทยาต่าง ๆ

การวิจัยครั้งนี้ได้ทำการศึกษาตัวอย่างจากแหล่งมรกตที่เป็นที่นิยมในตลาดอัญมณีจำนวน 149 ตัวอย่าง ซึ่งสามารถแบ่งเป็น 2 ประเภท ตามสภาพการเกิดทางธรณีวิทยาที่แตกต่างกัน คือ แบบที่ 1มรกตที่เกิดไม่สัมพันธ์กับหินชีสต์ (มรกตจากโคลัมเบีย และไนจีเรีย) และ แบบที่ 2 มรกตที่เกิดสัมพันธ์กับหินชีสต์ (มรกตจากบราซิล ได้แก่ แหล่ง Canaiba/Socoto, Itabira และ Santa Terezinha, มรกตจากมาดากัสการ์ และแซมเบีย)

ลักษณะบางอย่างของมรกตสามารถบ่งชี้ถึงแหล่งกำเนิดได้ พบว่าค่าดัชนีหักเหและค่าความถ่วงจำเพาะสัมพันธ์กับธาตุอัลคาไลน์ โดยมรกตที่มีสภาพการเกิดแบบที่ 1 มีค่าดัชนีหักเหและค่าความถ่วงจำเพาะปานกลาง ถึงสูงนั้น จะมีธาตุอัลคาไลน์ที่สูงด้วย ในทางตรงกันข้าม มรกตที่มีสภาพการเกิดแบบที่ 2 มีค่าดัชนีหักเหและค่าความถ่วงจำเพาะที่ต่ำ จะมีธาตุอัลคาไลน์ที่ต่ำ เช่นกัน มรกตที่มาจากแซมเบียและบราซิล (Carnaiba/Socoto) พบว่ามีปริมาณธาตุโซเดียมและซีเซียมสูง ส่วนมรกตจากมาดากัสการ์ พบว่ามีปริมาณโปแตสเซียมสูงมาก มรกตจากโคลัมเบีย พบว่ามีปริมาณเหล็กต่ำมาก ลักษณะมลทินภายในบางชนิดสามารถใช้จำแนกมรกตจากแหล่งต่าง ๆ ได้ เช่น ลักษณะรอบนอกคล้ายฟันปลาของมลทินของไหลชนิดสามสถานะที่พบในมรกตจากโคลัมเบียและไนจีเรีย พบว่ามรกตจากโคลัมเบียจะมีสัดส่วนของเหลว/ก๊าซ น้อยกว่าในมรกตจากไนจีเรีย เป็นต้น

สำหรับลักษณะทางสเปคตรัม ในส่วนของการดูดกลืนช่วงรังสี UV-Vis-NIR พบว่ามรกตส่วนใหญ่แสดงช่วงการดูดกลืนของ โครเมียม/วานาเดียม และเหล็ก ยกเว้นมรกตจากโคลัมเบียที่ไม่แสดงการดูดกลืนของเหล็ก จากการศึกษาสเปคตรัมของน้ำในมรกตช่วง NIR สามารถหาความสัมพันธ์ของโมเลกุลน้ำในโครงสร้างของมรกต (ชนิด 1 และ 2) กับลักษณะการเกิดของมรกตในแต่ละแหล่งได้ คือ มรกตที่มีสภาพการเกิดแบบที่ 1 อย่างไนจีเรียจะแสดงสเปคตรัมของน้ำชนิดที่ 1 เด่นชัด ส่วนมรกตที่มีสภาพการเกิดแบบที่ 2 โดยเฉพาะมรกตจาก Santa Terezinha จะแสดงสเปคตรัมของน้ำชนิดที่ 2 เด่นชัด

ภาควิชา………………ธรณีวิทยา…………ลายมือชื่อนิสิต……………………………………..
สาขาวิชา……………..โลกศาสตร์…………ลายมือชื่ออาจารย์ที่ปรึกษา………………………..
ปีการศึกษา……………2547………………..ลายมือชื่ออาจารย์ที่ปรึกษาร่วม…………………..

4772255023 : MAJOR Earth Science

KEY WORD: emerald / beryl / Brazil / Colombia / Madagascar / Zambia / Nigeria

THITINTHAREE PAVARO : COMPARATIVE STUDY OF EMERALDS FROM DIFFERENT GEOLOGICAL OCCURRENCES THESIS ADVISOR : ASSOC. PROF. VISUT PISUTHA-ARNOND, PH.D., THESIS CO-ADVISOR : WILAWAN ATICHAT, M.SC., 196 P., ISBN : 974-17-7069-3

Thailand is known as one of an important center for precious stones cutting, jewelry manufacturing and exporting. Rough or cutting emeralds have been imported to Thailand from foreign countries especially from Colombia, Brazil, Zambia, Madagascar and Nigeria. Determination of origin of emerald can be useful as value added factors in the gem marketing. This study aims at comparing the gemmological properties, internal characteristic, absorption spectra and chemical composition of emeralds from the different geological occurrences.

Totally 149 emerald samples from various types of important geological occurrence were acquired for this study. They can be divided into two different major categories: non-schist-related type I deposits (Nigeria and Colombia) and schist-related type II deposits (Carnaiba/Socoto, Itabira and Santa Terezinha in Brazil, Madagascar and Zambia).

Some characteristics are locality specific and can be used for origin determination. In addition, refractive index (RI) and specific gravity (SG) are related to alkali contents in emerald. The high to medium RI and SG values are found in emeralds from type II deposit which is high in alkali contents. In contrast the low RI and SG values are found in emeralds from type I deposit which is low in alkali contents. The emeralds from Zambia and Carnaiba/Socoto contain relatively high contents of Li and Cs, while the emeralds from Madagascar show exceptionally high K content. The Colombian emeralds show consistently very low iron content. Some inclusion features can be used to distinguish emeralds from different locality such as emeralds from Colombia and Nigeria contain different jagged outline in 3-phase inclusions in which those from Colombia have lower liquid/vapor ratios.

For the spectroscopic properties, UV-Vis-NIR absorption spectra of emeralds from most localities show a combination of Cr^{3+}/V^{3+} and $Fe^{2+,3+}$, except the spectrum of Colombian emerald has no $Fe^{2+,3+}$ absorptions. NIR absorption spectra of water molecules (type I and II) in emerald's structure show relationship to alkali contents. In addition, emeralds from Nigeria of type I deposit is dominated by the type I water. In contrast, emeralds from Santa Terezinha in Brazil of type II deposit is dominated by the type II water.

Department…………….Geology………………..Student's signature…………………………

Field of Study………… Earth Science…………Advisor's signature…………………………

Academic year…………2004……………………Co-advisor's signature…………………….

ACKNOWLEDGMENTS

I would like to express my sincere gratitude to my supervisor, Associate Professor Dr. Visut Pisutha-arnond for his crucial supervision, encouragement and critical review of the manuscript and Ms. Wilawan Atichat (my co-advisor and director of The Gem and Jewelry Institute of Thailand) for her encouragement and help many things in this research. I am grateful to the Gem and Jewelry Institute of Thailand (GIT) under Professor Sakda Siripant (former director) for financial supports and permission to use all gemological instruments.

I am indebted to Dr. Dietmar Schawarz for donation of many samples and suggestion about geological origin of the emeralds. I wish to express my appreciation to Mr. Thanong Leelawatanasuk for hospitality, valuable advises and discussion in all aspects.

Several people are deeply acknowledged for helping on various aspect at various stages in the realization of my work, in particular: Assistant Professor Dr. Pornsawat Wathanakul (Department of General Science, Kasetsart University) for encouragement and valuable advises in this research. I am indebted to Tin Tin Win who analysed chemical composition of emeralds at Macquarie University in Sydney, Australia. Many thanks to all laboratory staff of the Gem and Jewelry Institute of Thailand (GIT) for their help and hospitality and Mr. Sakrapee Saejoo for providing some documents.

Finally, I would like to give special thanks to my parents (Associate Professor Dr. Chitkavee Pavaro and Associate Professor Umphawan Pavaro) for their support and encouragement.

CONTENTS

LIST OF TABLES

Table Page

LIST OF FIGURES

Figure Page

Figure Page

Figure Page

Figure Page

Figure Page

Figure Page

Figure Page

Figure Page

Figure Page

Figure Page

Figure Page

Figure Page

CHAPTER I

INTRODUCTION

1.1 General Overview

Emerald is an intense green variety of beryl which is well-known as one of the most beautiful coloured gems. Other varieties of beryl are blue known as aquamarine, red as bixbite, yellow as heliodor and completely colourless as goshenite. Emerald is always a treasure for the appeal of attractive green colour calm, and the rich history of emerald combined with its beauty and rarity has made it the most valuable.

Emerald, as well as beryl, is composed of silicon, aluminum oxygen and beryllium which come from rocks of the continental crust. The elements that give the emerald its green colour are chromium and vanadium which concentrate below in upper mantle. The resulting folds and faults mobilized fluid that move along fractures. These fluids can dissolve and transport the necessary elements that have been brought together for emerald formation. As a result, In contrast to other varieties of beryl, emerald can only form in certain unique geological settings, and thus emerald generally does not occur in association with other varieties of beryl.

Emerald deposits are known from 5 continents namely Africa, South America, Asia, Europe and Australia. Emeralds can be found in several geological environments which are normally related to all potential source rocks of its component elements. The important production of emeralds are from South America, such as Colombia and Brazil, and from Africa, such as Zambia, Madagascar and Nigeria.

The first know emerald mine was the Cleopatra's mine in Egypt where it is generally accepted as the world's oldest source of emeralds. Egypt was the only significant source of emeralds until the 1500's, when the Spanish invaded the Americas (Ward, 1993). Up to that time, South America had been using emeralds in ornaments and ceremonies. The emeralds originated from Colombia and Brazil, were by far much larger, more transparent, and greener than those from Egypt. Since the 16^{th} century, large quantities of Colombian emeralds have entered the European market. In very fine qualities, Colombian emeralds can retail for over $20,000 a carat (Newman, 1995).

Thailand is known as one of an important center for precious stones cutting, jewelry manufacturing and exporting. The most important gemstones are ruby, sapphire and emerald. Rough emeralds have been imported from foreign countries especially from Colombia, Zambia and Brazil and cut in Thailand. Loose emeralds were then exported mainly to Europe, USA and Japan which according to the Thailand export statistics in 2003 the value was approximately 222.54 million baths or account to about 0.002% of gem and jewelry exporting revenue (http://www.git.or.th, Thailand Export Statistics).

Colombian emerald is by far the most desirable because of its splendor and clearer than those from the other deposits. Consequently, the emeralds from this source are considered the most valuable in the gem trades whereas most Brazilian emeralds contain large amount of inclusions, thus, are less desirable. It is therefore justifiable to study the well known deposits because emeralds in various countries of origins are different in their values.

1.2 Rationale and the Purpose of Study:

The country of origin of an emerald is one important aspect in gem identification. Many customers occasionally request a gem laboratory to issue the country of origin of an emerald in a gem identification report beside routine gem identification. Hence in order to be able to distinguish emeralds from different sources, it is necessary to collect and compare all available physical, optical and chemical data of emeralds from various sources. The assumption adopted in this study is that emeralds from different geologic occurrences should inherit some different gemological properties, internal characteristics as well as the chemical fingerprint that are able to give a clue to the country of origin of that emerald sample. Therefore the purpose of this research is 1) to study the gemmological properties, such as colour, refractive index, specific gravity, 2) to observe their internal characteristics, and 3) to compare the absorption spectra and trace element compositions of emeralds from different geological occurrences. The emerald samples used in this study were from Colombia, Brazil, Zambia, Madagascar and Nigeria that were obtained from a reliable person. The samples cover all major types of emerald deposits and are among the most important emeralds commercially available in the gem markets today.

1.3 The method of study

Firstly, literature survey of the previous works was carried out on all technical aspects of emerald. Then some representative samples of emerald from various sources were acquired from a reliable person. The samples used in this study were obtained from 5 different countries of origin, i.e. Colombia, Brazil, Zambia, Madagascar and Nigeria. The physical and optical properties (i.e. refractive index (IR), birefringence, specific gravity (SG) and luminescence under short wave and long wave) were determined on polished slabs cut perpendicular to the c axis. After that the observation of internal characteristics, such as minerals and liquid inclusions, was undertaken together with photomicrographing. Measurement of the absorption spectra of the samples were then carried out using a UV-Vis-NIR Spectrophotometer and a Fourier Transform Infra-red Spectrophotometer (FTIR) at The Gem and Jewelry Institute of Thailand (GIT). Some selected samples from each locality were subsequently analyzed for their trace elements contents (Li, Be, B, Na, Mg, Al, Si, P, K, Ca, Ti, V, Cr, Mn, Fe and Cs) using a Laser Abrasion Induced Coupled Plasma Mass Spectrometry (LA-ICP-MS) at the Macquarie University in Sydney, Australia. Results were then presented, discussed and concluded in the thesis report. The method of study can be summarized as follows (Figure 1.1)

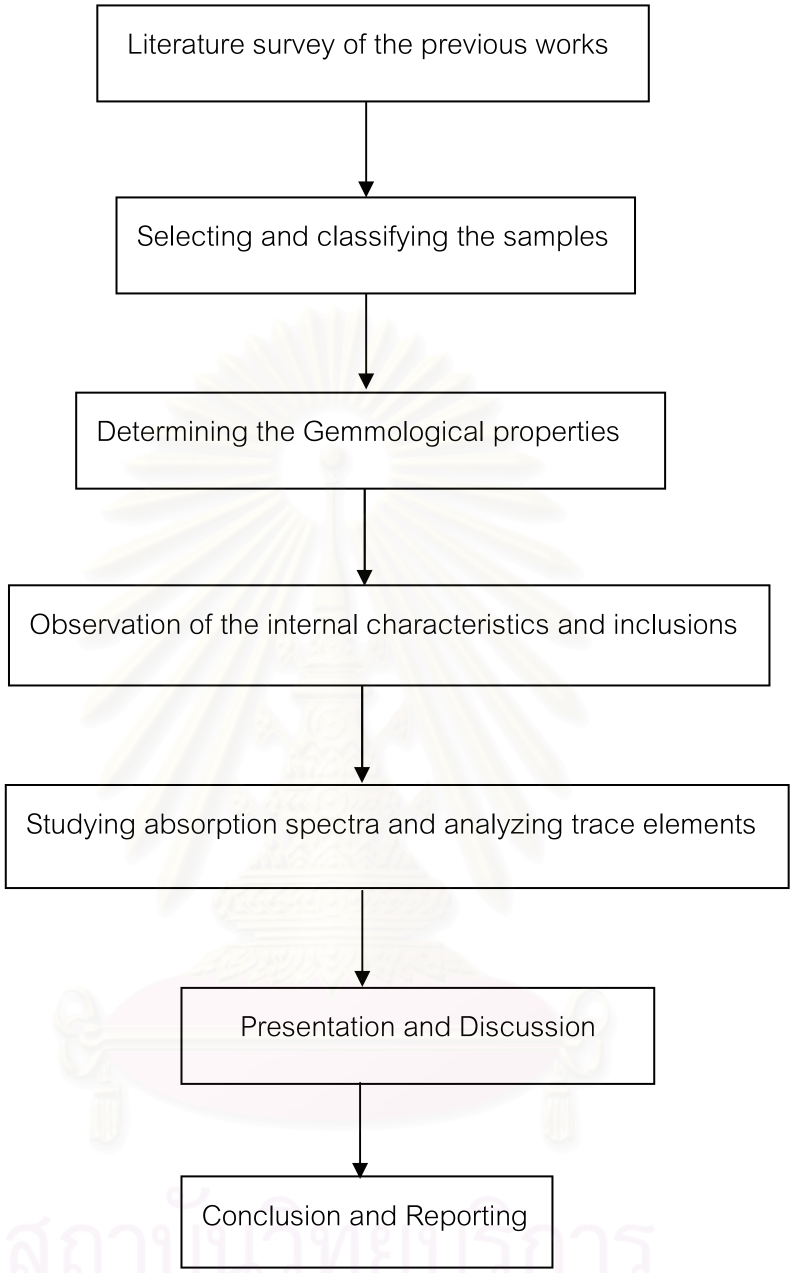

Figure 1.1: Flowchart of the method of study

CHAPTER II

GEOLOGY AND OCCURRENCES

An emerald is composed mainly of silicon, aluminum and oxygen. The forth primary component is beryllium, which is rare in the Earth's upper crust (∼1.5 ppm). Therefore emerald is not a common mineral that comes from rocks of the continental crust. The elements give emerald its colour are chromium and vanadium that can occur in sedimentary rocks, particular in black shales. These elements are also found in basalts of the oceanic crust, in peridotites and dunites of Earth's upper mantle (Schwarz et al., 2002).

Specifically geologic and geochemical conditions are required for chromium and/or vanadium to encounter beryllium. There are a few deposits in which the circulation processes inside one geologic environment are sufficient for emerald formation, such as the black shales of Colombia (see later section). But in general the source rocks must be first open to permit the circulation and mobilization of elements. Then the action of tectonic plate, the result of folds and faults could mobilize fluids along fractures. As those fluids moved they could dissolve and transport the elements necessary for emerald formation. Emeralds can crystallize from a fluid in schists and gneisses or miarolitic cavities or quartz lenses, faults, breccias, lenticular vugs, druses and isolated crystal pocket in geologic structure such as veins along fracture zones (Schwarz et al., 2002).

2.1 Classification of deposits of study emerald:

Emerald deposits are known from 5 continents namely Africa, South America, Asia, Europe and Australia. The important production of emerald is however from South America, such as Colombia and Brazil, and from Africa, such as Zambia, Madagascar and Nigeria.

Emeralds can be found in several geological environments which are normally related to all potential source rocks of its component elements. In general two main types of emerald deposits can be distinguished in this study; type I deposits are non-schist-related and type II deposits are schist-related. Both types are mainly controlled by tectonic structures, such as faults and shear-zones (Schwarz, et al, 2002).

The type I deposits (non-schist-related emerald mineralization) can be sub-divided into 2 sub-types:

Ia; pegmatite without schist; e.g., from Kaduna Plateau of Nigeria (NI) and

Ib; black shales with veins and breccias; e.g., from Cordillera Oriental of Colombia (CO).

The type II deposits (schist-related emerald mineralization) can be further sub-divided into 2 sub-types:

IIa; schist without pegmatite; e.g., from Santa Terezinha (STA) of Brazil and

IIb; schist with pegmatite; e.g., from Carnaiba/Socoto (CAR) and Itabira, (ITA) of Brazil, from Mananjary of Madagascar (MA) and from Ndola Rural district of Zambia (ZA). A summary of all the emerald deposits are shown in Table 2.1

Table 2.1: Summary of geological occurrences of emeralds from Brazil, Colombia, Madagascar, Zambia and Nigeria.

Type I Deposits (Non-schist-related)		Type II Deposits (Schist-related)				
Type Ia (Pegmatite without Schist)	Type Ib (Black Shales with Viens and Breccias)	Type IIa (Schist without Pegmatite	Type IIb (Pegmatite with Schist); emerald occur between contact zone of country rock and pegmatite veins			
Emerald crystallized in vugs of granitic - rock, which intruded to the country rock.	Host rock is black shales.	Host rock is talc-chlorite-amphibole-magnetite schist.	Host rock is phlogopite-carbonate - talc schist.	Host rock is amphibolite.	Host rock is serpentinite.	Host rock is talc.
Kaduna Plateau, Nigeria	Cordillera Oriental, Colombia	Santa Terezinha (Brazil)	Mananjary, Madagascar	Ndola Rural, Zambia	Carnaiba/ Socoto (Brazil)	Itabira (Brazil)

* The detail of each deposit is described below.

2.2 Type I: Non-schist-related emerald deposits;

2.2.1 Ia: Emeralds in granite and pegmatite vugs without schist seams, e.g. Kaduna and Plateau States of Nigeria

The emerald mineralization of the Kaduna and Plateau States in Nigeria is associated with two periods of magmatism and the accompanying intrusion of alkali granites: the Pan-African orogenesis (600 - 450 million years ago) and the Mesozoic orogenesis (190-144 million years ago). These deposits also contain significant elements, such as tin, niobium, tantalum and zinc (Schwarz, 1996).

To the east of the Nigeria River and north of the Benue River, there is an important pegmatite belt which is apparently not related to major granite intrusions. The pegmatites occur in an area bounded to the north by Kafanchan, to the south by the Afu Hills, to the east by the Jos Plateau and to the west by Nassarawa (Figure 2.1). These pegmatites vary considerably in their mineralogy. The bulk of those which are metal-bearing are complex albitized pegmatites with important gem potential.

The emerald occurs in small pegmatitic pockets in association with quartz, feldspar and topaz (Figures 2. 2 and 2.3). These pegmatite pockets, which can be up to 8 cm in size, are found at the contact of a granite with basement rocks and represent cavities created by gas loss from the cooling magma. The temperatures of crystallization of Nigerian emeralds were reported to be about 400 - 500 ^{o}c (Schwarz, 1996).

In the Pan-African pegmatites, emerald is associated with aquamarine, tourmaline and beryl. In the Mesozoic pegmatites, the emerald occurs in pegmatite cavities or in phlogopite-alkali-feldspar-granites with quartz, blue topaz and beryl/aquamarine (Schwarz et al., 2002).

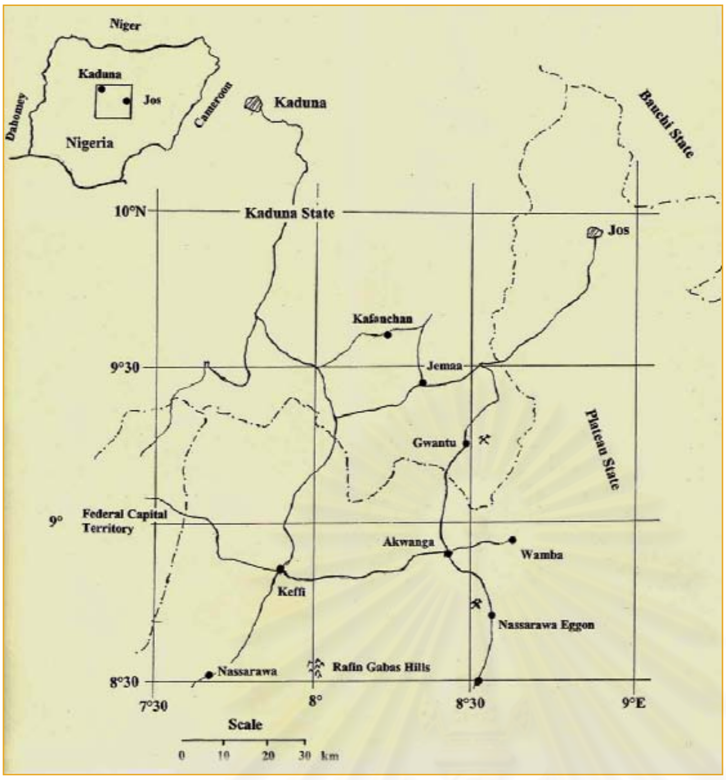

Figure 2.1: Location map with the emerald occurrences at the Kaduna and Plateau States in Central Nigeria (Schwarz, 1996).

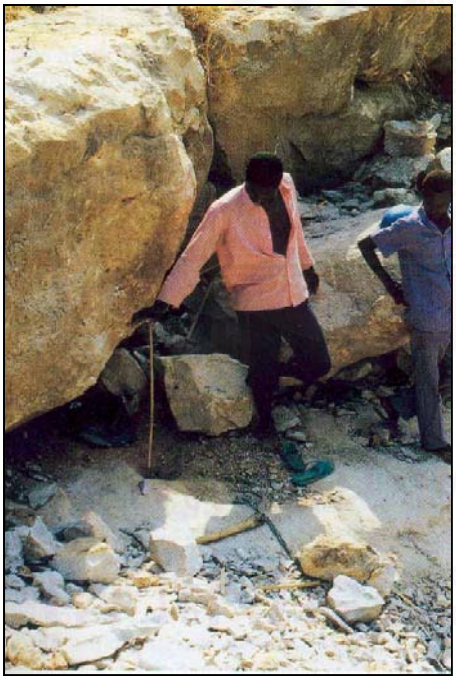

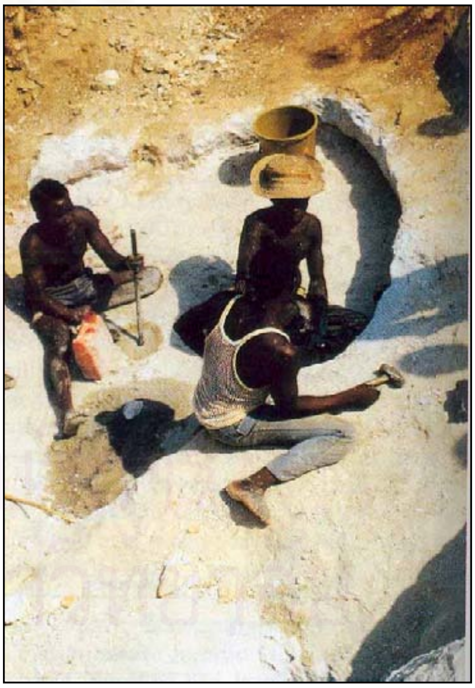

Figure 2.2: (left) and Figure 2.3: (right) Searching and drilled holes prepared for blasting to expose in the zone of granites (Schwarz, 1996).

According to Schwarz, et al. in 2002, the emeralds in Nigeria were probably formed between magmatic and hydrothermal stages. The alkali-granites were enriched with beryllium and fluorine. The beryllium might have been derived from the micas and feldspars of the granites and the chromium could have come from the mafic rocks. The magmatic origin of the mineralizing solution was indicated by the oxygen and hydrogen isotopic compositions of the emerald. Geologic structures and the type of mineralization were characterized by the interaction of solution with volcanic rocks.

2.2.2 Ib: Emeralds in veins and breccias in black shales: e.g. Cordillera Oreintal of Colombia

Colombian emeralds are significant in both quality and quantity. The deposits were exploited by the native before the appearance of Europeans in the 16th century and have been worked more or less afterward. The occurrences of emerald are so widespread in this area that new deposits have been found in modern times and the probability is still great to be discovered in the future (Sinkankas, 1981). The new and famous deposits are Muzo and Chivor mines (Figure 2.4), where renowned worldwide for the quality and quantity of their emeralds (Bosshart, 1991). There is also a large number of smaller deposits. These emerald occurrences form two narrow zones extending near and along the two multiphase fault boundaries of the Eastern Cordillera. These are the same original boundaries of the Cretaceous sedimentary basins. The eastern zone contains the mining districts of Chivor, the western zone is the districts of Muzo and Coscuez.

The Colombian emeralds occur in calcite veins intensely folded and invaded running vertically through dark shale (Figure 2.5) of early Cretaceous age (about 120 to 130 million years old). Emerald forms as an accessory mineral in hydrothermal albite-carbonate-pyrite veins (Keller, 1981). In all mining district, the emerald-bearing veins are crosscutting the strata and are spatially associated with breccias and albites. The dark rock series was chalky and argillaceous of marine origin and is therefore grey to black in colour (Figures 2.6).

Geochemical studies have indicated the absence of magmatic activity related to the origin of the emeralds. The composition of water from the structural channels and oxygen in Colombian emerald is consistent with basinal brines that have interacted with local evaporate deposits. These brines were likely reacted with organic matter in the black shales, releasing organically trapped beryllium, chromium and vanadium into the solution (Schwarz, 1998).

Since the early Tertiary period, the black shale series have been lifted, folded, faulted and mineralized. Many emerald appear in places, where large scale tectonic faults once cut into the sediments (Bosshart, 1991). In the course of sodium metasomatic interaction which probably took place at relatively low temperature of about 300°c, hydrothermal fluids leached the beryllium, chromium and vanadium from the black shales (Schwarz and Giuliani, 2002).

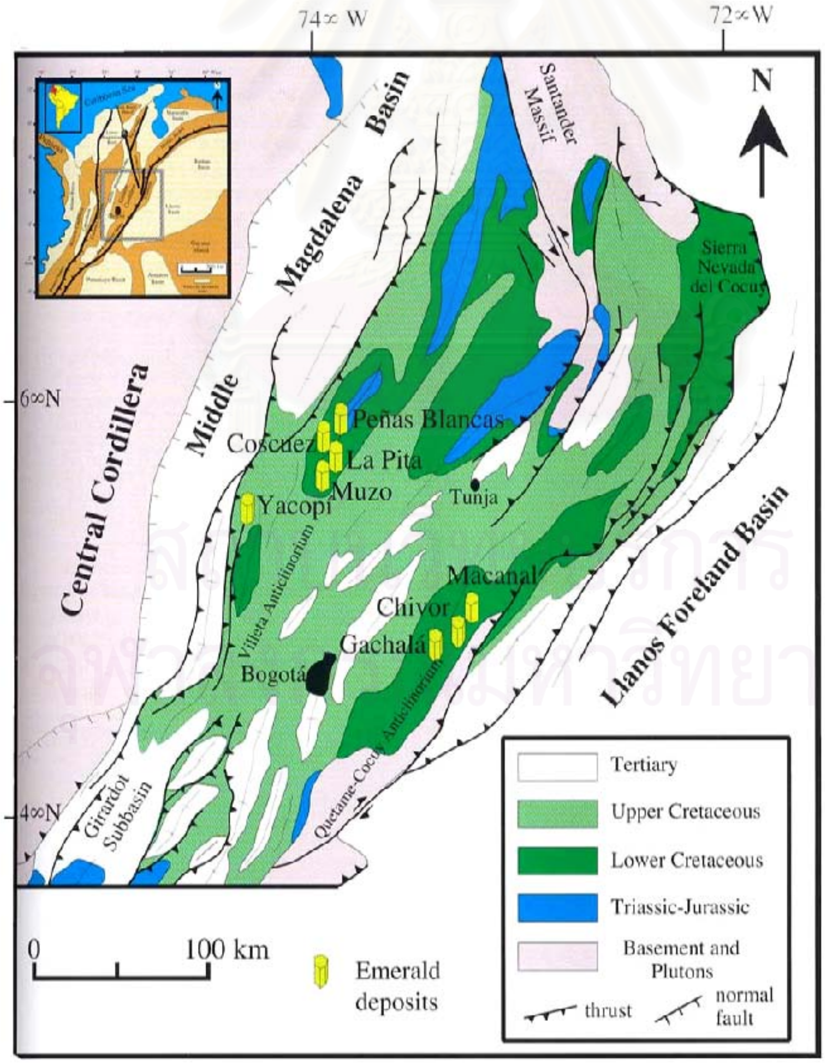

Figure 2.4: The geology in the area of Colombian emerald deposits showing the important mines (Branquet et al., 1999).

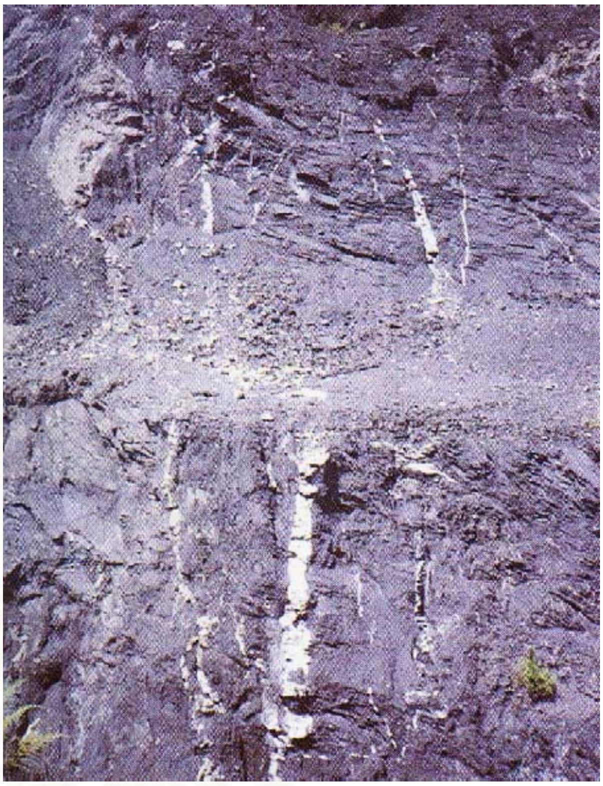

Figure 2.5: In Muzo, the Colombian emeralds occur in calcite veins vertically crosscutting in dark, carbonaceous shales with thin layer of limestones (Schwarz, 1998).

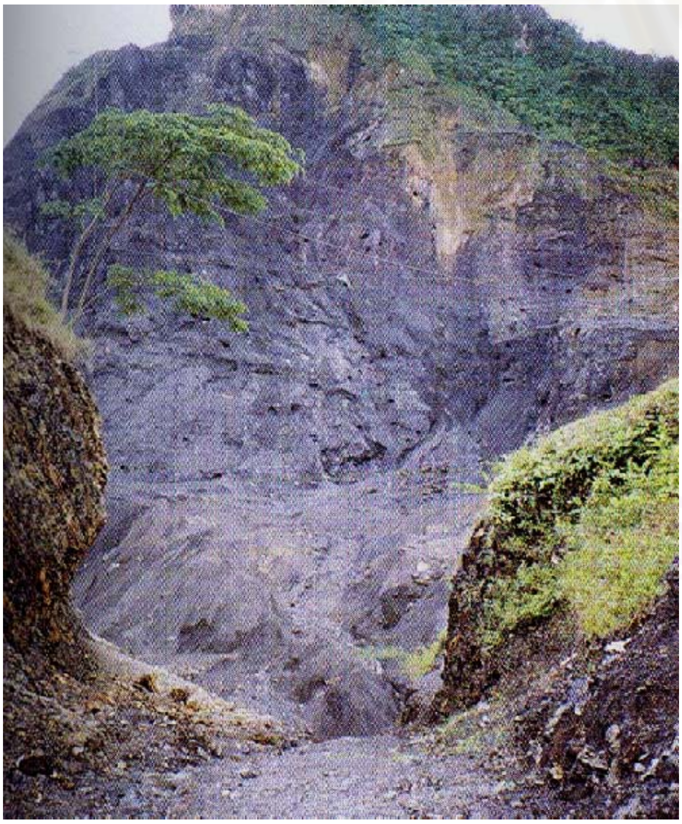

Figure 2.6: The Coscuez mine; Cordillera Oriental (Ward, 1993).

2.3 Type II: Schist-related emerald deposits;

2.3.1 IIa: Emeralds in schist without pegmatites: e.g. Santa Terezinha deposits in Goias State of Brazil

The Santa Terezinha deposits are situated at 230 km northwest of Brazilia (Figure 2.7) and about 275 km north of Goianua, the capital of the state of Goiás. This region is a part of the Brazilian Shield. In this region, the Middle Precambrian rocks (belong to the Araxá Group) consist mainly of mica schists and quartzites, varying in thickness from a few hundred to almost 2,000 meters.

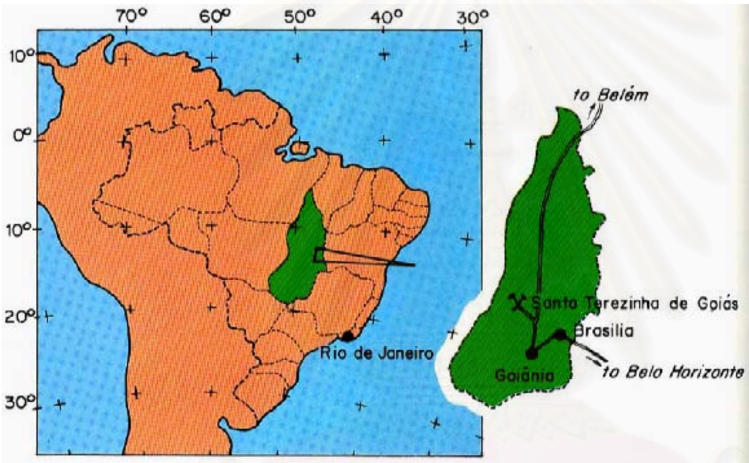

Figure 2.7: The location map of Santa Terezinha deposits at Goias State, Brazil (Cassedanne and Sauer, 1984).

The emeralds are disseminated in phlogopite schists and phlogopitized carbonate-talc-schists. In the deposit, faults thrusts and shear zones also controlled the infiltration of hydrothermal fluids. Emerald-rich zones are encountered in the core of sheared folds and along foliation planes. Two mineralization types were distinguishable: (Schwarz, 2002).

1) A carbonate-rich ore with dolomite, phlogopite, talc, quartz, chlorite, tremolite, spinel, pyrite and emerald;
2) A phlogopite-rich ore with quartz, carbonate, chlorite, talc, pyrite and emerald.

The emeralds grew in the talc schist (Figure 2.8) and incorporated inclusions of chromite, pyrite, and talc from the schist. Later tectonic folding caused fracturing of some of the pre-formed emeralds. The mineralized schist provides a high concentration of emerald crystals, for example, more than one kilogram of emeralds in six tons of mineralized schist. In general, the deposit is of the mica-oligoclase-beryl type as defined by Smirnov (1977). The beryllium most likely came from mica (phlogopite/biotite)-rich rocks while the chromium came from the host talc-schists (Schwarz and Giuliani, 2002).

Figure 2.8: The pits of the emerald-bearing talc schist are excavated to remove the ore at the part of the lateritic plateau in Santa Terezinha (Cassedanne and Sauer, 1984).

2.3.2 IIb: Emeralds in pegmatites with schist seams: e.g. Madagascar, Zambia and Brazil (Itabira, Carnaiba and Socoto)

Most schist-related emerald deposits are associated with granitic rocks, greisen, aplites, pegmatites and quartz veins. It normally shows a dark, clearly schistose zone developed at the contact between pegmatitic and mafic rocks (serpentinite, talc-schist or amphibolite).

These deposits are found in the Precambrian or Paleozoic volcano-sedimentary series. At first, pegmatites and aplites form in the roof region of plutons. The black wall schist around the pegmatites and aplites is composed of phlogopite and plagioclase, derived by exchange of elements (alkali-metasomatism) between granitic rock and the neighboring serpentinites, actinolite/tremolite schists or talc schists. In some deposits, greisen formation and tectonic deformation are characteristic for the contact zone and hydrothermal fluids to access the alteration zones where emeralds later formed.

The beryllium could come from the decomposition of beryl, feldspar, mica and from phenakite while the chromium may come from mafic rocks such as serpentinite and talc schist (Schwarz and Giuliani, 2002).

IIb (1): Mananjary region of Madagascar

The fourth largest island in the world is Madagascar, which is 1,580 km (1,000 miles) long and 580 km (365 miles) across at its widest. Two major groups of rocks cover the island: ancient Precambrian basement rock and younger sediments. The basement rocks, which cover most of the area, consist mainly of gneisses and schists overlain over wide areas by crystalline limestones and schist-quartzites. Numerous granite intrusions contributed pegmatite mineralization. The pegmatites contain various minerals and are commonly complex, including those suitable for gems and mineral specimens. Both common and gem beryl occur in many bodies (Murdock, 1963 cited in Schwarz, 1994).

Beryl is one of the important gem minerals (more than 50 minerals) found on Madagascar (Chikayama, 1989 cited in Schwarz, 1994). According to Lacroix, 1922 (cited in Schwarz, 1994) provided the first detailed survey account of occurrences of both primary and secondary (eg. alluvial) gem quality beryl there. The primary emerald occurrences are in the vicinity of Mananjary (Figure 2.9).

At the beginning of the 1990s, the worked area around Mananjary comprised at least 50 km^2 (Thomas, 1993 cited in Schwarz, 1994). The Morafeno Mining is performed by independent mine and a number of small mechanized operations (Figures 2.10). The mining have been exploited commercially-rich emerald mineralization that is embedded in mica schist and amphibole schists. Most crystals range from one to three carats, but are low quality crystals.

Figure 2.9: Map showing three commercially mining areas of the emerald deposits in Mananjary, Morafeno (Schwarz, 1994).

Figure 2.10: The overview of Morafeno mining operations shows some deposits. (Schwarz, 1994).

IIb (2): Ndola Rural district of Zambia

The main emerald-producing area in Zambia comprises two deposits, Kamakanga and Kafubu (both in Ndola Rural district), which lie within a few kilometers of each other. This emerald field is located between the Ndola Rural district and Kitwe district of northern Zambia (Figure 2.11), approximately 32 km south-west of Kitwe and 40 km west-northwest of Luansya, near the entrance of the Miku River into the Kafubu River (Bank,1974 cited in Koivula, 1982). Both Miku and Kafubu areas produce excellent, gem-quality emeralds; some crystals weigh well over 100 ct (Koivula, 1982).

The Zambian emerald deposits occur within rocks of the Muva Supergroup -- which are persistent bands of talc-chlorite-amphibole (tremolite/actinolite)-magnetite schist. They are intruded by pegmatites which occur as feldspar-quartz-muscovite bodies or as minor quartz-tourmaline veins. Contact aureoles of pegmatitic veins with the ultramafic schists are usually altered to phlogopite-biotite-tourmaline aggregates and the minor veins are often concordant to the foliation of the country rocks. The emeralds are found in the contact zones, and sometimes within the quartz-tourmaline veins (Figure 2.12). Muva Supergroup forms the youngest part of per-Katangan basement immediately southwest of the well known Copper belt of Zambia.

The chromium was probably derived from magnetite in the talc-magnetite schists, as the magnetite in these rocks shows to contain a low % chromium (Bank, 1974 cited in Koivula, 1982). The emeralds are found in biotite-phlogopite schists in which dark brown to black-tourmaline also occurs. Other rocks associated with the emerald-and-tourmaline-bearing mica schists are talc-magnetite schist with secondary quartz veining (Bank, 1974; Sinkankas,1981 cited in Koivula, 1982).

Figure 2.11: The map of the emerald bearing area in Zambia (Seifert et al, 2004).

Figure 2.12: Emerald associated with quartz and tourmaline veins in talc schist. (Moroz and Eliezri, 1998).

IIb (3): Carnaiba/Socoto deposits in Bahia State of Brazil

Carnaiba and Socoto deposits are in the district of Bahia. The geological situation in these regions are marked by the intrusion of granite batholiths into the Serra de Jacobina unit which is composed of schists, quartzites and serpentinites (Schwarz and Giuliani, 2002).

The rocks of the Serra de Jacobina were subdivided by Couto et al. in 1978 (cited in Schwarz and Eidt, 1989), into the Jacobina Group – which consists of an ultrabasic basement unit (with an age of 2.4-2.7 billion years) which, together with the granite, is important for the formation of the emerald occurrence) and the Itapicuru Complex in Figure 2.13 (Griffon et al., 1967; Barbosa, 1973; Santana et al., 1980; Santana et al., 1981 cited in Schwarz and Eidt, 1989).

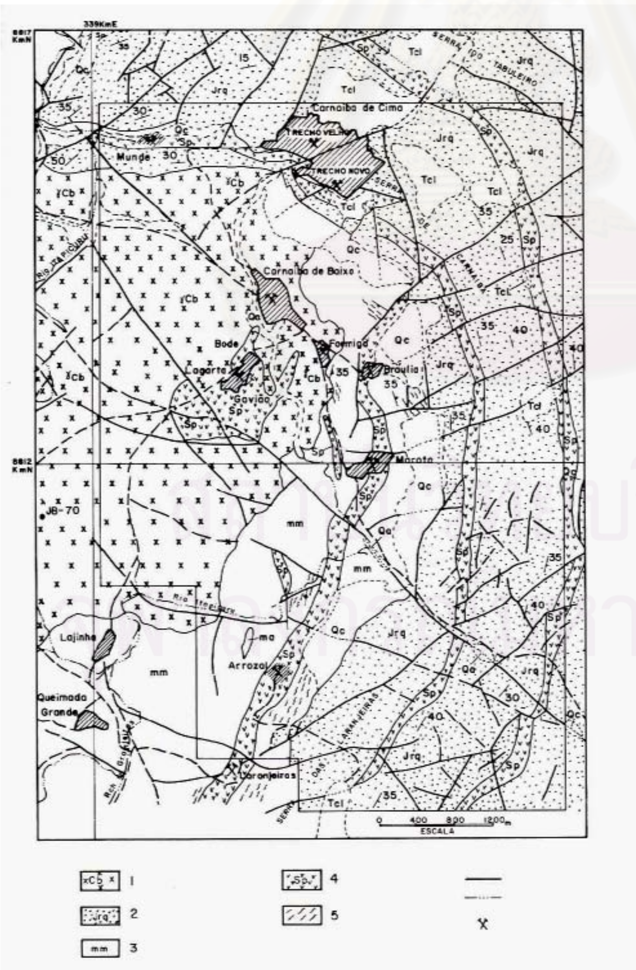

Figure 2.13: Geological map of the Carnaiba region (Schwarz and Eidt, 1989)

1- Carnaiba granite

2- Jacobina Group

3- Migmatites

4-Serpentinites

5- Cataclastic rocks

X Emerald mineralizations

----- Faults lithologic and/or stratigraphic contact

- - - River

(in: SEM-CBPM,Salvador 1978)

The Carnaiba/Socoto deposits were related to the zones of the strongest tectonic activities, which were characterized by the association of mafic-ultramafic rocks or their metamorphic derivatives (Cr/Fe source rocks) with pegmatites (provide Be) (Schwarz et al., 1990). It was the Cr-rich serpentinites and peridotites that were intruded by pegmatites and phlogopite or biotite/ phlogopite were in direct contact with the pegmatite and quartz veins. These micas are oriented parallel to the vein walls and show a lepidoblastic texture which gives the rock a schist-like appearance. The rock is therefore called mica-schist and is the emerald host rock. The emeralds occur either in the forms of aggregates or as single crystals, (Griffon et al, 1967, Barbosa, 1973, Santana et al, 1980, Santana et al, 1981 Couto and Almeida, 1982, Moreina and Santana, 1982 and Couto, 1985 cited in Schwarz and Eidt, 1989).

In these deposits, it is believed that metasomatic processes accompanying the intrusion of pegmatite bodies into the ultramasic rocks are responsible for the formation of emerald. The temperature of geochemical processes resulting in mineral association range of 600 - 800 °c (Griffon et al., 1967 cited in Schwarz and Eidt, 1989).

A mining attempt usually begins with a limited open pit and is worked with uncomplicated hand tools (Figure 2.14). These quarries are known in Brazil as garimpo, as they are worked by independent miners as called ‘garimpeiros’.

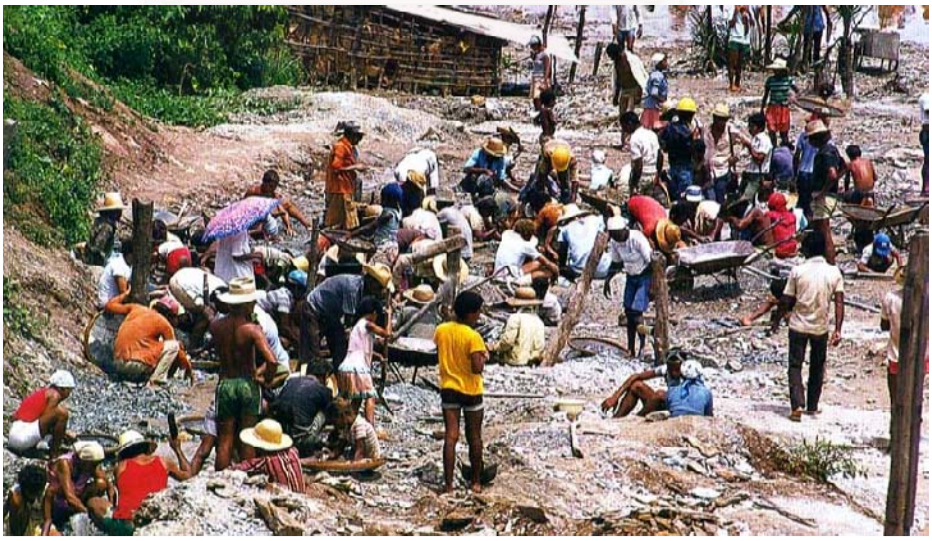

Figure 2.14: The ‘garimpeiros’ who are working by hand with pick, hammer, chisel and crowbar (Schwarz, 2002).

IIb (4): Itabira deposits in Minas Gerais State of Brazil

The significant emerald deposits of Itabira township are Capoeirana and Belmont mines (Figure 2.15). The Belmont mine lies 13 km SE of the town of Itabira and 120 km E of Belo Horizonte, the state capital of Minas Gerais State (Schwarz and Giuliani, 2002). The Capoeirana mine was discovered only about 10 km SE of Belmont mine in Figures 2.16 (Epstein, 1989).

According to Schwarz and Giuliani (2002), the stratigraphy of the Itabira region is characterized by two rock series of Precambrian age: the crystalline basement (so-called 'Série pré Minas' after Pfulg, 1968) and the overlying meta-sediments (so-called 'Supergrupo Minas'). The basement rocks are composed mainly of paragneiss and poly-metamorphic migmatites.

In the area of the emerald occurrence, a belt of schists dominates, stretching in a north to north-easterly direction. The width of the belt varies between 750 and 1200 meters. Leuco-gneisses occur symmetrically on both sides of this belt. The schist belt, together with the mafic rocks were strongly folded. Emeralds occur in black biotite/phlogopite schists in green chlorite schists or in kaolin masses (altered pegmatite). Crystals of lower quality are also found in quartz masses (Schorscher, 1973; Schorscher and Guimarães, 1976; Schorscher et al., 1982 cited in Hanni, Schwarz and Fischer, 1987).

The average emerald-content of the biotite schist is 165s/ton. The both mines are the richest emerald occurrence in Brazil so far as emerald-content of the parent rock in relation to the average quality of the emeralds is concerned (Hänni, 1987).

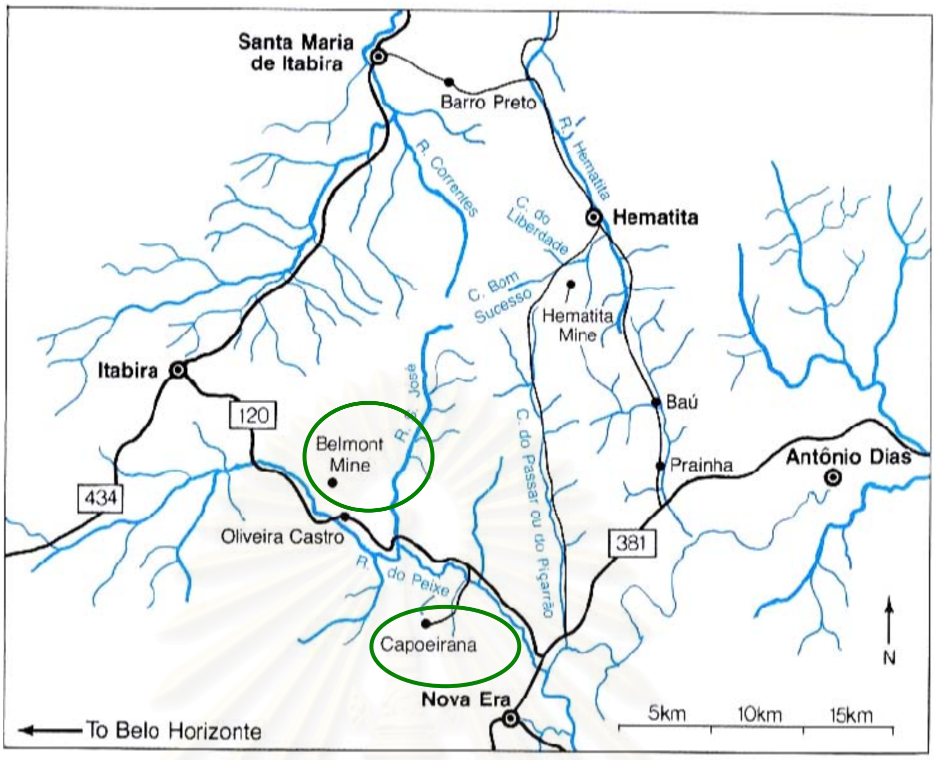

Figure 2.15: The map of two important emerald deposits-the Capoeirana and the Belmont mines in Itabira township, Brazil (Epstein, 1989).

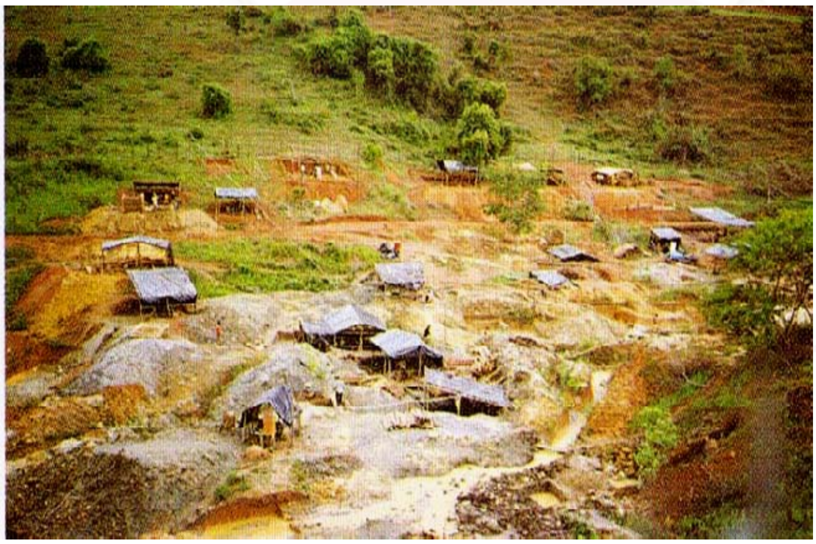

Figure 2.16: The present working of the Capoeirana emerald deposits (Schwarz, 1998).

CHAPTER III

GENERAL OBSERVATION

3.1 Crystal habits and Structure

Emerald which is a variety of beryl belongs to the highest symmetry class of the hexagonal crystal system. The emerald crystal looks the same from both the top and the bottom, as the opposite poles are identical. Hexagonal crystals can exhibit habits ranging from acicular through prismatic to thin tabular. The c-axis is the principal axis of symmetry and is six-fold, that is the crystal can rotate in six increments of 60°. Emerald crystals are more modest, as they only form more or less prismatic crystals shown in Figure 3.1. Very few tabular emerald crystals exist that can be rather complex with maximum number of crystal faces. This applies less to the prism faces than to the terminations, which can be bound by numerous faces of the most varied forms, mainly bipyramidal forms (Vrba, 1881 cited in Hochleitner, 2002)..

Emerald often forms in tectonically active areas. As a result the crystals are broken and commonly contain many fractures. Broken emerald crystals are sometimes found frozen in calcite (Figure 3.2: B). The individual pieces are slightly separated from one another during period of tectonic activity. Generally, the most complex emerald crystals are from localities in which crystal form in vugs or cavities.

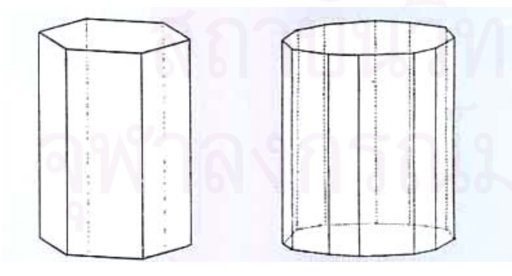

Figure 3.1: Hexagonal prism (left) and dihexagonal prism (right) of emerald crystals (Vrba, 1881 cited in Hochleitner, 2002).

A B

Figure 3.2: Specimens of emeralds with dark organic matter (A) and its specimen associated with calcite (B) from Muzo, Colombia (Photo by Pavaro, T.).

The primary elements of emerald are beryllium, aluminum, oxygen and silicon, that has the general formula: $Be_3Al_2(Si_6O_{18})$. The dominant features in the structure consists of rings of silicon atoms, each surrounded by four oxygen atom in tetrahedral arrangement. These rings forming hollow columns parallel to the *c*-axis of the crystal. Between the rings lie the aluminium and beryllium atoms, each aluminium atom is surrounded and coordinated with an octahedral group of six oxygen atoms, while each beryllium atom is surrounded by four oxygen atoms on a distorted tetrahedron. The linked silicon-oxygen of neighbourings Si_6O_{18} rings both laterally and vertically in the beryl structure is called cyclosilicate (Figure 3.3). The structure is thus like a honeycomb without atomic centre nearer than 2.55 A° to a centre of the open channels that forms parallel to the c-axis (Deer, 1992 cited in Hochleitner, 2002). Other elements not included in the general formula, such as potassium, sodium and cesium, can fit into these hollow channels. In addition, molecules such as the water or carbon dioxide commonly reported in beryl can also fit into these spaces. The colour of emerald is determined by foreign elements that are built into the lattice. The important ones are chromium and vanadium (Hochleitner, 2002).

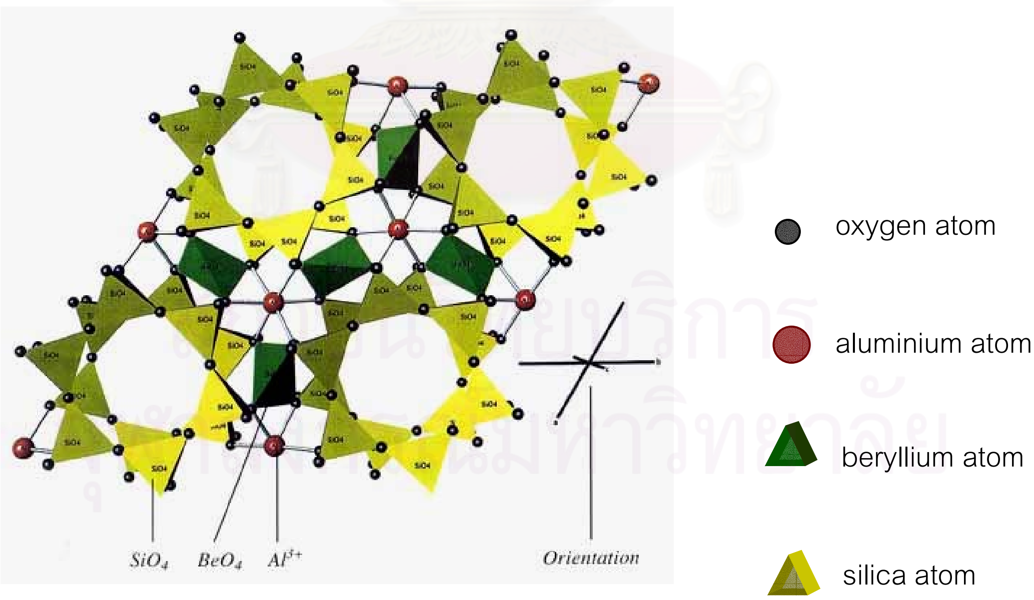

Figure 3.3: The beryl structure composed of ring-shaped arrangement of SiO4 tetrahedra (Hochleitner, 2002).

Two types of water may occur, the “type I” water molecule occurs alone, and is oriented in the hollow channels with its oriented by 90° to the c- axis of the beryl. The “type II” water molecule is associated with nearby alkali ion on the molecule dipole and lies with its symmetry axis parallel to the hexagonal c-axis direction (Figures 3.4a, 3.4b and 3.4c) (Wood and Nassau,1976).

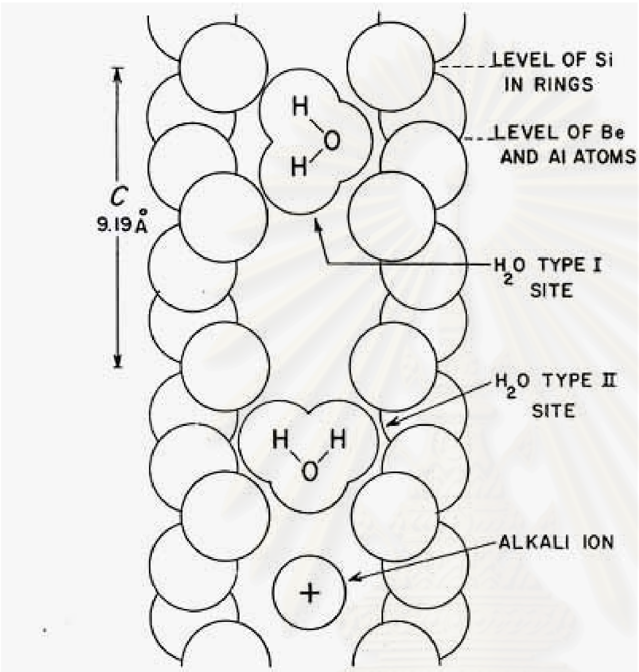

Figure 3.4: Side view of a beryl structure, only the oxygen atoms of the wall being shown, with possible positions and orientations of alkali ions and both types of water molecules located in channels sites, (Sinkankas, 1989).

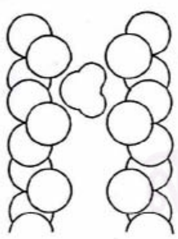

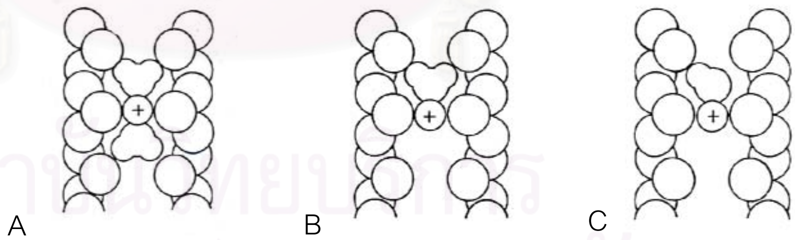

Figure 3.5: Non-alkali bonded type I water molecules Schmetzer and Kiefert, 1990).

Figure 3.6: Alkali bonded type II water molecules; (A) type IIa water molecules showing in sequence H_2O-Na-H_20, (B) type IIb water molecules showing H_2O-Na-X and (C) type IIc water molecules showing OH-Na-X (hydroxyl groups), with X representing vacancies in channel sites of the beryl structure (Schmetzer and Kiefert, 1990).

3.2 Visual appearance

All emerald samples used in this study consists of 148 polished and one cabochon stones from 5 countries of origin, namely Brazil (29 samples), Colombia (30 samples), Madagascar (30 samples), Zambia (30 samples) and Nigeria (30 samples). The samples are mostly transparent to semi-transparent and vitreous luster. Their weights are from approximately 0.3 to 2.8 carats. They are slightly different hue and tone, mostly ranges of colour are between bluish green to green (Figure 3.5).

<table>
<tr><td>A. (CAR 1-10)
</td><td colspan="2">B (ITA 1-9)
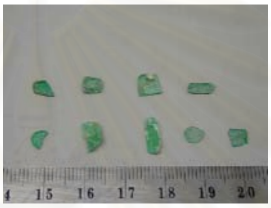</td><td>C (STA 1-10)
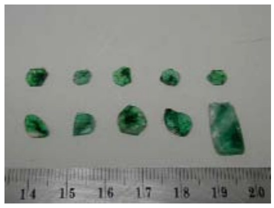</td></tr>
<tr><td>Brazil/Carnaiba-Socoto</td><td colspan="2">Brazil/Itabira</td><td>Brazil/Santa Terezinha</td></tr>
<tr><td>D (CO 1-15)
</td><td>E (CO 16-30)
</td><td>F (MA 1-15)
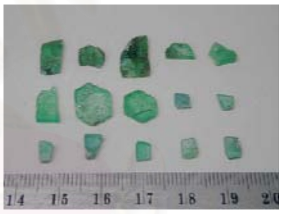</td><td>G (MA 16-30)
</td></tr>
<tr><td colspan="2">Colombia/Cordilla Oriental; Coscues,Muzo</td><td colspan="2">Madagascar/Mananjary region</td></tr>
<tr><td>H (ZA 1-15)
</td><td>I (ZA 16-30)
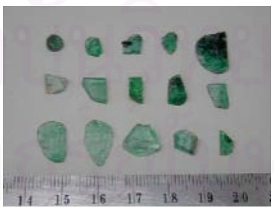</td><td>J (NI 1-15)
</td><td>K (NI 16-30)
</td></tr>
<tr><td colspan="2">Zambia/Kafubu</td><td colspan="2">Nigeria/Kaduna Platua</td></tr>
</table>

Figure 3.7: Showing all samples in this study; 29 samples of Brazilian emeralds (A to C), 30 samples of Colombian emeralds (D to E), 30 samples of emeralds from Madagascar (F to G), 30 samples of Zambian emeralds (H to I) and 30 samples of Nigerian emeralds (J to K).

The colours of 149 emerald samples are compared with the standard gem colour of Gemological Institute of America (GIA GemSets) under the daylight lamp. The lamp's temperature is 6500 K. The colour code comprises hue, tone and saturation. Hue is its colour. Tone is the lightness to darkness of the hue, the higher number is the darker tone (scale 0 -10). Saturation is the strength and purity of the hue, the higher number is the stronger hue (scale 1-6). In this study, the range of colour (depending on the depth of samples) or colour code of emeralds from each area are reported by the following sequence, tone / saturate / hue. In general, Nigerian emeralds are very light to medium light / very slightly grayish to moderately strong / very slightly bluish green to green. The Colombian emeralds are very light to medium / very slightly grayish to moderately strong / very slightly bluish green to green. The Brazilian emeralds are very light to dark / very slightly grayish to moderately strong / very slightly bluish green to green. The emeralds from Madagascar are light to medium / very slightly grayish to strong / very slightly bluish green to bluish green. Finally, the emeralds from Zambia are very light to medium / very slightly grayish to strong / very slightly bluish green to bluish green. The colour codes of all the samples are listed in Appendix I (Figure I.1 and Table I.2).

3.3 Physical and Optical properties

Beryl is one of the durable minerals. For example, large numbers of beryl crystals have been found to retain traces of crystal faces despite prolonged chemical attack and abrasion with other stones. Fracture surfaces are usually brilliant, smooth and conchoidally curved like freshly broken glass.

The specific gravity (SG) and optical properties, such as refractive index (RI), birefringence and fluorescence were examined. A summary of the results are shown in Table 3.1 and the results of all samples are given in Appendix I (Table I.3).

High optical values are found in emeralds from (Santa Terezinha) Brazil. Medium to high optical values are found in emeralds from Madagascar, Zambia, (Carnaiba/Socoto and Itabira) Brazil. Low to medium optical values are found in emeralds from Colombia and Nigeria. High specific gravity values are found in emeralds from Brazil, Madagascar and Zambia whereas emeralds from Colombia and Nigeria are low.

Table 3.1: Summary of the gemological properties of emeralds from Brazil, Madagascar, Zambia, Nigeria and Colombia.

Sample	RI		Birefringence	SG	Fluorescence	
	e-ray	o-ray			LW	SW
Nigeria/NI (Type Ia)	1.560 – 1.570	1.569 – 1.582	0.007 – 0.016	2.601 – 2.687	Inert	Inert
Colombia/CO (Type Ib)	1.561 – 1.572	1.571 – 1.582	0.007 – 0.018	2.612 – 2.731	Inert	Inert
Brazil / STA (Santa Terezinha) (Type IIa)	1.579 – 1.586	1.592– 1.597	0.010 – 0.014	2.723 – 2.812	Inert	Inert
Madagascar/MA (Type IIb)	1.570 – 1.584	1.581 – 1.598	0.008 – 0.023	2.661 – 2.785	Inert	Inert
Zambia/ZA (Type IIb)	1.573 – 1.590	1.580 – 1.597	0.006 – 0.016	2.582 – 2.782	Inert	Inert
Brazil / CAR (Carnaiba/Socoto) (Type IIb)	1.571– 1.581	1.581 – 1.591	0.009– 0.014	2.705 – 2.769	Inert	Inert
Brazil / ITA (Itabira) (Type IIb)	1.571 – 1.580	1.581 – 1.591	0.006 – 0.011	2.690 – 2.727	Inert	Inert

3.4 Internal Characteristics

Certain inclusions, especially in emerald, are distinctive and sometimes can even serve to identify a particular deposit from which they came. Inclusions also provide evidence as to the geochemical environment in which the emerald crystals grew. In general inclusions can be divided into two types based on the time of formation as follows:

1. Primary inclusions are minerals or fluids which formed before or contemporaneously with the host emerald and were enveloped by the emerald crystal as it grew, such as some fluid inclusion; tube and foreign mineral inclusions; mica, quartz, pyrite, etc.
2. Secondary inclusions are those which developed afterwards; such as iron stained in fissures, micas developed to hematite.

In this study, a GIA binocular microscope with magnifications up to 70 times (70x) was used to examine internal and external characteristics of emeralds from different country of origins. Among the common internal features in those emeralds are foreign crystal inclusions, liquid inclusions and growth structures. Some mineral inclusions were further identified their species by using a Ranishaw Laser Raman spectroscope System 1000 attached with a Leica microscope at the GIT. The inclusions were also studied under objective lenses with x5 x20 and x50 magnifications in both transmitted and reflected light microscope. The identification of a mineral inclusion by Raman spectroscopy was done by matching the pattern of Raman peak shift with those of the Renishaw and GIT databases (Figures 3.8 and 3.9).

Williams et al. (1997) reported the database of the Raman Shift peaks of common inclusions which are summarized in Appendix I (Table I.4). Some inclusions were photo-micrographed by a Nikon digital camera model Coolpix 950 attached to a gem microscope or by the Leica microscope attached to the Laser Raman spectroscope.

Figure 3.8: A binocular microscope at the Gem and Jewelry Institute of Thailand (GIT)

Figure 3.9: A Renishaw Laser Raman Spectroscope at the Gem and Jewelry Institute of Thailand (GIT).

3.4.1 Nigeria:

Kaduna Platua

Some of 30 samples of Nigerian emerald examined in this study contain mica inclusions (Figure 3.10 and Figure 3.11 with the Raman spectrum). One sample exhibits opaque-black platelets inclusions of ilmenite as identified by Laser Raman (Figure 3.12). Raman spectrum shows rutile inclusions in Figure 3.13. Raman spectrum of carbonate daughter crystals in multi-phase inclusions is shown in Figure 3.14. Strong relief, colourless to grey mineral inclusions of fluorite are shown in Figure 3.15. Various types of fluid inclusions, such as 2 phase (l,g) , 3 phase (s,l,g) or multi-phase inclusions (Figures 3.16 and 3.17), which look like the ‘classic’ fluid inclusions observed in Colombian emeralds in Figure 3.18. Growth phenomena, such as internal growth lines and coloured zoning can be observed by looking in the direction of c-axis (Figure 3.19). Elongated, strong relief negative crystal can be observed in Figure 3.20.

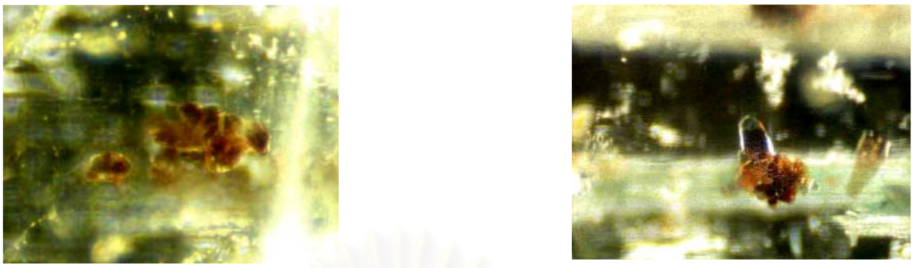

Figure 3.10: Reddish brown to dark brown biotite inclusions in cluster (left) NI10, 70x and book-like appearance (right), d; NI12, 100x.

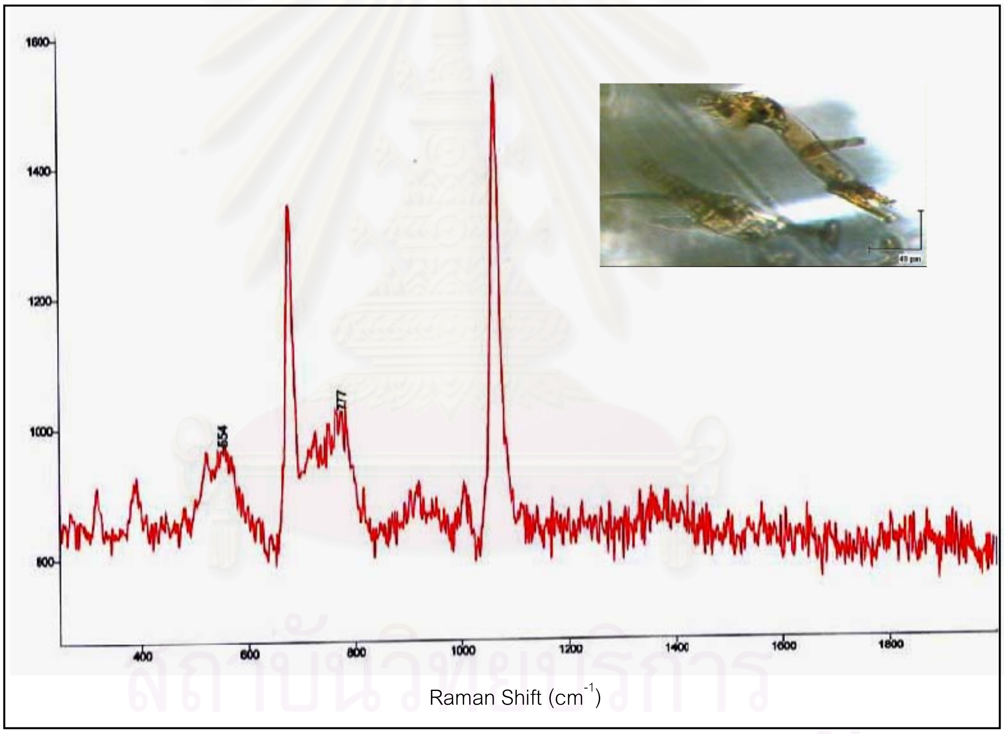

Figure 3.11: Raman spectrum of irregularly shaped biotite inclusions in NI13 (peaks at 554 and 777 cm^{-1}).

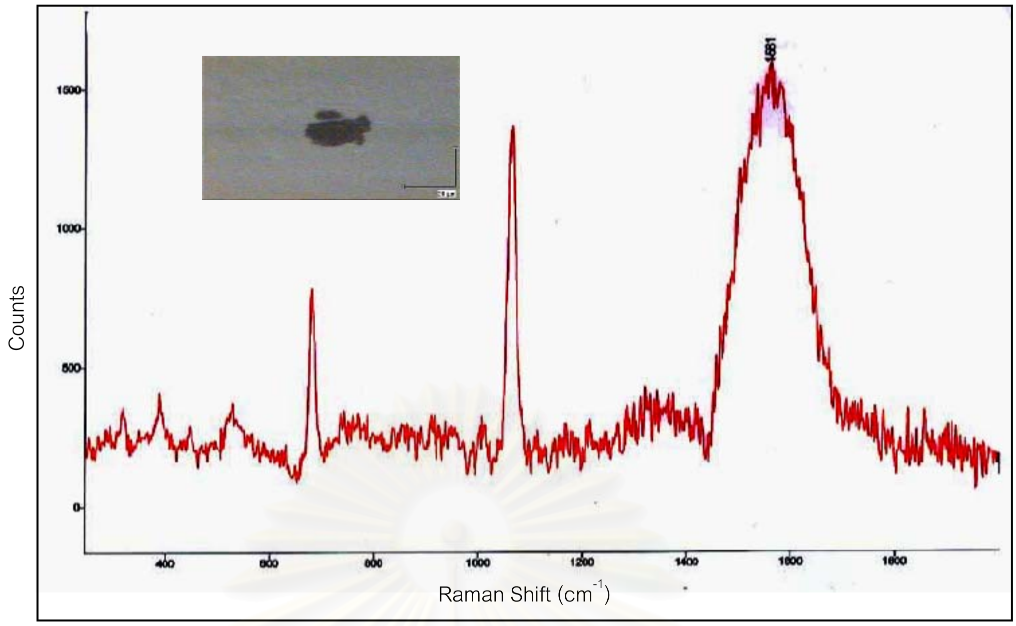

Figure 3.12: Raman spectrum of ilmenite inclusions, which is irregularly shaped grains with metallic luster (NI24, peaks at 398, 681, 1377 and 1581 cm^{-1}).

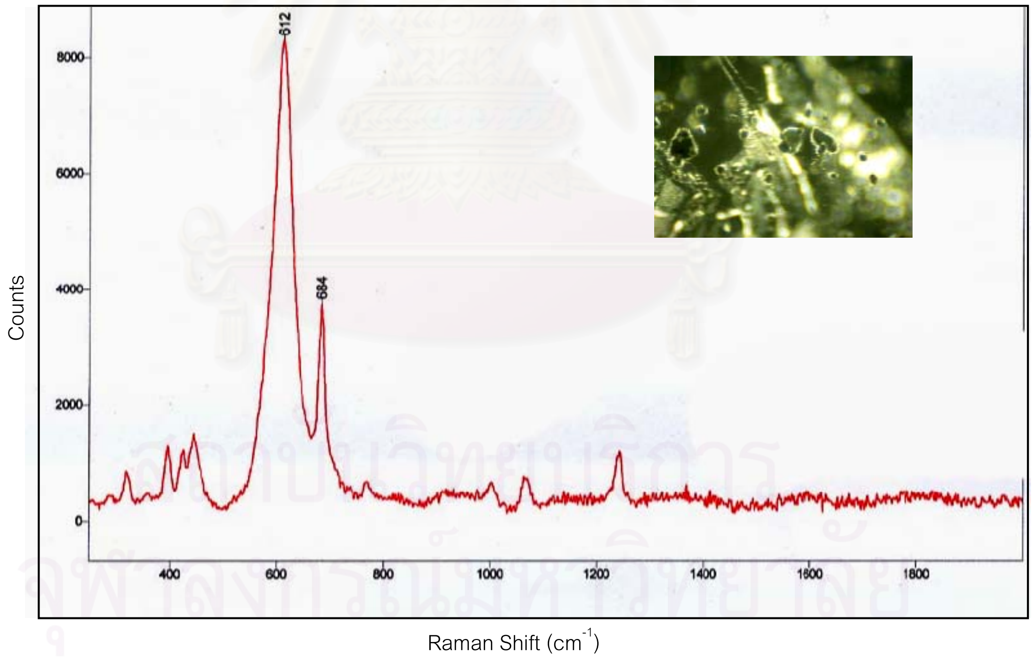

Figure 3.13: Raman spectrum of rutile inclusions, showing strong relief with metallic luster (NI30, peaks at 241, 448 and 612 cm^{-1}).

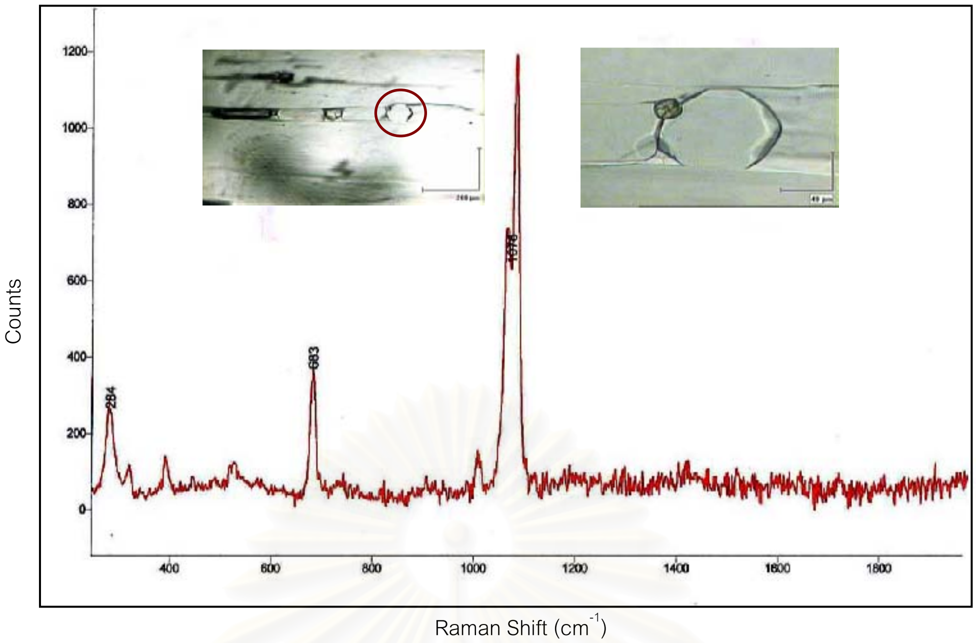

Figure 3.14: Raman spectrum of carbonate daughter crystal in multi-phase inclusions (NI19, peaks at 284, 683 and 1076 cm^{-1}).

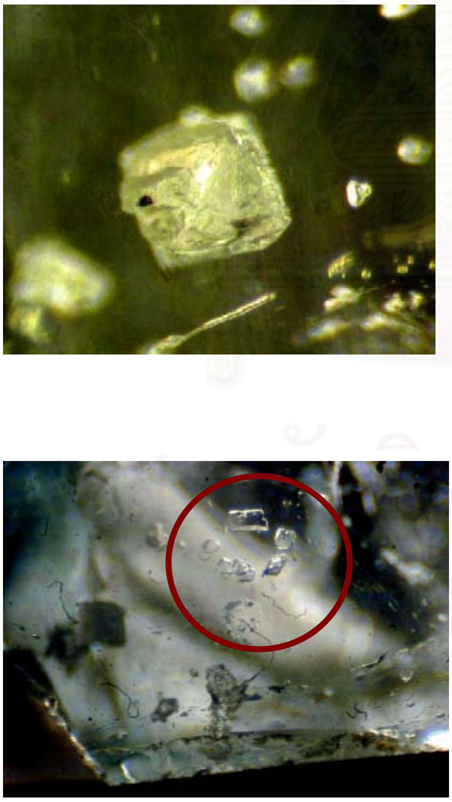

Figure 3.15: Strong relief, colourless to grey perfectly developed octahedral crystals (top) and irregularly shaped mineral inclusions (bottom) of probable fluorite (NI21, 120X).

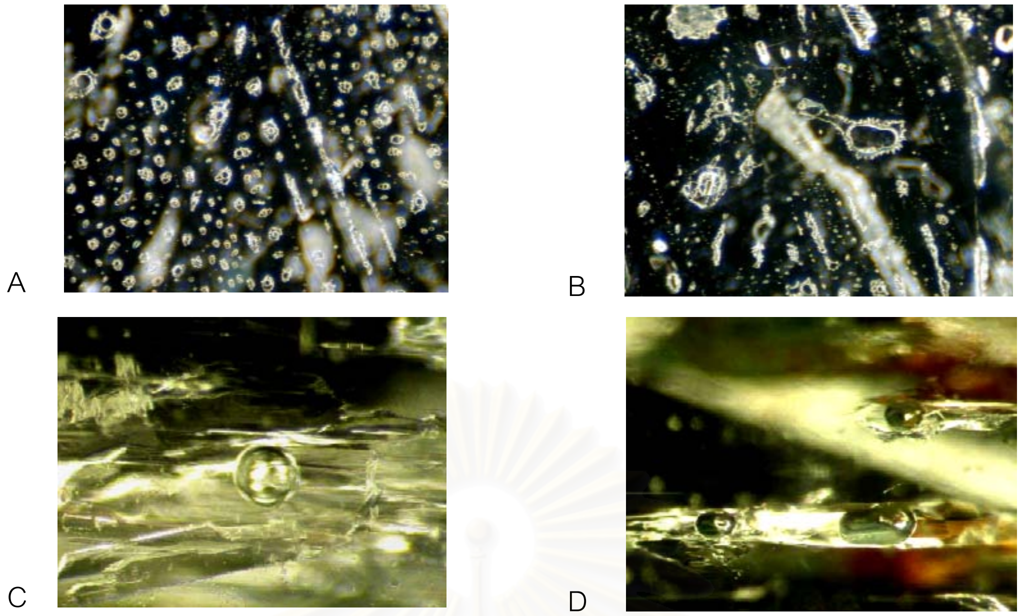

Figure 3.16: Secondary cavities in healing fissures showing rounded, irregularly shaped or 'jagged' outlines in (NI15, 70x); (A and B). And 2-phase fluid inclusion of the 'l,g' type (NI16, 120x); (C) and 3-phase fluid inclusions of the 's,l,g' type (NI10, 100x); (D).

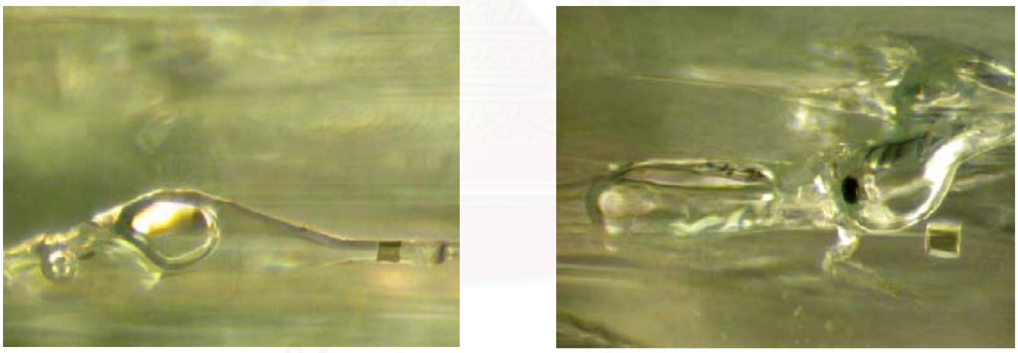

Figure 3.17: Both of primary multi-phase fluid inclusions of the '2s,l,g' type with rhombohedral (may be carbonate) and brown to very dark brown crystal (NI10, 120x).

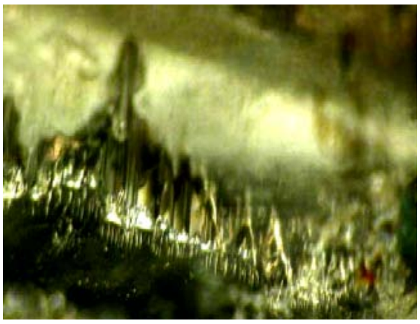

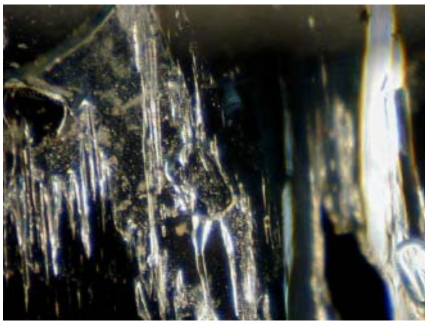

Figure 3.18: The cavities may show elongated (partly jagged) outlines. Mostly cavities often more or less flattened, and the cavity walls seem to be uneven (NI10 and NI12, 70x).

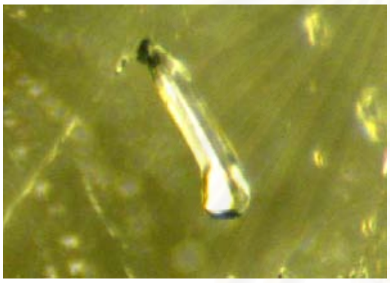

Figure 3.19: Elongate shape of isolated negative crystal in NI10, 100x.

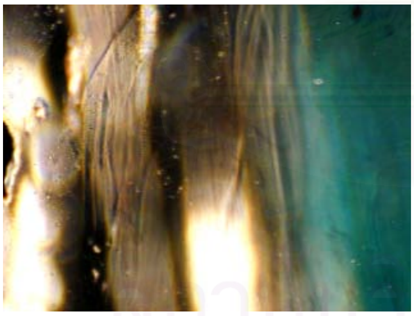

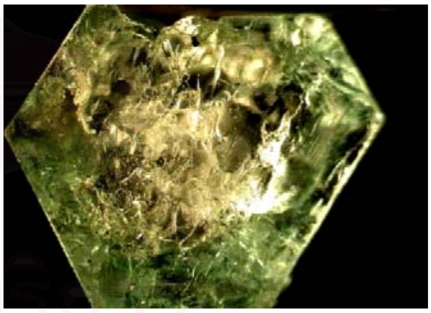

Figure 3.20: Pronounced hexagonal-concentric growth structures, parallel to the prism, and the basal faces (internal growth lines in NI12, 70X) and (colour zoning in NI9, 40X).

3.4.2 Colombia:

Cordillera Oriental, Muzo, Coscues and Chivor mines

The common mineral inclusions of Colombian emerald found in this study include pyrite (Figure 3.21), albite, carbonate and organic matters, which can be identified by Raman spectra (Figures 3.22 to 3.25). Most samples show compact aggregate of black tiny organic matters and carbonate inclusions (Figure 3.26). Elongated or jagged outlines of 2, 3 or multi-phase inclusions are characteristic in Colombian emerald (Figure 3.27). Primary elongated cavities parallel to the emerald's c-axis (growth tube) and strongly developed growth structures are shown in Figures 3.28 and 3.29.

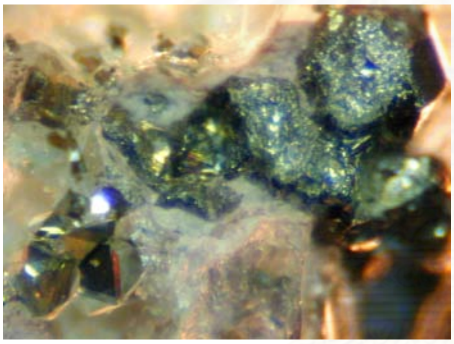

Figure 3.21: Pyrite crystals with golden-yellow metallic luster exposed on the surface (CO3, 60X).

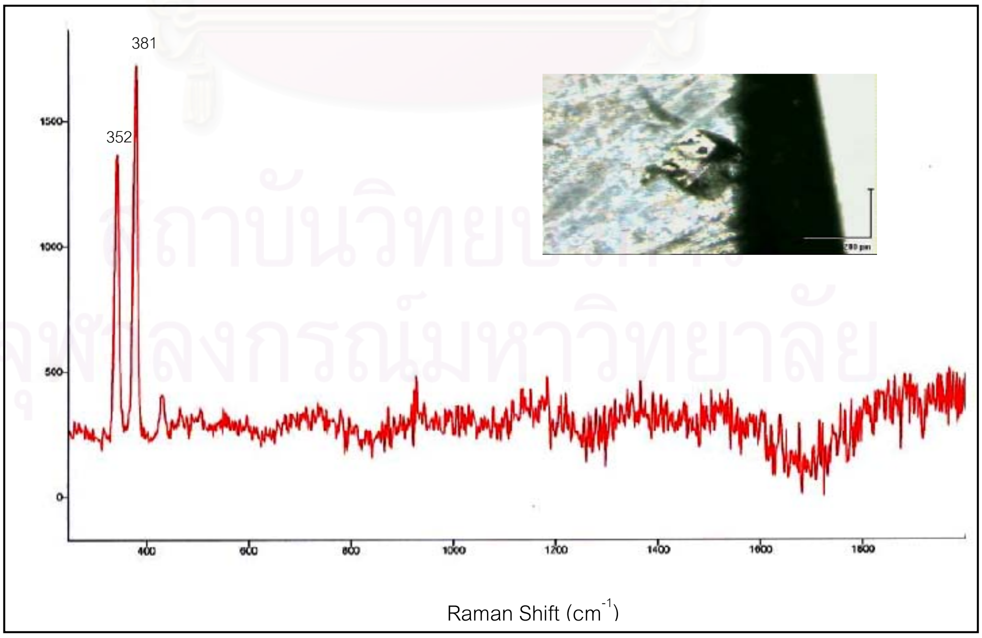

Figure 3.22: Raman spectrum of pyrite inclusion (CO9, peaks at 352, 381 and 443 cm^{-1}).

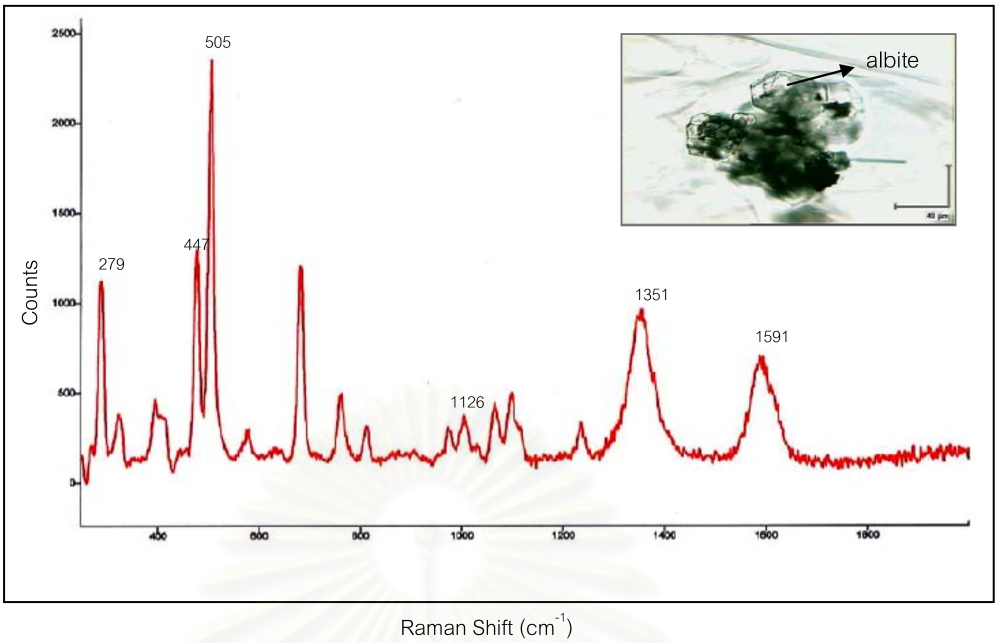

Figure 3.23: Raman spectrum of albite (colourless to greyish) inclusions associated with black organic matters in CO2; (albite: peaks at 279 and 1126) and (organic peaks at 447, 505, 1351 and 1591 cm^{-1}).

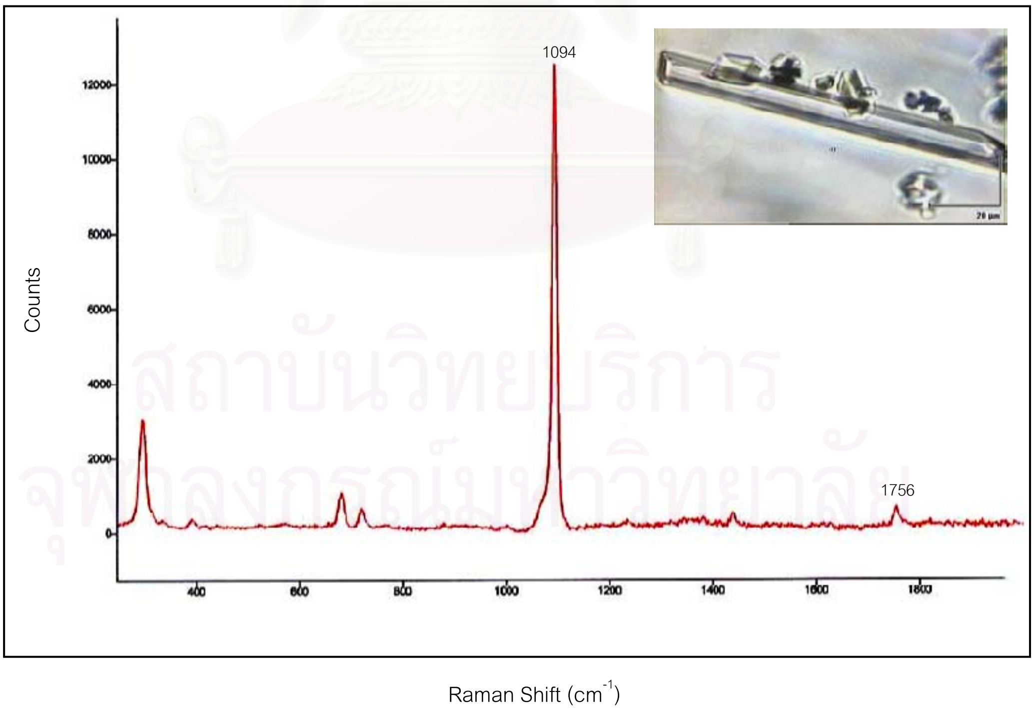

Figure 3.24: Raman spectrum of translucent elongated carbonate crystals (strong relief), (CO4, peaks at 1094 and 1756 cm^{-1}).

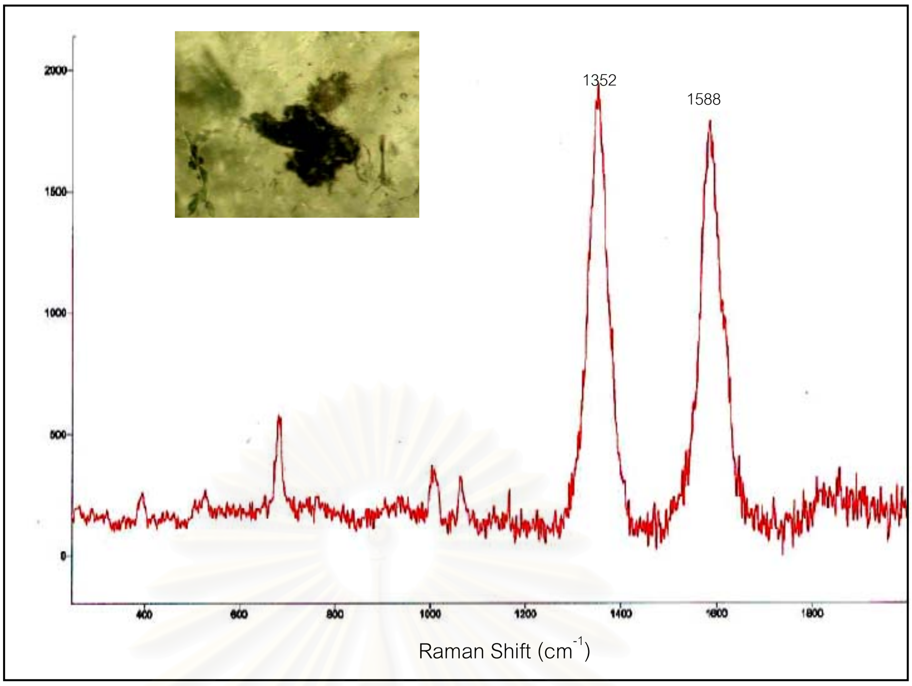

Figure 3.25: Raman spectrum of compact aggregated black organic matter (strong relief), (CO21, peaks at 1352 and 1588 cm^{-1}).

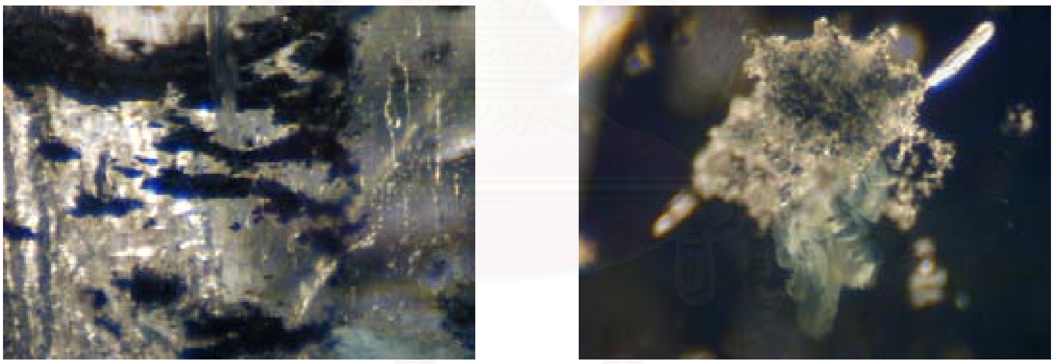

Figure 3.26: Compact aggregated black organic (left); CO-26, 50x and strong relief of gray agglomerate carbonate inclusions (right); CO13, 70x.

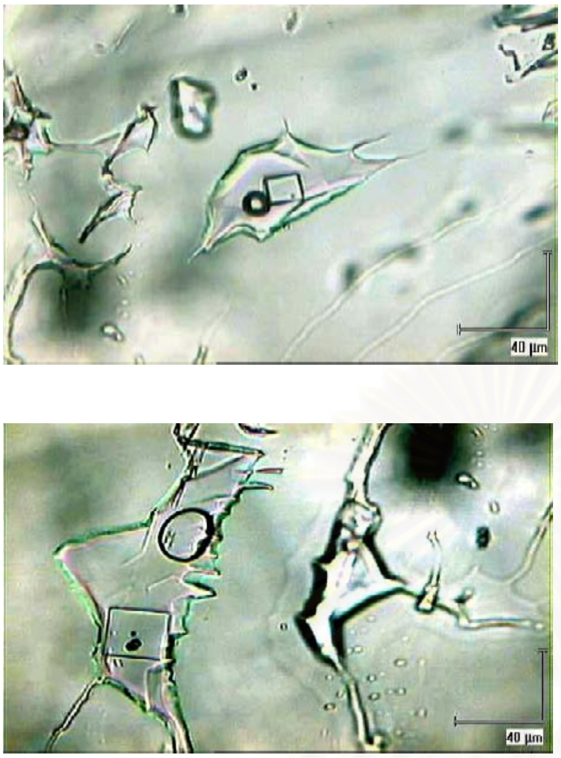

Figure 3.27: Primary cavities with a 3-phase inclusion, which composed of s,l,g (Top) and the multi-phase inclusions containing a rounded vapor bubble, a square shaped crystal and a black crystals (2s,l,g); (bottom) showing jagged outline in CO3.

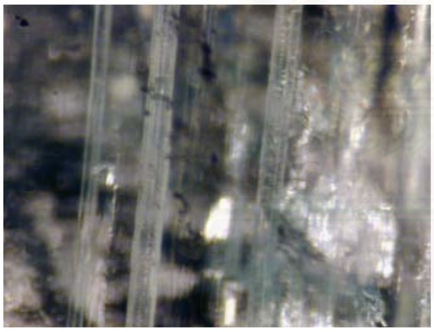

Figure 3.28: Elongated large growth tubes (CO26, 70x).

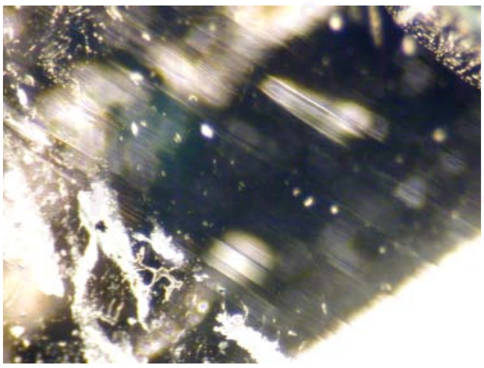

Figure 3.29: Well developed growth structures perpendicular to c-axis (CO7, 40x).

3.4.3 Santa Terezinha deposits of Goias State in Brazil:

The most important inclusions in 10 emerald samples from Santa Terezinha deposits of Goias State are pyrite, carbonate and chromite (Figures 3.30 to 3.32), which some of these inclusions were confirmed by the Laser Raman shown in Figures 3.33 to 3.34. Raman spectra of low relief quartz and talc inclusions (transparent, colourless and irregularly-shaped) are shown in Figures 3.35 and 3.36. Among the other inclusions numerous black-opaque inclusions of spinel were also observed and in general formed more or less compact aggregates (Figures 3.37 and its Raman spectrum in Figure 3.38). Light brown, irregularly-shaped mica inclusions are randomly distributed in the host crystal as shown in Figure 3.39 together with its Raman spectrum. ‘Dust-particles’ and secondary inclusions of iron stain in fissures and fractures can be seen in Figures 3.40 and interference colour of oil-filling in Figure 3.41.

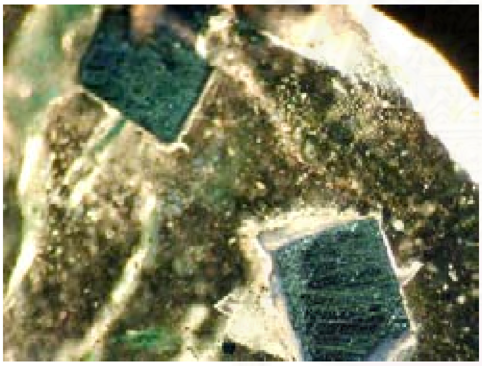

Figure 3.30: Numerous large pyrite crystals (partly cubes cut at surface) with many faces showing a typical yellowish metallic luster (STA5, 50x).

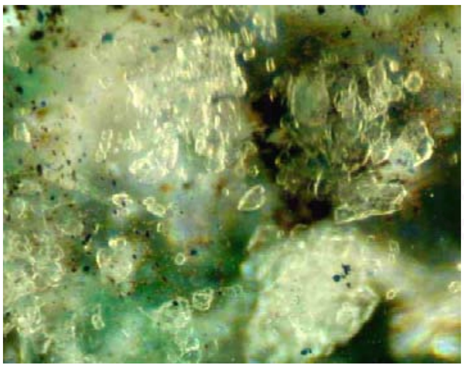

Figure 3.31: Colourless to brownish, transparent carbonate crystals with strong relief (STA10, 70x).

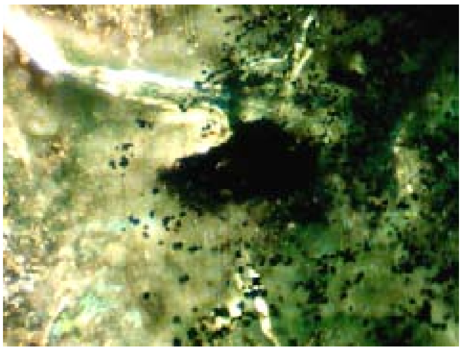

Figure 3.32: Chromite is present as black rounded crystals or in octahedrons. The large individual crystals are mostly isolated, and some form irregular clouds or films (STA1, 70x).

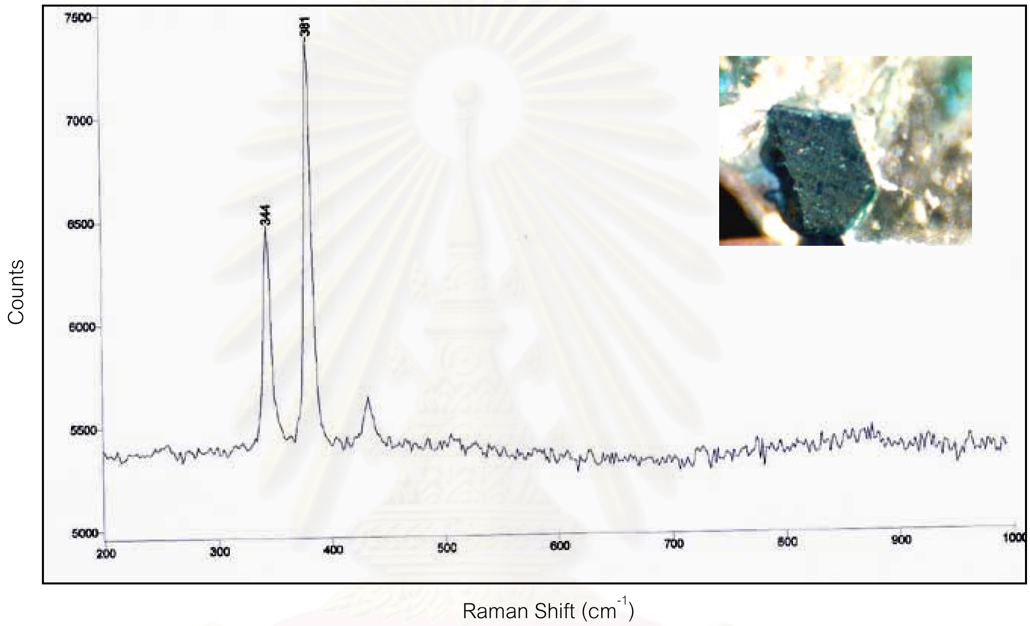

Figure 3.33: Raman spectrum of a pyrite inclusion which is common in emerald of the Santa Terezinha deposits (STA2; peaks at 344 and 381 cm^{-1}).

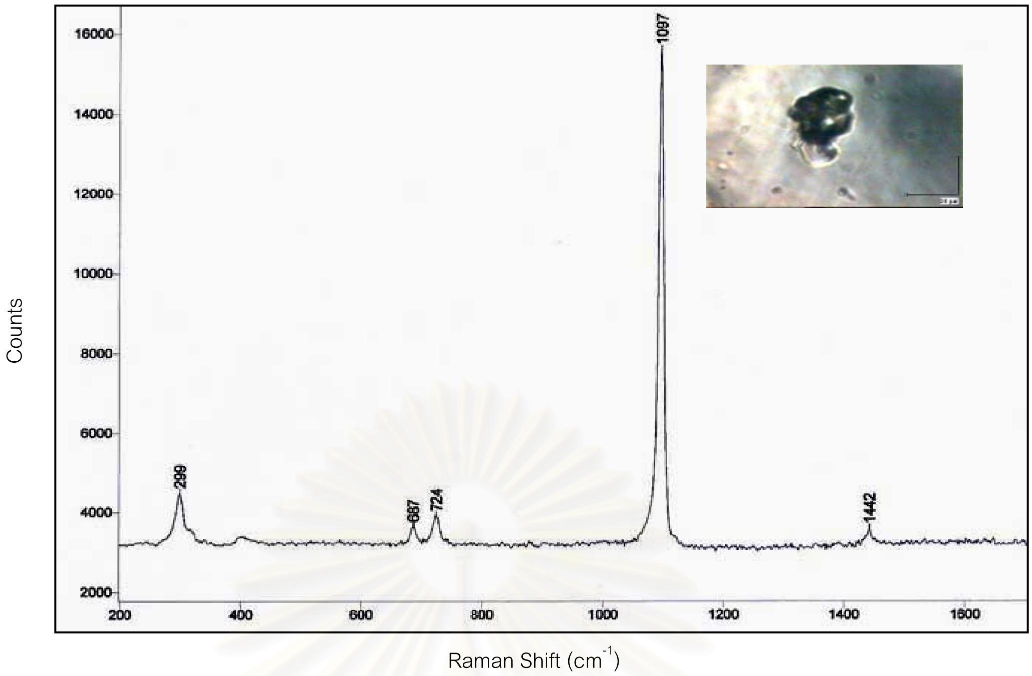

Figure 3.34: Raman spectrum of a whitish to grayish-transparent to translucent carbonate inclusions (strong relief) that may be calcite or dolomite (STA7; peaks at 724, 1097 and 1442 cm^{-1}).

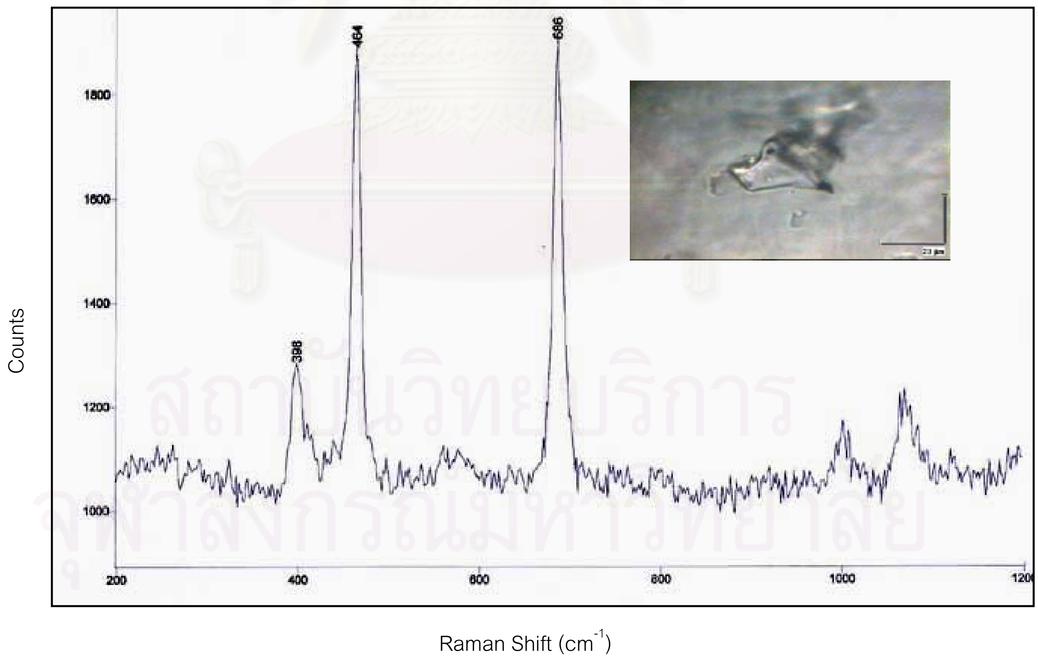

Figure 3.35: Raman spectrum of whitish transparent irregularly-shaped quartz inclusions (low relief); (STA10; peaks at 398 and 464 cm^{-1}).

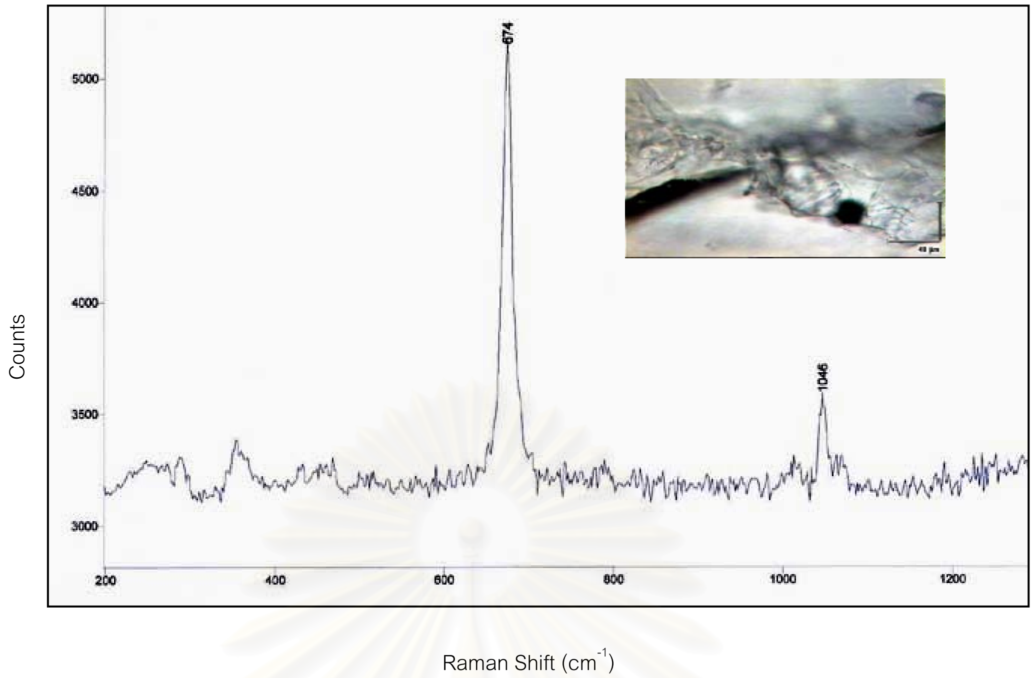

Figure 3.36: Raman spectrum of isolated colourless-trasparent talc platelets. They show a faint relief and are randomly distributed in the host crystal (STA9; peaks at 674 and 1046 cm^{-1}).

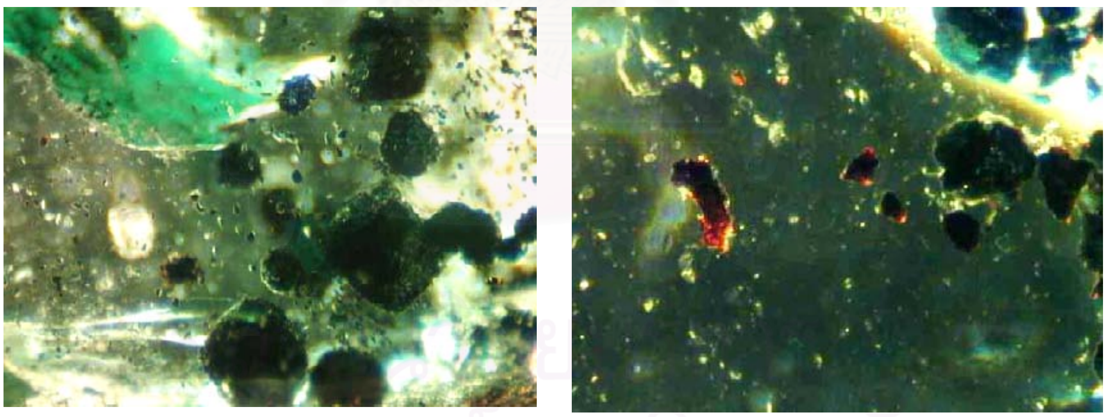

Figure 3.37: On the left, Numerous black-opaque spinel crystals, generally formed more or less compact aggregates (STA9, 70x) and on the right, small black grains of opaque Fe-Cr spinel, which are commonly dispersed along (healed) fissures (STA6, 70x).

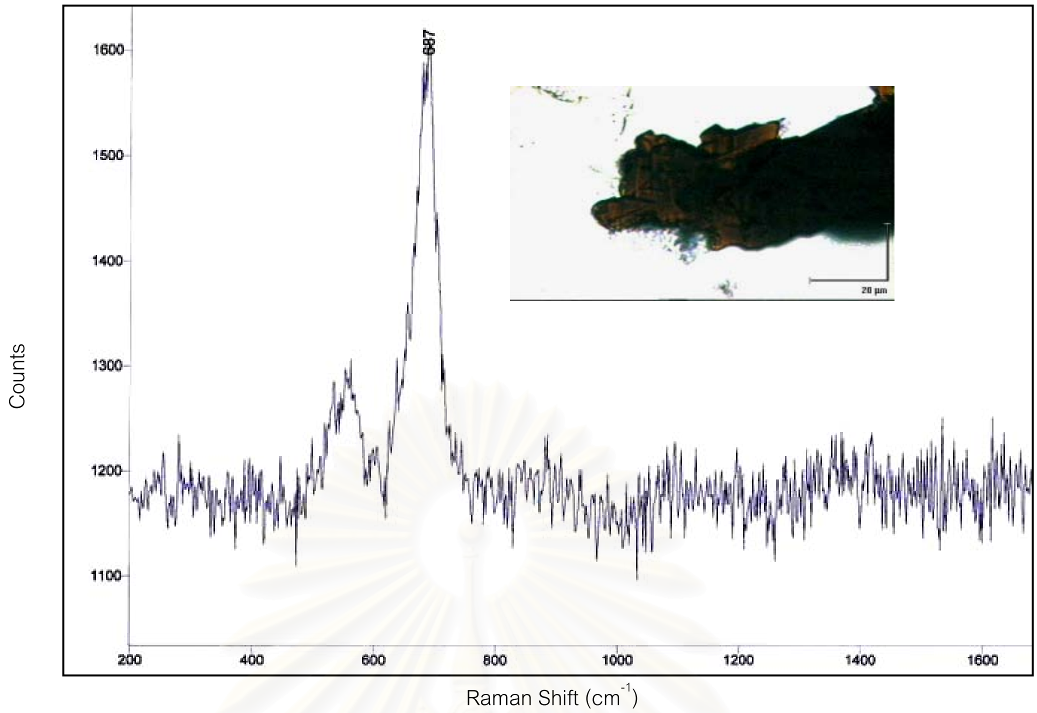

Figure 3.38: Raman spectrum of a compact aggregate crystal, possibly Cr-Fe spinel inclusions with iron stain (STA9; peaks at about 555 and 687 cm^{-1}).

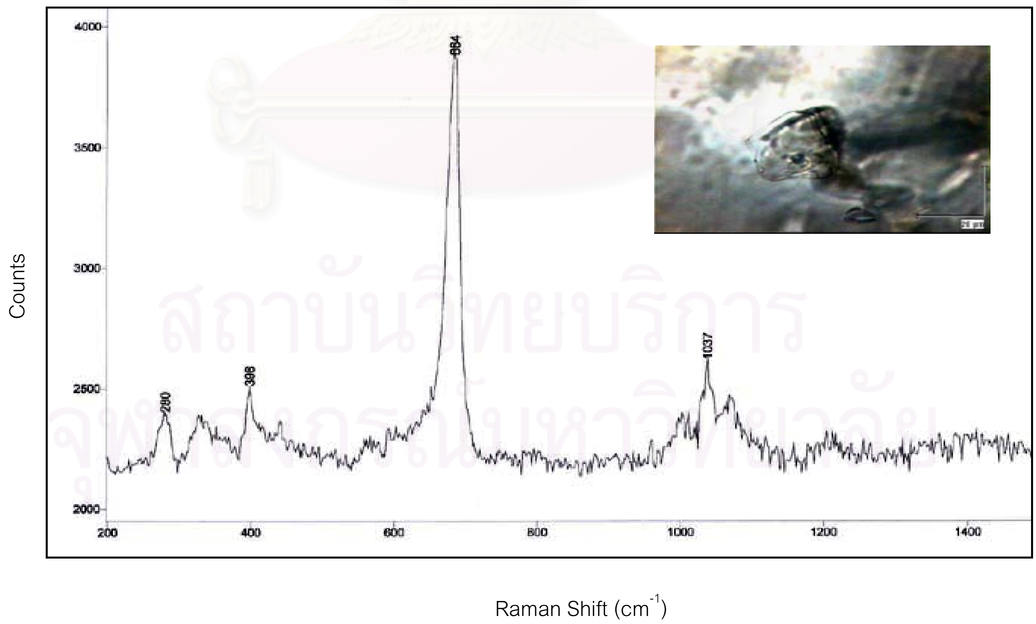

Figure 3.39: Raman spectrum of a light brownish transparent flake of mica, may be biotite or phlogopite inclusions in Brazilian emerald from Santa Terezinha de Goias (STA5; peaks at 280, 359, 398 and 1037 cm^{-1}).

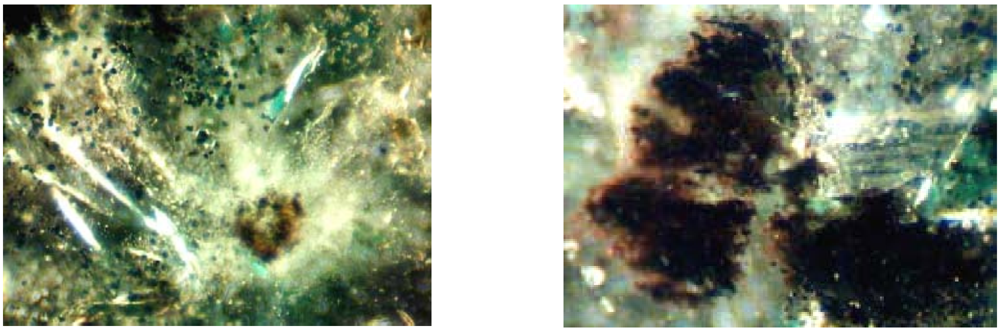

Figure 3.40 (Both pictures) Most of fluid inclusions are so small that they look like 'dust-particles' and secondary inclusions of iron stain in fissures and fractures (STA1, 3; 70x).

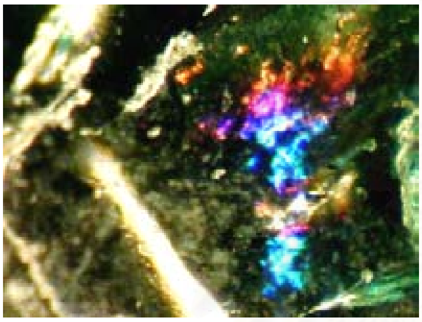

Figure 3.41 Fracture-filling with oil showing interference colour (STA3, 60x).

3.4.4 Madagascar:

Mananjary deposits of Madagascar

The most common mineral inclusions in 30 emerald samples from the Mananjary deposits are quartz, which can be divided, similar to those observed by Schwarz (1994), in 4 categories on the basic of their morphology and manner of occurrences such as, 1) Transparent, colourless, elongated, prismatic crystals, often associated with primary fluid inclusions in Figures 3.42, 2) Rounded or spherical grains, not associated with fluid inclusions or 3) Irregularly rounded crystals, some of which had corroded rough surface; in Figures 3.43 and 4) Isolated crystals, which were baby crystals of former fluid-filled cavities can be shown with Raman spectrum in Figures 3.44.

Mica (biotite/phlogopite) inclusions normally can be observed from worldwide occurrences related to mica schists (Zambia, Madagascar and Brazil). In these samples, mica inclusions appear as dark brown transparent crystals which may have an hexagonal outline or prismatic shape (Figures 3.45 and 3.46 with the Raman spectrum). The amphibole inclusions can be seen in emeralds due to host rocks (mica schist) grade into amphibole schist. These mineral inclusions are green and show a long prismatic habit of actinolite which was identified by Laser Raman (Figure 3.47). Compact aggregates composed of amphibole and talc crystals are also observed in the border region of the sample (Figure 3.48).

Low relief well-developed rhombohedral carbonate inclusion is also noted (Figures 3.49) and in Figure 3.50 shows Raman spectra of daughter carbonate crystals in CO_2-rich fluid inclusions. Large numbers of primary fluid inclusions occur as elongated cavities which look like 'rain effect' in Figures 3.51. Some fluid inclusions (negative crystals) show high relief in Figure 3.52. A sample in Figure 3.53 exhibits the healed fissures filled with foreign substances (may be oil) and some samples show coloured zones with primary fluid inclusions oriented perpendicular to c-axis (Figure 3.54)

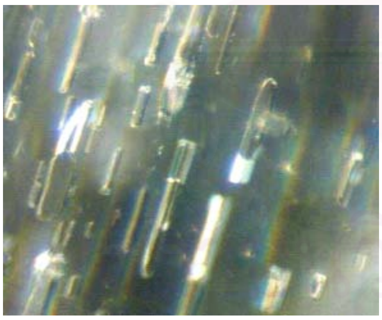

Figure 3.42: Elongated, prismatic quartz inclusions, often associated with primary fluid inclusions (MA-17, 100X).

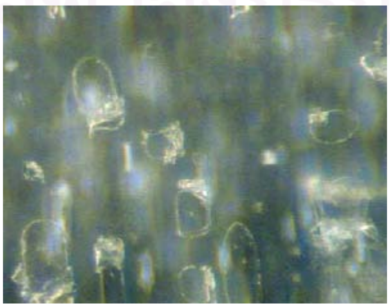

Figure 3.43: Colourless transparent, irregularly rounded quartz inclusions, some of which had corroded rough surface (MA-18, 90X).

.

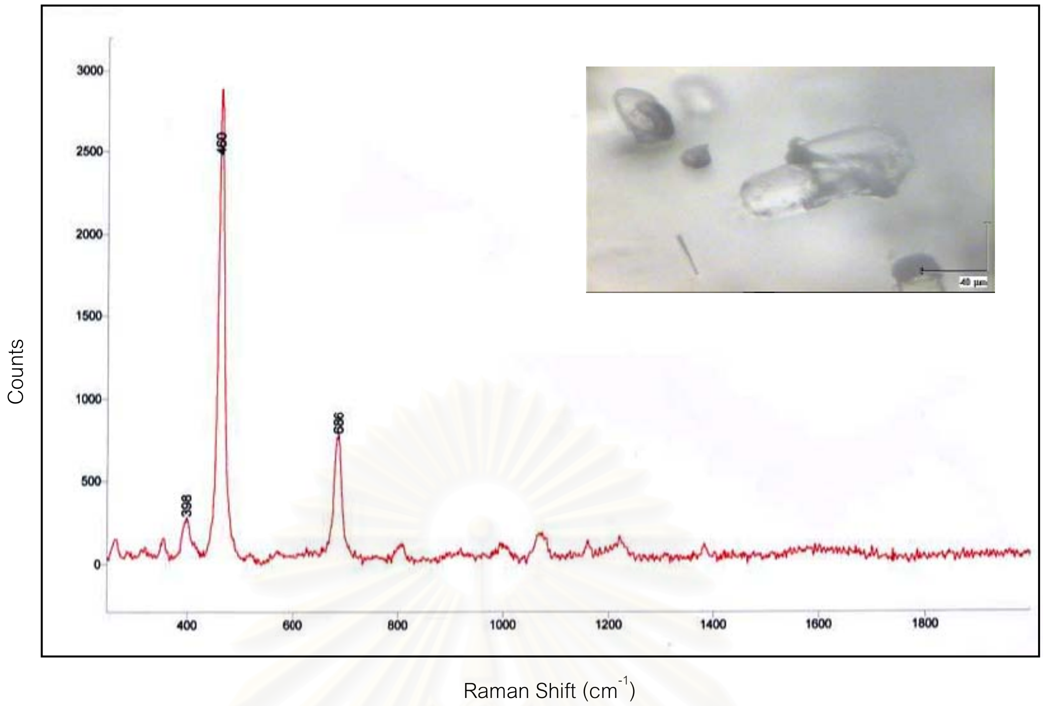

Figure 3.44: Raman spectrum of isolated elongated, prismatic colourless quartz inclusion, often associated with primary fluid inclusions (MA-11; peaks at 398 and 460 cm^{-1}).

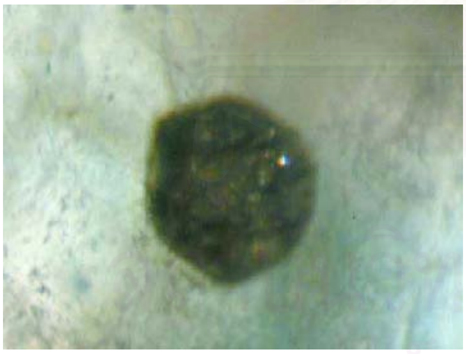

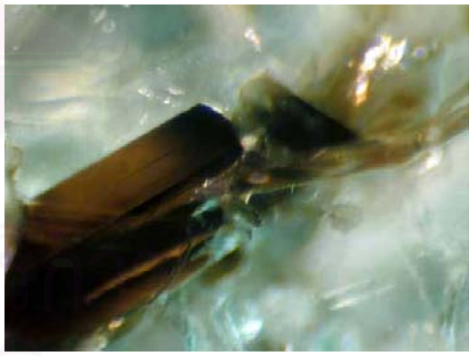

Figure 3.45: Perfect (pseudo-), hexagonal outline of a dark brown mica inclusion on the left (MA2,120x) and dark brown elongate crystals or ‘books’ of mica inclusions on the right (MA4, 60X).

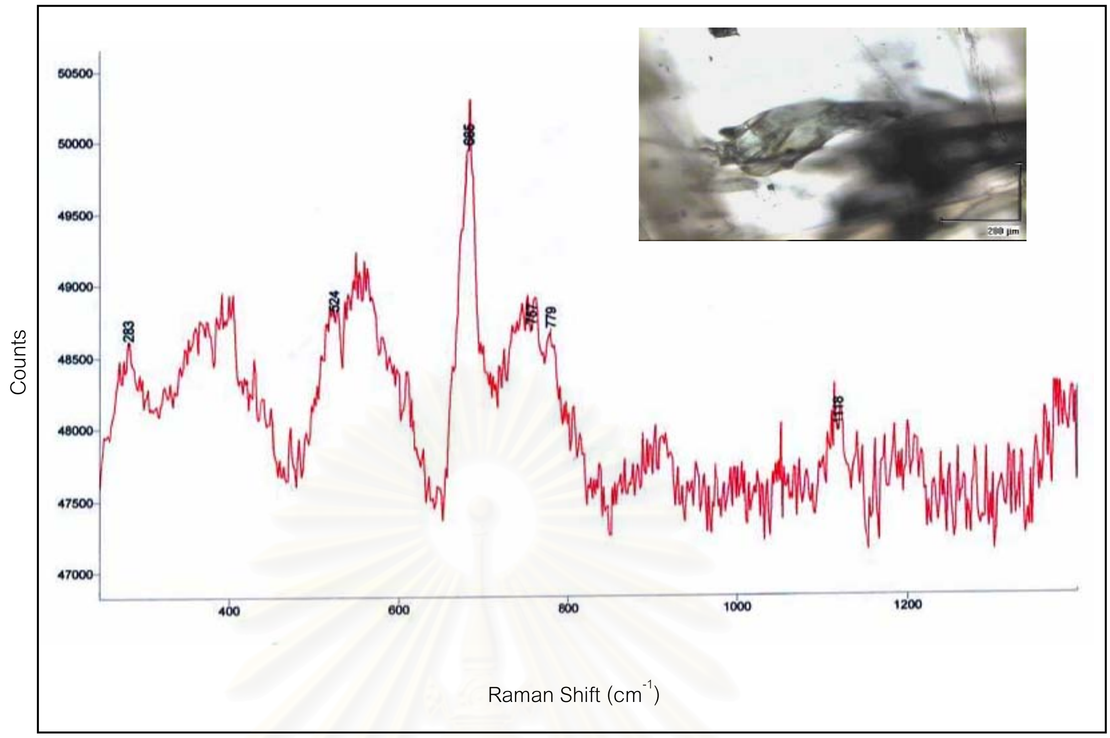

Figure 3.46: Raman spectrum of brown mica crystals are irregularly rounded and randomly orientated in the emerald host (MA1; peaks at 283, 406, 524, 557, 563, 767 and 779 cm^{-1}).

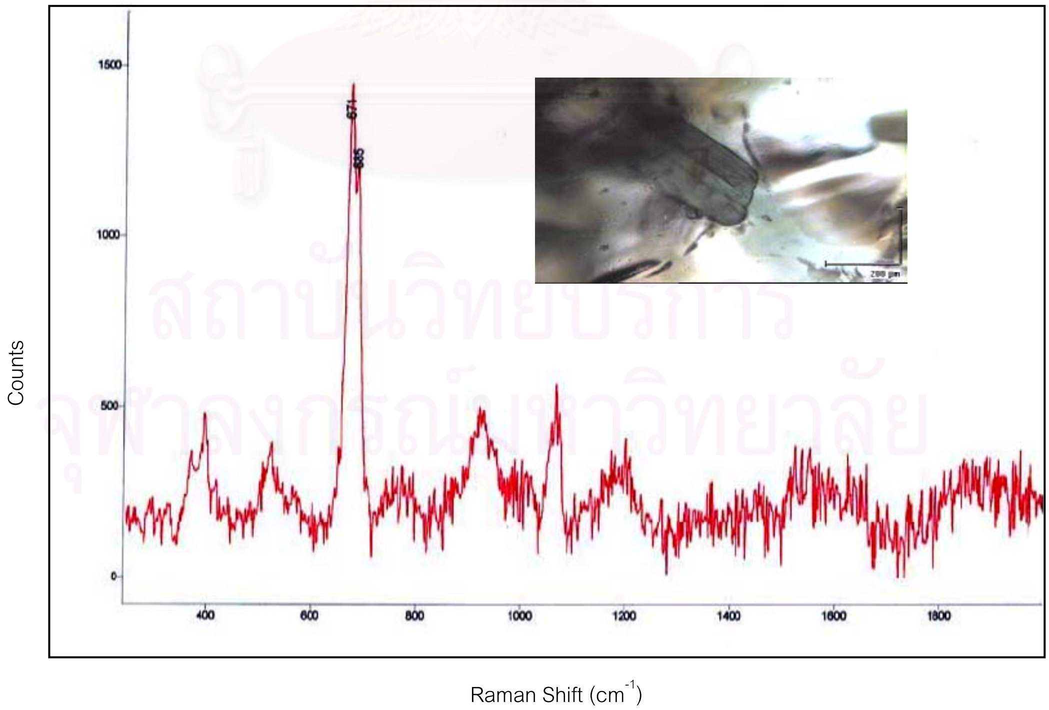

Figure 3.47: Raman spectrum of long prismatic, transparent green amphibole (actinolite) inclusions (MA3; peaks at 383 and 671cm^{-1}).

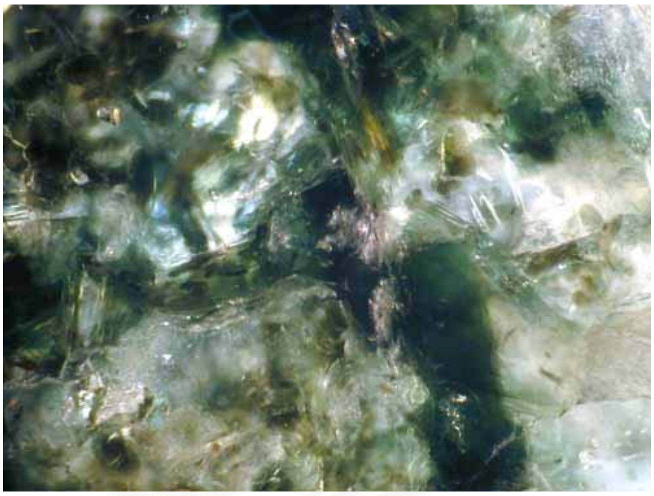

Figure 3.48: Compact aggregates composed of green amphibole (actinolite) and talc (colourless to whitish mineral inclusions) at the rim of the sample (MA3, 100x).

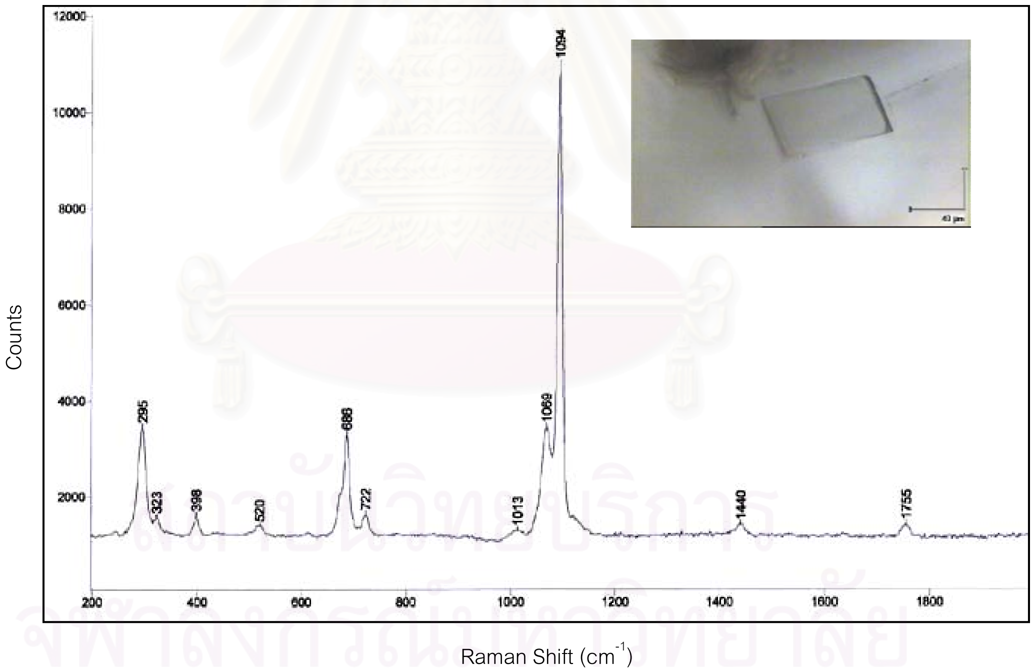

Figure 3.49: Raman spectrum of rhombohedral light brown carbonate crystal can be seen in some of the Mananjary emeralds (MA3; peaks at 295, 722, 1069, 1094, 1440 and 1755 cm^{-1}).

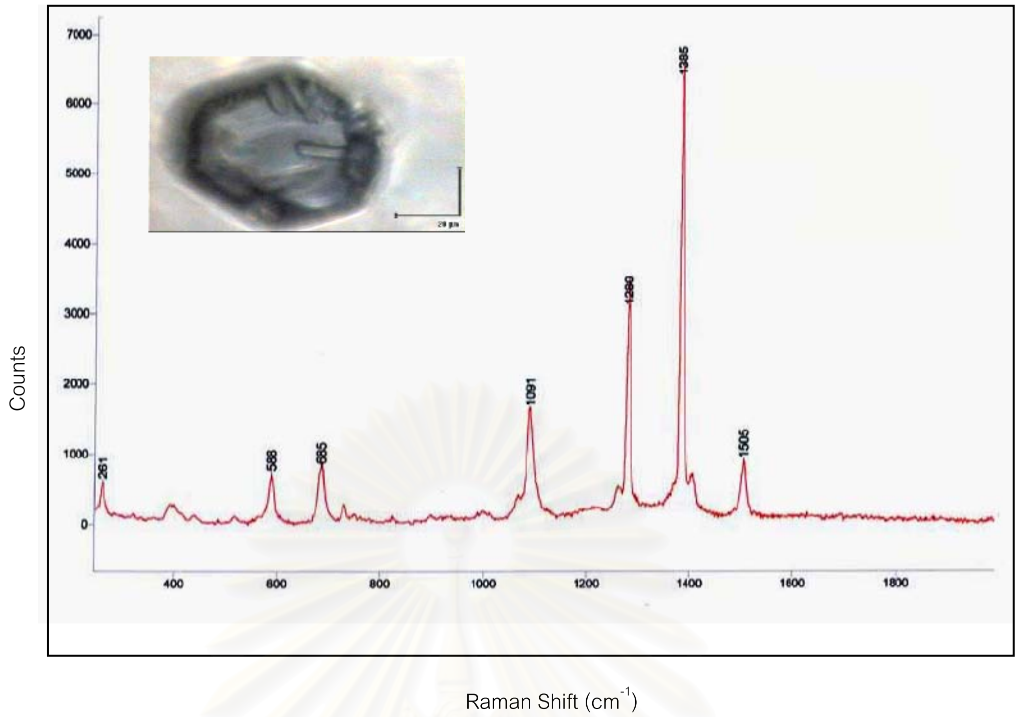

Figure 3.50: Raman spectra of several daughter carbonate crystals and CO_2 in negative crystal inclusions have been identified by Laser Raman spectroscopy in sample MA20 (carbonate peaks at 261, 1091 and 1505 cm^{-1} and CO_2 at 1280 and 1385 cm^{-1}).

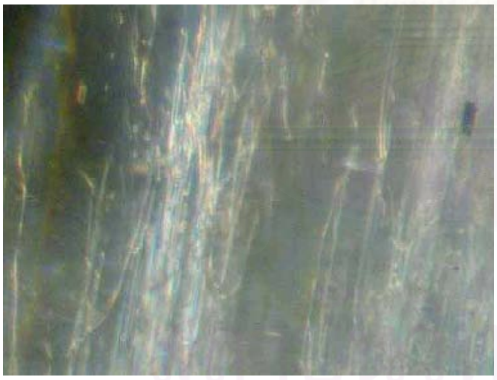

Figure 3.51: Some samples showing primary fluid inclusions occurred as elongated cavities, look like 'rain effect' (MA24, 90x).

Figure 3.52: Well developed rectangular outlines of high relief negative crystal (MA20, 120x).

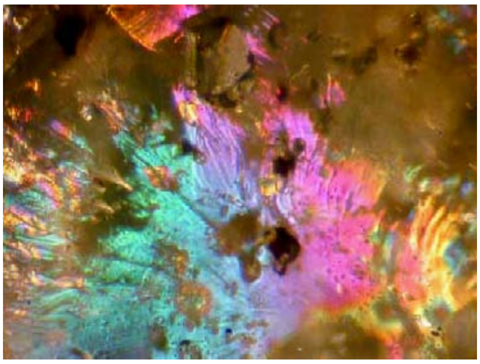

Figure 3.53: Oil-filling in fractures showing interference colour (MA20, 50x).

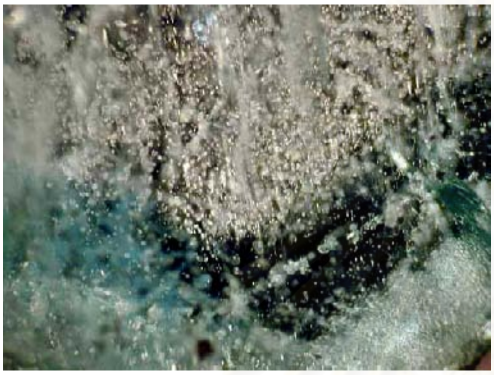

Figure 3.54: Syngenetic inclusions formed along growth and coloured zones, perpendicular with c-axis (MA8, 30x).

3.4.5 Zambia:

Kafubu area in Ndola Rural district

The most common mineral inclusions in 30 samples of Zambian emerald are micas, which include phlogopite/biotite platelets, euhedral and irregularly rounded transparent, brown crystals (Figures 3.55 and Figure 3.56 with the Raman spectrum). The next common mineral inclusions are green, elongated prismatic actinolite inclusions and their Raman spectra shown in Figures 3.57 and 3.58. Raman spectroscopy can identified the following daughter crystals in muti-phase fluid inclusions; colourless – whitish to grayish, transparent to translucent carbonate crystals (high relief) in multi-phase (1l,2s,1g) inclusions (Figure 3.59), low relief, colourless-transparent quartz crystals and orange hematite platelets (Figures 3.60 and 3.61), and both hematite and quartz multi-phase (Figure 3.62). Other internal features are unhealed fissures showing a frosted appearance (Figure 3.63) and strongly developed growth structures and coloured zoning parallel to the emerald's prism faces (Figure 3.64). In Figure 3.65 shows brown foreign substances filled in fissures exhibiting dendritic pattern. And unhealed fissures show mirror-like reflection effect which are, partly, relative planer to the run more or less parallel to the emerald's c-axis (Figure 3.66). Growth tubes containing iron stains and primary fluids are shown in Figure 3.67.

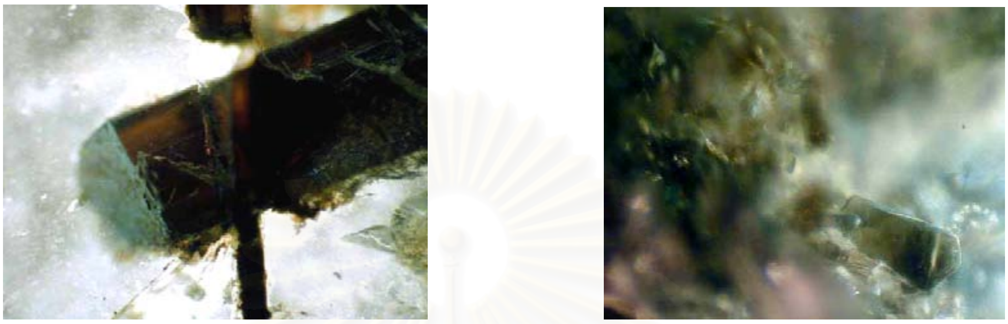

Figure 3.55: 'Booklets' of mica (left); (ZA13, 120x) and cluster of brown irregularly rounded mica platelets of biotite/phlogopite (right), which do not show any crystallographic orientation in the emerald host; (ZA30, 100x).

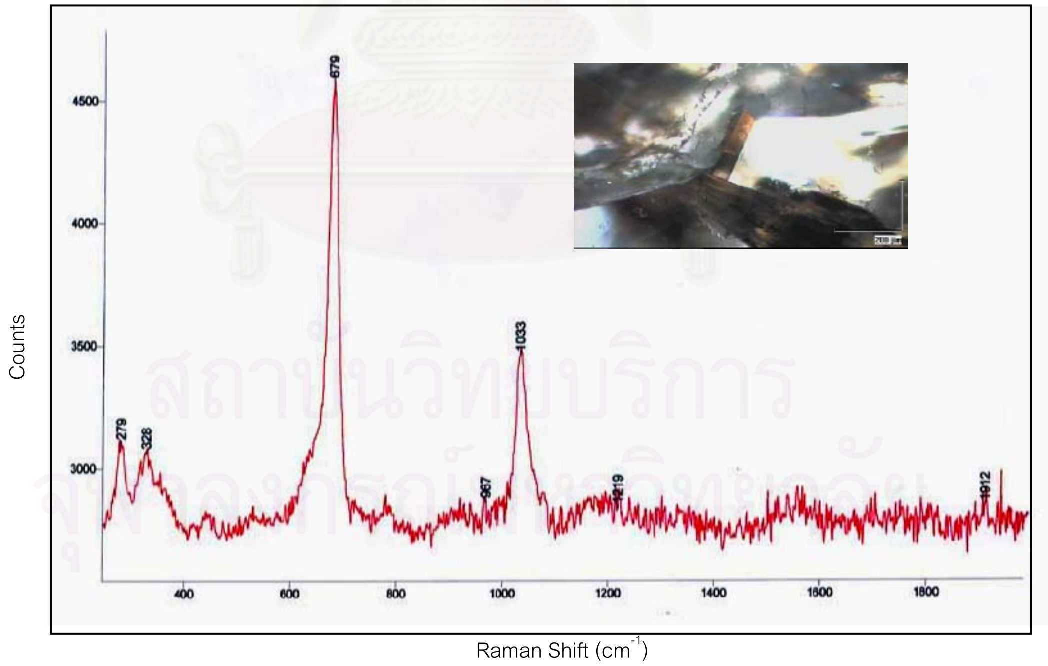

Figure 3.56: Raman spectram of isolated mica platelets (ZA20; peaks at 279, 328 and 679 cm^{-1}).

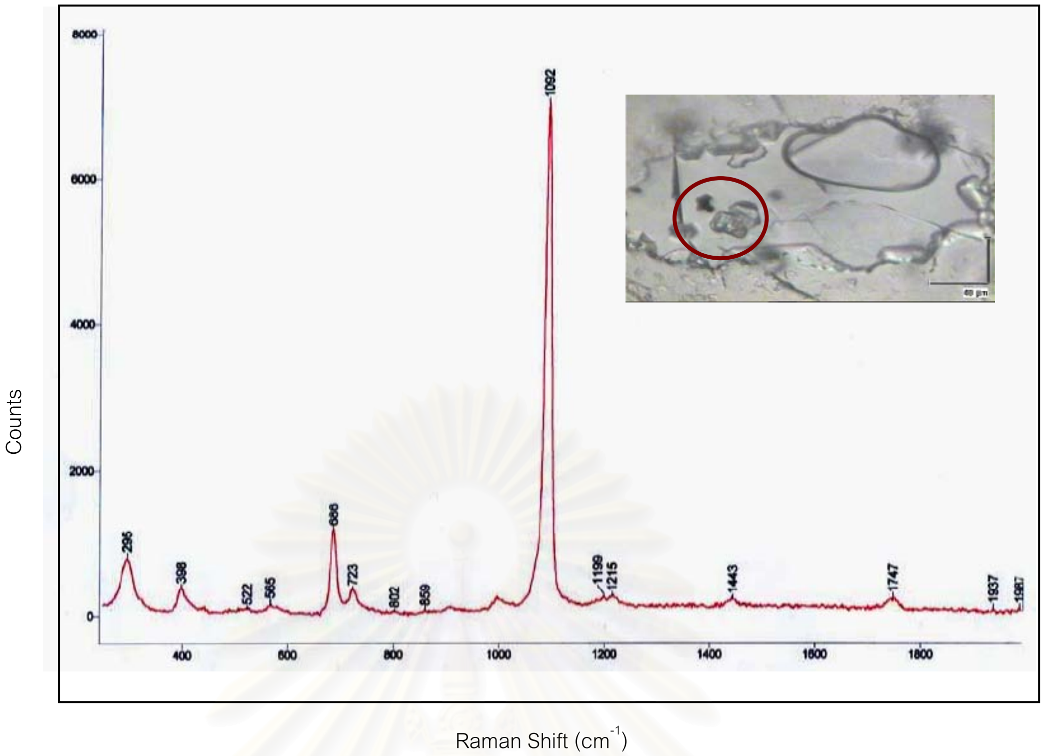

Figure 3.57: Raman spectrum of carbonate crystals (high relief) in a multi-phase (1l,2s,1g) inclusion (ZA23; peaks at 565, 723, 802 and 1092 cm^{-1}).

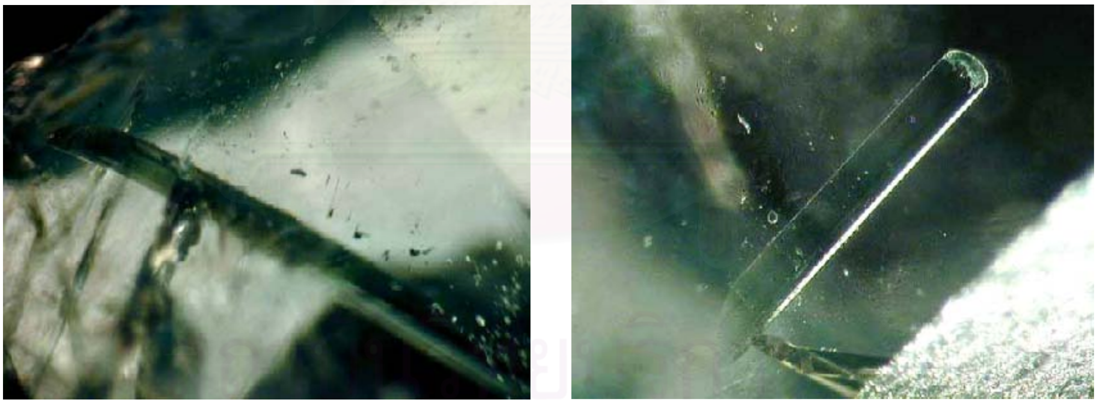

Figure 3.58: elongated prismatic actinolite inclusions in both pictures (high relief); (ZA17, 120x).

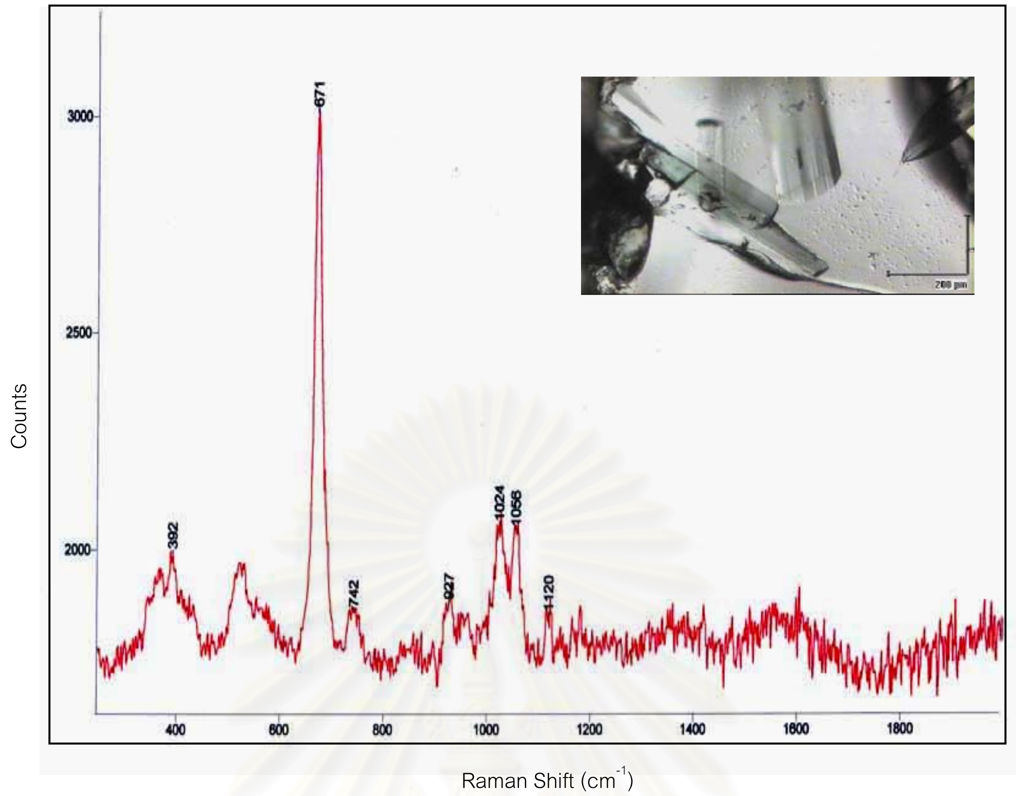

Figure 3.59: Raman spectrum of actinolite inclusions in Zambian emerald (ZA17; peaks at 383, 671,742 and 1058 cm^{-1}).

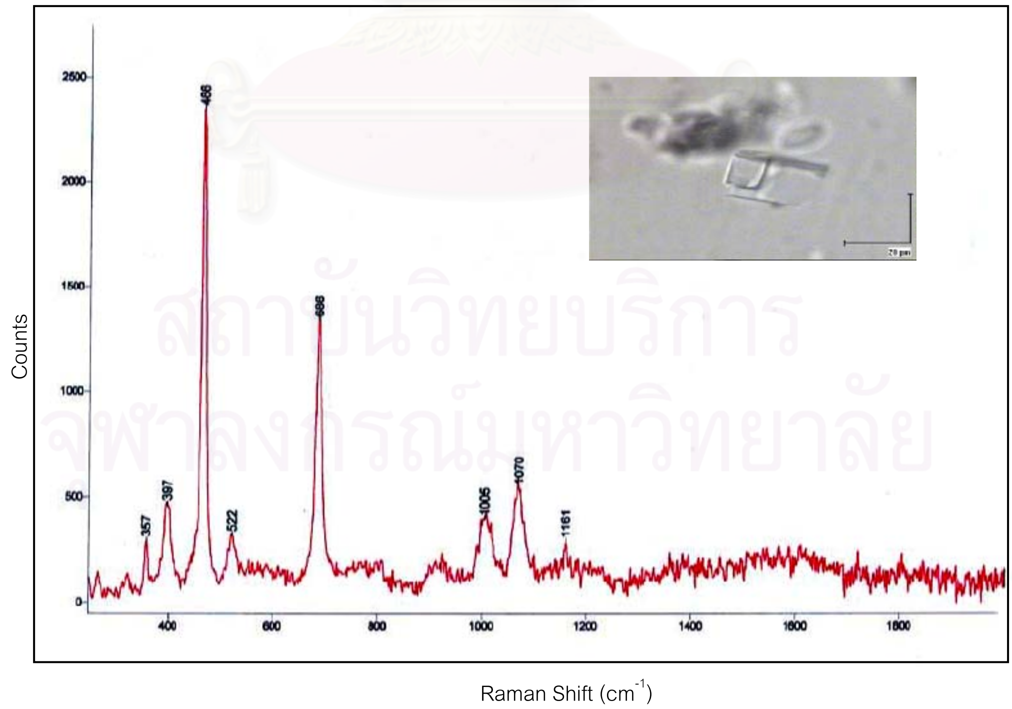

Figure 3.60: Raman spectrum of transparent, colourless quartz inclusions in low relief (ZA25; peaks at 357, 397, 466 and 1161 cm^{-1}).

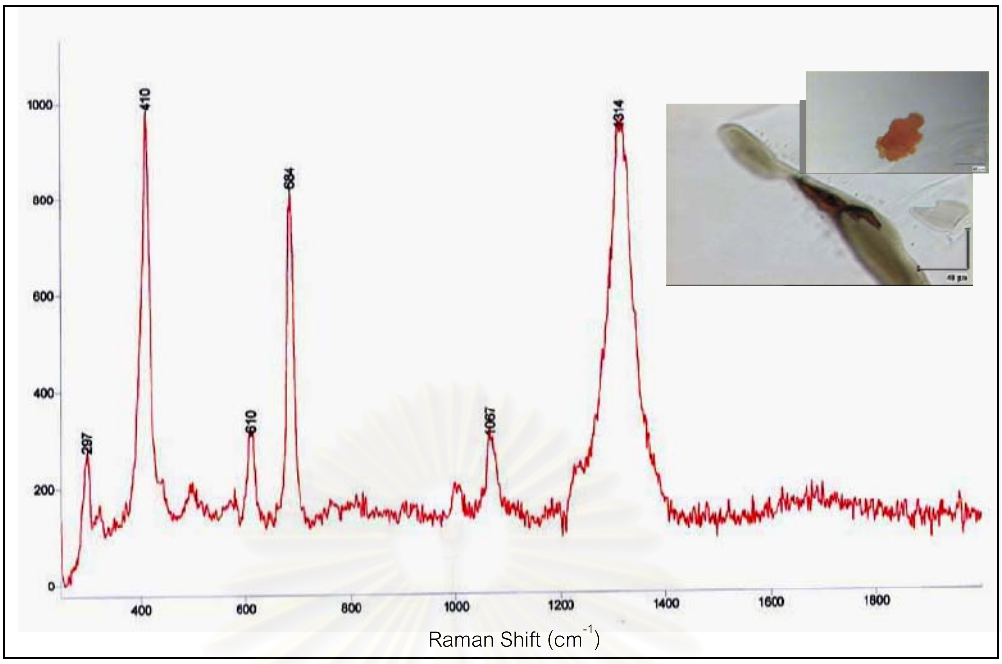

Figure 3.61: Raman spectra of mica altered to hematite (bottom) in Za21; (mica showing peaks at 297 and 1067 cm^{-1} and hematite showing peaks at 410, 610 and 1314 cm^{-1}), high relief of orange hematite platelets (top).

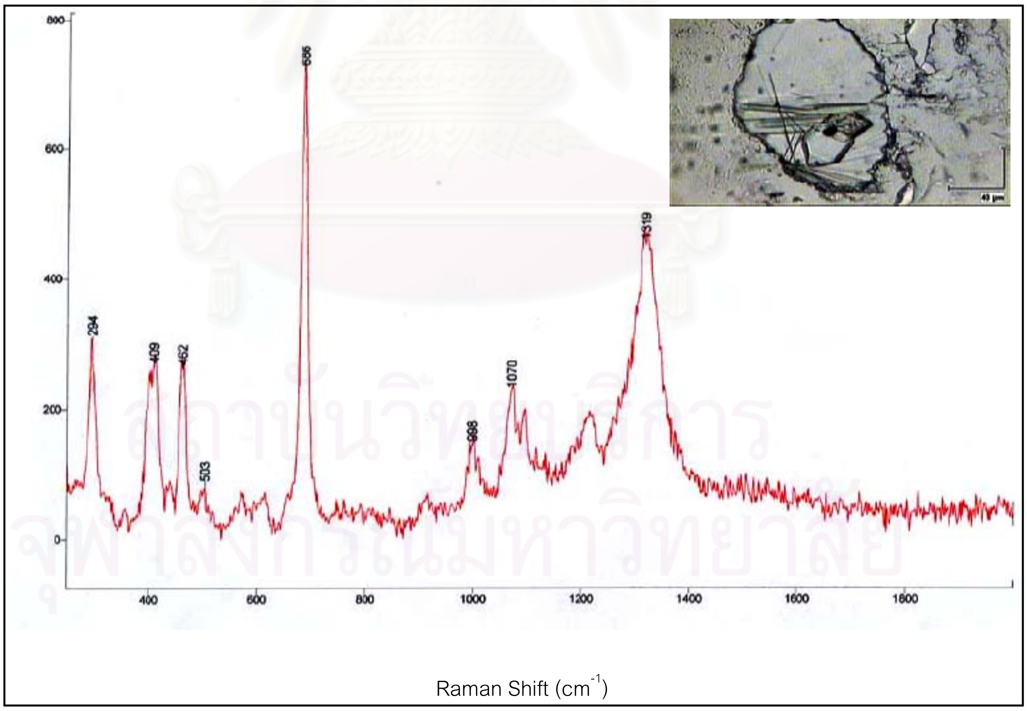

Figure 3.62: Raman spectra of sample ZA23 showing a combination of hematite (peaks at 294, 409, 503, 1070 and 1319 cm^{-1}) and quartz (peaks at 462 cm^{-1}) in a multi-phase inclusion.

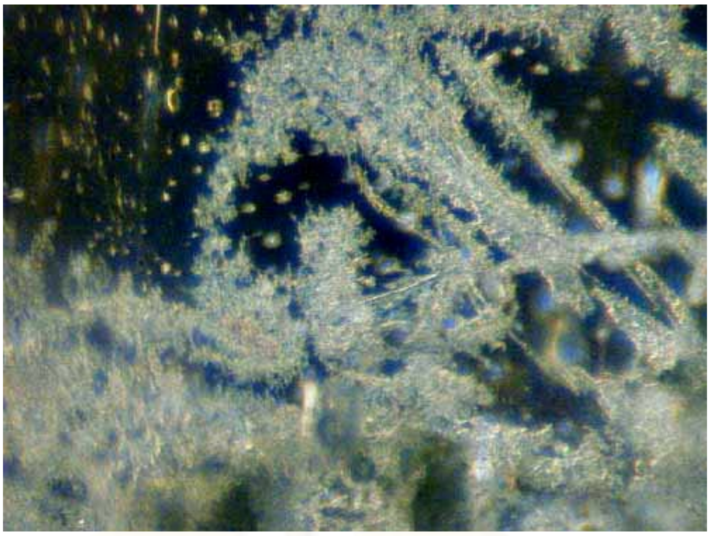

Figure 3.63: Unhealed fissures showing a frosted appearance (ZA22, 120x).

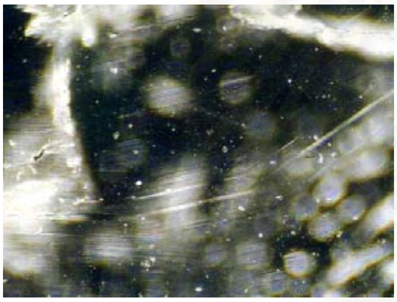

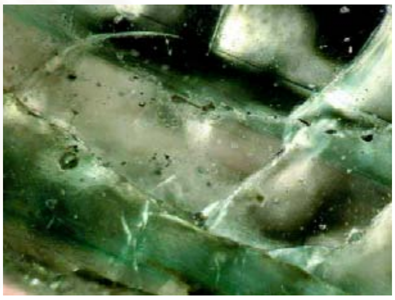

Figure 3.64: Strongly developed growth structures (ZA4, 70x) and coloured zoning parallel to the emerald's prism faces (ZA23, 70x).

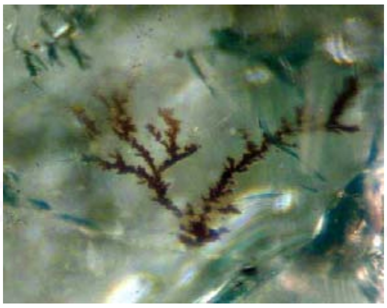

Figure 3.65: Unhealed fissures, partly with foreign material (ZA5, 100x).

Figure 3.66: Reflection from unhealed fissures showing mirror-like effect (ZA1, 70x).

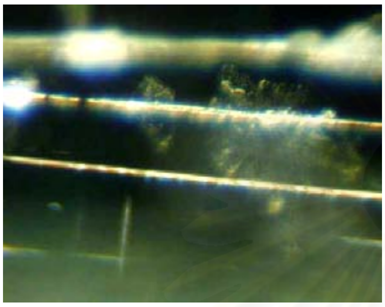

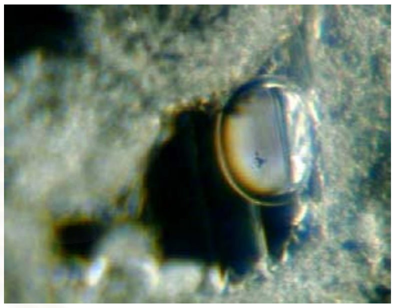

Figure 3.67: Growth tubes containing iron stain and fluids (left); (ZA29, 120x) and primary fluid inclusions (2-phase) showing a high relief gas bubble (right); (ZA29, 140x).

3.4.6 Canaiba-Socoto Deposits in Bahia State in Brazil:

The most common mineral inclusions found in 10 emerald samples from the Canaiba-Scototo deposits of Bahia State were brown irregular-shaped mica platelets and greenish-brown chlorite, which were randomly distributed in the emerald host crystals (see Figures 3.68 and 3.69). Raman spectra confirmed a mica inclusion of probably biotitic or phlogopitic composition (Figures 3.70) and a chlorite inclusion (Figure 3.71). Growth phenomena (internal growth lines and coloured zoning) can be observed by looking in the direction of c-axis (Figure 3.72). Iron stain and thin channel-like growth were found in some samples (Figure 3.73). Most of fluid inclusions are very small, that look-like 'dust-particles' and other 'dust-particles' form 'flake-like' agglomerations (Figure 3.74).

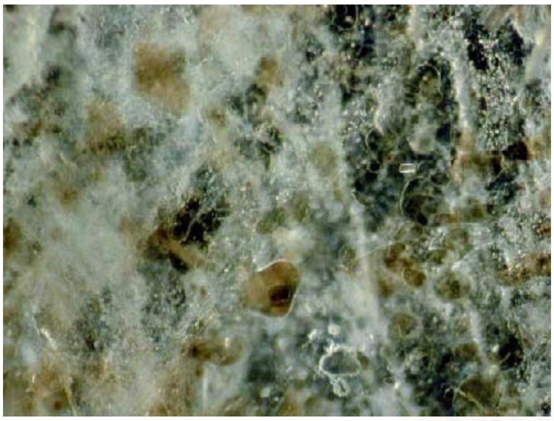

Figure 3.68: Numerous brown booklets and crystals of biotite inclusions (CAR6, 70x).

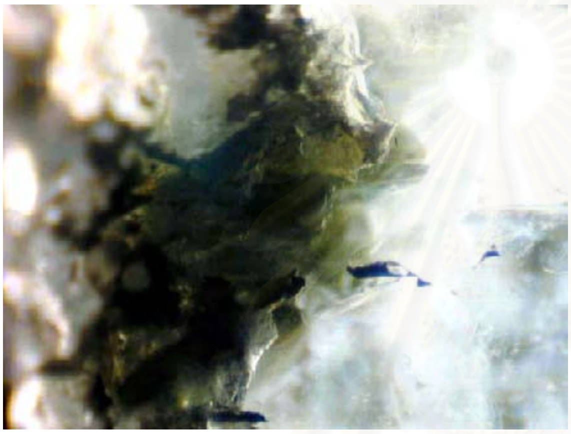

Figure 3.69: Typical chlorite inclusions showing irregularly shaped and greenish brown crystals (CAR8, 70x).

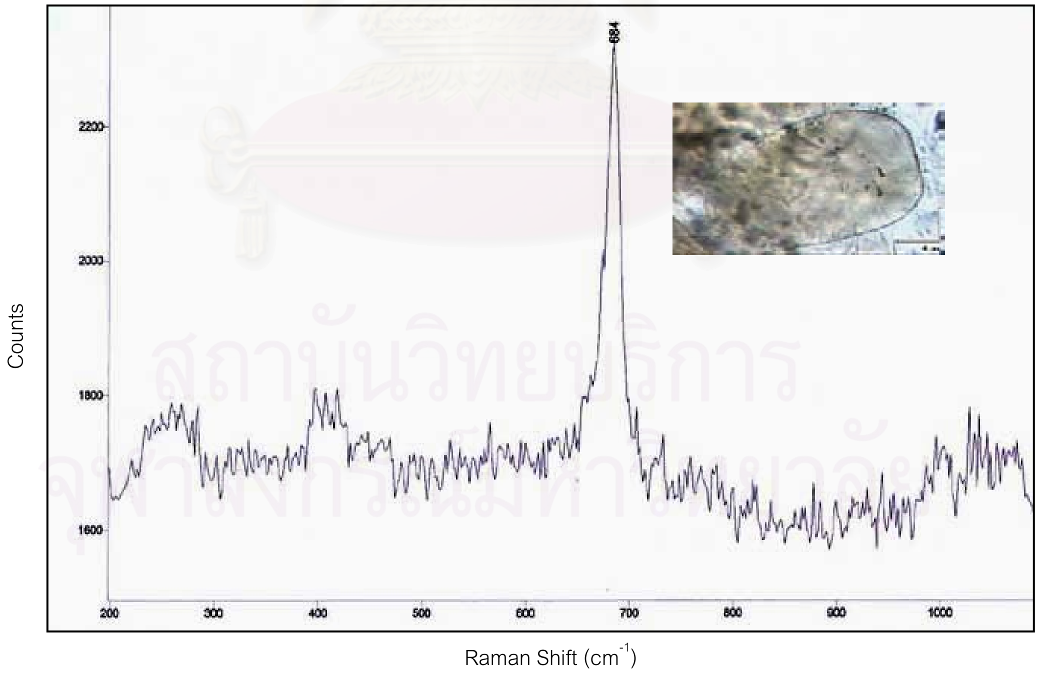

Figure 3.70: Raman spectrum of a biotite inclusion in a Brazilian emerald from the Caniaba-Socoto deposits (CAR6; biotite peaks at 406, 684 cm^{-1}).

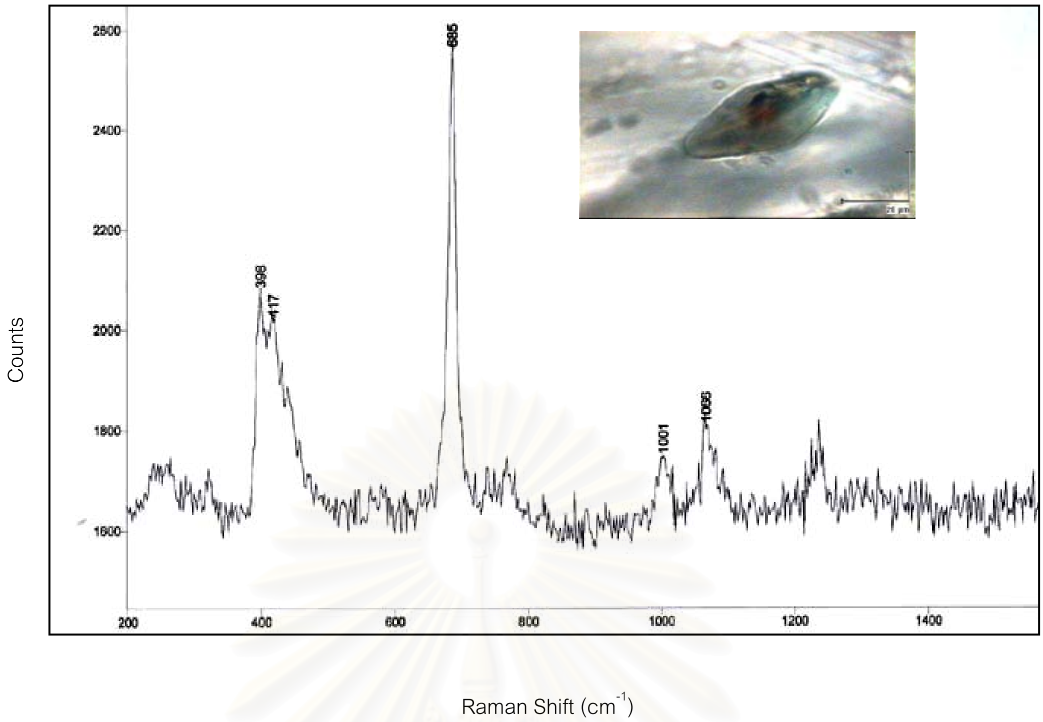

Figure 3.71: Raman spectrum of a chlorite inclusion associated with the biotite inclusion in a Brazilian emerald from Caniaba-Socoto deposits (CAR10; chlorite peaks at 398, 685,1011 and 1088 cm^{-1}).

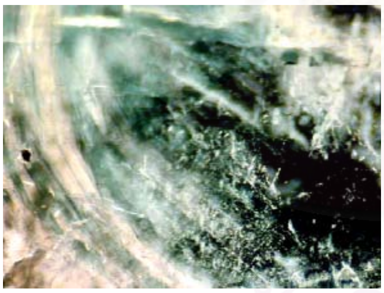

Figure 3.72: Well developed growth structures and coloured zoning (parallel to the emerald's prism face) (CAR5, 60x.).

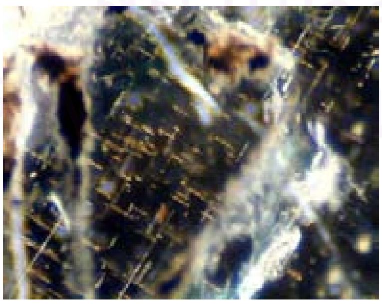

Figure 3.73: Small fluid inclusions look like 'dust-particles' and some of these healed with iron stain (CAR9, 70x).

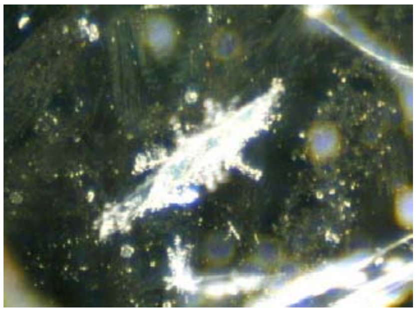

Figure 3.74: On the left, ‘particles’ showing sugar grain like’ structures (CAR4, 70x) and on the right healed fissures have a quite compact aspect, other ‘dust-particles’ form ‘flake-like’ agglomerations (CAR7, 70x).

3.4.7 Itabira deposits in Minas Gerais State of Brazil:

Under the optical microscope, most inclusions of 10 emerald samples from the Belmont mine at Itabira deposit of Minas Gerais state are biotite micas, on one hand, exhibit deep brown colour and thick translucent to opaque platelets (Figure 3.75). Mica inclusions, on the other hand, are usually strongly round and Raman spectra of these mica inclusions (biotite and phlogopite) are shown in Figure 3.76. Quartz inclusions were found as Isolated, colourless-transparent and irregularly-shaped crystals with weak relief as shown in Figure 3.77 together with its Raman spectrum. A peak of carbon dioxide, within negative crystal is shown by Raman spectra (figure 3.78). There are numerous primary fluid inclusions in the form of growth tubes. These fluid inclusions are partly associated with quartz crystals dispersed over fissure planes (Figure 3.79). Two and three phase fluid inclusions were commonly found in short barrel-shaped primary negative crystals (Figure 3.80). In general, tiny growth tubes (primary cavities/fluid inclusions) and very small fluid inclusions can be observed in some samples (Figure 3.81).

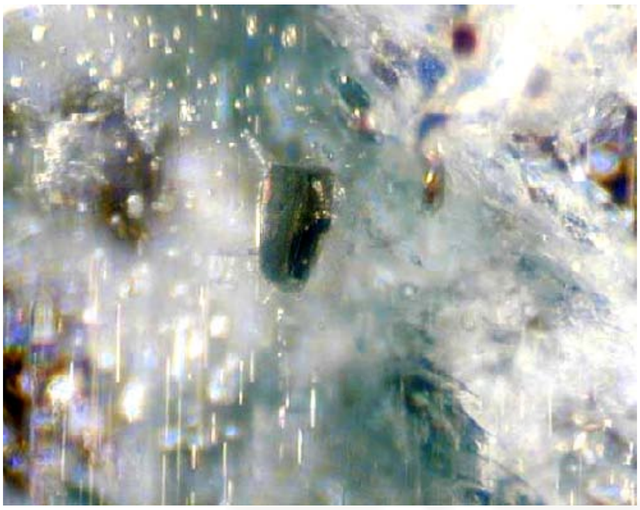

Figure 3.75: High relief dark brown biotite inclusions which are randomly distributed in the host crystal (ITA10, 60x).

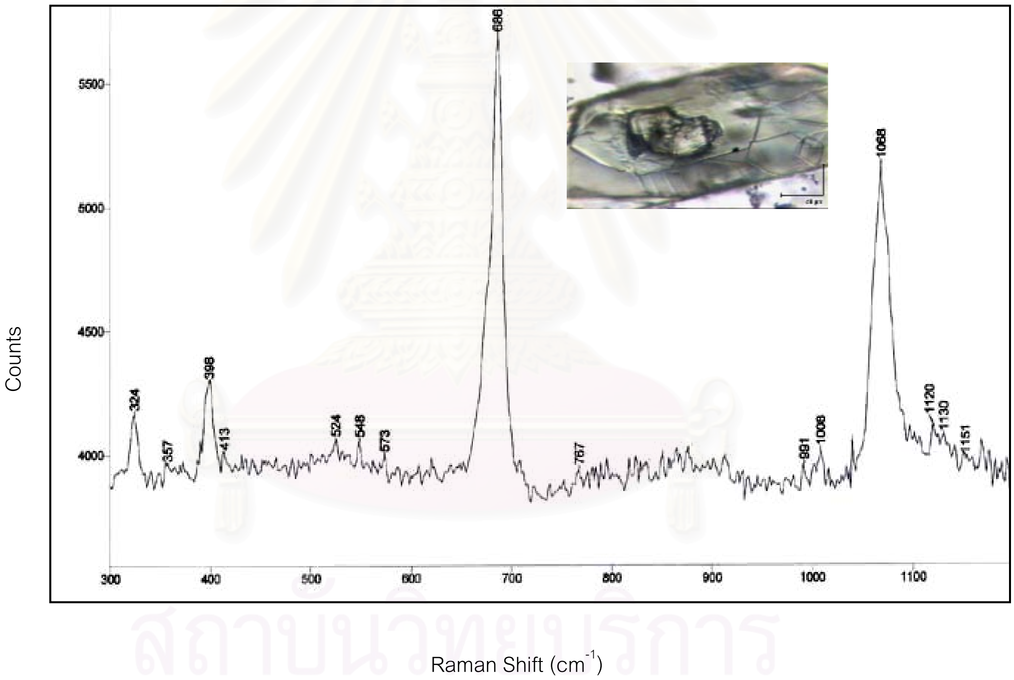

Figure 3.76: Raman spectrum of transparent flakes of micas may be biotite/phlogopite inclusions in Brazilian emerald from Itabira (ITA1; peaks at 357, 688, 413, 548, 787 and 1088 cm^{-1}).

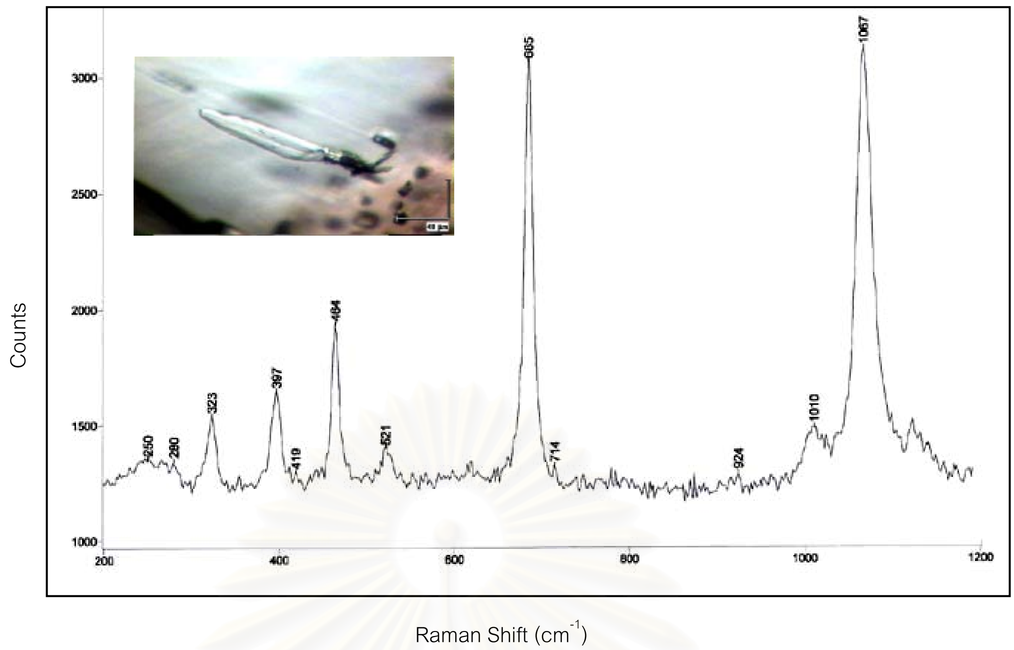

Figure 3.77: Raman spectrum of a colourless-transparent irregularly-shaped quartz inclusion (ITA10; peaks at 464 cm^{-1}).

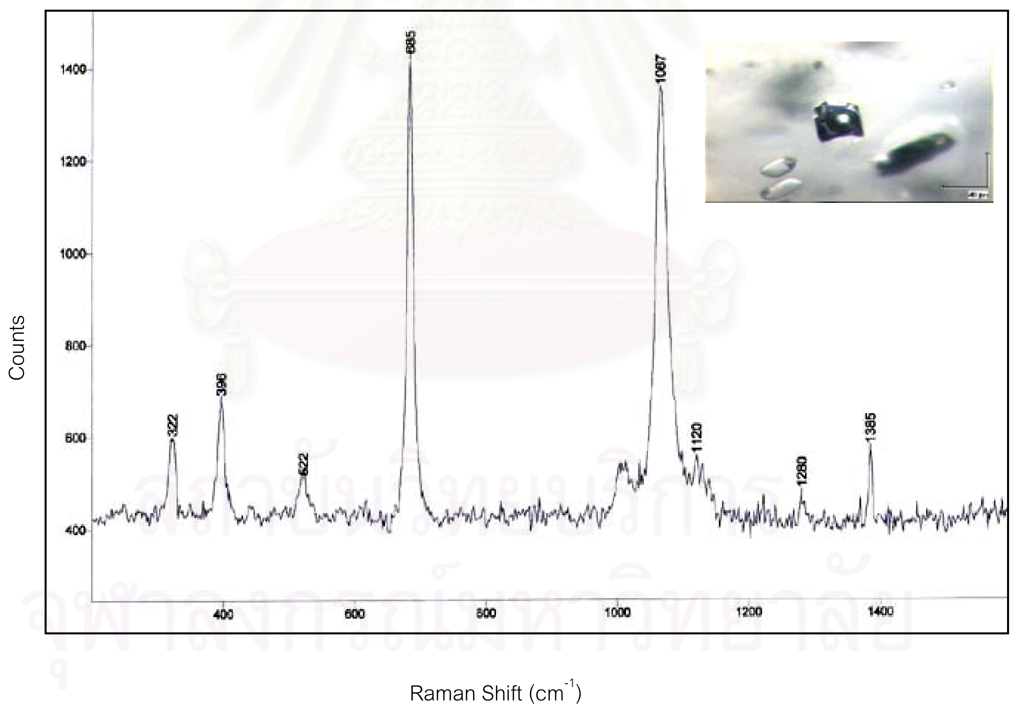

Figure 3.78: Raman spectrum of carbon dioxide within the negative crystal inclusions (ITA8; peaks at 1280 and 1385 cm^{-1}).

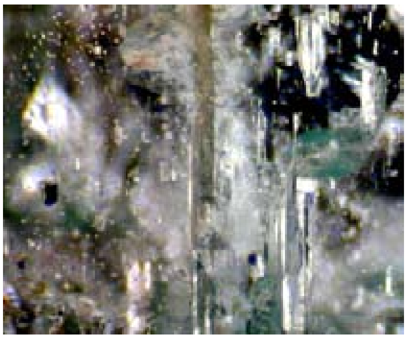

Figure 3.79: Elongated Growth tubes filled with fluids and the associated quartz inclusions (ITA3, 70x).

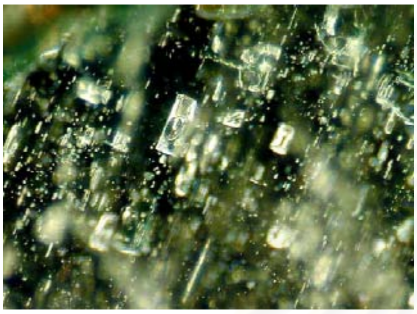

Figure 3.80: Barrel-shaped fluid inclusions (ITA1, 70x).

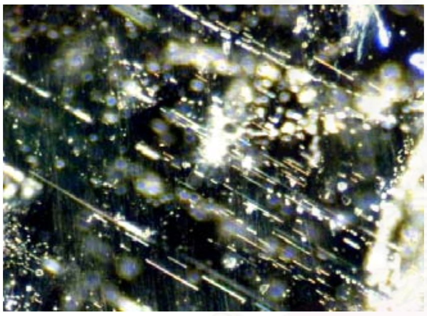

Figure 3.81: On the left; tiny growth tubes filled with fluids (ITA9, 70x) and on the right; some fluid inclusions having 'dust-like' appearance (ITA7, 70x).

CHAPTER IV

CHEMICAL ANALYSIS

4.1 Introduction

The major components of a natural beryl are BeO, Al_2O_3 and SiO_2 which are normally accompanied by minor alkali elements such as Na, Mg, Cs,… (Bosshart, 1991). Other important chromophoric elements are Cr, V, Fe. In addition, water molecules are commonly found in channels of ring of cyclosilicate structure of emerald (see Figure 3.3)

The ideal formula of a beryl is $Be_3Al_2Si_6O_{18}$, in which alkali, water and other trace elements can substitute into emerald/beryl lattice or structural channels, as follows (Feklichev et al., 1963 in (a) and Schaller et al., 1962 in (b) cited in Sinkankas, 1989):

a) $Be_3Al_2Si_6O_{18} \longrightarrow R_1^{+}\ {-}_nR^{2+}{}_nBe_{2.51/2n}\ Al_2Si_6O_{18}$

where: $R^{+} = Cs^{+}, Li^{+}, Rb^{+}, Na^{+}, K^{+}$

where: $R^{2+} = Ca^{2+}, Ba^{2+}, Sr^{2+}$; and n = 0,1

b) $Be_3Al_2Si_6O_{18} \longrightarrow Be_3R^{3+}\ Si_6O_{18}$

where: $R^{3+} = Al^{3+}, Fe^{3+}, Cr^{3+}, Sc^{3+}$

The fact that many cations can substitute into the emerald structure, it is expected that emeralds from different geological environments should contain different amounts of trace elements in their structures. Hence trace element contents should be applicable as a chemical fingerprint of emeralds from various geologic occurrences. It is therefore the aim of this study to look into the trace element concentration of emeralds from various locations.

4.2 Samples and Procedure

In this study, the chemical analysis of emerald was carried out by a Laser ablation Inductively Coupled Plasma Mass Spectrometry (LA-ICP-MS). This technique is suitable for analysis of trace elements in particular the light elements such as Li, Be, B, Na, Mg, despite the fact that it is a “destructive” technique.

The LA-ICP-MS unit at the Macquarie University in Australia was used in this study (Figure 4.1). Detailed descriptions of LA-ICP-MS instrumentation analytical and calibration procedures are similar to those given by Norman et al. (1996). The UV laser ablation microprobe (a New Wave Research 213 nm Nb:YAG) is coupled to an Agilent 7500S ICP-MS. All analyses were done with a pulse rate of 5 Hz and a beam energy of approximately 0.5 mJ per pulse, producing a spatial resolution 50 micrometers. The beam is used to vaporize an extremely small sample of material (in this case, emerald). The ablated sample is carried by a stream of inert gas, usually argon, into a high-temperature field, causing dissociation of molecules and ionization of atoms.

The MS identifies and quantifies elements in terms of mass and charge. Some 41 elements and their relative amounts can be detected even when present in only a few parts per billion.Quantitative results for 16 trace elements (Li, Be, B, Na, Mg, Al, Sr, P, K, Ca, Ti, V, Cr, Mn, Fe and Cs of the emerald samples) were obtained through calibration of relative element sensitivities using the NIST-610 multi-element glass standard and an emerald with 12.5 wt% BeO as internal standards. The BCR2G basaltic glass standard was also used as an external standard. The detection limits vary from analysis to analysis and are typically less than 1 ppm for Li, Be, V and Cs; less than 4 ppm for Mg, Al, Ti, Mn and Cr; less than 13 ppm for B and Na; less than 80 ppm for P and Fe; less than 300 ppm for Si and K and less than 500 ppm for Ca.

In this study a total of 23 emerald samples from 7 different geological occurrences (2-4 representative samples from each locality) were selected for chemical analysis. In each sample at least 5 spots were analyzed across the polished surface normally cut perpendicular to c axis. The detailed positions of the spots analyzed are presented in Figures 4.2 to 4.8.

Figure 4.1: Laser ablation Inductively Coupled Plasma Mass Spectrometry Laser Ablation (LA-ICPMS) unit at Macquarie University, Australia used for chemical analysis in this study.

The representative laser points of 23 samples from different geological occurrences in below:

NI 1

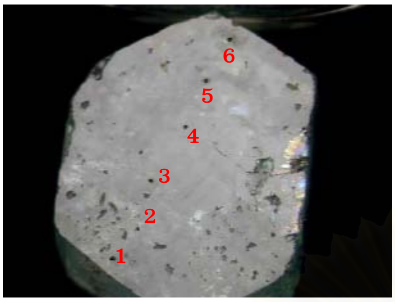

NI 11

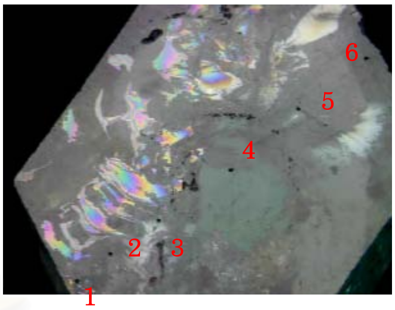

NI 16

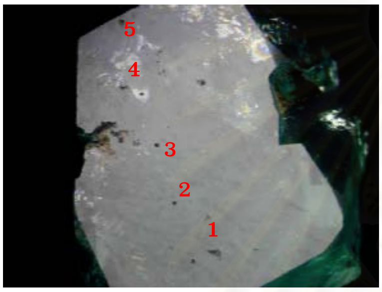

NI 27

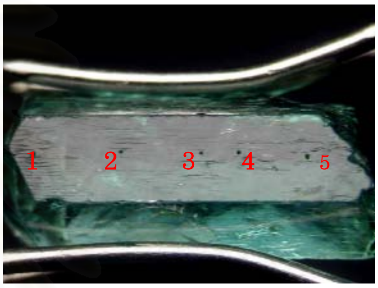

Figure 4.2: Showing the 4 samples of emerald from Kaduna Plateau, Nigeria.

CO 1

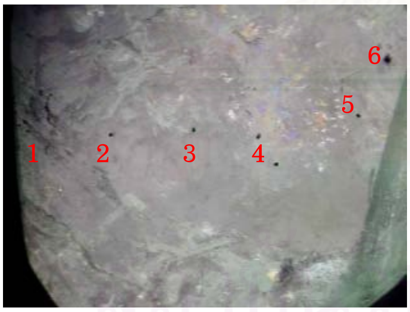

CO 11

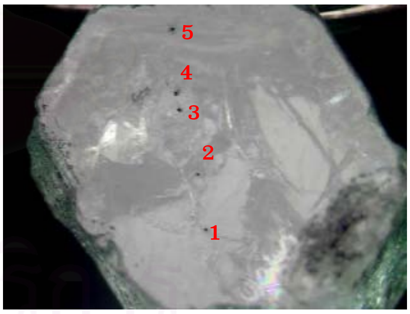

CO 18

CO 22

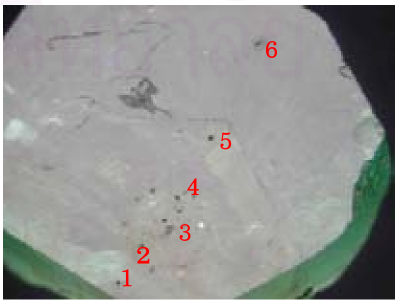

Figure 4.3: Showing the 4 samples of emerald from Cordillera Oriental, Colombia.

STA 1

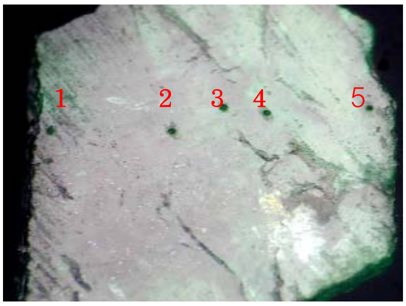

STA 3

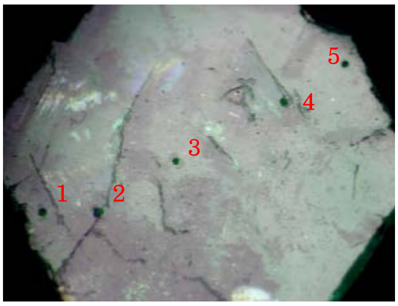

STA 8

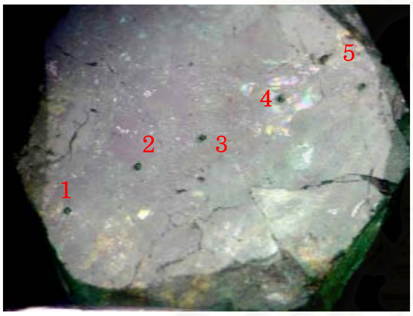

Figure 4.4: Showing the 3 samples of emerald from Santa Terezinha de Goais, Brazil.

MA 4

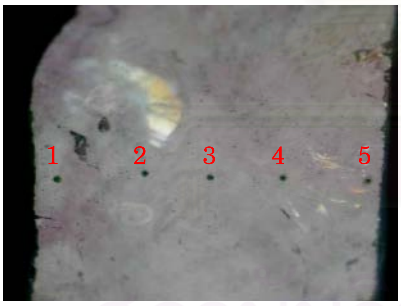

MA 7

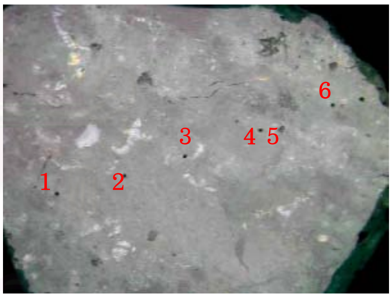

MA 8

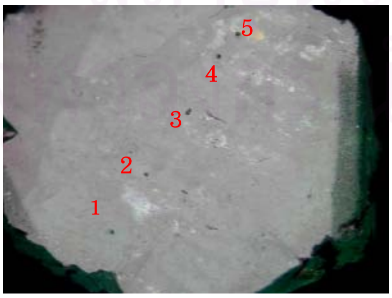

MA 18

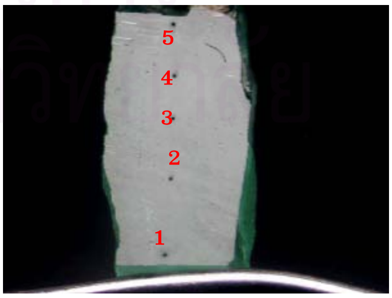

Figure 4.5: Showing the 4 samples of emerald from Mananjary region, Madagascar.

ZA 5

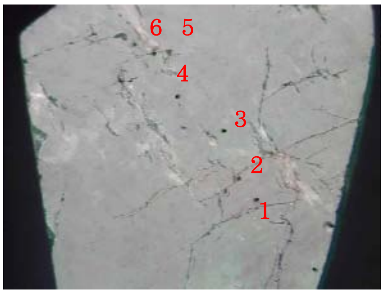

ZA 6

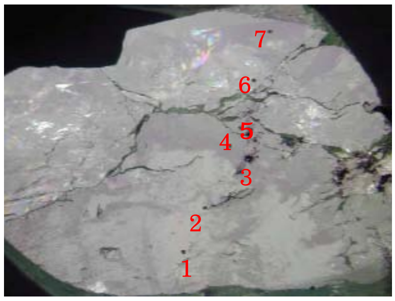

ZA 23

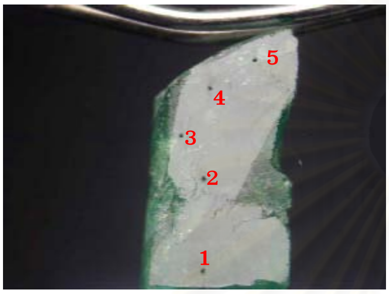

ZA 25

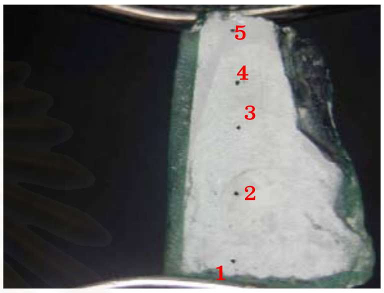

Figure 4.6: Showing the 4 samples of emerald from Ndola Rural district, Zambia.

CAR 4

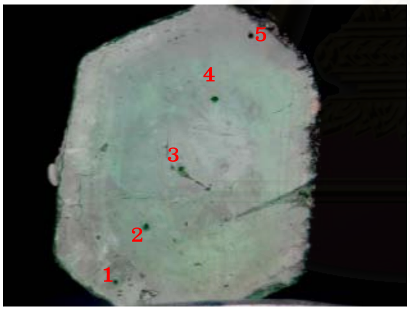

CAR 7

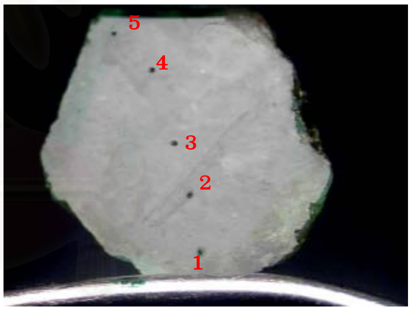

Figure 4.7: Showing the 2 samples of emerald from Carnaiba/Socoto, Bahia State, Brazil.

ITA 2

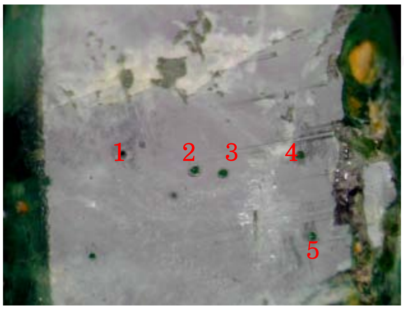

ITA 10

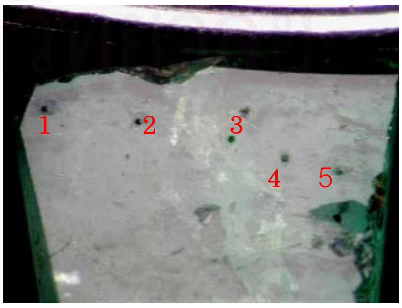

Figure 4.8: Showing the 2 samples of emerald from Itabira, Minas Gerias state in Brazil.

4.3 Results

The average concentrations of 16 trace elements; Li, Be, B, Na, Mg, Al, Si, P, K, Ca, Ti, V, Cr, Mn, Fe and Cs of each emerald sample analyzed in this study after recalculation into atom mole ppm are listed in Tables 4.1 to 4.3. The analytical concentrations in ppm by weight of original data, the plot of averages ($\overline{X}$) and standard deviation (STD) are shown in Appendix IV

From the chemical data shown Tables 4.1 to 4.3, the elements of emeralds from this study are mainly as alkalis and iron. Amount of these elements are characteristic, which related to geological environments.

4.4 Cross plots

Cross plots of Na versus Fe (or Na vs Fe), Na vs Li, Na vs Mg, Na vs Cs, Na vs Ti, Na vs B, Na vs (Mg+Fe), Li vs K, Li vs Fe, Li vs Cs and Al vs sum of all monovalent+divalent+trivalent ions contents of all the emeralds in this study are shown in Figures 4.9 to 4.19. The majority of the plots include alkali elements because of the fact that they are the major trace elements which have the strongest influence on the optical, physical and chemical properties of emeralds.

A good correlation between Na and Mg is seen in Figures 4.11 and between Na and (Mg+Fe) in Figure 4.15 regardless of localities. The remaining cross plots seem to show no correlation of other pair of elements. With regard to Figures 4.11 and 4.15, the contents of Na and Mg and probably Fe are highest in emeralds from Santa Terezinha, relatively high to moderate in those from Madagascar, Zambia, Carnaiba/Socoto and Itabira, relatively low in those from Colombia and lowest in those from Nigeria.

The emeralds from Zambia and Carnaiba/Socoto contain relatively high contents of Li and Cs (Figure 4.18). The emeralds from Madagascar show exceptionally high K content (Figure 4.16). The Colombian emeralds show consistently low iron content (Figures 4.9 and 4.17). These unusual high or low contents of Li, Cs, K and Fe contents may be used as locality specific criteria for those emeralds.

The emeralds from Brazil, Madagascar and Zambia (Type II deposits) show relatively moderate to high values of Na, Mg, Li and Cs (alkali elements) and Fe (as well as the total foreign elements) as compared with those of emeralds from Nigeria and Colombia (Type I deposits) (Figure 4.19). The highest contents of foreign elements can be found in the Santa Terezinha emerald from Goias State of Brazil (Type IIa) whereas the lowest contents are in Kaduna Plateau of Nigeria (Type Ia) (Figure 4.19).

Table 4.1: Chemical data of 16 trace elements of Nigerian emeralds (NI), and Colombian emeralds (CO) show atom mole ppm 16 major and trace elements.

Cation (atom mole ppm)	Nigeria (Kaduna Plateau)				Colombia (Cordillera Oriental)			
	NI 1	NI 11	NI 16	NI 27	CO 1	CO 11	CO 18	CO 22
Li	174.38	129.03	118.70	110.39	420.19	174.86	86.24	71.56
Be	102944.42	86637.46	86420.81	102404.53	99083.28	95835.41	97121.61	98043.19
B	40.87	35.06	46.93	46.40	42.90	55.15	62.00	55.90
Na	700.57	957.51	1032.32	444.05	3198.94	1893.79	2411.65	2046.69
Mg	318.14	262.99	238.77	217.96	3096.22	1859.98	2538.37	2148.45
Al	61525.47	64903.11	64397.83	61605.85	70778.95	72223.64	71509.80	71244.78
Si	211173.05	223081.16	223696.21	212241.29	201870.96	206546.76	204782.83	204771.24
P	10.51	10.52	11.21	9.71	77.15	13.82	14.32	65.92
K	84.54	39.00	97.90	70.85	27.93	54.92	118.62	113.73
Ca	61.84	51.64	67.47	79.19	126.47	150.56	140.36	113.20
Ti	3.60	7.22	5.48	1.90	2.54	1.10	1.00	0.83
V	145.26	165.05	159.88	108.04	90.64	50.88	49.24	137.27
Cr	105.49	88.90	115.23	121.48	28.75	27.69	27.32	112.07
Mn	2.39	2.97	5.70	1.78	0.49	0.54	0.51	1.23
Fe	1674.49	2591.87	2516.78	1472.44	152.99	54.42	70.24	72.67
Cs	0.06	0.09	24.02	16.02	1.62	1.09	1.00	1.28
Total atom mole %	**37.90**	**37.90**	**37.90**	**37.90**	**37.90**	**37.89**	**37.89**	**37.90**

Table 4.2: Chemical data of 16 trace elements of emeralds from Santa Terezinha (STA; Brazil) and Madagascar (MA) show atom mole ppm 16 major and trace elements.

Cation (atom mole ppm)	Brazil (Santa Terezinha)			Madagascar (Mananjary)			
	STA 1	STA 3	STA 8	MA 4	MA 7	MA 8	MA 18
Li	361.17	382.93	498.33	283.32	216.36	193.46	132.98
Be	95938.26	95213.29	96584.19	97419.18	99566.39	96865.60	99501.36
B	31.51	32.23	27.67	43.57	30.66	44.37	43.45
Na	12395.65	12048.93	12134.87	11737.03	8795.89	9006.50	9809.61
Mg	11396.61	11445.15	11613.44	11621.37	9593.88	9309.79	9707.25
Al	53464.63	53359.60	52854.39	49331.88	51076.70	50975.58	51060.39
Si	201007.10	201268.48	199574.99	204602.02	204334.76	206903.82	204963.37
P	40.96	62.75	44.46	14.12	10.61	9.23	10.48
K	172.04	166.71	193.87	1265.27	2962.34	2738.60	1270.28
Ca	44.28	50.16	140.37	159.65	118.27	129.17	88.51
Ti	1.83	2.81	6.78	2.05	2.51	2.54	2.33
V	134.90	139.76	116.57	20.23	17.35	25.88	19.96
Cr	1358.84	1810.83	1249.17	377.58	237.43	440.39	353.78
Mn	2.39	7.61	7.75	4.27	6.33	3.56	3.99
Fe	2587.58	2947.36	3866.50	2027.88	1985.30	2292.87	1972.50
Cs	62.26	61.40	86.64	35.48	12.17	18.71	16.50
Total atom mole %	**37.90**	**37.90**	**37.90**	**37.89**	**37.90**	**37.90**	**37.90**

Table 4.3: Chemical data of 16 trace elements of Zambian emeralds (ZA), and Brazilian emeralds from Carnaiba/Socoto (CAR) and Itabira (ITA) show atom mole ppm 16 major and trace elements.

Cations (atom mole ppm)	Zambia (Ndola Rural)				Brazil (Carnaiba/Socoto)		Brazil (Itabira)	
	ZA 5	ZA 6	ZA 23	ZA 25	CAR 4	CAR 7	ITA 2	ITA 10
Li	1514.17	751.11	848.70	1015.47	1049.89	1524.12	170.20	150.43
Be	87742.93	103036.66	99042.54	100880.81	97278.73	97170.22	96628.48	97011.45
B	35.85	31.07	43.53	39.44	40.69	40.82	35.74	30.19
Na	10211.18	5997.84	12034.73	11456.83	6537.02	4521.65	7793.51	7142.84
Mg	7887.79	3670.29	10033.31	8965.03	5757.24	3656.60	8265.43	7277.90
Al	54608.98	58180.92	48744.60	50686.17	64315.87	69233.37	62242.63	62203.61
Si	213278.52	205095.17	203645.75	202114.72	201515.61	201159.38	201960.21	202768.27
P	7.11	8.98	10.16	6.71	10.50	8.82	7.46	45.18
K	99.63	91.34	295.83	164.94	178.32	245.33	163.87	134.81
Ca	52.12	61.18	139.97	58.95	86.25	67.16	111.52	134.75
Ti	1.92	1.62	3.36	2.34	2.13	1.83	1.10	2.06
V	34.76	15.85	44.80	33.99	21.88	6.78	24.10	20.54
Cr	461.13	77.07	550.24	481.26	695.87	520.83	416.59	381.39
Mn	11.72	8.69	5.54	4.62	4.73	12.64	1.58	3.02
Fe	2886.09	1859.85	3440.19	2952.58	1267.13	696.27	1128.40	1682.50
Cs	130.33	79.10	72.28	105.81	204.93	101.55	9.33	11.07
Total atom mole %	37.90	37.90	37.90	37.90	37.90	37.90	37.90	37.90

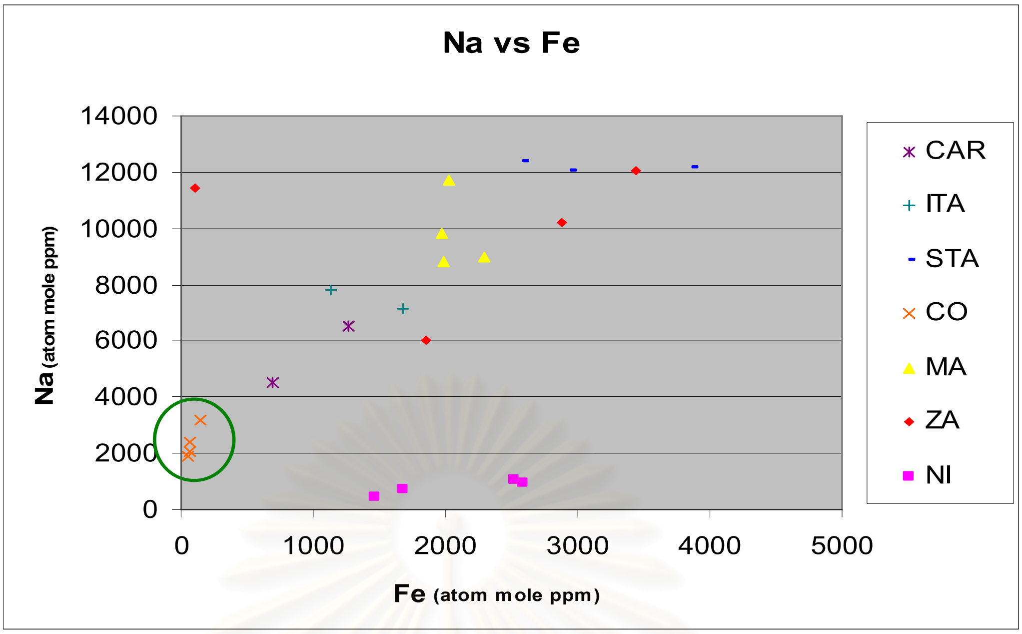

Figure 4.9: Plot of the average Na versus Fe contents of 23 emeralds from different geological occurrences show consistently low iron content in Colombian emerald.

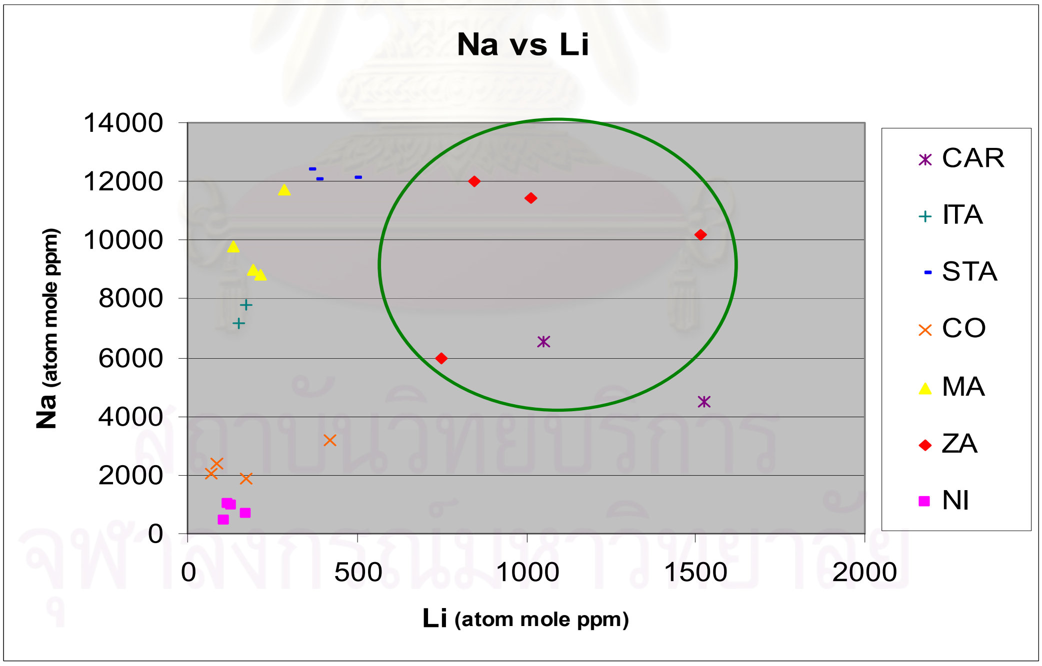

Figure 4.10: Plot of the average Na versus Li contents of 23 emeralds from different geological occurrences show moderate to high lithium content in Zambian emerald.

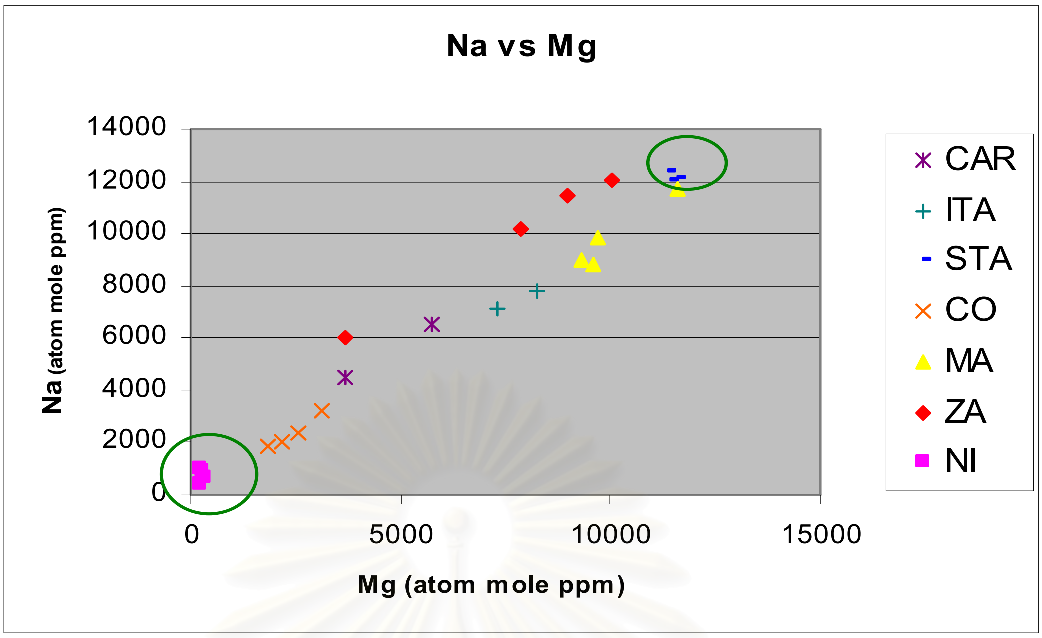

Figure 4.11: Plot of the average Na versus Mg contents of 23 emeralds from different geological occurrences showing the low sodium and magnesium (alkali) content in Nigerian emerald and the highest alkali content in Santa Terezinha from Brazil

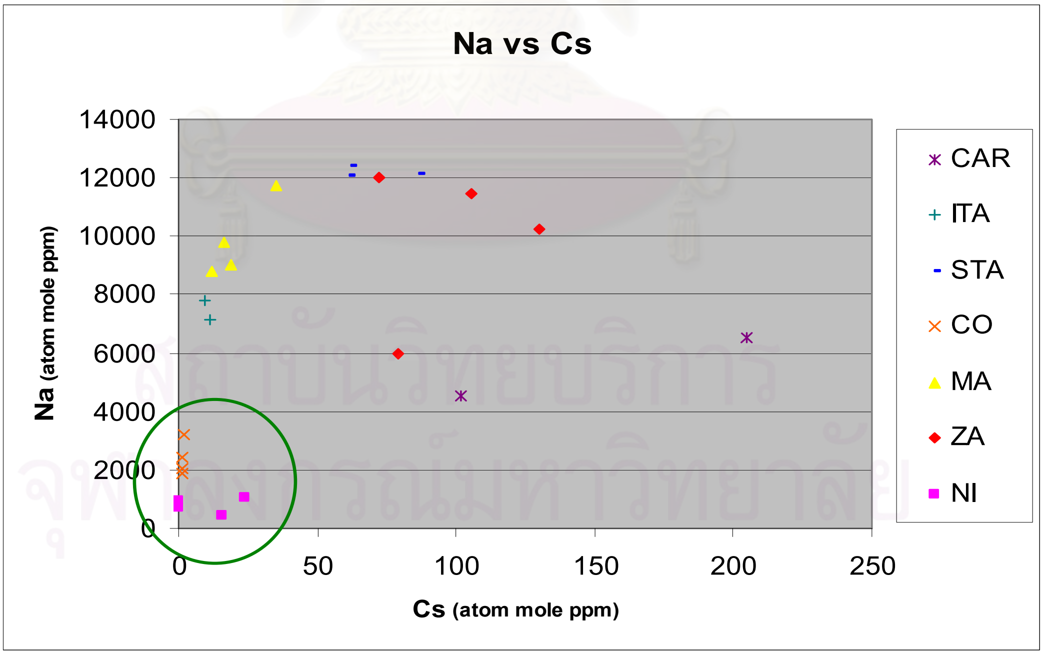

Figure 4.12: Plot of average Na versus Cs contents of 23 emeralds from different geological occurrences show low sodium and cesium content in emerald from Colombia and Nigeria.

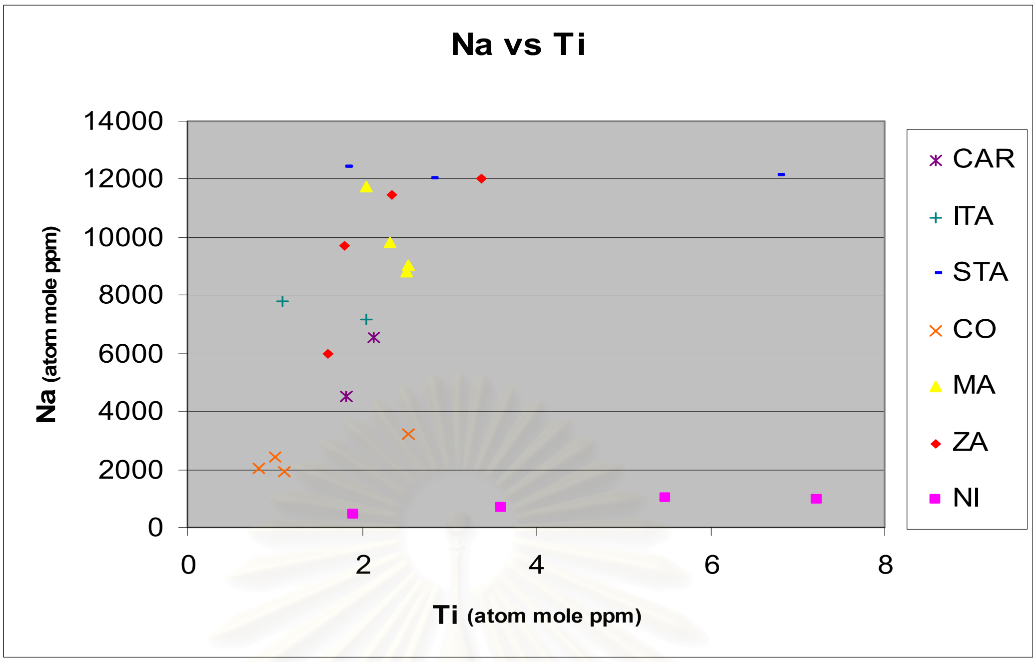

Figure 4.13: Plot of average Na versus Ti contents of 23 emeralds from different geological occurrences show no correlation of other pair of elements.

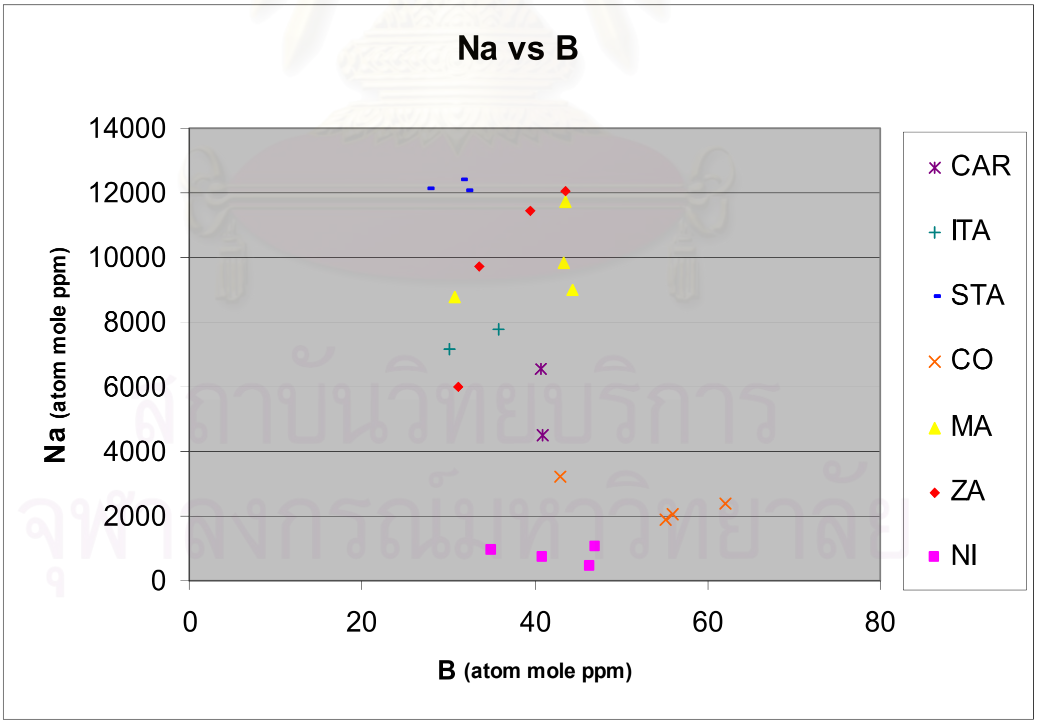

Figure 4.14: Plot of average Na versus B contents of 23 emeralds from different geological occurrences show no correlation of other pair of elements.

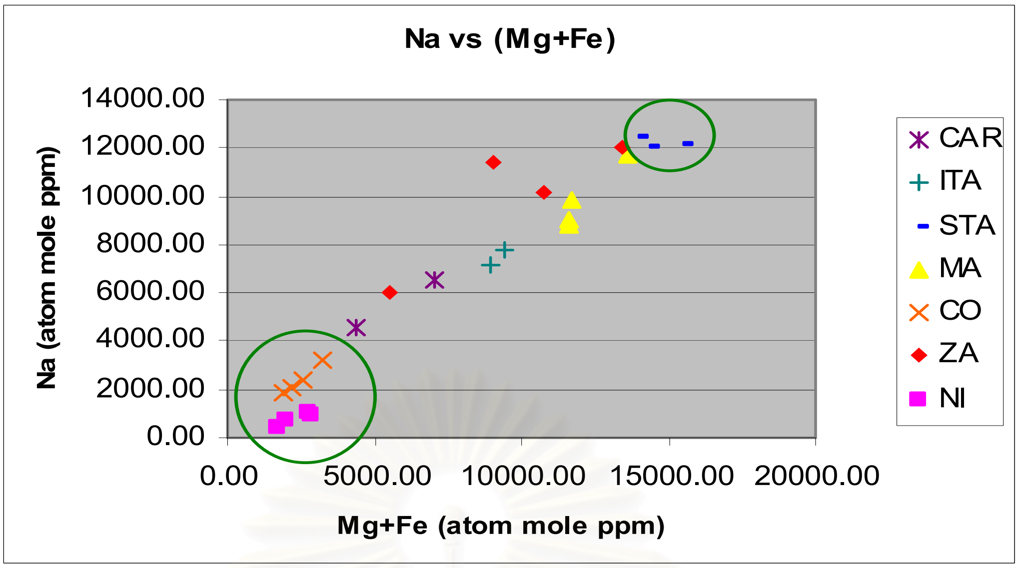

Figure 4.15: Plot of average Na versus (Mg+Fe) contents of 23 emeralds from different geological occurrences show low sodium and (magnesium plus iron) content in emerald from Nigeria and Colombia whereas consistently high these elements content in Santa Terezinha from Brazil.

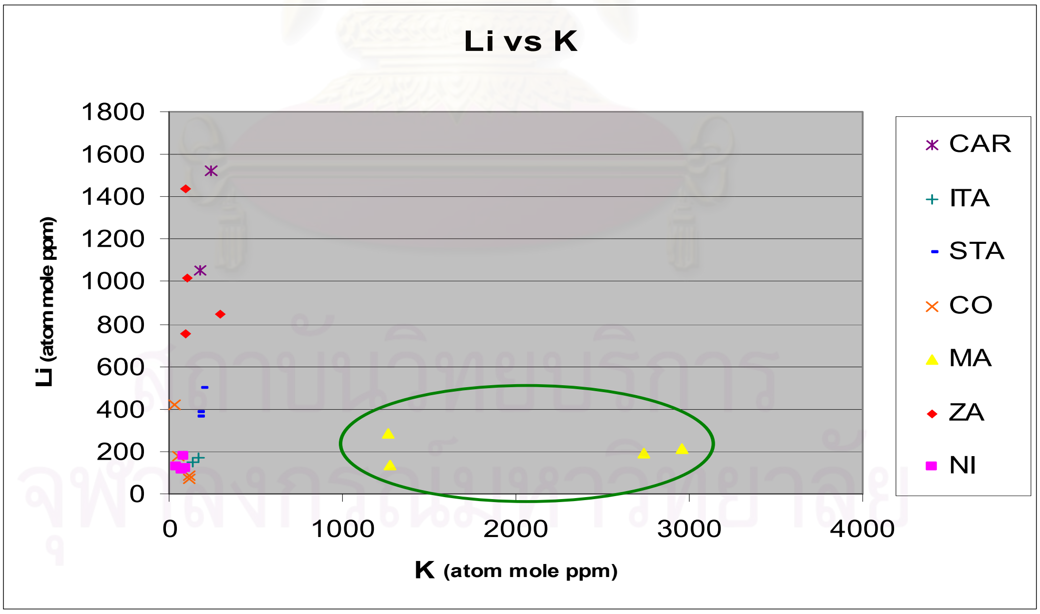

Figure 4.16: Plot of average Li versus K contents of 23 emeralds from different geological occurrences show consistently moderate to high potassium content in emerald from Madagascar.

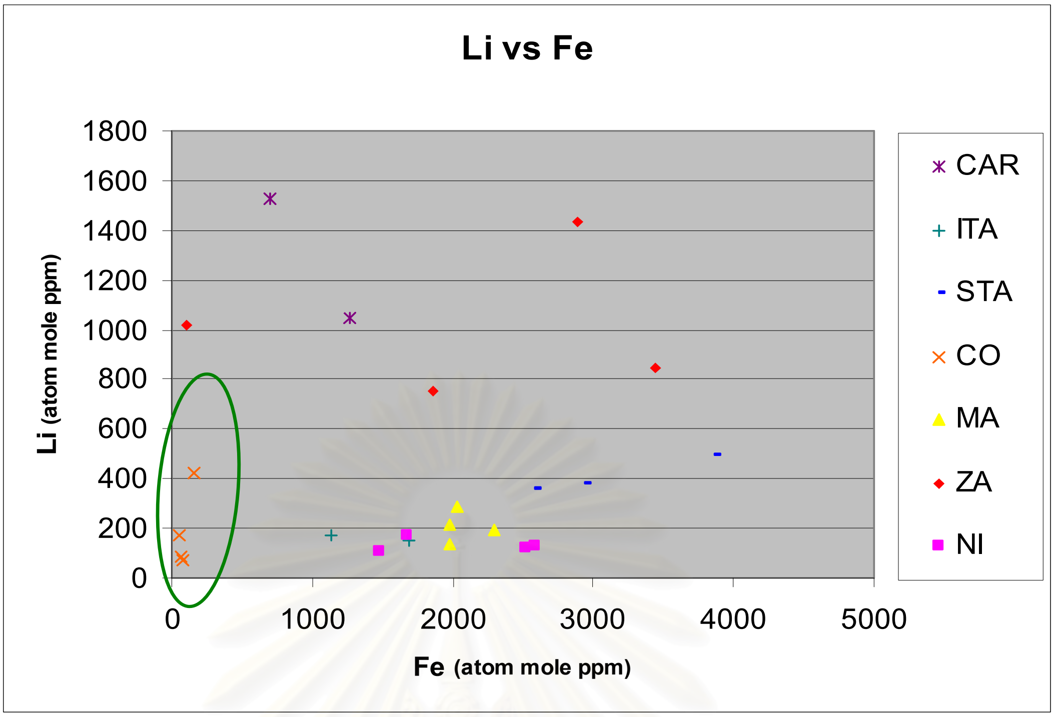

Figure 4.17: Plot of average Li versus Fe contents of 23 emeralds from different geological occurrences show consistently low iron content in Colombian emerald.

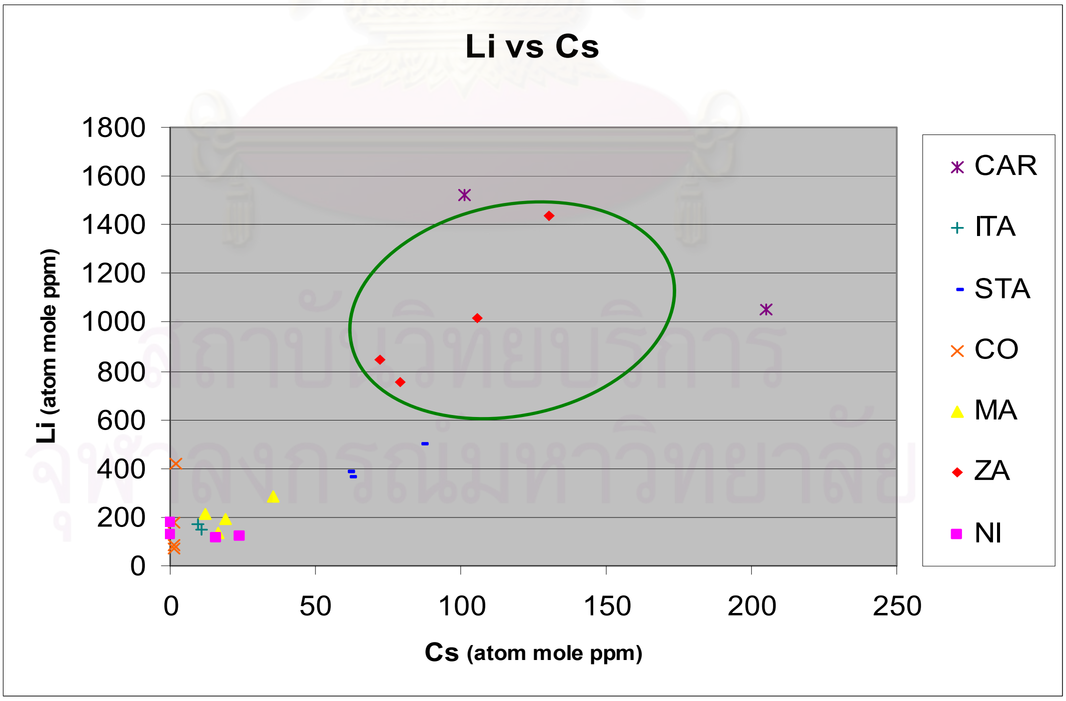

Figure 4.18: Plot of average Li versus Cs contents of 23 emeralds from different geological occurrences show moderate lithium and cesium content in Zambian emerald.

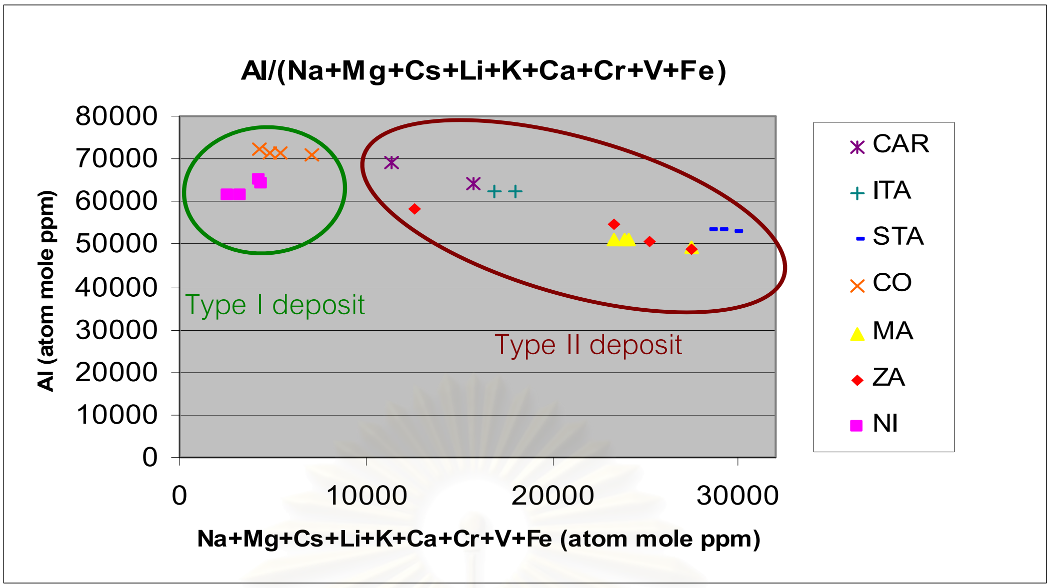

Figure 4.19: Plot of average Al versus sum of all Monovalent+Divalent+Trivalent ions contents from 7 different geological occurrences.

In most emeralds, the contents of sodium and magnesium are higher than the contents of chromophores, except those in Nigerian emeralds. Comparison of significant alkali elements (Na and Mg) and colouring elements (Cr, V and Fe) is shown below. Among those emeralds, the Colombian's contain lowest chromophoric elements because the Colombian emeralds have the lowest iron content (Figures 4.9 and 4.17).

	SUM(Na+Mg) (atom mole ppm)		SUM(Cr+V+Fe) (atom mole ppm)
Nigeria (NI):	1043.07	$<$	2316.23
Colombia (CO):	4798.52	$>$	218.54
Santa Terezinha (STA):	23678.22	$>$	4190.93
Madagascar (MA):	19895.33	$>$	2442.79
Zambia (ZA):	17564.25	$>$	3209.45
Carnaiba/Socoto (CAR):	10236.26	$>$	775.92
Itabira (ITA):	15239.84	$>$	1826.75

CHAPTER IV

CHEMICAL ANALYSIS

4.1 Introduction

The major components of a natural beryl are BeO, Al_2O_3 and SiO_2 which are normally accompanied by minor alkali elements such as Na, Mg, Cs,… (Bosshart, 1991). Other important chromophoric elements are Cr, V, Fe. In addition, water molecules are commonly found in channels of ring of cyclosilicate structure of emerald (see Figure 3.3)

The ideal formula of a beryl is $Be_3Al_2Si_6O_{18}$, in which alkali, water and other trace elements can substitute into emerald/beryl lattice or structural channels, as follows (Feklichev et al., 1963 in (a) and Schaller et al., 1962 in (b) cited in Sinkankas, 1989):

a) $$Be_3Al_2Si_6O_{18} \longrightarrow R^{+}_{1-n}R^{2+}_{n}Be_{2.51/2n}\,Al_2Si_6O_{18}$$

where: $R^{+} = Cs^{+}, Li^{+}, Rb^{+}, Na^{+}, K^{+}$

where: $R^{2+} = Ca^{2+}, Ba^{2+}, Sr^{2+}$; and n = 0,1

b) $$Be_3Al_2Si_6O_{18} \longrightarrow Be_3R^{3+}\,Si_6O_{18}$$

where: $R^{3+} = Al^{3+}, Fe^{3+}, Cr^{3+}, Sc^{3+}$

The fact that many cations can substitute into the emerald structure, it is expected that emeralds from different geological environments should contain different amounts of trace elements in their structures. Hence trace element contents should be applicable as a chemical fingerprint of emeralds from various geologic occurrences. It is therefore the aim of this study to look into the trace element concentration of emeralds from various locations.

4.2 Samples and Procedure

In this study, the chemical analysis of emerald was carried out by a Laser ablation Inductively Coupled Plasma Mass Spectrometry (LA-ICP-MS). This technique is suitable for analysis of trace elements in particular the light elements such as Li, Be, B, Na, Mg, despite the fact that it is a “destructive” technique.

The LA-ICP-MS unit at the Macquarie University in Australia was used in this study (Figure 4.1). Detailed descriptions of LA-ICP-MS instrumentation analytical and calibration procedures are similar to those given by Norman et al. (1996). The UV laser ablation microprobe (a New Wave Research 213 nm Nb:YAG) is coupled to an Agilent 7500S ICP-MS. All analyses were done with a pulse rate of 5 Hz and a beam energy of approximately 0.5 mJ per pulse, producing a spatial resolution 50 micrometers. The beam is used to vaporize an extremely small sample of material (in this case, emerald). The ablated sample is carried by a stream of inert gas, usually argon, into a high-temperature field, causing dissociation of molecules and ionization of atoms.

The MS identifies and quantifies elements in terms of mass and charge. Some 41 elements and their relative amounts can be detected even when present in only a few parts per billion.Quantitative results for 16 trace elements (Li, Be, B, Na, Mg, Al, Sr, P, K, Ca, Ti, V, Cr, Mn, Fe and Cs of the emerald samples) were obtained through calibration of relative element sensitivities using the NIST-610 multi-element glass standard and an emerald with 12.5 wt% BeO as internal standards. The BCR2G basaltic glass standard was also used as an external standard. The detection limits vary from analysis to analysis and are typically less than 1 ppm for Li, Be, V and Cs; less than 4 ppm for Mg, Al, Ti, Mn and Cr; less than 13 ppm for B and Na; less than 80 ppm for P and Fe; less than 300 ppm for Si and K and less than 500 ppm for Ca.

In this study a total of 23 emerald samples from 7 different geological occurrences (2-4 representative samples from each locality) were selected for chemical analysis. In each sample at least 5 spots were analyzed across the polished surface normally cut perpendicular to c axis. The detailed positions of the spots analyzed are presented in Figures 4.2 to 4.8.

Figure 4.1: Laser ablation Inductively Coupled Plasma Mass Spectrometry Laser Ablation (LA-ICPMS) unit at Macquarie University, Australia used for chemical analysis in this study.

The representative laser points of 23 samples from different geological occurrences in below:

NI 1

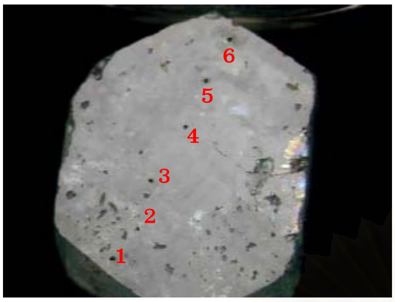

NI 11

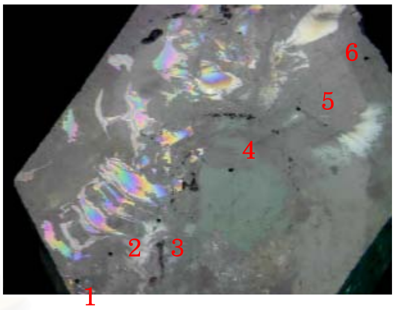

NI 16

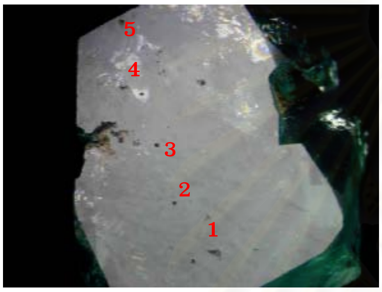

NI 27

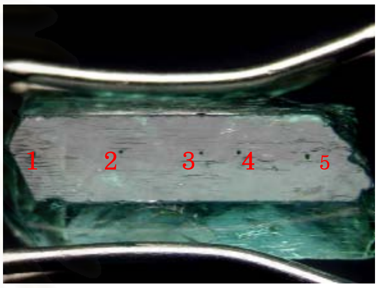

Figure 4.2: Showing the 4 samples of emerald from Kaduna Plateau, Nigeria.

CO 1

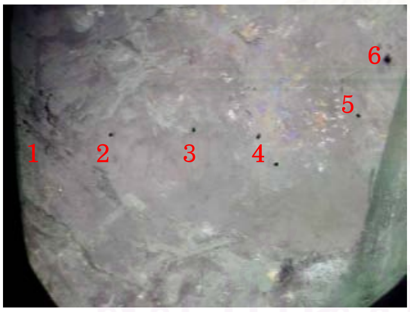

CO 11

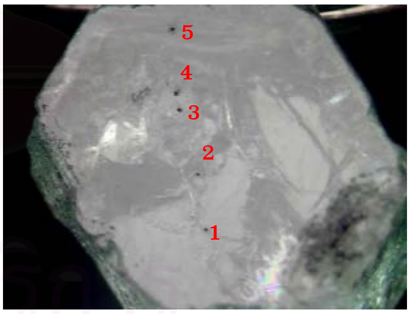

CO 18

CO 22

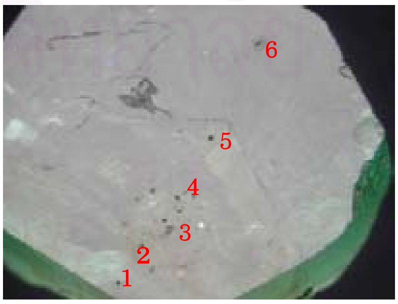

Figure 4.3: Showing the 4 samples of emerald from Cordillera Oriental, Colombia.

STA 1

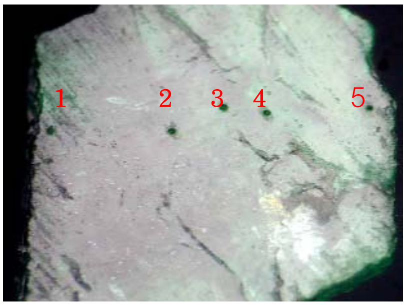

STA 3

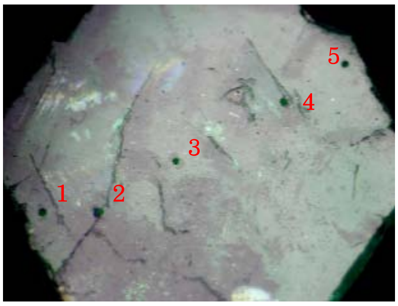

STA 8

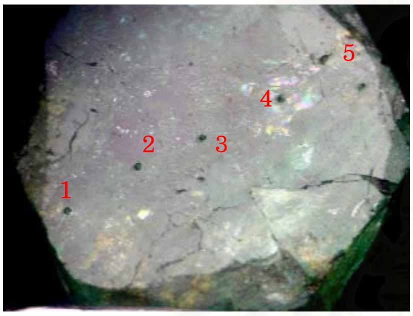

Figure 4.4: Showing the 3 samples of emerald from Santa Terezinha de Goais, Brazil.

MA 4

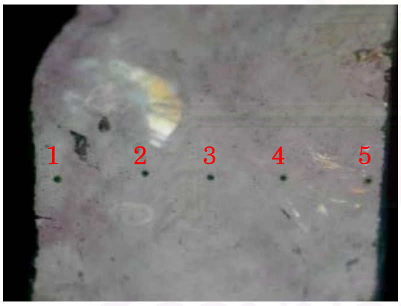

MA 7

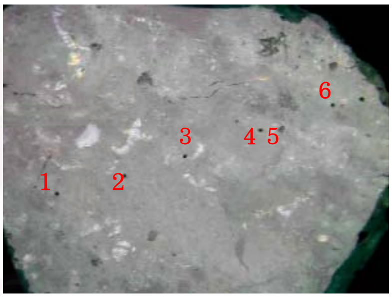

MA 8

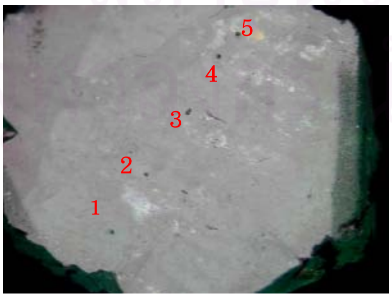

MA 18

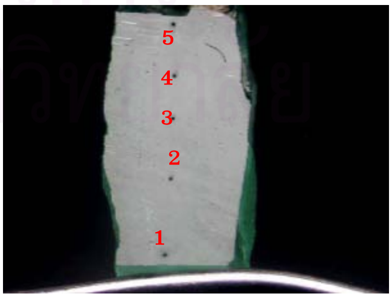

Figure 4.5: Showing the 4 samples of emerald from Mananjary region, Madagascar.

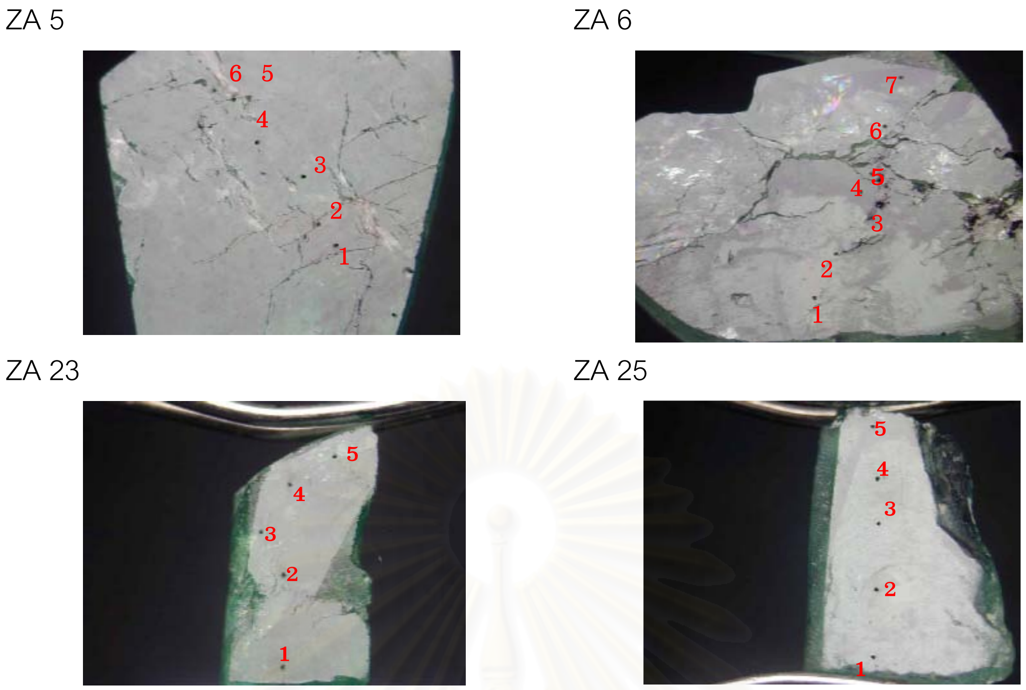

Figure 4.6: Showing the 4 samples of emerald from Ndola Rural district, Zambia.

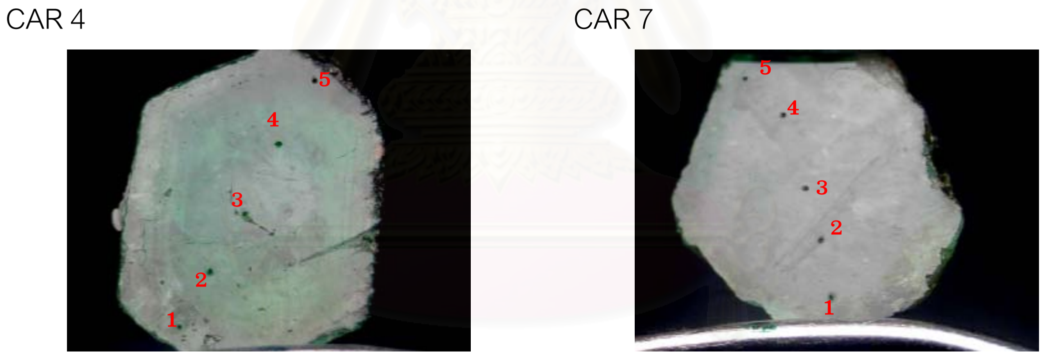

Figure 4.7: Showing the 2 samples of emerald from Carnaiba/Socoto, Bahia State, Brazil.

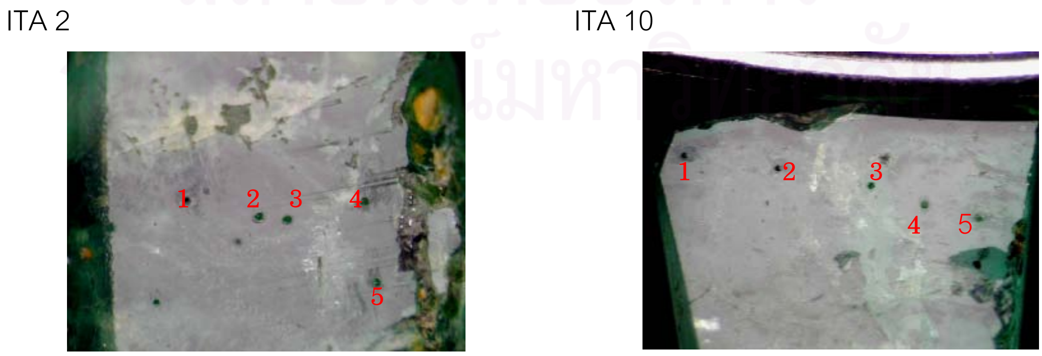

Figure 4.8: Showing the 2 samples of emerald from Itabira, Minas Gerias state in Brazil.

4.3 Results

The average concentrations of 16 trace elements; Li, Be, B, Na, Mg, Al, Si, P, K, Ca, Ti, V, Cr, Mn, Fe and Cs of each emerald sample analyzed in this study after recalculation into atom mole ppm are listed in Tables 4.1 to 4.3. The analytical concentrations in ppm by weight of original data, the plot of averages ($\overline{X}$) and standard deviation (STD) are shown in Appendix IV

From the chemical data shown Tables 4.1 to 4.3, the elements of emeralds from this study are mainly as alkalis and iron. Amount of these elements are characteristic, which related to geological environments.

4.4 Cross plots

Cross plots of Na versus Fe (or Na vs Fe), Na vs Li, Na vs Mg, Na vs Cs, Na vs Ti, Na vs B, Na vs (Mg+Fe), Li vs K, Li vs Fe, Li vs Cs and Al vs sum of all monovalent+divalent+trivalent ions contents of all the emeralds in this study are shown in Figures 4.9 to 4.19. The majority of the plots include alkali elements because of the fact that they are the major trace elements which have the strongest influence on the optical, physical and chemical properties of emeralds.

A good correlation between Na and Mg is seen in Figures 4.11 and between Na and (Mg+Fe) in Figure 4.15 regardless of localities. The remaining cross plots seem to show no correlation of other pair of elements. With regard to Figures 4.11 and 4.15, the contents of Na and Mg and probably Fe are highest in emeralds from Santa Terezinha, relatively high to moderate in those from Madagascar, Zambia, Carnaiba/Socoto and Itabira, relatively low in those from Colombia and lowest in those from Nigeria.

The emeralds from Zambia and Carnaiba/Socoto contain relatively high contents of Li and Cs (Figure 4.18). The emeralds from Madagascar show exceptionally high K content (Figure 4.16). The Colombian emeralds show consistently low iron content (Figures 4.9 and 4.17). These unusual high or low contents of Li, Cs, K and Fe contents may be used as locality specific criteria for those emeralds.

The emeralds from Brazil, Madagascar and Zambia (Type II deposits) show relatively moderate to high values of Na, Mg, Li and Cs (alkali elements) and Fe (as well as the total foreign elements) as compared with those of emeralds from Nigeria and Colombia (Type I deposits) (Figure 4.19). The highest contents of foreign elements can be found in the Santa Terezinha emerald from Goias State of Brazil (Type IIa) whereas the lowest contents are in Kaduna Plateau of Nigeria (Type Ia) (Figure 4.19).

Table 4.1: Chemical data of 16 trace elements of Nigerian emeralds (NI), and Colombian emeralds (CO) show atom mole ppm 16 major and trace elements.

Cation (atom mole ppm)	Nigeria (Kaduna Plateau)				Colombia (Cordillera Oriental)			
	NI 1	NI 11	NI 16	NI 27	CO 1	CO 11	CO 18	CO 22
Li	174.38	129.03	118.70	110.39	420.19	174.86	86.24	71.56
Be	102944.42	86637.46	86420.81	102404.53	99083.28	95835.41	97121.61	98043.19
B	40.87	35.06	46.93	46.40	42.90	55.15	62.00	55.90
Na	700.57	957.51	1032.32	444.05	3198.94	1893.79	2411.65	2046.69
Mg	318.14	262.99	238.77	217.96	3096.22	1859.98	2538.37	2148.45
Al	61525.47	64903.11	64397.83	61605.85	70778.95	72223.64	71509.80	71244.78
Si	211173.05	223081.16	223696.21	212241.29	201870.96	206546.76	204782.83	204771.24
P	10.51	10.52	11.21	9.71	77.15	13.82	14.32	65.92
K	84.54	39.00	97.90	70.85	27.93	54.92	118.62	113.73
Ca	61.84	51.64	67.47	79.19	126.47	150.56	140.36	113.20
Ti	3.60	7.22	5.48	1.90	2.54	1.10	1.00	0.83
V	145.26	165.05	159.88	108.04	90.64	50.88	49.24	137.27
Cr	105.49	88.90	115.23	121.48	28.75	27.69	27.32	112.07
Mn	2.39	2.97	5.70	1.78	0.49	0.54	0.51	1.23
Fe	1674.49	2591.87	2516.78	1472.44	152.99	54.42	70.24	72.67
Cs	0.06	0.09	24.02	16.02	1.62	1.09	1.00	1.28
Total atom mole %	**37.90**	**37.90**	**37.90**	**37.90**	**37.90**	**37.89**	**37.89**	**37.90**

Table 4.2: Chemical data of 16 trace elements of emeralds from Santa Terezinha (STA; Brazil) and Madagascar (MA) show atom mole ppm 16 major and trace elements.

Cation (atom mole ppm)	Brazil (Santa Terezinha)			Madagascar (Mananjary)			
	STA 1	STA 3	STA 8	MA 4	MA 7	MA 8	MA 18
Li	361.17	382.93	498.33	283.32	216.36	193.46	132.98
Be	95938.26	95213.29	96584.19	97419.18	99566.39	96865.60	99501.36
B	31.51	32.23	27.67	43.57	30.66	44.37	43.45
Na	12395.65	12048.93	12134.87	11737.03	8795.89	9006.50	9809.61
Mg	11396.61	11445.15	11613.44	11621.37	9593.88	9309.79	9707.25
Al	53464.63	53359.60	52854.39	49331.88	51076.70	50975.58	51060.39
Si	201007.10	201268.48	199574.99	204602.02	204334.76	206903.82	204963.37
P	40.96	62.75	44.46	14.12	10.61	9.23	10.48
K	172.04	166.71	193.87	1265.27	2962.34	2738.60	1270.28
Ca	44.28	50.16	140.37	159.65	118.27	129.17	88.51
Ti	1.83	2.81	6.78	2.05	2.51	2.54	2.33
V	134.90	139.76	116.57	20.23	17.35	25.88	19.96
Cr	1358.84	1810.83	1249.17	377.58	237.43	440.39	353.78
Mn	2.39	7.61	7.75	4.27	6.33	3.56	3.99
Fe	2587.58	2947.36	3866.50	2027.88	1985.30	2292.87	1972.50
Cs	62.26	61.40	86.64	35.48	12.17	18.71	16.50
Total atom mole %	**37.90**	**37.90**	**37.90**	**37.89**	**37.90**	**37.90**	**37.90**

Table 4.3: Chemical data of 16 trace elements of Zambian emeralds (ZA), and Brazilian emeralds from Carnaiba/Socoto (CAR) and Itabira (ITA) show atom mole ppm 16 major and trace elements.

Cations (atom mole ppm)	Zambia (Ndola Rural)				Brazil (Carnaiba/Socoto)		Brazil (Itabira)	
	ZA 5	ZA 6	ZA 23	ZA 25	CAR 4	CAR 7	ITA 2	ITA 10
Li	1514.17	751.11	848.70	1015.47	1049.89	1524.12	170.20	150.43
Be	87742.93	103036.66	99042.54	100880.81	97278.73	97170.22	96628.48	97011.45
B	35.85	31.07	43.53	39.44	40.69	40.82	35.74	30.19
Na	10211.18	5997.84	12034.73	11456.83	6537.02	4521.65	7793.51	7142.84
Mg	7887.79	3670.29	10033.31	8965.03	5757.24	3656.60	8265.43	7277.90
Al	54608.98	58180.92	48744.60	50686.17	64315.87	69233.37	62242.63	62203.61
Si	213278.52	205095.17	203645.75	202114.72	201515.61	201159.38	201960.21	202768.27
P	7.11	8.98	10.16	6.71	10.50	8.82	7.46	45.18
K	99.63	91.34	295.83	164.94	178.32	245.33	163.87	134.81
Ca	52.12	61.18	139.97	58.95	86.25	67.16	111.52	134.75
Ti	1.92	1.62	3.36	2.34	2.13	1.83	1.10	2.06
V	34.76	15.85	44.80	33.99	21.88	6.78	24.10	20.54
Cr	461.13	77.07	550.24	481.26	695.87	520.83	416.59	381.39
Mn	11.72	8.69	5.54	4.62	4.73	12.64	1.58	3.02
Fe	2886.09	1859.85	3440.19	2952.58	1267.13	696.27	1128.40	1682.50
Cs	130.33	79.10	72.28	105.81	204.93	101.55	9.33	11.07
Total atom mole %	37.90	37.90	37.90	37.90	37.90	37.90	37.90	37.90

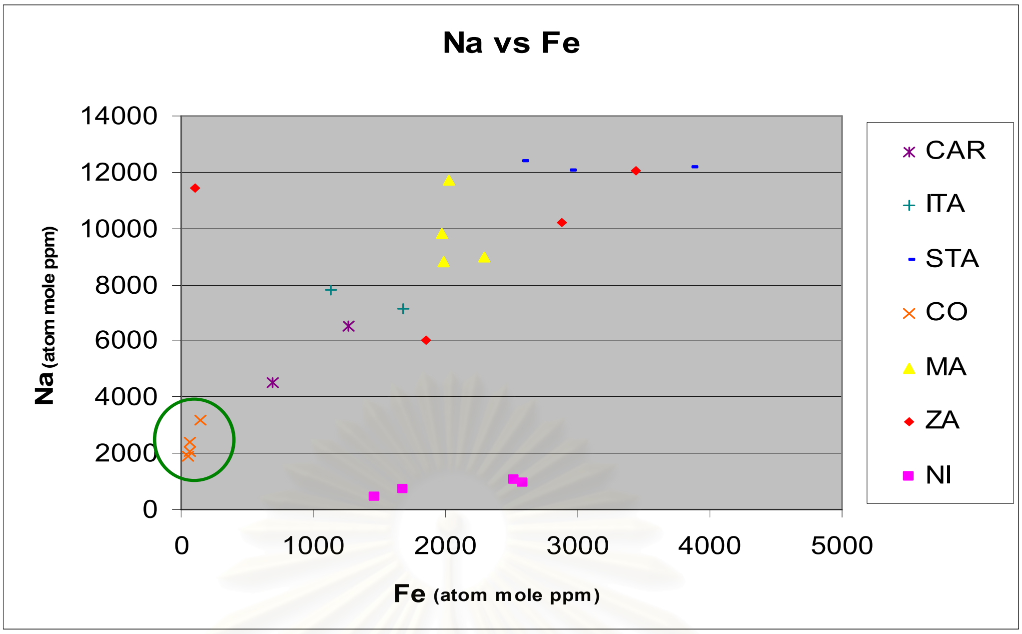

Figure 4.9: Plot of the average Na versus Fe contents of 23 emeralds from different geological occurrences show consistently low iron content in Colombian emerald.

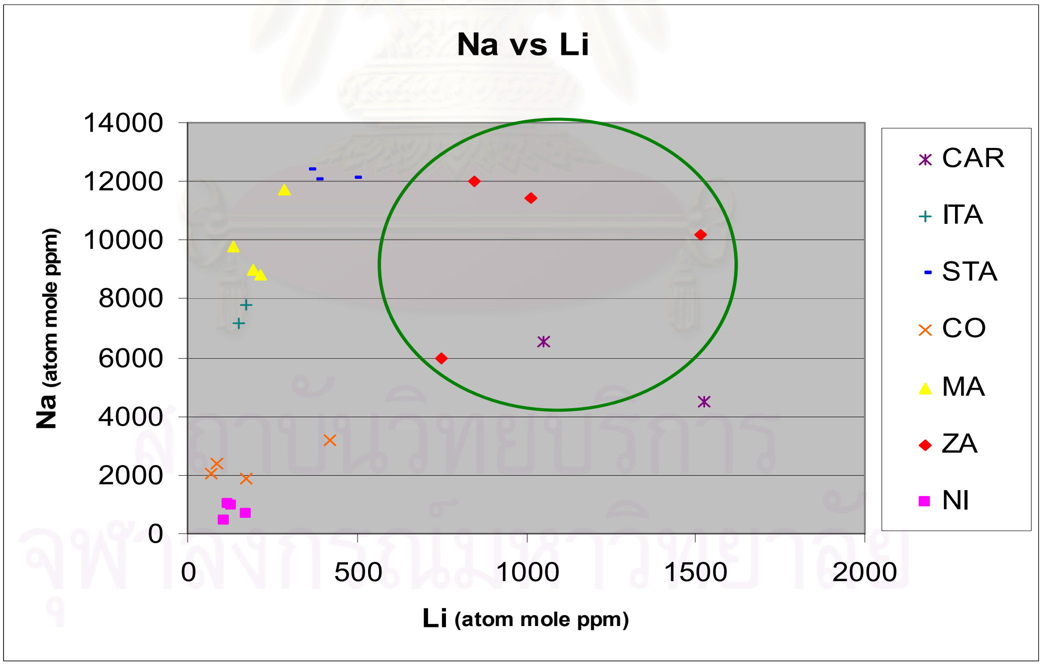

Figure 4.10: Plot of the average Na versus Li contents of 23 emeralds from different geological occurrences show moderate to high lithium content in Zambian emerald.

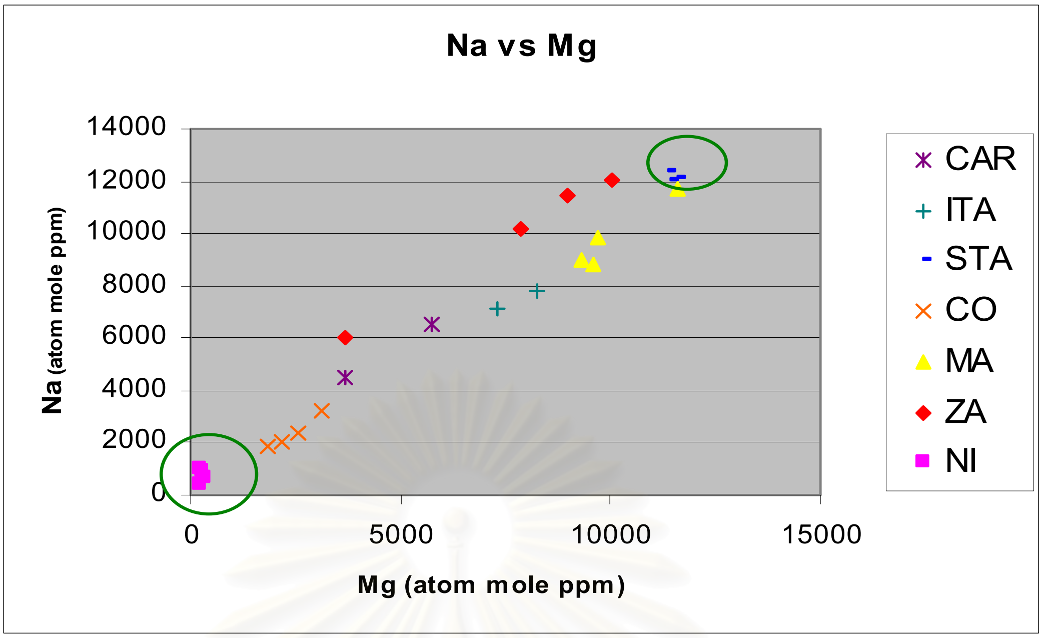

Figure 4.11: Plot of the average Na versus Mg contents of 23 emeralds from different geological occurrences showing the low sodium and magnesium (alkali) content in Nigerian emerald and the highest alkali content in Santa Terezinha from Brazil

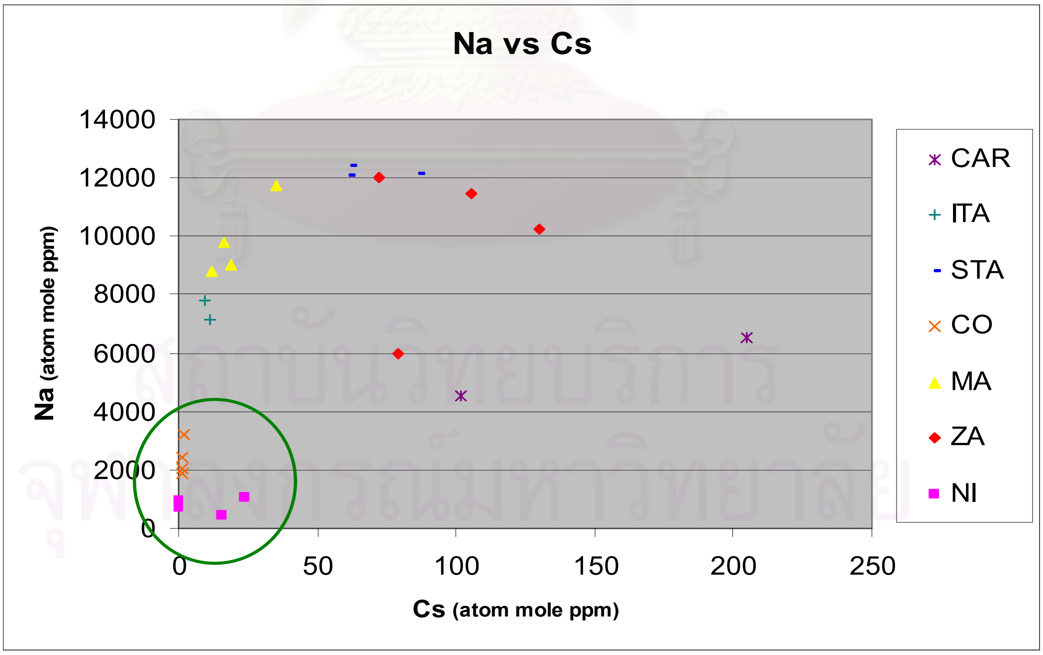

Figure 4.12: Plot of average Na versus Cs contents of 23 emeralds from different geological occurrences show low sodium and cesium content in emerald from Colombia and Nigeria.

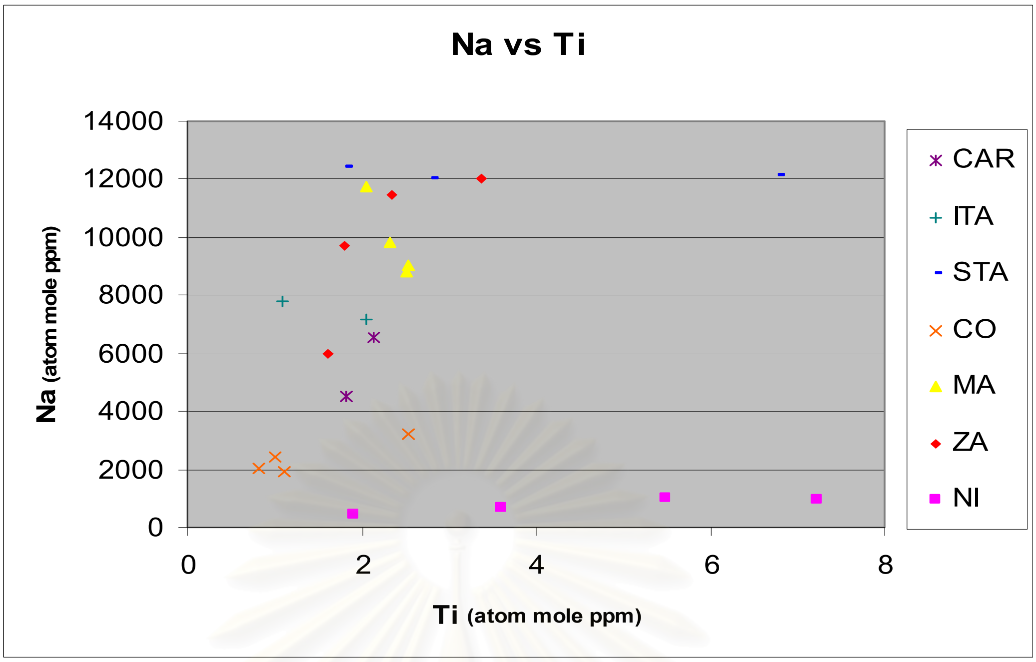

Figure 4.13: Plot of average Na versus Ti contents of 23 emeralds from different geological occurrences show no correlation of other pair of elements.

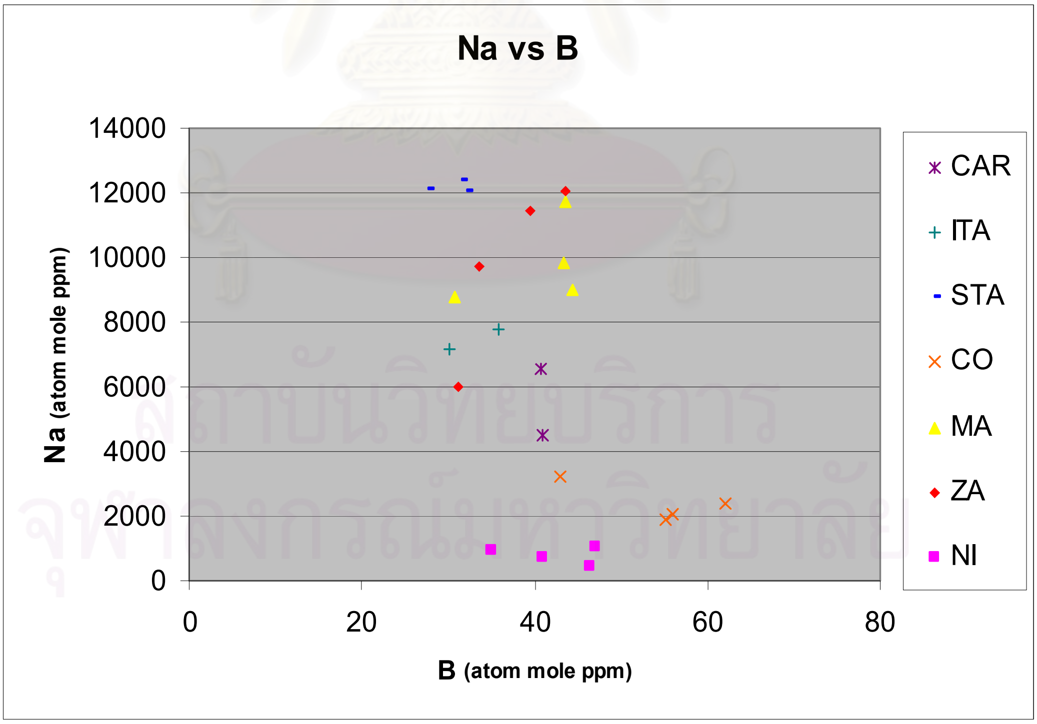

Figure 4.14: Plot of average Na versus B contents of 23 emeralds from different geological occurrences show no correlation of other pair of elements.

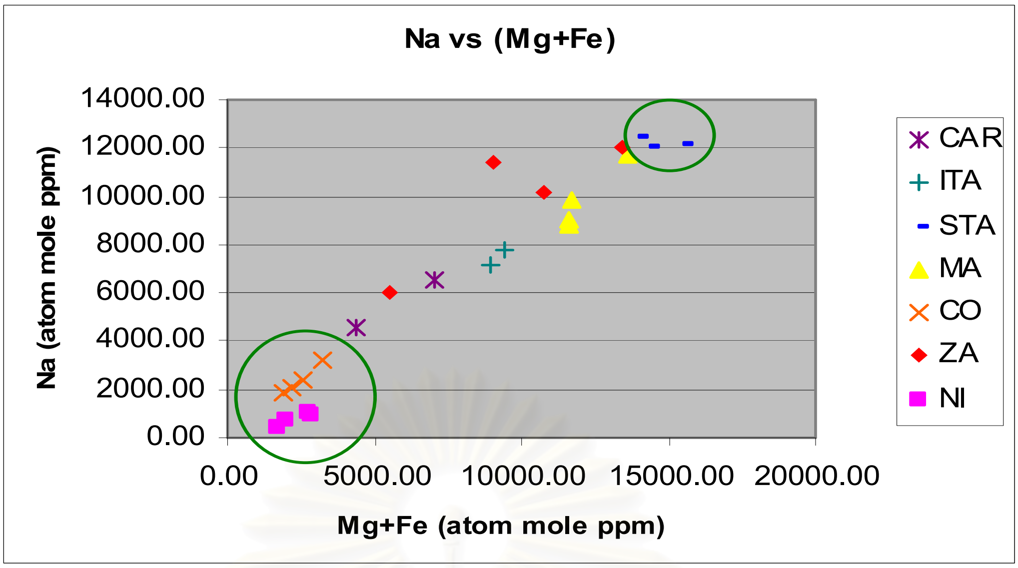

Figure 4.15: Plot of average Na versus (Mg+Fe) contents of 23 emeralds from different geological occurrences show low sodium and (magnesium plus iron) content in emerald from Nigeria and Colombia whereas consistently high these elements content in Santa Terezinha from Brazil.

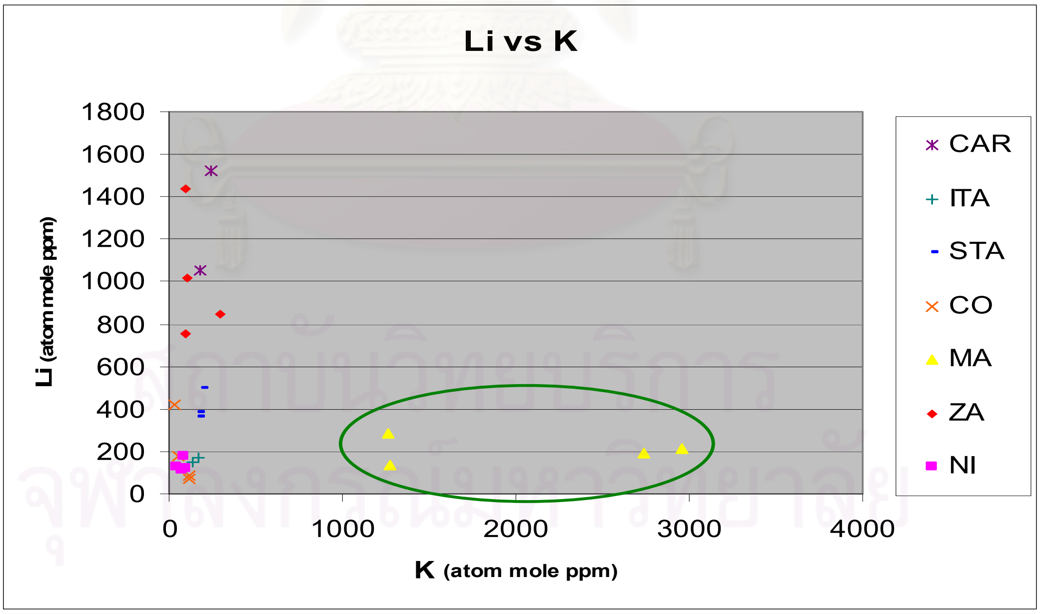

Figure 4.16: Plot of average Li versus K contents of 23 emeralds from different geological occurrences show consistently moderate to high potassium content in emerald from Madagascar.

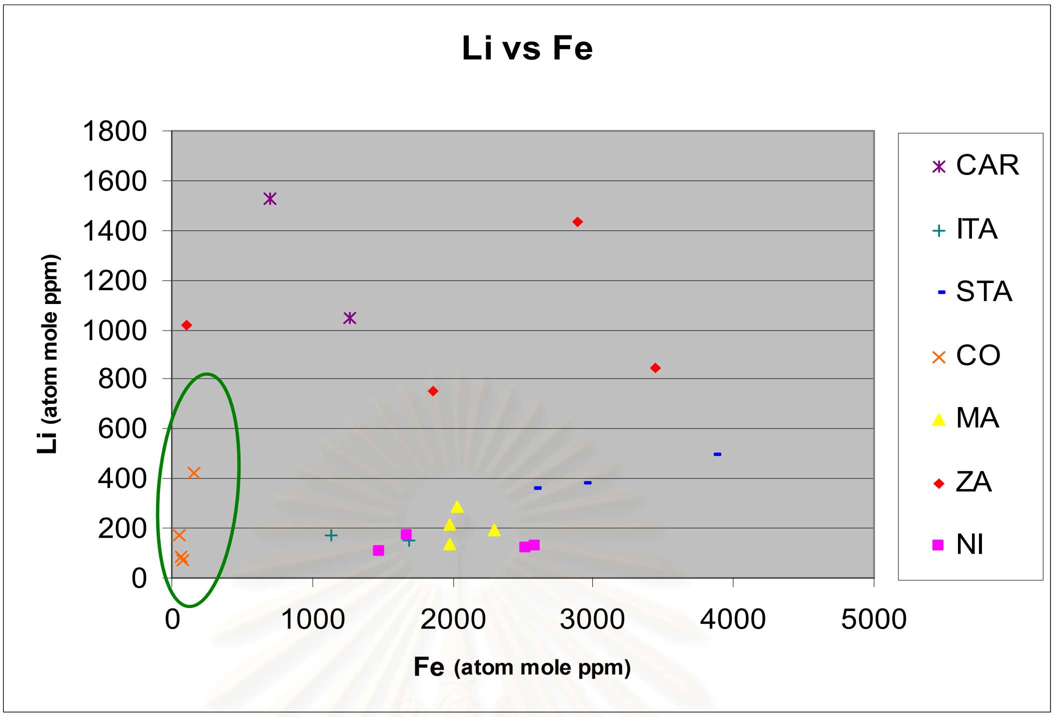

Figure 4.17: Plot of average Li versus Fe contents of 23 emeralds from different geological occurrences show consistently low iron content in Colombian emerald.

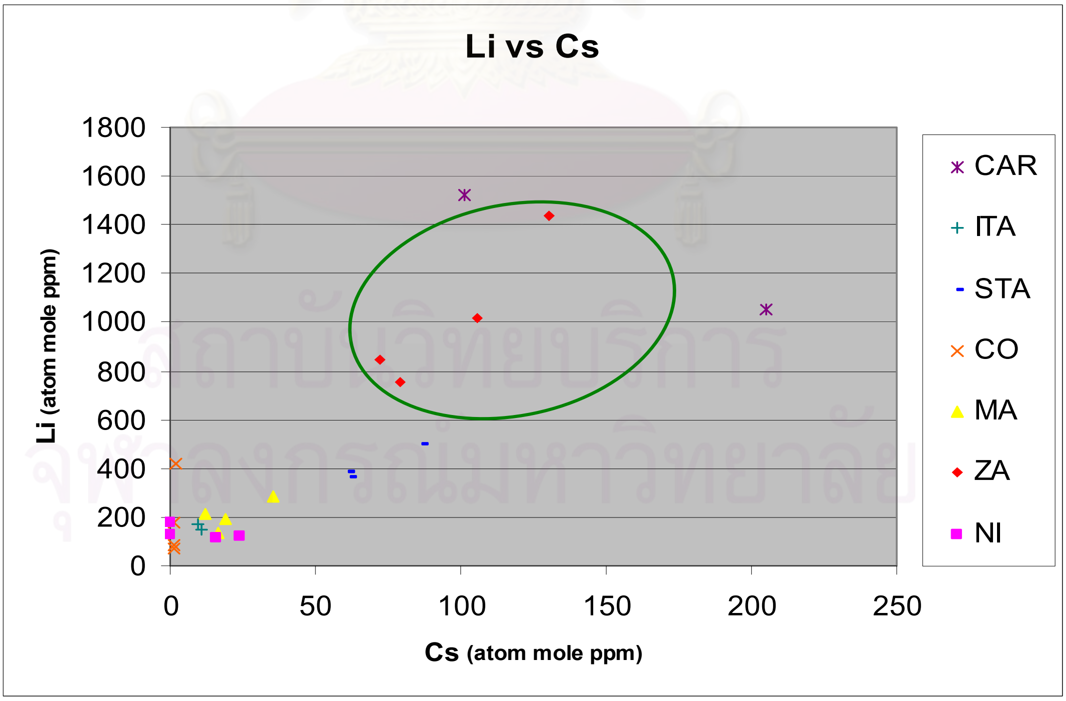

Figure 4.18: Plot of average Li versus Cs contents of 23 emeralds from different geological occurrences show moderate lithium and cesium content in Zambian emerald.

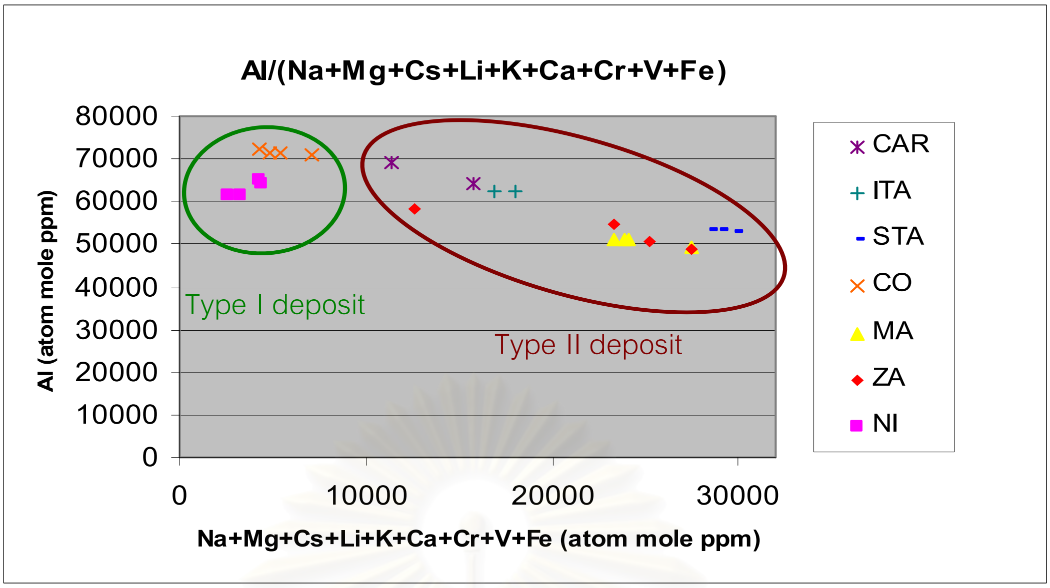

Figure 4.19: Plot of average Al versus sum of all Monovalent+Divalent+Trivalent ions contents from 7 different geological occurrences.

In most emeralds, the contents of sodium and magnesium are higher than the contents of chromophores, except those in Nigerian emeralds. Comparison of significant alkali elements (Na and Mg) and colouring elements (Cr, V and Fe) is shown below. Among those emeralds, the Colombian's contain lowest chromophoric elements because the Colombian emeralds have the lowest iron content (Figures 4.9 and 4.17).

	SUM(Na+Mg) (atom mole ppm)		SUM(Cr+V+Fe) (atom mole ppm)
Nigeria (NI):	1043.07	<	2316.23
Colombia (CO):	4798.52	>	218.54
Santa Terezinha (STA):	23678.22	>	4190.93
Madagascar (MA):	19895.33	>	2442.79
Zambia (ZA):	17564.25	>	3209.45
Carnaiba/Socoto (CAR):	10236.26	>	775.92
Itabira (ITA):	15239.84	>	1826.75

CHAPTER V

SPECTROSCOPIC EXAMINATION

In addition to those chemical data, spectroscopic examination was also carried out in this study which was divided into two intervals, namely Ultraviolet-Visible-Near InfarRed (UV-Vis-NIR) region and InfarRed (IR) region. The absorption spectra in the UV-Vis-NIR region are usually measured by a UV-Vis-NIR spectrophotometer whereas those in the IR region are measured by a Fourier Transform InfraRed (FTIR) Spectrophotometer.

5.1 UV-Vis-NIR spectrophotometry

The UV-Vis-NIR spectrophotometer is an equipment used for measurement of the absorption spectra in the UV-Vis-NIR region which can help understand the causes of colour. Typical features of absorption spectra as recorded by the spectrophotometer are assigned to certain trace elements indicating the role of these elements as colouring agents.

5.1.1 Instrument and Analytical condition

In this study, the UV-Vis-NIR absorption spectra of the emerald samples were measured by the spectrophotometer Model HITACHI U-4001 that has the wavelength ranging from 240 to 2500 nm (Figure 5.1) located at the GIT. The spectra were collected with scanning speed of 300 nm/min. and slit opening of 4.00 nm. The spectra were collected at two automatic sampling interval; at the wavelength 240-340 nm of the ultraviolet region (UV), the light sources of deuterium (D2) discharge tube was used ; and at the wavelength 320-1000 nm of the visible and near infrared region, a 50 W iodine tungsten lamp was used. Photomultiplier (for ultraviolet-visible region) and cooled-type PbS cell (for near infrared region) detectors incorporated with automatic wavelength calibration function were used to obtain the spectra with wavelength accuracies of +/-0.2 nm in ultraviolet-visible region and +/-1.0 nm in near infrared region. A standard PC computer with an installed program was used to collect and store the spectra including data processing and analysis. The spectra were recorded with both light polarized parallel (e-ray) and perpendicular (o-ray) to the c-axis by using a Polaroid filter.

Figure 5.1: A UV-Vis-NIR spectrophotometer Model HITACHI model U-4001 at the GIT.

5.1.2 Results

The UV-Vis-NIR absorption spectra of 7 emerald samples from Nigeria, Colombia, Santa Terezinha, Carnaiba/Socoto and Itabira (Brazil), Madagascar and Zambia were measured and representative spectra from each location are shown in Figures 5.2 to 5.8. The spectra of most emeralds except that of the Colombian emerald show typical absorption bands of chromium (Cr^{3+}) and vanadium (V^{3+}) mixed with iron (Fe^{2+} and Fe^{3+}). The two wide absorption bands of Cr^{3+} and V^{3+}, the so-called ‘emerald component’, in 400 – 480 nm and 590 – 640 nm are dominant in those spectra. The narrow Cr^{3+} absorption bands in red to orange region (611, 638, 648, 662, 685 nm) are overlapped by a wide absorption band of the so-called ‘aquamarine component’ (Fe^{2+}/ Fe^{3+} IVCT: inter-valence charge transfer) in 600 – 750 nm and one or two board band of Fe^{2+} in 820 nm (o-ray) and 760 - 920 nm (e-ray). The V^{3+} absorption bands (390 – 405 and 570 – 575) are slightly shifted against the Cr^{3+} peaks. Other two narrow bands of Fe^{3+} are in violet region at about 370 and 426 nm. In contrast the spectra of Colombian emerald show only absorption bands due to Cr^{3+} and V^{3+} without contribution from iron absorption. The absorption characteristics can be summarized in Table 5.1. Similar results have previously been reported by Schmetzer and Bank (1981), Schwarz and Henn (1992), Schwarz (2002), Petrov and Neumeier (2002) and Bosshart (1982).

Table 5.1: Summary of the absorption bands of emeralds in UV-Vis-NIR ranges found in this study as well as previously reported by Schmetzer and Bank (1981), Bosshart (1982), Schwarz and Henn (1992), Mathew (1998), Schwarz (2002) ,Petrov and Neumeier (2002)

Wave number (nm)	Assignment
about 370, 426	Two narrow bands of Fe^{3+}
611, 638, 648, 662, 685	Narrow bands of Cr^{3+}
400 – 480 and 590 – 640	Two wide bands of emerald component; Cr^{3+} and V^{3+}
600 – 750	A wide band of aquamarine component; Fe^{2+}/ Fe^{3+} inter-valence charge transfer
820 (o-ray; in channel site) and 760 – 920 (e-ray; at octahedral Al site)	One or two band of Fe^{2+}
390 – 405 and 570 - 575	V^{3+} are slightly shifted against the Cr peaks

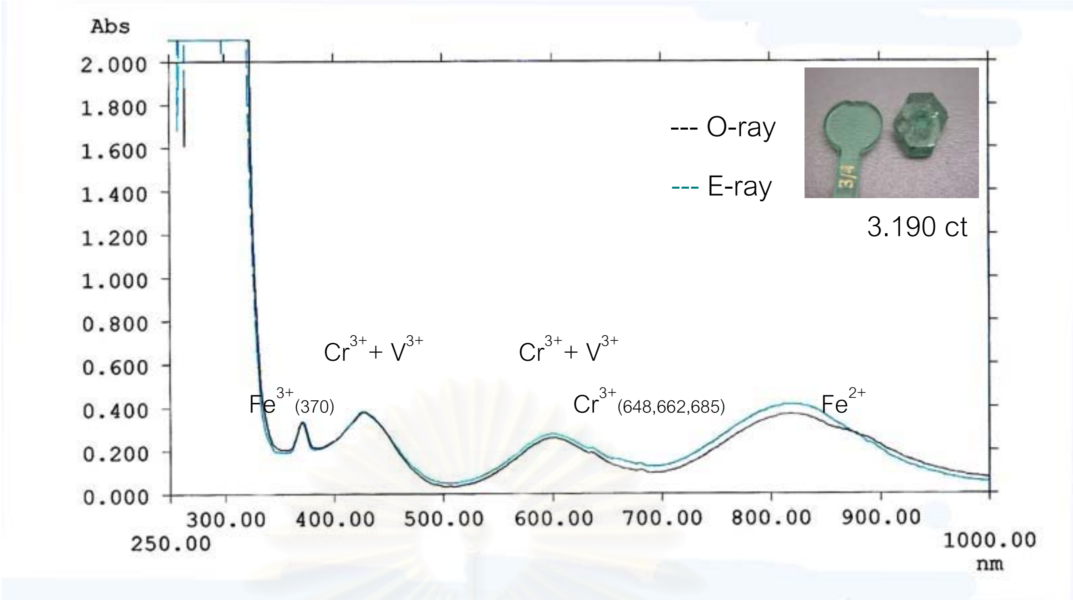

Figure 5.2: UV-Vis-NIR spectra of Nigerian emerald (NI-11) showing chromium-vanadium spectrum, ferric iron (Fe^{3+}) bands in ultraviolet and ferrous iron (Fe^{2+}) band in near-infrared.

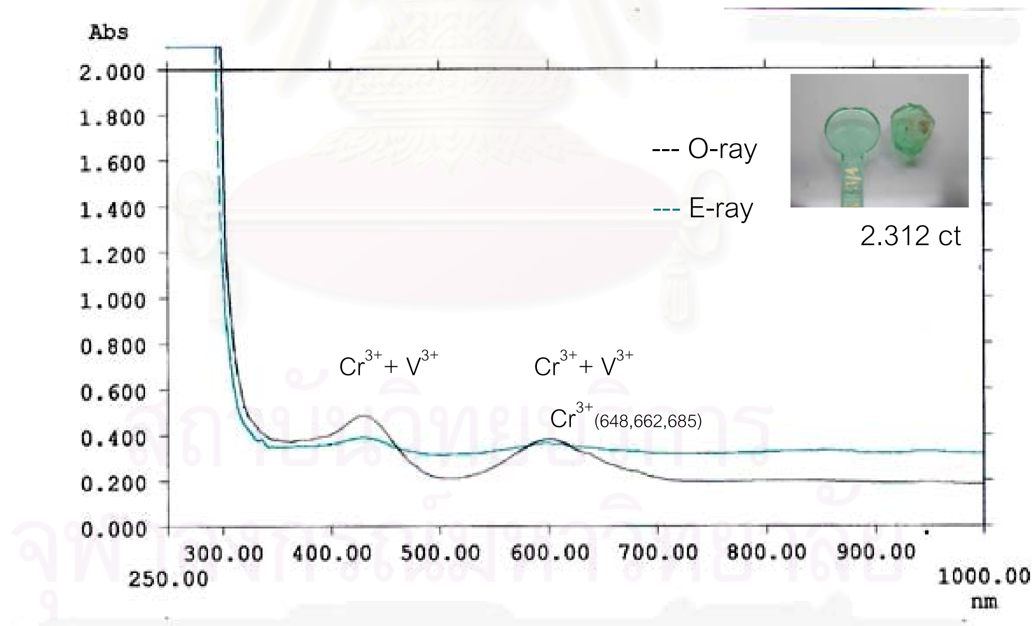

Figure 5.3: UV-Vis-NIR spectra of Colombian emerald (CO-22) showing chromium-vanadium spectrum without iron bands.

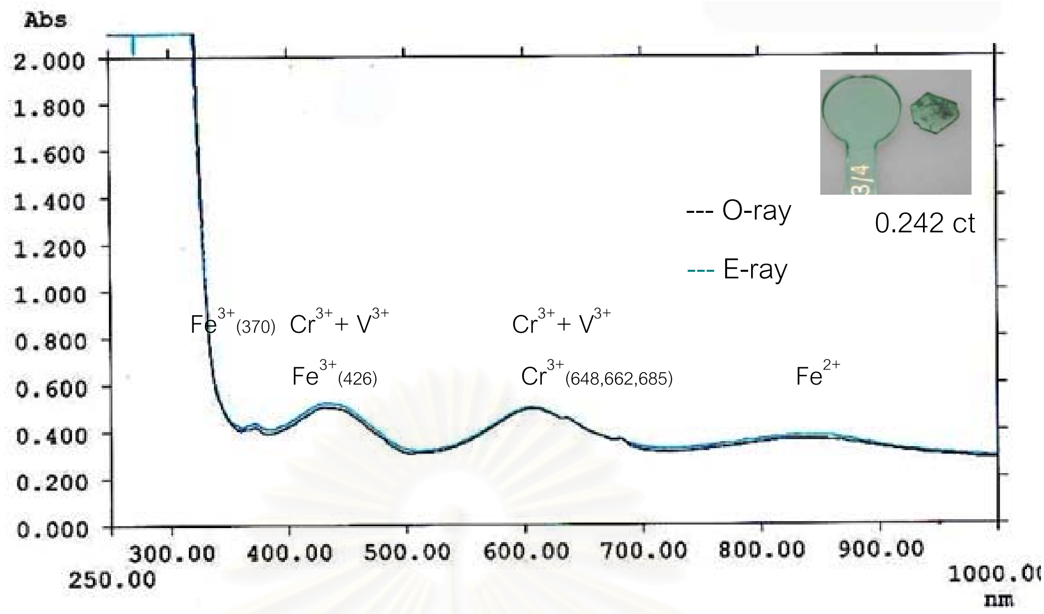

Figure 5.4: UV-Vis-NIR spectra of Santa Terezinha emerald from Brazil (STA-3) showing chromium-vanadium spectrum, ferric iron (Fe^{3+}) bands in ultraviolet and ferrous iron (Fe^{2+}) band in near-infrared.

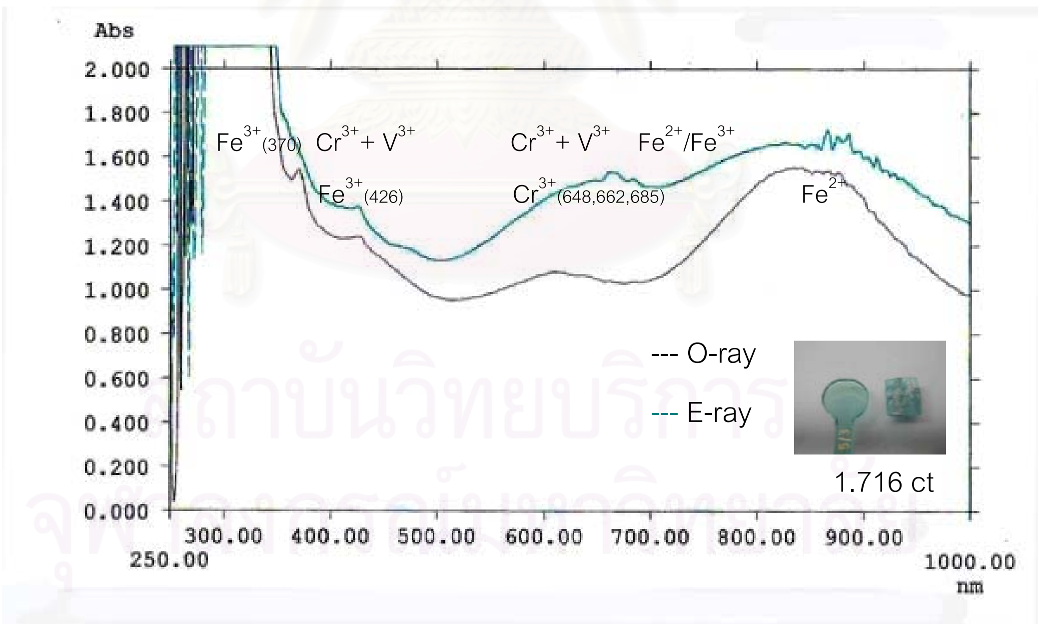

Figure 5.5: UV-Vis-NIR spectra of emerald from Madagascar (MA-28) representing a typical mixed spectrum containing both an emerald component with Fe^{2+} and Fe^{3+} bands. The main Cr^{3+} absorption bands are overlapped by Fe^{3+} absorption.

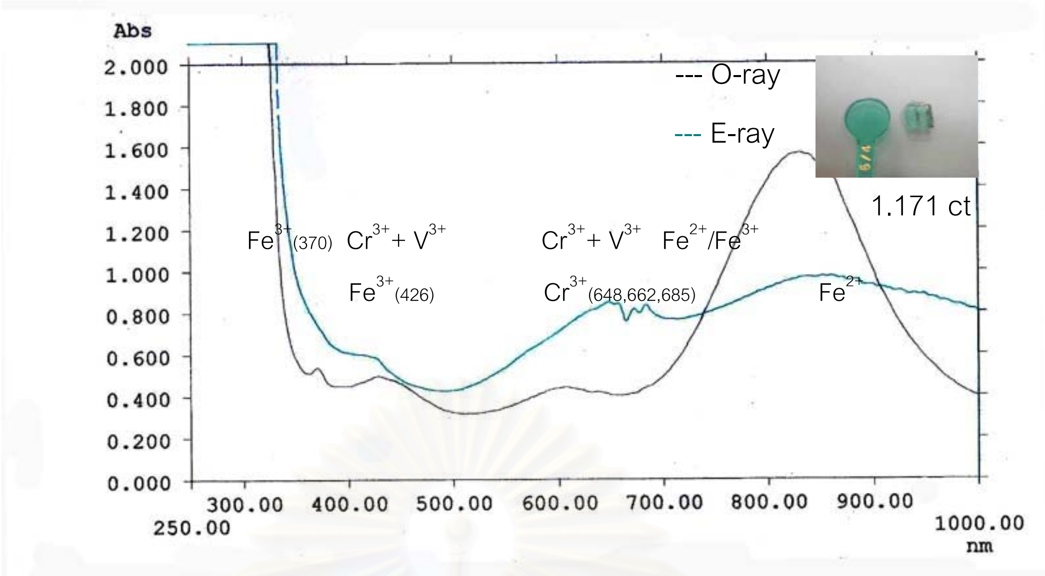

Figure 5.6: UV-Vis-NIR spectra of Zambian emerald (ZAM-29) showing a typical mixed spectrum containing both an emerald component with $Fe^{2+}$and Fe^{3+} bands. The main Cr^{3+} absorption bands are overlapped by Fe^{3+} absorption.

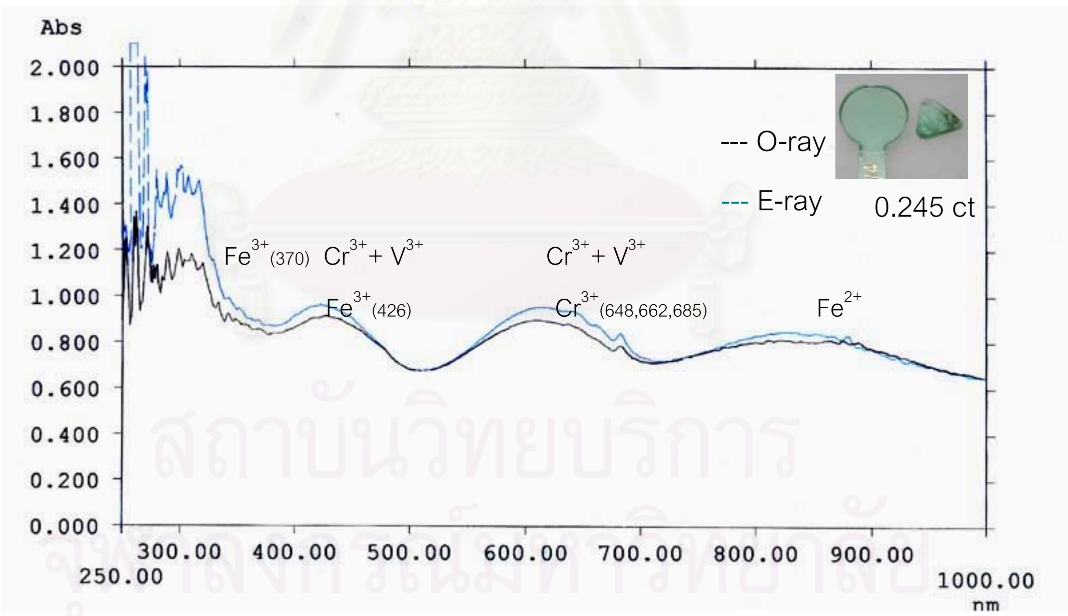

Figure 5.7: UV-Vis-NIR spectra of Carnaiba/Socoto emerald from Brazil (CAR-2) showing chromium-vanadium spectrum, ferric iron (Fe^{3+}) bands in ultraviolet and ferrous iron (Fe^{2+}) band in near-infrared.

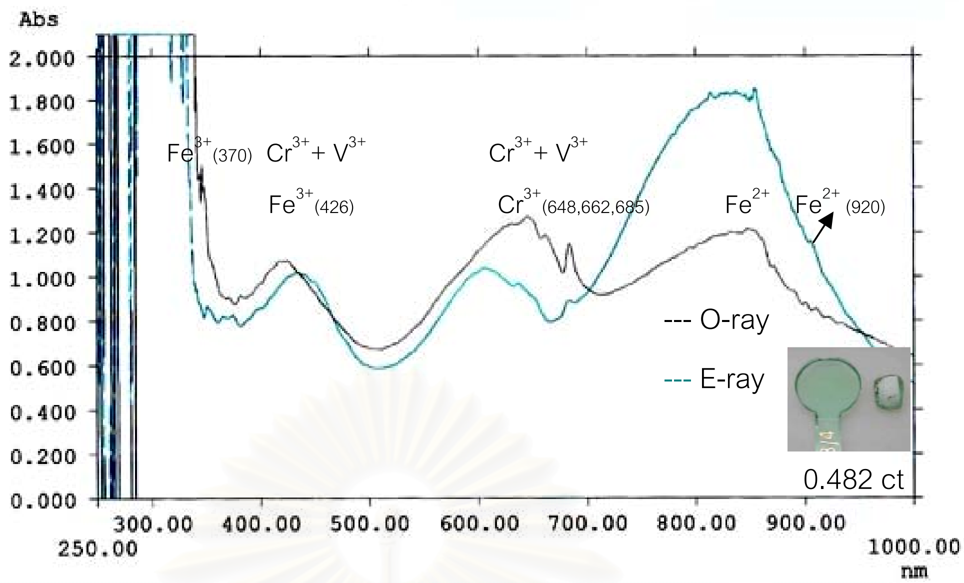

Figure 5.8: UV-Vis-NIR spectra of Itabira emerald from Brazil (ITA-2) showing chromium-vanadium spectrum, ferric iron (Fe^{3+}) bands in ultraviolet and ferrous iron (Fe^{2+}) band in near-infrared.

5.2 Fourier Transform InfraRed Spectrophotoscopy (FTIR)

The infrared region of the electromagnetic spectrum is the energy range just beyond the red end of the visible spectrum. In fact the term infrared is derived from being lower in energy 'infra-' than the red end. The unit by which infrared energy is usually measured is the wave number (number of waves per centimeter), which is expressed in reciprocal centimeters (cm^{-1}). The infrared is thus referred to as the energy range between 13,333 cm^{-1} (the edge of the red) and 33 cm^{-1} (a limit determined by use and technology). This broad region is divided on the basic of experimental techniques and applications into three parts: near infrared (13,500 – 4,000 cm^{-1}), mid infrared (4,000 - 350 cm^{-1}), and far infrared (350 – 33 cm^{-1}). For most gemological purposes, infrared energy is express in cm^{-1}; energies above 400 cm^{-1} that is, the mid infrared and the near infrared are of greatest interest gemologically.

Infrared spectroscopy in itself is not new, having become generally available to scientists about 50 years ago. However, technological advances in instrumentation in the past 10 years have made infrared spectra much more readily and rapidly accessible. Infrared spectroscopy is now widely used in gem laboratories to characterize natural, treated and synthetic stones. It is a powerful tool for gem identification and research. Absorptions of a gem material in the infrared region of the electromagnetic spectrum are due to vibrations in the crystal structure; they can be used to help separate one gem material from another or to detect certain types of treatments. 'Water', either molecular (H_2O) or as hydroxyl groups (OH) is combined in various forms in many gemstones or is present as an impurity. These various forms of water have characteristic patterns in the mid infrared and can be good indicators of structure, origin, or treatment

5.2.1 Instrument and Analytical condition

The author use Nicolet FTIR Spectrophotometer (Model NEXUS 670 with OMNIC software, see Figure 5.9) at GIT, the FTIR spectra were measured with the transmission mode and display as absorbance mode in the near infrared range at 4000 - 8000 cm^{-1} (wavenumber) in this study.

5.2.2 Results

The absorption bands of most emeralds appear in near infared ranges due to the vibration of water molecules in the channel sites of the beryl structure. The assignment of each absorption band to two types of water molecules has previously been studied and are summarized in Tables 5.2 - 5.3 and shown in Figures 5.10 - 5.11, respectively (Schwarz and Henn, 1992; Schmetzer et al, 1997). The type I water exhibit absorption bands at 5110, 5275, 5450, 5590, 6826, 7138 and 7267 cm^{-1} whereas the type II water exhibits absorption bands at about 5271 and 7077 cm^{-1}. Especially for Nigerian emeralds show other three small peaks at 4882, 4804 and 4650 cm^{-1} that may be type I H_2O.

Figure 5.9: Nicolet FTIR Spectrophotometer (Model NEXUS 670) of GIT, the FTIR spectra were measured with the transmission mode in the near infrared.

Table 5.2: H_2O vibration bands in the 4500 – 7500 cm^{-1} range of emerald from Morafeno area, Manajary, Madagascar (Schwarz and Henn, 1992)

Wavenumber (cm^{-1})	Wavelength (nm)	Type H_20
5271	1897	II
5590	1789	I
6826	1465	I
7077	1413	II
7138	1401	I
7267	1376	I

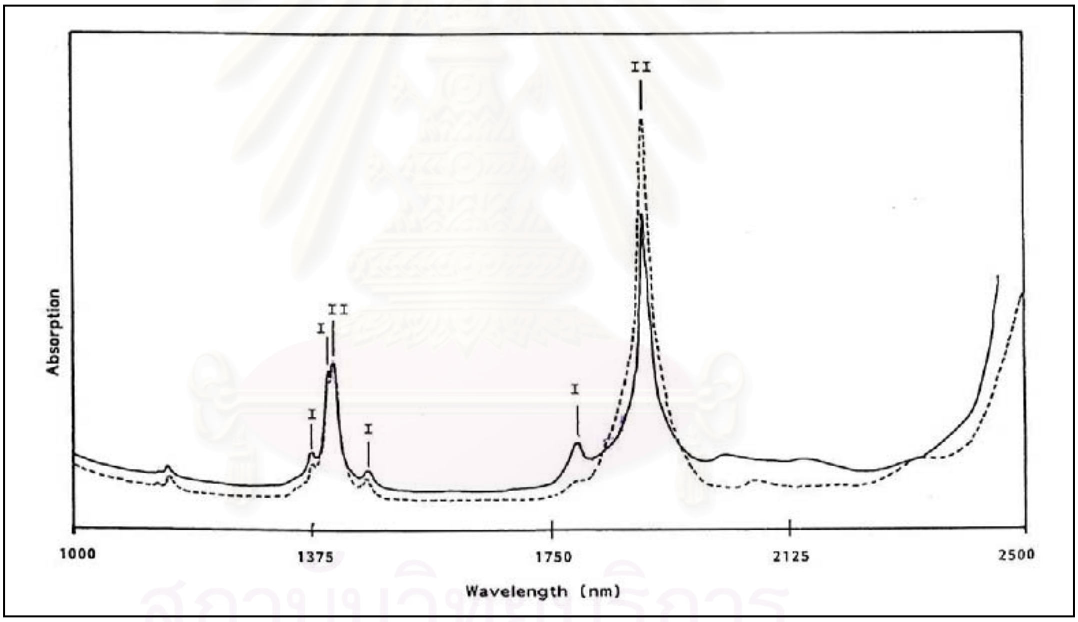

Figure 5.10: A representative FTIR spectra of vibration water molecules of emerald from Morafeno, Madagascar representing the type I H_2O at 5590, 6826, 7138 and 7267 cm^{-1} and the type II H_2O at 5271 and 7077 cm^{-1} (see table 5.2).

Table 5.3: H_2O vibration bands in the 5000 - 6,000 cm^{-1} range of synthetic hydrothermal emerald (Schmetzer et al, 1997) and show spectrum in Figure 5.11

Wavenumber (cm^{-1})	Type H_20
5110	I
5275	
5450	

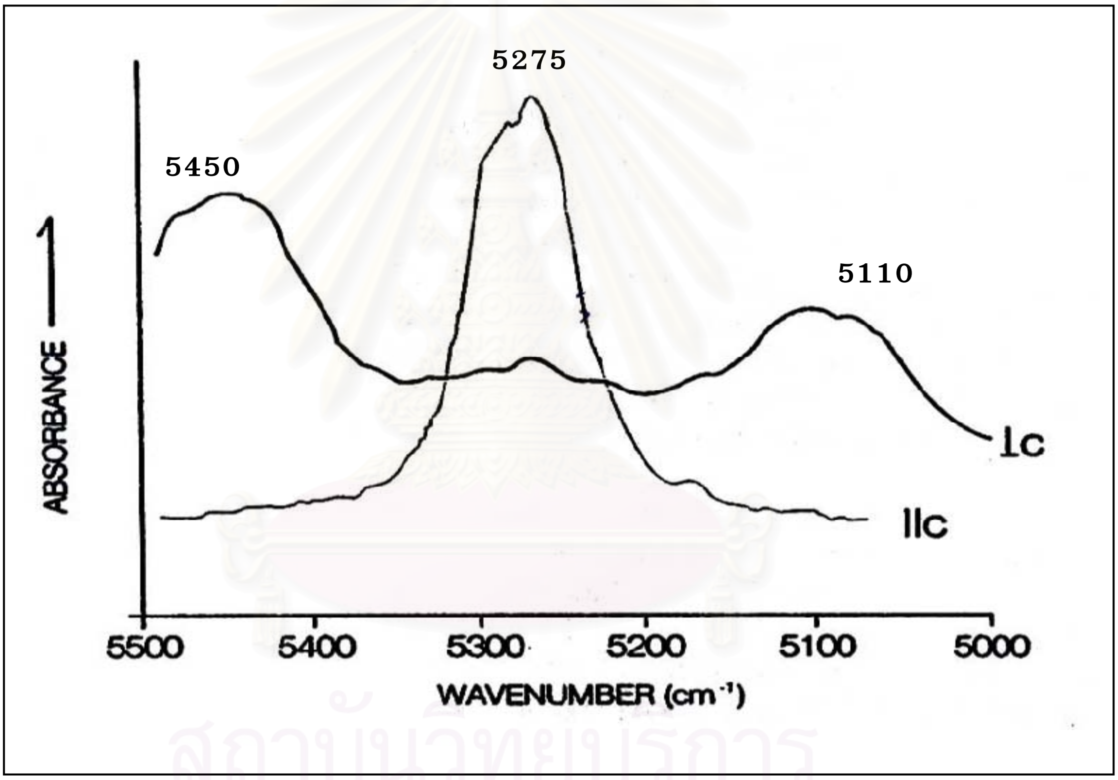

Figure 5.11: A sample of FTIR spectra in range 5000-5500 cm^{-1} of vibration water molecules of Chinese hydrothermal synthetic emerald representing type I H_2O when the beam is polarized parallel to the c-axis, the band at 5275 cm^{-1} whereas the beam is polarized parallel to the c-axis, the band at 5110 and 5450 cm^{-1}.

The representative FTIR absorption spectra of emeralds from each locality (Brazil, Madagascar, Zambia, Nigeria and Colombia) are shown in Figure 5.12 to 5.18.

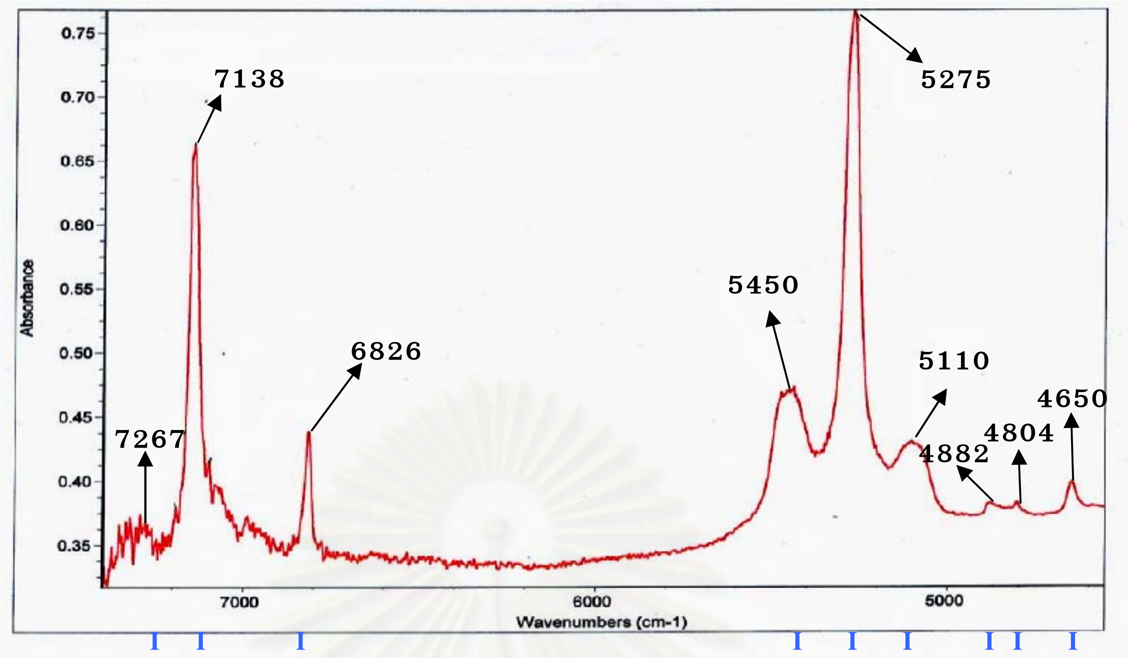

Figure 5.12: FTIR spectra of emerald from Nigeria (NI-24) dominated by type I H_2O at 5110, 5450, 5275, 6826, 7138 and 7267 cm^{-1} and three small peaks at 4882, 4804 and 4650 cm^{-1} that may also be of type I H_2O.

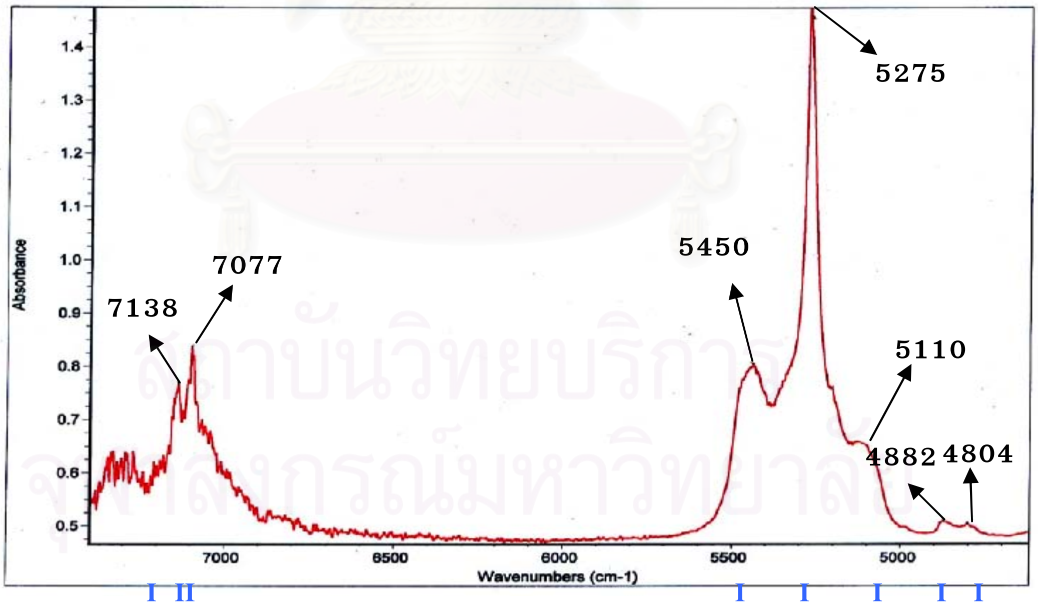

Figure 5.13: FTIR spectra of emerald from Colombia (CO-18) showing type I H_2O at 5110, 5275, 5450 and 7138 cm^{-1} and type II H_2O at 7077 cm^{-1} , that may also be of type I H_2O at 4882 and 4804 cm^{-1}.

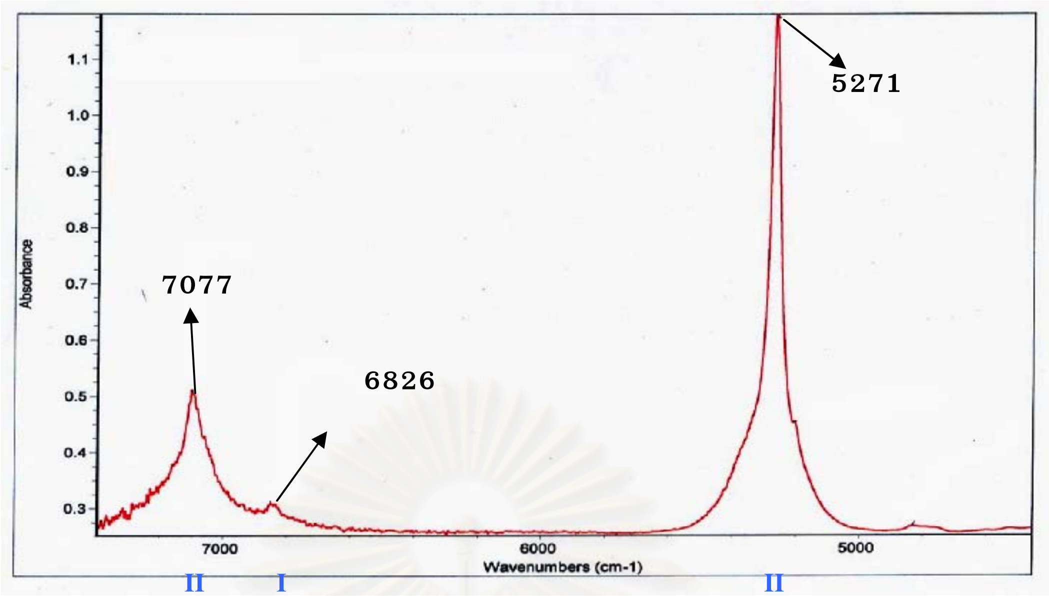

Figure 5.14: FTIR spectra of Santa Terezinha emerald from Goais, Brazil (STA-3) dominated by type II H_2O at 5271 and 7077 cm^{-1} while the type I H_2O at 6826 cm^{-1} is insignificant.

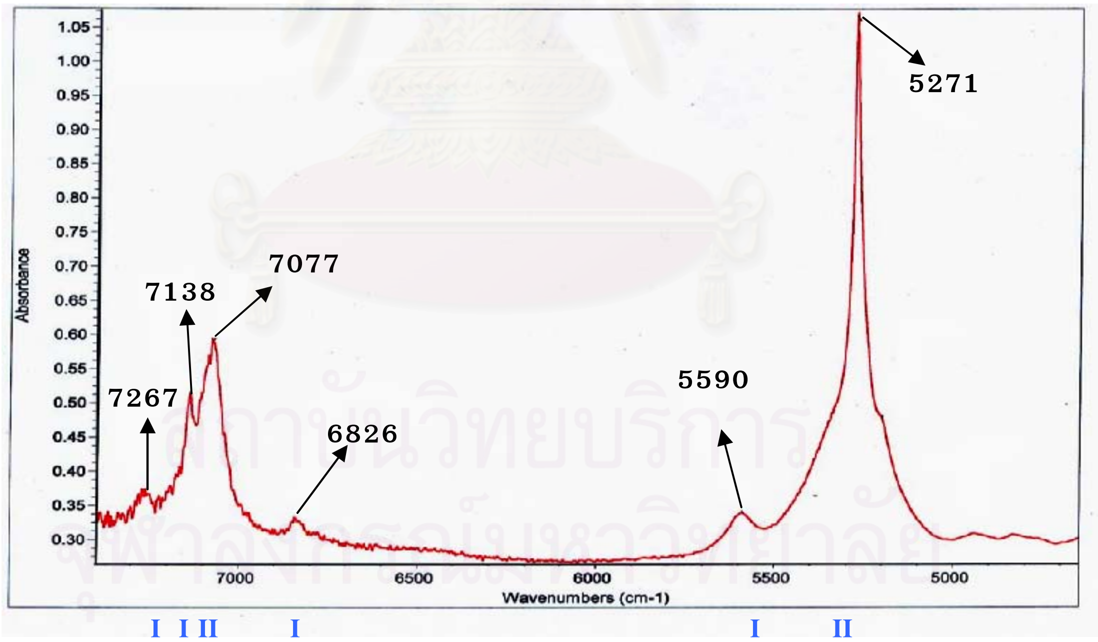

Figure 5.15: FTIR spectra of emerald from Mananjary, Madagascar (MA-21) showing type I H_2O at 5590, 6826, 7138 and 7267 cm^{-1} and type II H_2O at 5271 and 7077 cm^{-1}.

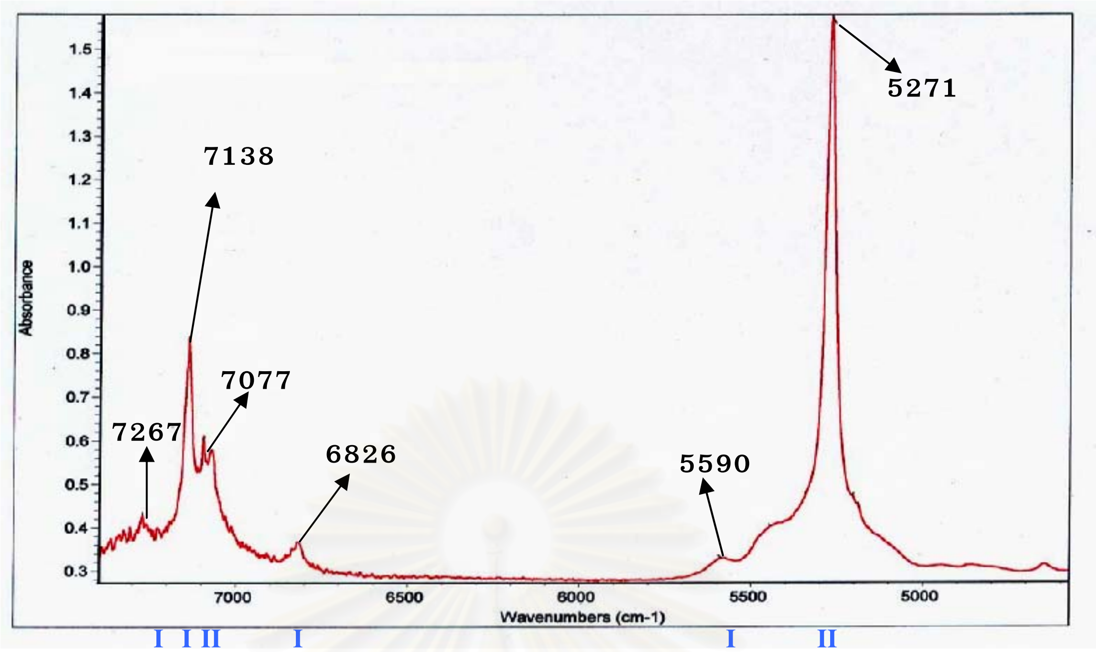

Figure 5.16: FTIR spectra of emerald from Zambia (ZA-3) showing type I H_2O at 5590, 6826, 7138 and 7267 cm^{-1} and type II H_2O at 5271 and 7077 cm^{-1}.

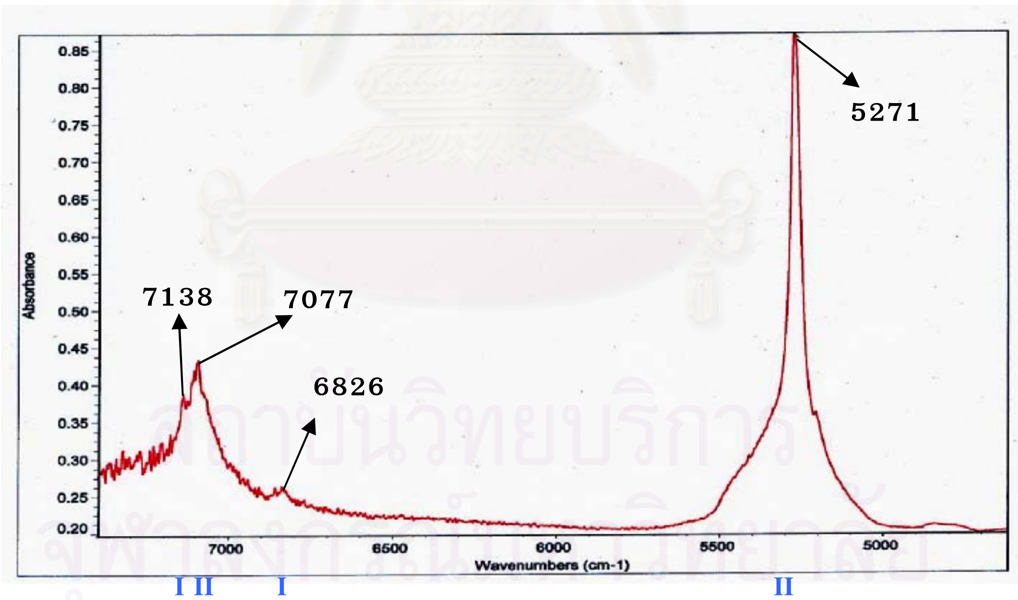

Figure 5.17: FTIR spectra of Canaiba/Socoto emerald from Bahia, Brazil (CAR-3) showing type I H_2O at 6826 and 7138 cm^{-1} and type II H_2O at the 5271 and 7077 cm^{-1}.

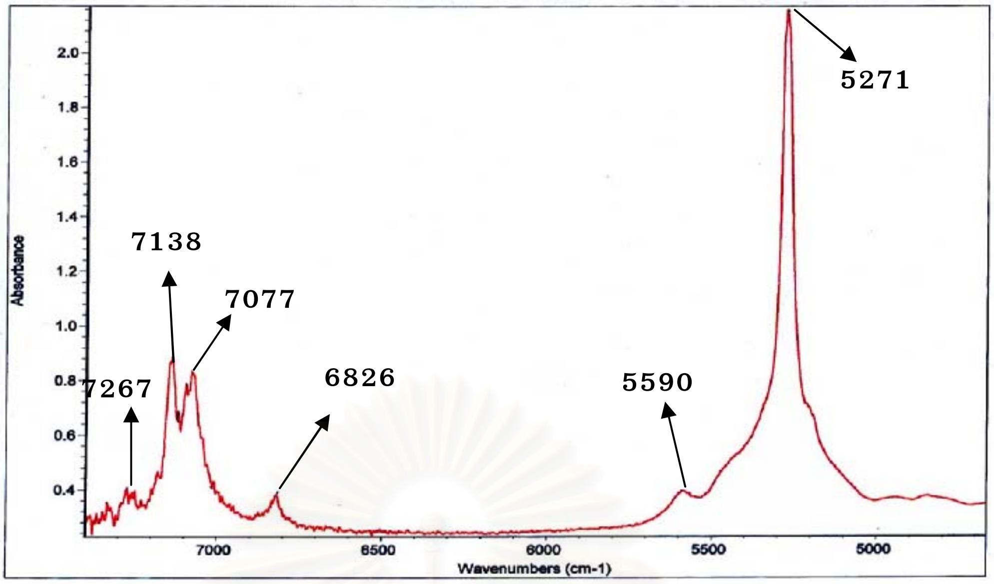

Figure 5.18: FTIR spectra of Itabira emerald from Minas Gerais, Brazil (ITA-7) showing type I H_2O at 5590, 6826, 7138 and 7267 cm^{-1} and type II H_2O at 5271 and 7077 cm^{-1}.

The spectra of almost all of these emeralds (i.e. from Madagascar, Zambia, Carnaiba/Socoto and Itabira of Brazil and Colombia) indicate similarly the presence of both types of water molecules except those of the Nigerian emerald and the Brazilian emerald from Santa Terezinha. The spectrum of Nigerian emerald is dominant by the type I water which is related to low alkali contents whereas that of the Brazilian emerald from Santa Terezinha is dominant by the type II water which is related to high alkali contents.

CHAPTER VI

DISCUSSION AND CONCLUSION

6.1 Discussion

6.1.1 Geological Occurrences:

In this study, emerald deposits have been classified and categorized in two major specific geological occurrences which are summarized and displayed again in Table 6.1.

Table 6.1: Summary of geological occurrences of emeralds from Brazil, Colombia, Madagascar, Zambia and Nigeria

Type I Deposits (Non-schist-related)		Type II Deposits (Schist-related)				
Type Ia (Pegmatite without Schist)	Type Ib (Black Shales with Viens and Breccias)	Type IIa (Schist without Pegmatite	Type IIb (Pegmatite with Schist); emerald occur between contact zone of country rock and pegmatite veins			
Emerald crystallized in vugs of granitic - rock, which intruded to the country rock.	Host rock is black shales.	Host rock is talc-chlorite-amphibole-magnetite schist.	Host rock is phlogopite-carbonate - talc schist.	Host rock is amphibolite.	Host rock is serpentinite.	Host rock is talc.
Kaduna Plateau, Nigeria	Cordillera Oriental, Colombia	Santa Terezinha (Brazil)	Mananjary, Madagascar	Ndola Rural, Zambia	Carnaiba/ Socoto (Brazil)	Itabira (Brazil)

In this chapter the author will try to relate their geologic occurrences (type of deposits) with some physical properties and internal characteristics.

6.1.2 Physical and Optical properties:

Schwarz (2004) has classified emerald's refractive indices (e-ray and o-ray) and birefringence into low, medium and high values based on over 1,000 measurements from various localities as follows:

	low	*medium*	*high*
e-ray	*<1.570*	*1.570-1.580*	*>1.580*
o-ray	***<1.580***	***1.580-1.590***	***>1.590***
birefringence	*<0.006*	*0.006-0.008*	*>0.008*

From the refractive indices (o-ray) of emeralds measured in this study, the high values are found in emeralds from Santa Terezinha of Brazil and the medium to high values are found in emeralds from Madagascar, Zambia, Carnaiba/Socoto and Itabira of Brazil. These emeralds occur in geologically type II deposit. In contrast the low to medium values are found in emeralds from Colombia and Nigeria which occur in geologically type I deposit (Table 6.2).

The type II emerald deposits also show high specific gravity values whereas the type I emerald deposits give low values. The variation of SG values with the type of emerald deposits are consistent with those found in RI values (Table 6.2). As will be shown later that the variations of both RI and SG are related to the alkaline contents substitute in those emerald structures.

Table 6.2: Refractive indices (RI) of o-ray and specific gravity (SG) of emeralds from Brazil, Colombia, Madagascar, Zambia and Nigeria

Deposit type		Locality	RI (O-ray)	SG
Type I deposits (Non-schist related)	Ia	Nigeria (NI)	1.569 –1.582	2.601-2.687
	Ib	Colombia (CO)	1.571 –1.582	2.612-2.731
Type II Deposits (Schist related)	IIa	Brazil; Santa Terezinha (STA)	1.592– 1.597	2.723-2.812
	IIb	Madagascar (MA)	1.581 – 1.598	2.661-2.785
	IIb	Zambia (ZA)	1.580 – 1.597	2.582-2.782
	IIb	Brazil; Carnaiba/Socoto (CAR)	1.581 –1.591	2.705-2.769
	IIb	Brazil; Itabira (ITA)	1.581 –1.591	2.690-2.727

6.1.3 Internal Characteristics:

The common internal features of emeralds found in this study are both solid inclusions and fluid inclusions. Among them mineral inclusions are the most common internal features which are summarized in Table 6.3.

Table 6.3: Summary of mineral and other solid inclusions in emeralds from Brazil, Colombia, Madagascar, Zambia and Nigeria

Mineral inclusions	Type I (Non-schist related)		Type II (Schist related)				
	Nigeria; Kaduna Plateau	Colombia; Cordilla Oriental	Santa Terezinha (Brazil)	Carnaiba/ Socoto (Brazil)	Itabira (Brazil)	Madagas car; Mananjary	Zambia; Ndola Rural
Pyrite		X	X				
Spinel			X				
Talc			X				
Carbonates	X	X	X			X	X
Mica	X		X	X	X	X	X
Albite		X					
Quartz			X		X	X	X
Hematite						X	X
Fluorite	X						
Chlorite				X			
Rutile	X						
Ilmenite	X						
Amphibole						X	X
Organic substance		X					

Inclusion features can provide evidence as to the geochemical environment in which the emerald crystals grew and they can also be used to distinguish emeralds from different locality. As would be expected, micas of probably biotitic or phlogopitic composition are commonly found in emeralds from the schist-related type II deposits of Brazil, Madagascar and Zambia, whereas muscovite may be found in Nigerian emerald of the non-schist related type I deposits. In contrast Colombian emerald has no mica. Talc, quartz, chlorite, hematite and amphibole inclusions are not found in emeralds from both Nigeria and Colombia (type I; non-schist related). Along with the other characteristic mineral inclusions are dark organic substances, which are distinguished Colombian emerald from the others.

Fluid inclusions are generally found in emeralds from all deposits. However the characteristic 3-phase inclusions of emeralds are only occurred in emeralds from Colombia and Nigeria. Although the 3-phase inclusions from both deposits show jagged outline, but those of Columbia have lower liquid/vapor ratios than and can be distinguished from those of Nigeria (see Figure 3.74 for Nigeria and Figure 3.90 for Colombia).

6.1.4 Trace element mineral chemistry:

Besides the major elements, such as Si, Al, O and Be that are formed an emerald, the other foreign elements, such as Cr, V and Fe (chromophores), sodium, magnesium, cesium (alkalis) etc. can be replaced or built into emerald/beryl lattice or structural channels (see Figure 3.3). Structural and chemical considerations indicated that the following substitutions in emerald could be applicable in chemical formula (Hänni et al., 1987), as a follows:

a) Al^{3+} (octahedral) = $(Mg, Fe)^{2+}$ + Na^{+} (channel site)

b) Al^{3+} (octahedral) = $(Cr, Fe, V)^{3+}$

Divalent (doubly charged) ions substitution by alkalis such as Mg^{2+} mainly replace Al^{3+} on the lattice sites of structure of natural emerald while the larger sizes such as Na^{+} is built into the ring channels for balancing electric charge compensation. As seen in Tables 4.1 - 4.3 the major trace element substitution in those emerald structures are Na and Mg with subordinate Fe (except for the major Fe substitution in emeralds from Nigeria where there are only minor Na and Mg substitution) while other trace element substitutions are relatively minor. Therefore Na, Mg and probably Fe substitution should have the largest influence on the emerald's optical and physical properties. As shown in the cross-plots of RI versus Na+Mg+Fe (Figure 6.1) and SG versus Na+Mg+Fe (Figure 6.2), a good correlation can be seen in both diagrams which suggest the dependence of both RI and SG on the Na+Mg+Fe substitution in those emerald structure.

As also shown in Figures 6.1 and 6.2 and mentioned earlier that both RI and SG are relatively high in the Type II emerald deposits and low in the Type I emerald deposits. This data may also suggest that the Type II schist-related deposits could inherently have strong influence from the alkali content during their formation as compared with those of the Type I non-schist-related deposits.

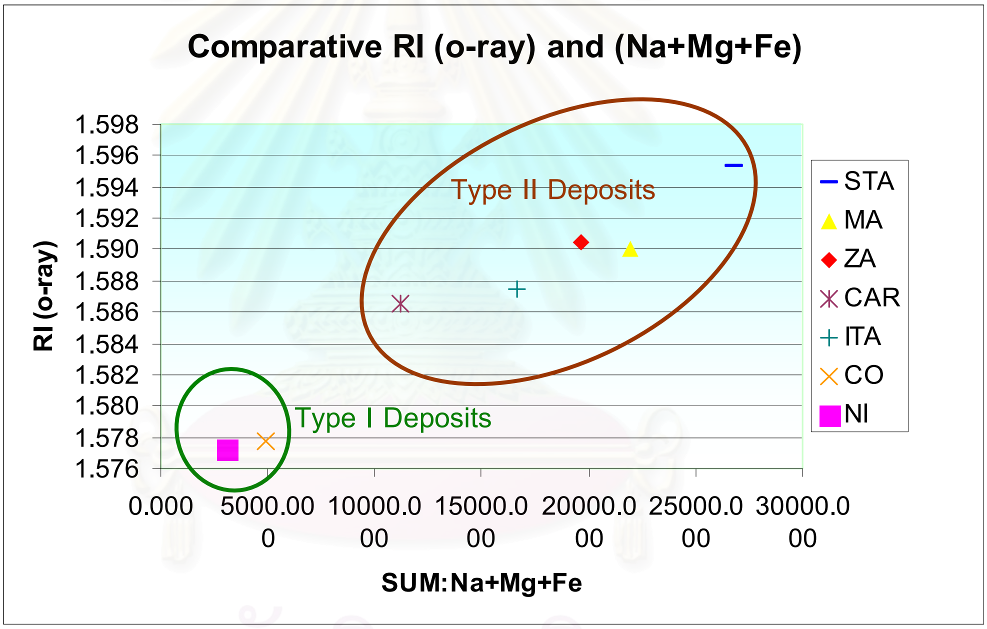

Figure 6.1: Correlation Diagram shows the highest optical values are found in Santa Tererzinha (STA) from Brazil, which also contain the highest values percentages of foreign elements whereas the lowest optical values are found in Nigeria (NI), also lowest foreign elements.

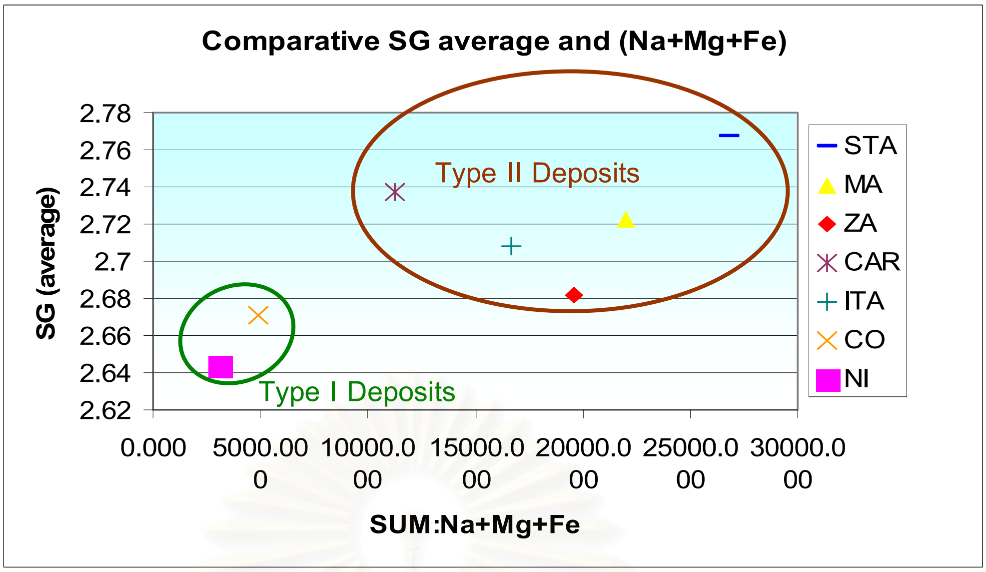

Figure 6.2: Correlation Diagram exhibits the highest specific gravity values are found in Santa Tererzinha (STA) from Brazil, which also contain the highest values percentages of foreign elements whereas the lowest specific gravity values are found in Nigeria (NI), also lowest foreign elements.

The diagram of Figure 6.3 shows that the rising of sodium plus magnesium and probably sodium plus iron plus magnesium in Figure 6.4, content of the emeralds is accompanied by a decreasing of the aluminum concentration. This variation suggest that the following substitution reaction for charge balance is likely to occur;

$$Al^{3+} = Na^{+} + (Mg, Fe)^{2+}$$

This can be confirmed by the strong correlation of Na vs Mg plot (R^2 = 0.95) in Figure 6.5 and Na vs (Mg+Fe) plot (R^2 = 0.93) in Figure 6.6. This assumption may imply that the majority of iron substitution in emeralds in this study could be in the form of divalent iron (Fe^{2+}). The substitution of Al^{3+} by Fe^{3+} is probably less significant as there is no clear correlation of Al vs Fe plot in Figure 6.7 (R^2 = 0.45). A good correlation of Al vs sum of all monovalent+divalent+trivalent ions contents (R^2 = 0.74) also suggests that all the cations probably substitute for Al^{3+} in octahedral site rather than for Be^{2+} in tetrahedral site (Figure 6.8).

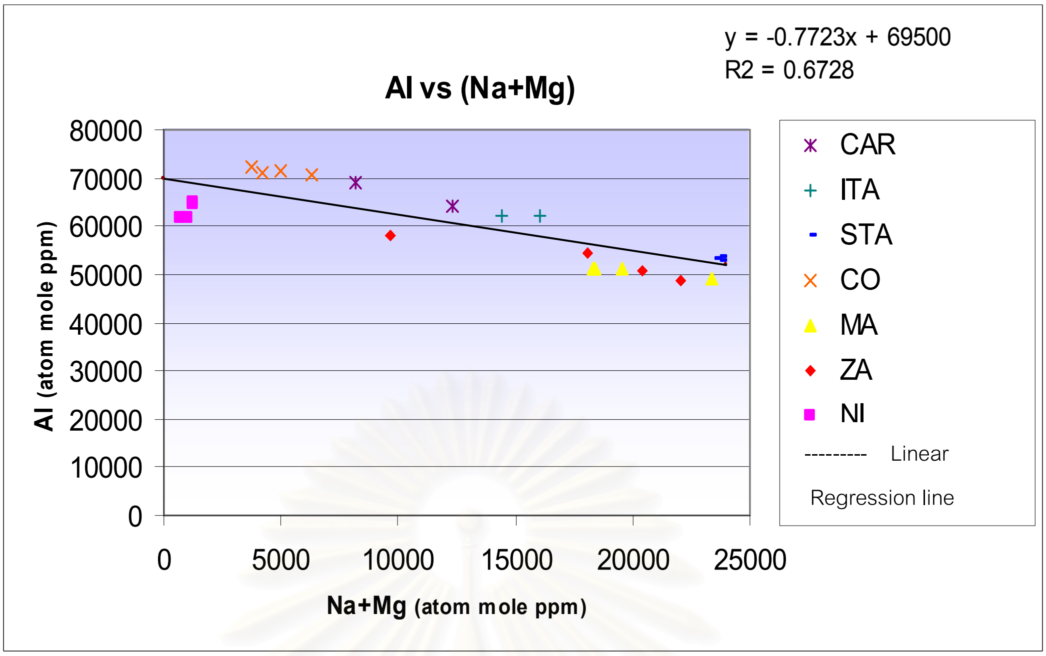

Figure 6.3: Plot of average Al versus Na+Mg contents of 23 emeralds from different geological occurrences.

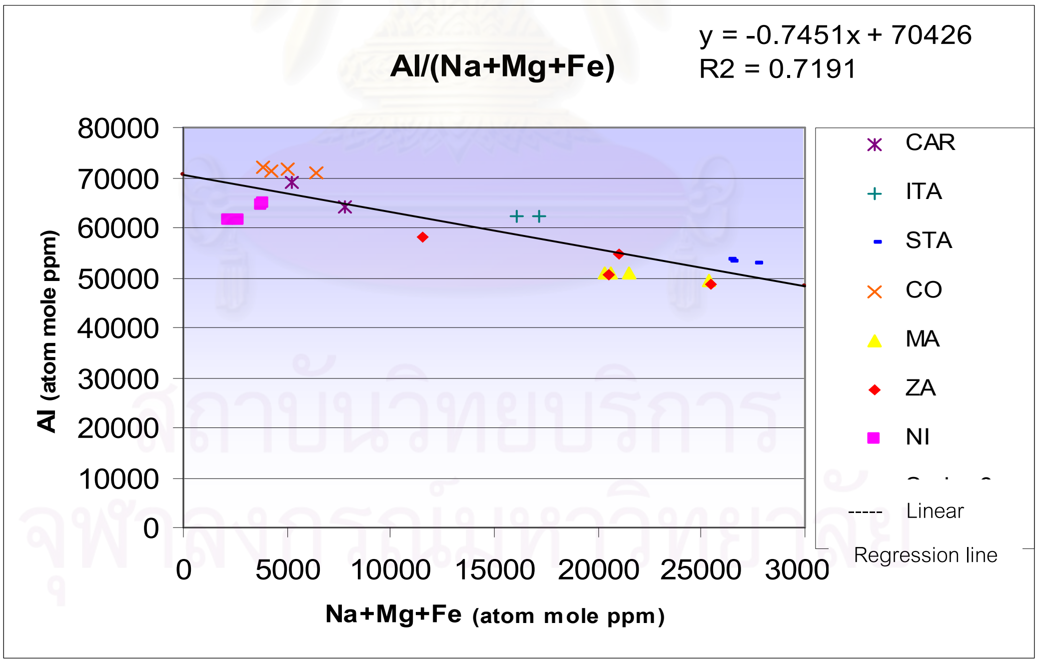

Figure 6.4: Plot of average Al versus Na+Fe+Mg contents of 23 emeralds from different geological occurrences.

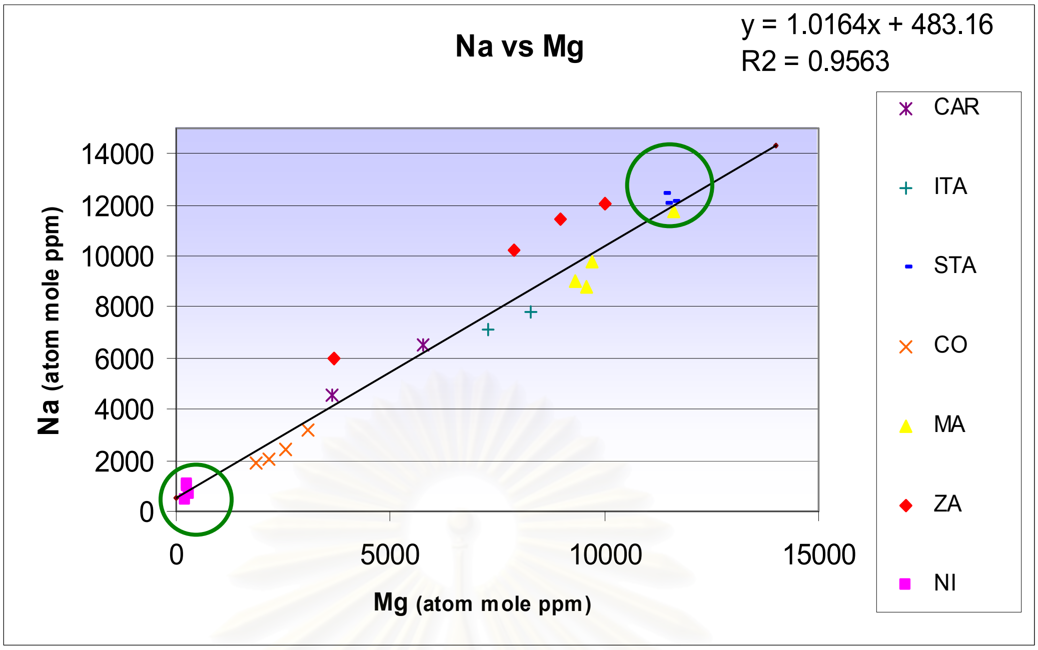

Figure 6.5: Plot of the average Na versus Mg contents of 23 emeralds from different geological occurrences.

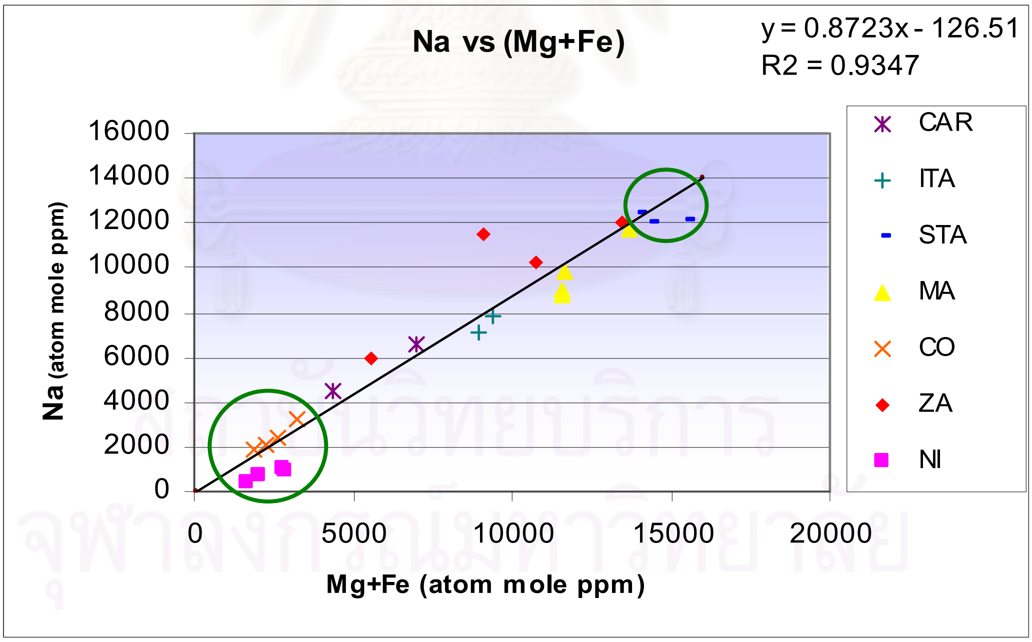

Figure 6.6: Plot of average Na versus (Mg+Fe) contents of 23 emeralds from different geological occurrences.

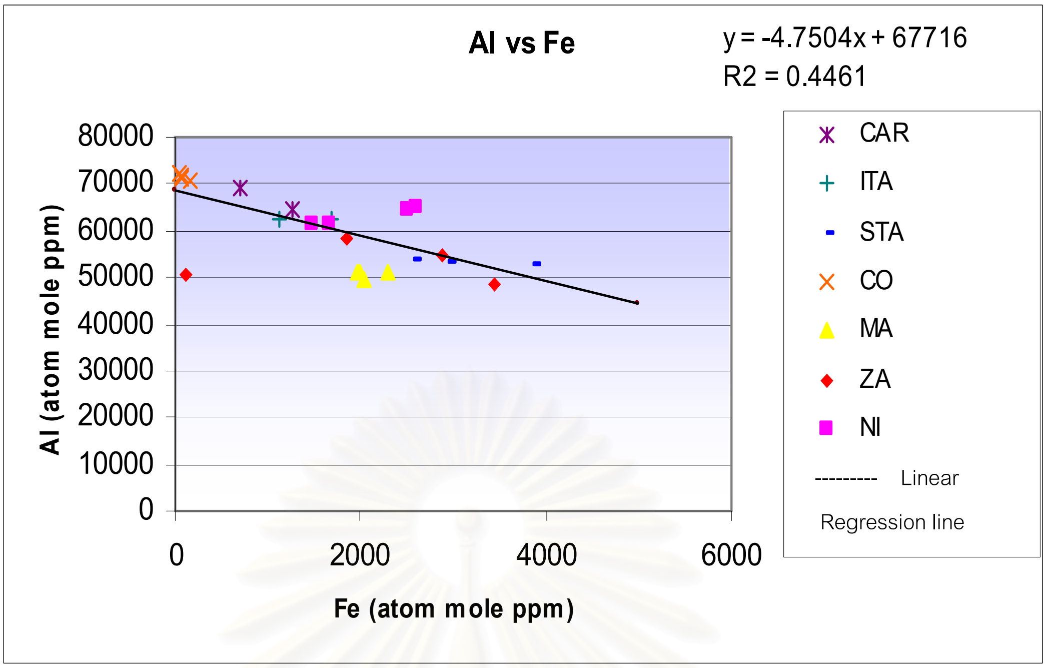

Figure 6.7: Plot of average Fe versus Al contents of 23 emeralds from different geological occurrences.

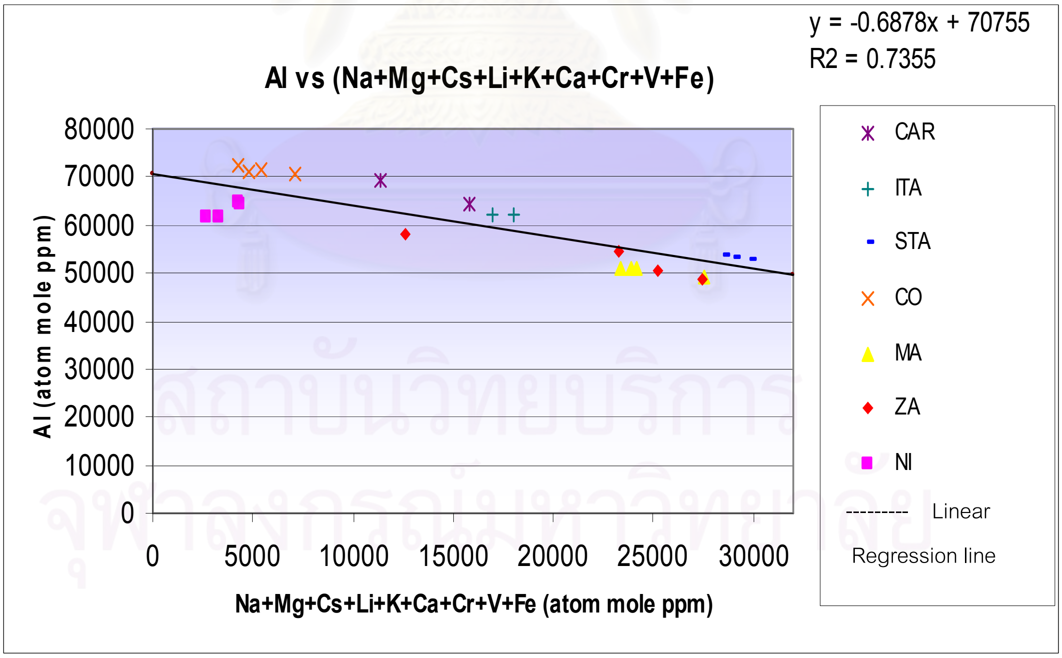

Figure 6.8: Plot of average Al versus sum of all Monovalent+Divalent+Trivalent ions contents from 7 different geological occurrences.

Figure 6.9 shows the relation of Cr and V. The emeralds from the Type II deposits (Santa Terezinha, Carnaiba/Socoto and Itabira, Zambia and Madagascar) contain higher Cr than V contents (Cr/V > 1) whereas those of the Type I deposits (Colombia and Nigeria) have lower or approximately equal proportion of Cr and V contents (Cr/V < or ~ 1). This data may imply that Cr might have been the important colouring element in the Type II schist-related deposits while both Cr and V are equally significant colouring elements in the Type I non-schist-related deposits.

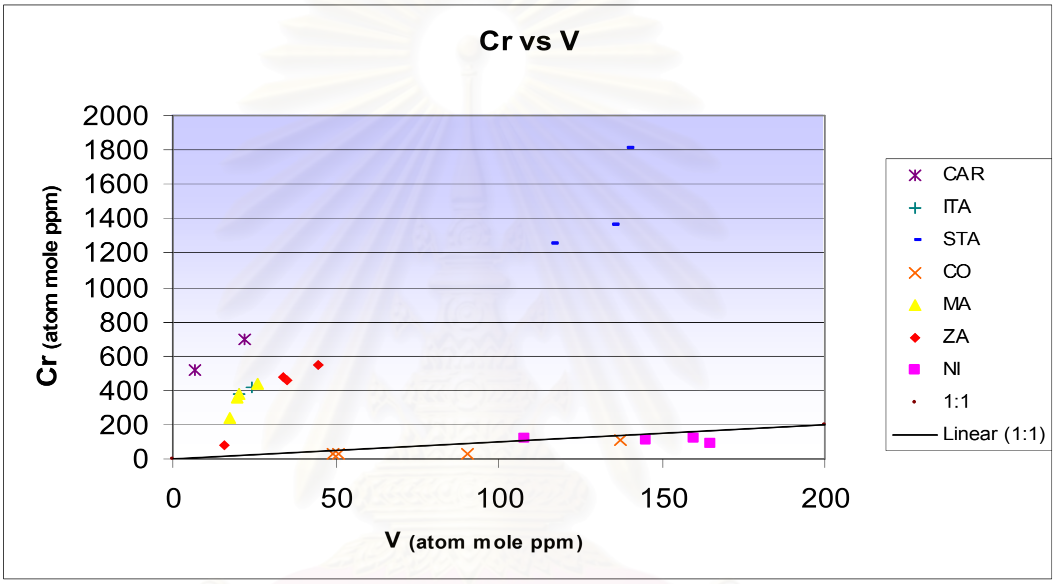

Figure 6.9: Plot of average Cr versus V contents of 23 emeralds from different geological occurrences.

6.1.5 Spectroscopic properties:

Most UV-Vis-NIR absorption spectra of emeralds measured in this study revealed the typical absorption bands of Cr^{3+} and V^{3+} combined with Fe^{2+} and Fe^{3+}, except those of Colombian emeralds without the iron absorption bands. This observation is consistent with the trace element data which show rather low content of iron in the Colombian emeralds. Furthermore all the spectra show almost identical positions of the major absorption bands for Cr^{3+} and V^{3+}. However as shown in the trace element data, most emeralds in this study contain both chromium and vanadium in which the Type II schist-related deposits are dominated mainly by Cr while the Type I non-schist-related deposits are dominated by both Cr and V. However, the respective portions of the (Cr^{3+} and V^{3+}) absorption bands exhibit essential identical spectra which cannot be separated from one another. Consequently, the contribution of these two elements to their respective colour of an emerald is therefore likely to be very similar.

The infrared spectra of almost all of the emeralds examined in this study indicate similarly the presence of both type I and type II water molecules except those of the Nigerian emerald and the Brazilian emerald from Santa Terezinha. The spectrum of Nigerian emerald is dominant by the type I water which is a free water type and indicate low alkali contents. In contrast the spectrum of the Brazilian emerald from Santa Terezinha is dominant by the type II water which is the electric dipole water molecule oriented and bonded to neighboring alkali or other cations in the ring channels. Therefore the emerald dominated by type II water indicates high alkali contents. These results are consistent with the trace element data which show the lowest alkali content in the Nigerian emeralds and the highest content in the Brazilian emeralds from Santa Terezinha. The spectra of emeralds from Madagascar, Zambia, Carnaiba/Socoto and Itabira and Colombia show a mixture of type I and type II water which are related to intermediate alkali contents.

6.2 Conclusions

It is rather difficult to separate between emeralds from similar geologic environments based on gemological data. However, if specific characteristics of geological occurrences are present distinctly, it is possible to determine the origin of an emerald.

1. In this study, emerald deposits have been classified and categorized in two major specific geological occurrences, non-schist-related type I deposits and schist-related type II deposits.

2. Inclusion features can be used to distinguish emeralds from different locality. As would be expected from mineral inclusions, biotite or phlogopite are commonly found in

emeralds from the schist-related type II deposits but they not found in non-schist related type I deposits. Emeralds from Colombia and Nigeria contain different jagged outline in 3-phase inclusions in which those from Colombia have lower liquid/vapor ratios.

3. It is shown in this study that some foreign elements such as Na, Mg and Fe have a strong influence on RI and SG of those emeralds in which the type II schist-related deposits show relatively higher values (the highest values are found in emerald from Santa Terezinha) while the type I non-schist-related deposits have somewhat lower values (the lowest values are found in emeralds from Nigeria).

4. It is likely that the majority of iron substitution in emeralds in this study could be in the form of divalent iron (Fe^{2+}). And all cations probably substitute for Al^{3+} in octahedral site rather than for Be^{2+} in tetrahedral site.

5. It was found that Cr might be the important colouring element in the type II schist-related deposits while both Cr and V have equally significant colouring elements in the type I non-schist-related deposits.

6. The emeralds from Zambia and Carnaiba/Socoto contain relatively high contents of Li and Cs, while the emeralds from Madagascar show exceptionally high K content. In the Colombian emeralds, both trace element data and UV-Vis-NIR spectra show consistently very low content of iron.

7. Nigerian emerald is dominated by the type I water and indicates low alkali contents. In contrast the Brazilian emerald from Santa Terezinha is dominated by the type II water which indicates high alkali contents.

8. These locality specific characteristics should be very useful for origin determination.

REFERENCES

Abduriyim, A. and Kitawaki H. (n.d.). Analysis on Cs Pink "Beryl" using a Laser Abltion System with Inductively Coupled Plasma Mass Spectrometer (LA-ICP-MS). www.Zenhokyo.co.jp

Arem, J.E. 1987. Beryl. Color encyclopedia of gemstones, 2nd edition. 50 – 55

Bosshart, G. 1982. Distinction of Natural and Synthetic Rubies by ultra violet spectrophotometry. Journal Gem and Gemmology, 18, 2: 145 – 160

Bosshart, G. 1991. Emeralds from Colombia (Part 1). Journal Gemmology, 22, 6: 355 - 361

Bosshart, G. 1991. Emeralds from Colombia (Part 2). Journal Gemmology, 22, 7: 409 - 425

Bosshart, G. 1991. Emeralds from Colombia (Part 1). Journal Gemmology, 22, 8: 500 - 503

Campbell, I.C.C. 1973. Emeralds Reputed to be of Zambian Origin. Journal Gemmology, 13, 5: 169 – 179

Cassedanne, J.P. and Sauer, D.A. 1984. The Santa Terezinha de Goiás Emerald Deposit. Gem & Gemology, 20,1: 4 – 13

Epstein, D.S. 1989. The Capoeirana Emerald Deposit near Nova Era, Minas Gerais, Brazil. Gem & Gemology, 25,3:150 – 158

Eppler, W.F. 1960. A Brazilian Emerald. Journal gemology, 7, 5: 221 - 225

Graziani, G., Gubelin, E. and Lucchesi, S. 1984. Report on the Investigation of an Emerald from the Kitwe District, Zambia. The Australian Gemmologiust, August: 227 – 233

Hänni, H., Schwarz, D. and Fischer, M. 1987. The emeralds of the Belmont Mine, Minas Gerais, Brazil. Journal Gemmology, 20, 7/8: 446 – 456

Hänni, H. 1992. Blue-green Emerald from Nigeria (A consideration of terminology). The Australian Gemmologist, 18, 1: 16 – 18

Hänni, H. et al. 1997. A Raman microscope in the gemological laboratory: first experiences of application. Journal Gem and Gemmology, 25, 6: 394 – 406

Hochleitner, R. 2002. The Emerald Mineralogically a Beryl. Emerald of the world, 10 - 15

Johnson, P.W. 1961. The Chivor Emerald mine. Journal Gemmology, 8, 4: 126 – 152

Keller, P.C. 1981, Emeralds of Colombia. Gem & Gemology,17, 2: 80 – 92

Koivula, J.I. 1982. Tourmaline as an Inclusion in Zambian Emeralds. Gem & Gemology, 18,4: 225 – 227

Koivula, J.I. 1984. Mineral inclusions in Zambian Emeralds. The Australian Gemmologiust, August: 235 – 239

Lind, T. 1986. Blue and green beryls (aquamarines and emeralds) of gem quality from Nigeria. Journal Gemmology, 20, 1: 40 – 48

Mathew, G., et al. 1988. Maxixe-type colour centre in natural colourless beryl from Orissa, India: an ESR and OA investigation. Journal Gem and Gemmology, 26, 4: 238 – 251

Miyata, T., et al. 1987. On the inclusion in emeralds from Santa Terezinha de Goiás, Brazil. Journal Gemmology, 20, 6: 377 – 379

Moroz, I.I. and Eliezri, I.Z. 1998. Emerald Chemistry from different deposits – An electron microprobe study. The Australian Gemmologist, 20, 2: 64 – 69

Newman, R. 1996. Emerald and Tanzanite Buying Guide. 155 p.

Pulz., G.M., et al. 1998. The Chemical signature of emeralds from the Campos Verdes-Santa Terezinha Mining District, Goiás, Brazil. Journal Gemmology, 26, 4: 252 - 261

Schmetzer, K., et al. 1997. Characterization of Chinese Hydrothermal Synthetic Emerald. Gem & Gemology, 33, 4: 276 – 291

Schmetzer, K. and Bank, H. 1981. An unusual pleochroism in Zambian emeralds. Journal Gem and Gemmology, 27, 7: 443 – 446

Schmetzer, K. and Kiefert, L. 1990. Water in Beryl – a contribution to the separability of natural and synthetic emeralds by infrared spectroscope. Journal Gemmology, 22, 4: 215 – 223

Schwarz, D. and Eidt, T. 1989. The Brazilian emeralds and their occurrences: Carnaíba, Bahia. Journal Gemmology, 21, 8: 474 – 486

Schwarz, D. 1990. The Brazilian emeralds and their occurrences: Socotó, Bahia. Journal Gemmology, 22, 3: 147 – 163

Schwarz, D. and Henn, U. 1992. Emerald from Madagascar. Journal Gem and Gemmology, 23, 3: 140 – 149

Schwarz, D. 1992. The Chemical Properties of Colombian emeralds. Journal Gemmology, 23, 4: 225 – 233

Schwarz, D. 1994. Emeralds from the Manajary region, Madagascar: Internal Features. Gem & Gemology, 30, 2: 88 – 101

Schwarz, D., et al. 1996. Emerald and green beryl from Central Nigeria. Journal Gemmology, 25, 2: 117 – 141

Schwarz, D. 2000. Gemmological Europa VII. Milano. Italy: Servizio Pubblico per il Controllo di Qualita dei Materiali Gemmologici: 221 p.

Schwarz, D. and Giuliani, G. 2001. Emerald Deposits - A Review. The Australian Gemmologist, 21, 1: 17 – 23

Schwarz, D., et al. 2002. The Origin of Emerald. Emerald of the World. Lapis International, Germany: 18 - 35.

Schwarz, D. and Giuliani, G. 2002. South America: Colombia. Emerald of the World. Lapis International, Germany: 36 - 45.

Schwarz, D. and Giuliani, G. 2002. South America: Brazil. Emerald of the World. Lapis International, Germany: 46 - 51.

Seifert, A.V., et al. 2004. Emerald mineralization in the Kafubu area, Zambia. Bulletin of Geosciences, 79, 1: 1 – 40

Sliwa, A.S. and Nguluwe, C.A. 1984. Geological Setting of Zambian Emerald Deposits. Precambrian Research. 25: 213 – 228

Sinkankas, J. 1989. Emerald and Other Beryls. Geoscience Press, Prescott, Arizona: 665 p.

Treryakova, L.I., et al. 1997. A combined spectroscopic method for non-destructive gem identification. Journal Gem and Gemmology, 29, 8: 532 – 539

Ward, F. 1993. Emerald. Gem Book Publishers: 64 p.

Williams, K.P.J., et al. 1997. The Renishaw Raman database of gemological and mineralogical materials. issue 2 July

APPENDICES

APPENDIX I

Figure I.1: GIA GemSet colour specimens; showing the range of emerald colouration in this study (right).

- Hue is very strong bluish green (A)
- Hue is very slightly bluish green (B and C)
- Hue is bluish green (D)
- Hue is green (E)

* All under daylight

A

B

C

D

E

Table I.1: List of hue, tone and saturation terms for describing gem colors, with their abbreviations.

Hue			
P	Purple	slyG	Slightly yellowish Green
Rp	reddish Purple	G	Green
RP/PR	red-purple or purple-red	VslbG	Very slightly bluish Green
slpR	slightly purplish Red	BG	Bluish Green
stpR	strongly purplish Red	VstbG	Very strongly bluish Green
R	Red	GB/BG	GREEN-BLUE or BLUE-GREEN
oR	Orangy red	VstgB	Very strongly greenish Blue
RO/OR	Red-orange-Orange-red	gB	Blue
rO	reddish Orange	vslgB	violetish Blue
O	Orange	B	bluish Violet
yO	yellowish Orange	vB	Violet
Oy	Orangy Yellow	bV	Bluish Purple
Y	Yellow	V	Pink
gY	greenish Yellow	bP	Brown
YG/GY	Yellow-Green or Green Yellow	Pk	
styG	strongly yellowish Green	Br	
yG	yellowish Green		

TONE		SATURATION	
0	colorless or white	1	grayish (brownish)
1	extremely light	2	slightly grayish (brownish)
2	very light	3	very slight grayish (brownish)
3	light	4	moderately strong
4	medium light	5	strong
5	medium	6	vivid
6	medium dark		
7	dark		
8	very dark		
9	extremely dark		
10	black		

Table I.2: Colour codes of emeralds in this study from different areas based on the GIA Gemset

Origin/ Sample		GIA Gemset colour Code	(Tone, Saturation, Hue)
Nigeria (Kaduna Platua)	NI-14	vslbG2/3	very light, very slightly greyish, very slightly bluish Green
	NI-8,9,11,26	vslbG3/4	light, moderately strong, very slightly bluish Green
	NI-2,3,10,16,25	vslbG4/4	medium light, moderately strong, very slightly bluish Green
	NI-13,17,30	bG2/3	very light, very slightly greyish, bluish Green
	NI-1,7,19,20,24	bG3/3	light, very slightly greyish, bluish Green
	NI-4,5,6,12,18,21,22,27,28, 29	bG4/3	medium light, very slightly greyish, bluish Green
	NI-15,23	G3/1	light, grayish, Green
	NI-14	vslbG2/3	very light, very slightly greyish, very slightly bluish Green
	NI-8,9,11,26	vslbG3/4	light, moderately strong, very slightly bluish Green

Origin	Sample	GIA Gemset colour Code	(Tone, Saturation, Hue)
	NI-2,3,10,16,25	vslbG4/4	medium light, moderately strong, very slightly bluish Green
Colombia (Cordilla Oreintal-Coscues, Muzo)	CO-1,5,7,9,14,16,21,24	vslbG2/3	very light, very slightly grayish, very slightly bluish Green
	CO-6,22,29	vslbG3/4	light, moderate strong, very slightly bluish Green
	CO-10,15	vslbG4/4	medium light, moderate strong, very slightly bluish Green
	CO-23,26	vslbG5/3	medium, very slightly grayish, very slightly bluish Green
	CO-18,27,28	bG2/3	very light, very slightly greyish, bluish Green
	CO-2,12,13,17,19,25,30	bG3/3	light, very slightly greyish, bluish Green
	CO-8	bG4/4	medium light, moderately strong, bluish Green

Origin	Sample	GIA Gemset colour Code	(Tone, Saturation, Hue)
	CO-3,4,11,20	G3/1	light, greyish, Green
Brazil: (Santa Terezinha in Goais State)	STA-2,3,4,5,8	vslbG3/4	light, moderately strong, very slightly bluish Green
	STA-7,9	vslbG4/4	medium light, moderately strong, very slightly bluish Green
	STA-1,6	vslbG7/3	dark, very slightly grayish, very slightly bluish Green
	STA-10	bG4/3	medium light, very slightly grayish, bluish Green
Madagascar (Manajary region)	MA-25	vstbG4/5	medium light, strong, very strongly bluish Green
	MA-24,28	vstbG5/3	medium, very slightly greyish, very strongly bluish Green
	MA-3,10	vslbG3/4	light, moderate strong, very slightly bluish Green
	MA-1,4,7,8,11,13,17,18,19, 22	vslbG4/4	medium light, moderate strong, very slightly bluish Green
	MA-2,5,6,26,29,30	vslbG5/5	medium, strong, very slightly bluish Green

Origin	Sample	GIA Gemset colour Code	(Tone, Saturation, Hue)
	MA-14	bG3/3	light, very slightly greyish, bluish Green
	MA-9,12,15,16,20,21,23	bG4/3	medium light, very slightly grayish, bluish Green
	MA-15,27	bG4/4	medium light, moderate strong, bluish Green
Zambia (Ndola Rural district, Kafubu area	ZA-1	vstbG2/3	very light, very slightly grayish, very strongly bluish Green
	ZA-29	vstbG6/4	medium dark, moderate strong, very strongly bluish Green
	ZA-21	vslbG2/3	very light, very slightly greyish, very slightly bluish Green
	ZA-2,3,4,7,8,10,13,22	vslbG3/4	light, moderately strong, very slightly bluish Green
	ZA-9,17,30	vslbG4/4	medium light, moderately strong, very slightly bluish Green
	ZA-14	vslbG5/3	medium, very slightly greyish, very slightly bluish Green
	ZA-5,15,16,19,20,23	vslbG5/5	medium, strong, very slightly bluish Green

Origin	Sample	GIA Gemset colour Code	(Tone, Saturation, Hue)
	ZA-24	vslbG6/4	medium dark, moderately strong, very slightly bluish Green
	ZA-28	bG3/3	light, very slightly greyish, bluish Green
	ZA-6,11,12,18,26,27	bG4/3	medium light, very slightly greyish, bluish Green
	ZA-25	bG4/4	medium light, moderately strong, bluish Green
Brazil: (Carnaiba/ Socoto in Bahia State)	CAR-10	vslbG2/3	very light, very slightly grayish, very slightly bluish Green
	CAR-2	vslbG3/4	light, Moderately strong, very slightly bluish Green
	CAR-3,4	vslbG4/4	medium light, moderately strong, very slightly bluish Green
	CAR-7	bG2/3	very light, very slightly grayish, bluish Green
	CAR-8	bG3/3	light, very slightly grayish, bluish Green

Origin	Sample	GIA Gemset colour Code	(Tone, Saturation, Hue)
	CAR-1	G4/3	medium light, very slightly grayish, Green
	CAR-5,9	G3/1	light, grayish, Green
	CAR-6	G4/2	medium light, slightly grayish, Green
Brazil: (Itabira in Minas Gerais State)	ITA-2,3,5,8	vslbG3/4	light, moderately strong, very slightly bluish Green
	ITA-1,6	vslbG4/4	medium light, moderately strong, very slightly bluish Green
	ITA-7,9,10	bG4/3	medium light, very slightly grayish, bluish Green

Table I.3: List the gemological properties of emeralds from Brazil, Colombia, Madagascar, Zambian and Nigeria

Brazil (Carnaiba/Socoto)

Sample no. (ct)	RI		Birefringence	SG	Fluorescence	
	ne	no		Approximately	LWUV	SWUV
CAR1 (0.208)	1.581	1.590	0.009	2.77	inert	inert
CAR2 (0.245)	1.580	1.591	0.011	2.74	inert	inert
CAR3 (0.229)	1.580	1.589	0.009	2.76	inert	inert
CAR4 (0.303)	1.581	1.591	0.010	2.74	inert	inert
CAR5 (0.378)	1.572	1.581	0.009	2.70	inert	inert
CAR6 (0.405)	1.571	1.585	0.014	2.73	inert	inert
CAR7 (0.189)	1.571	1.582	0.011	2.73	inert	inert
CAR8 (0.308)	1.572	1.585	0.013	2.71	inert	inert
CAR9 (0.589)	1.575	1.584	0.005	2.72	inert	inert
CAR10 (0.264)	1.572	1.581	0.005	2.73	inert	inert

Brazil (Itabira)

ITA1 (0.342)	1.576	1.582	0.006	2.69	inert	inert
ITA2 (0.482)	1.579	1.586	0.007	2.70	inert	inert
ITA3 (0.852)	1.579	1.585	0.006	2.71	inert	inert
ITA5 (0.265)	1.570	1.581	0.010	2.69	inert	inert
ITA6 (0.178)	1.580	1.591	0.010	2.70	inert	inert
ITA7 (1.178)	1.580	1.589	0.009	2.70	inert	inert
ITA8 (0.713)	1.580	1.589	0.009	2.69	inert	inert
ITA9 (0.211)	1.580	1.589	0.009	2.72	inert	inert
ITA10 (0.292)	1.580	1.589	0.009	2.72	inert	inert

Brazil (Santa Terezinha)

STA1 (0.330)	1.583	1.596	0.013	2.72	inert	inert
STA2 (0.245)	1.586	1.598	0.012	2.80	inert	inert
STA3 (0.242)	1.585	1.595	0.010	2.74	inert	inert
STA4 (0.257)	1.579	1.593	0.014	2.73	inert	inert
STA5 (0.192)	1.586	1.597	0.011	2.81	inert	inert
STA6 (0.590)	1.582	1.595	0.013	2.76	inert	inert
STA7 (0.419)	1.585	1.592	0.012	2.76	inert	inert
STA8 (1.025)	1.583	1.595	0.012	2.72	inert	inert

Table I.3: List the gemological properties of emeralds from Brazil, Colombia, Madagascar, Zambian and Nigeria (*Brazil (Santa Terezinha)*

Sample no. (ct)	RI		Birefringence	SG	Fluorescence	
	ne	no		Approximately	LWUV	SWUV
STA9 (0.593)	1.586	1.596	0.010	2.77	inert	inert
STA10 (2.702)	1.582	1.594	0.012	2.76	inert	inert

Colombia

CO1 (1.286)	1.569	1.581	0.012	2.70	inert	inert
CO2 (0.059)	1.571	1.580	0.009	2.62	inert	inert
CO3 (0.458)	1.571	1.580	0.009	2.71	inert	inert
CO4 (0.524)	1.570	1.578	0.008	2.73	inert	inert
CO5 (0.959)	1.571	1.581	0.010	2.70	inert	inert
CO6 (0.826)	1.566	1.576	0.008	2.66	inert	inert
CO7 (1.714)	1.569	1.580	0.011	2.68	inert	inert
CO8 (1.190)	1.572	1.580	0.008	2.70	inert	inert
CO9 (0.498)	1.570	1.579	0.009	2.69	inert	inert
CO10 (1.519)	1.561	1.571	0.010	2.64	inert	inert
CO11 (1.806)	1.562	1.575	0.013	2.66	inert	inert
CO12 (2.104)	1.570	1.582	0.012	2.70	inert	inert
CO13 (1.832)	1.569	1.580	0.018	2.64	inert	inert
CO14 (1.207)	1.570	1.581	0.011	2.67	inert	inert
CO15 (2.070)	1.570	1.579	0.009	2.69	inert	inert
CO16 (1.117)	1.569	1.576	0.007	2.69	inert	inert
CO17 (1.368)	1.571	1.582	0.011	2.67	inert	inert
CO18 (1.764)	1.569	1.576	0.007	2.64	inert	inert
CO19 (2.110)	1.570	1.579	0.009	2.67	inert	inert
CO20 (2.427)	1.568	1.578	0.010	2.70	inert	inert
CO21 (0.863)	1.570	1.580	0.010	2.69	inert	inert
CO22 (2.312)	1.570	1.579	0.009	2.68	inert	inert
CO23 (4.423)	1.570	1.579	0.009	2.61	inert	inert
CO24 (3.208)	1.571	1.580	0.009	2.65	inert	inert
CO25 (1.012)	1.571	1.579	0.008	2.69	inert	inert
CO26 (1.352)	1.570	1.579	0.009	2.65	inert	inert
CO27 (0.574)	1.569	1.580	0.018	2.70	inert	inert

Table I.3: List the gemological properties of emeralds from Brazil, Colombia, Madagascar, Zambian and Nigeria (continued)

Colombia

Sample no.	RI		Birefringence	SG	Fluorescence	
	ne	no			LWUV	SWUV
CO28 (1.769)	1.567	1.575	0.008	2.69	inert	inert
CO29 (0.709)	1.570	1.579	0.009	2.71	inert	inert
CO30 (0.709)	1.570	1.580	0.010	2.70	inert	inert

Madagascar

MA1 (1.316)	1.572	1.581	0.009	2.74	inert	inert
MA2 (0.865)	1.584	1.594	0.010	2.71	inert	inert
MA3 (1.663)	1.581	1.590	0.009	2.74	inert	inert
MA4 (0.666)	1.580	1.591	0.011	2.69	inert	inert
MA5 (0.818)	1.584	1.593	0.009	2.75	inert	inert
MA6 (0.892)	1.581	1.591	0.010	2.71	inert	inert
MA7 (2.131)	1.580	1.590	0.010	2.70	inert	inert
MA8 (1.271)	1.580	1.589	0.009	2.71	inert	inert
MA9 (0.309)	1.582	1.591	0.009	2.73	inert	inert
MA10 (0.279)	1.581	1.580	0.009	2.66	inert	inert
MA11 (0.359)	1.570	1.589	0.010	2.66	inert	inert
MA12 (0.481)	1.576	1.591	0.013	2.72	inert	inert
MA13 (0.314)	1.582	1.590	0.008	2.75	inert	inert
MA14 (0.264)	1.582	1.591	0.009	2.77	inert	inert
MA15 (1.316)	1.580	1.590	0.010	2.72	inert	inert
MA16 (0.182)	1.579	1.591	0.012	2.78	inert	inert
MA17 (0.334)	1.581	1.591	0.010	2.66	inert	inert
MA18 (0.447)	1.580	1.590	0.010	2.71	inert	inert
MA19 (1.531)	1.582	1.598	0.016	2.71	inert	inert
MA20 (1.301)	1.582	1.592	0.010	2.72	inert	inert
MA21 (0.431)	1.580	1.591	0.011	2.68	inert	inert
MA22 (0.303)	1.581	1.590	0.009	2.74	inert	inert
MA23 (0.338)	1.584	1.593	0.009	2.66	inert	inert
MA24 (0.418)	1.575	1.598	0.023	2.74	inert	inert
MA25 (0.466)	1.580	1.590	0.010	2.73	inert	inert

Table I.3: List the gemological properties of emeralds from Brazil, Colombia, Madagascar, Zambian and Nigeria (continued)

Madagascar

Sample no.	RI		Birefringence	SG	Fluorescence	
	ne	no			LWUV	SWUV
MA26 (0.758)	1.579	1.592	0.013	2.73	inert	inert
MA27 (0.443)	1.584	1.596	0.012	2.71	inert	inert
MA28 (1.716)	1.580	1.590	0.010	2.70	inert	inert
MA29 (1.236)	1.580	1.590	0.010	2.71	inert	inert
MA30 (1.763)	1.584	1.595	0.011	2.72	inert	inert

Zambia

ZA1 (0.364)	1.580	1.591	0.011	2.74	inert	inert
ZA2 (7.753)	1.575	1.586	0.011	2.70	inert	inert
ZA3 (1.651)	1.578	1.584	0.006	2.72	inert	inert
ZA4 (1.899)	1.578	1.591	0.013	2.72	inert	inert
ZA5 (2.986)	1.581	1.591	0.010	2.72	inert	inert
ZA6 (3.988)	1.579	1.589	0.010	2.71	inert	inert
ZA7 (4.081)	1.580	1.589	0.009	2.71	inert	inert
ZA8 (8.351)	1.579	1.589	0.010	2.72	inert	inert
ZA9 (1.027)	1.578	-	-	2.73	inert	inert
ZA10 (0.847)	1.582	1.590	0.008	2.78	inert	inert
ZA11 (0.580)	1.578	1.586	0.008	2.68	inert	inert
ZA12 (0.365)	1.581	1.590	0.009	2.58	inert	inert
ZA13 (0.779)	1.581	1.590	0.009	2.69	inert	inert
ZA14 (0.384)	1.573	1.588	0.015	2.73	inert	inert
ZA15 (0.628)	1.574	1.589	0.015	2.70	inert	inert
ZA16 (0.551)	1.582	1.597	0.015	2.71	inert	inert
ZA17 (0.654)	1.584	1.592	0.008	2.74	inert	inert
ZA18 (0.557)	1.586	1.596	0.010	2.73	inert	inert
ZA19 (0.451)	1.578	1.598	0.016	2.70	inert	inert
ZA20 (2.447)	1.582	1.592	0.010	2.75	inert	inert
ZA21 (0.696)	1.575	1.588	0.013	2.70	inert	inert
ZA22 (1.091)	1.582	1.591	0.009	2.70	inert	inert
ZA23 (1.038)	1.579	1.591	0.012	2.72	inert	inert

Table I.3: List the gemological properties of emeralds from Brazil, Colombia, Madagascar, Zambian and Nigeria (continued)

Zambia

Sample no.	RI		Birefringence	SG	Fluorescence	
	ne	no			LWUV	SWUV
ZA24 (1.579)	1.580	1.589	0.009	2.74	inert	inert
ZA25 (0.589)	1.579	1.591	0.012	2.73	inert	inert
ZA26 (0.969)	1.580	1.590	0.010	2.73	inert	inert
ZA27 (0.823)	1.580	1.589	0.009	2.74	inert	inert
ZA28 (2.890)	1.578	1.590	0.012	2.71	inert	inert
ZA29 (1.171)	1.578	1.590	0.012	2.70	inert	inert
ZA30 (0.353)	1.580	1.590	0.010	2.72	inert	inert

Nigeria

NI1 (1.022)	1.562	1.578	0.016	2.61	inert	inert
NI2 (1.057)	1.561	1.575	0.014	2.65	inert	inert
NI3 (1.446)	-	1.572	-	2.64	inert	inert
NI4 (1.531)	1.562	1.570	0.008	2.64	inert	inert
NI5 (0.828)	1.560	1.573	0.013	2.66	inert	inert
NI6 (2.660)	1.560	1.571	0.011	2.66	inert	inert
NI7 (0.678)	1.565	1.572	0.007	2.66	inert	inert
NI8 (1.154)	1.561	1.570	0.009	2.62	inert	inert
NI9 (0.698)	1.568	1.575	0.007	2.63	inert	inert
NI10 (0.874)	1.576	1.582	0.016	2.66	inert	inert
NI11 (3.190)	1.569	1.579	0.010	2.61	inert	inert
NI12 (2.416)	1.568	1.575	0.007	2.67	inert	inert
NI13 (0.189)	1.561	1.569	0.008	2.60	inert	inert
NI14 (0.312)	1.568	1.576	0.008	2.64	inert	inert
NI15 (2.064)	1.569	1.578	0.009	2.63	inert	inert
NI16 (4.110)	1.570	1.579	0.009	2.64	inert	inert
NI17 (0.805)	1.561	1.571	0.001	2.65	inert	inert
NI18 (2.316)	1.563	1.571	0.008	2.60	inert	inert
NI19 (0.472)	1.567	1.580	0.013	2.61	inert	inert
NI20 (0.606)	1.568	1.577	0.009	2.66	inert	inert
NI21 (0.602)	1.569	1.582	0.013	2.66	inert	inert

Table I.3: List the gemological properties of emeralds from Brazil, Colombia, Madagascar, Zambian and Nigeria (continued)

Nigeria

Sample no.	RI		Birefringence	SG	Fluorescence	
	ne	no			LWUV	SWUV
NI22 (1.850)	1.565	1.573	0.008	2.65	inert	inert
NI23 (0.612)	1.562	1.570	0.008	2.65	inert	inert
NI24 (0.848)	1.560	1.570	0.010	2.66	inert	inert
NI25 (0.877)	1.562	1.571	0.009	2.65	inert	inert
NI26 (1.108)	1.563	1.571	0.008	2.60	inert	inert
NI27 (1.640)	1.563	1.573	0.010	2.68	inert	inert
NI28 (1.068)	1.567	1.577	0.010	2.67	inert	inert
NI29 (4.083)	1.565	1.574	0.009	2.67	inert	inert
NI30 (0.813)	1.569	1.578	0.009	2.68	inert	inert

Table I.4: Major Raman Shift peaks of the mineral inclusions in this study (William et al., 1997)

Minerals	Major Raman Shift peaks at 200 – 2000 cm^{-1}
Actinolite	383, 665, 669, 1066
Albite	279, 472, 510, 1126
Apatite	433, 434, 593, 965, 966, 1056
Barytocalcite	227, 228, 264, 703, 1087
Beryl	323, 324, 398, 399, 402, 451, 526, 529, 532, 686, 687, 690, 691, 1012, 1013, 1019, 1060, 1070, 1072, 1075, 1240
Biotite	204, 359, 362, 406, 413, 543, 549, 552, 556, 557, 563, 714, 715, 752, 756, 782, 787, 789, 802, 805, 913, 1070, 1073, 1082, 1287
Calcite	278, 283, 285, 714, 716, 1083, 1087, 1088, 1434, 1437, 1746
Chlorite	203, 352, 361, 549, 676, 678, 679, 1081
Chromite	222, 538, 549, 573, 583, 586, 658, 671, 700, 703, 752, 1580
Dolomite	300, 301, 302,724, 725, 727, 1097, 1099, 1100, 1440, 1442, 1444, 1758, 1760
Emerald	315, 319, 322, 323, 393, 394, 395, 397, 398, 681, 683, 1033, 1066, 1067, 1068, 1069, 1071
Feldspar	212, 285, 286, 293, 455, 459, 476, 478, 481, 510, 514, 766, 817, 1101
Fluorite	320, 837, 840, 841, 913, 920, 926, 929, 946, 947, 950, 1031, 1125, 1154, 1253, 1293, 1294, 1297, 1358, 1360, 1364, 1391, 1395, 1398, 1449, 1466, 1505, 1576, 1580
Hematite (Fe_2O_3)	202, 227, 230, 248, 250, 260, 292, 295, 298, 303, 350, 392, 412, 413, 416, 417, 499, 500, 504, 615, 617, 666, 675, 804, 1078, 1157, 1321, 1324, 1337, 1342
Magnetite	313, 555, 668, 680,729, 738, 739,
Phlogopite	282, 331, 565, 685,746, 785, 1091
Pyrite	347, 352, 381, 388, 433, 443
Pyroxene	230, 321, 323, 386, 387, 506, 526, 559, 664, 666, 858, 1012, 1014

Table I.4: William et al. (1997), Major Raman Shift peaks of the mineral inclusions in this study (continued).

Spinel	402, 664, 718, 762, 763, 803, 930
Rutile	237, 238, 240, 242, 441, 448, 449, 610, 612, 613, 800
Sulpher / Sulphide	217, 245, 437, 472
Talc	289, 362, 434, 468, 678, 793
Quartz	204, 207, 208, 214, 264, 265, 354, 356, 391, 398, 412, 462, 465, 466, 467, 505, 693, 697, 799, 813, 1159, 1163, 1164

APPENDIX II

FTIR spectra of emerald samples from Nigeria, Colombia, Brazil, Madagascar and Zambia;

- 15 samples of Kaduna Plateau emeralds from Nigeria: NI3, NI4, NI5, NI11, NI12, NI14, NI15, NI17, NI10, NI20, NI23, NI24, NI25, NI28, NI30

- 12 samples of Cordillera Oriental emeralds from Colombia: CO1, CO2, CO4, CO6, CO8, CO11, CO13, CO18, CO20, CO22, CO26, CO27

- 4 samples of Santa Terezinha from Goais State, Brazil: SAN3, SAN7, SAN8, SAN10

- 14 samples of Manajary emeralds from Madagascar: MA1, MA3, MA9, MA15, MA17, MA18, MA21, MA23, MA24, MA26, MA27, MA28, MA30

- 14 samples of emeralds from Ndola Rural district: ZA3, ZA4, ZA5, ZA11, ZA12, ZA14, ZA15, ZA17, ZA20, ZA23, ZA24, ZA25, ZA28, ZA30

- 5 samples of Carnaiba/Socoto emeralds from Bahia State, Brazil: CAR2, CAR3, CAR4, CAR8, CAR9

- 5 samples of Itabira emeralds from Minas Gerias State, Brazil: ITA1, ITA2, ITA3, ITA7, ITA9

FTIR spectra of emerald samples from Nigeria: *Pure Type I H_2O (Ia)*

NI 3	NI 4
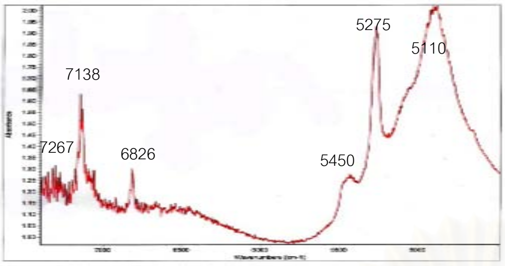	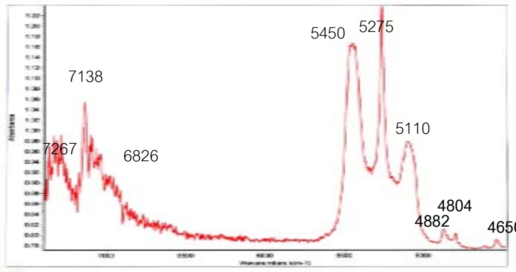
NI 5	**NI 11**
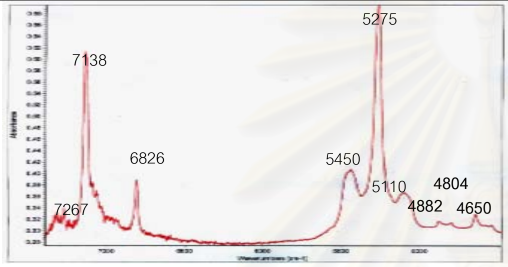	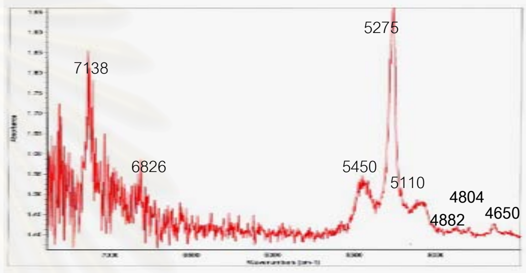
NI 12	**NI 14**
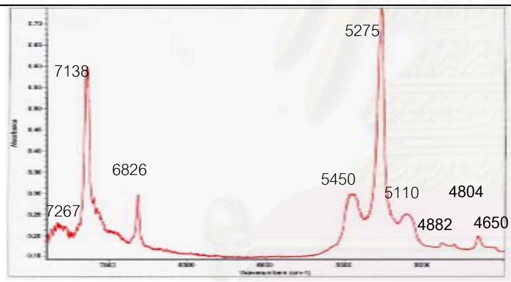	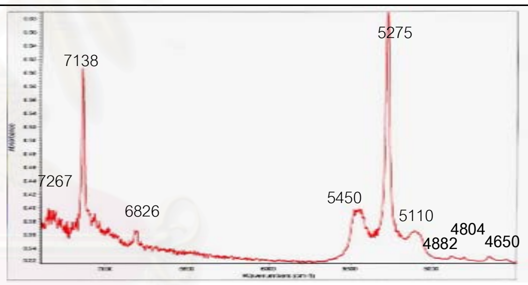
NI 15	**NI 17**
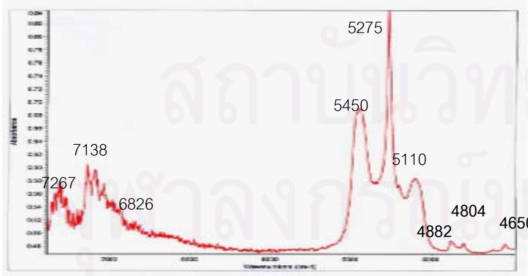	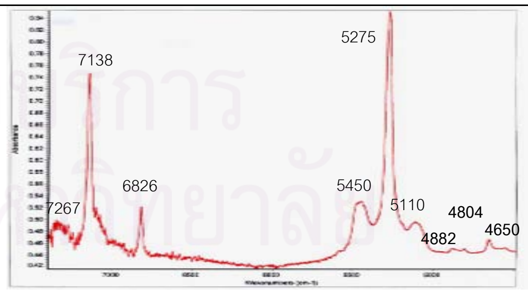

FTIR spectra of emerald samples from Nigeria: *Pure Type I H_2O (Ia), continue*

NI 20

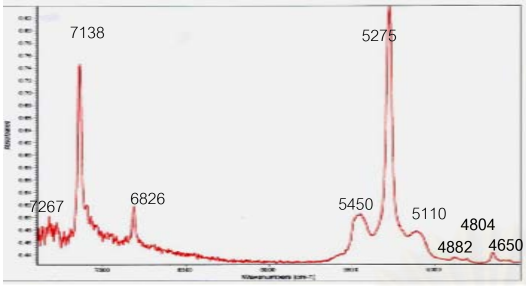

NI 23

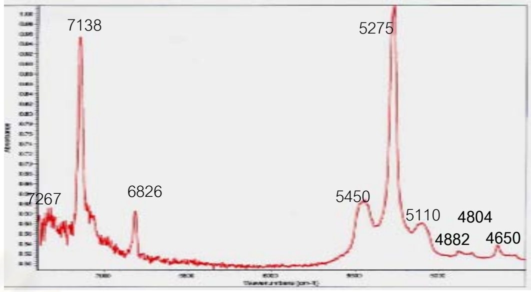

NI 24

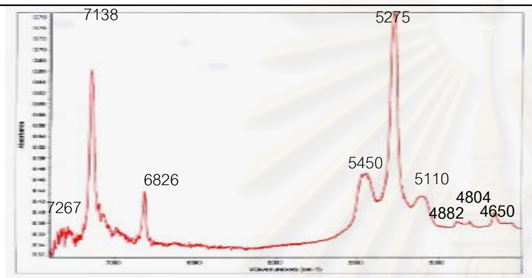

NI 25

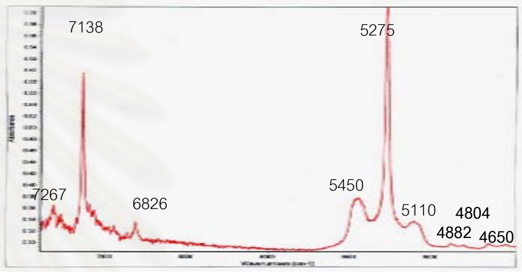

NI 28

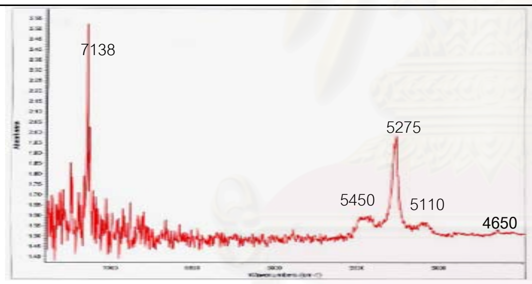

NI 30

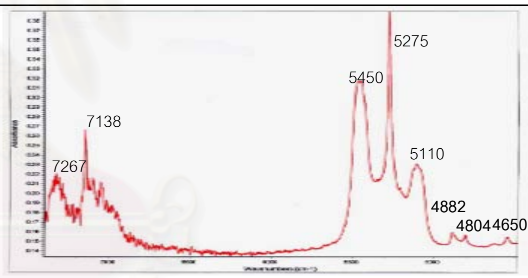

FTIR spectra of emerald samples from Colombia: *Type I H_2O dominant + II H_2O (Ib)*

CO 1

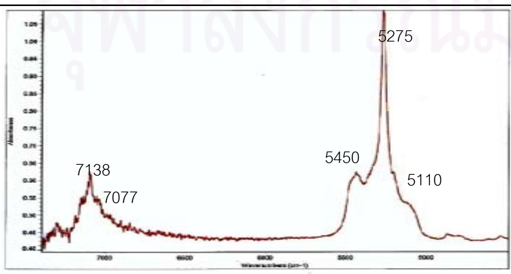

CO 2

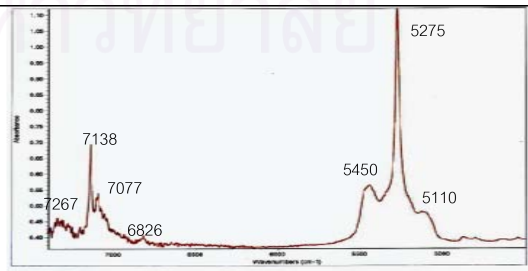

FTIR spectra of emerald samples from Colombia: *Type I H_2O dominant + II H_2O (Ib)*, continue

CO 4	CO 6
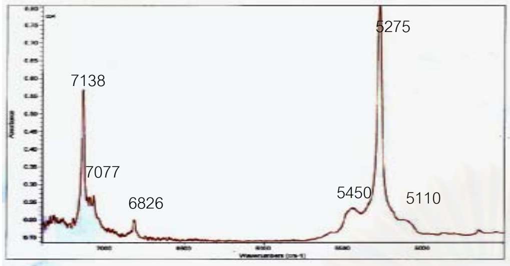	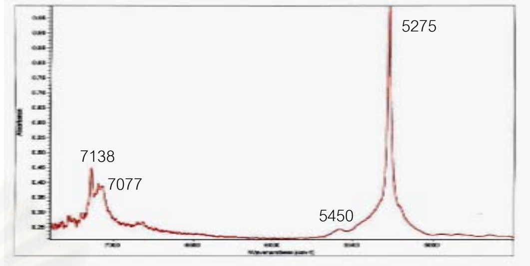
CO 8	**CO 11**
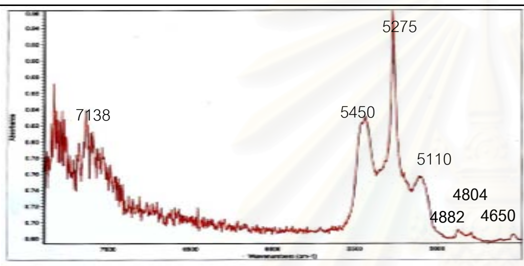	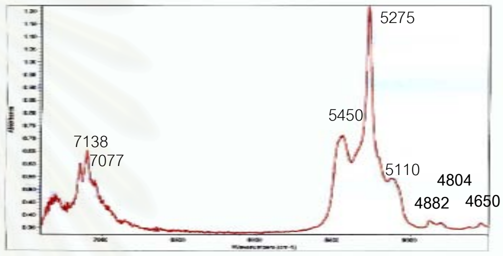
CO 13	**CO 18**
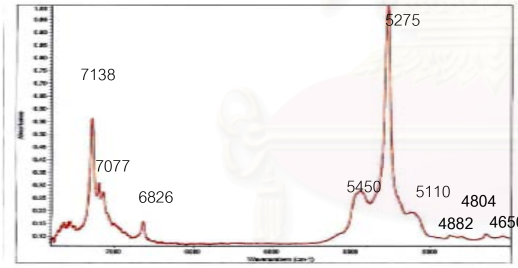	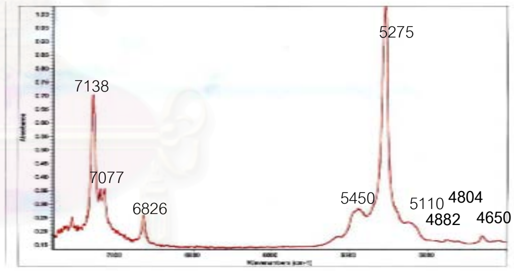
CO 20	**CO 22**
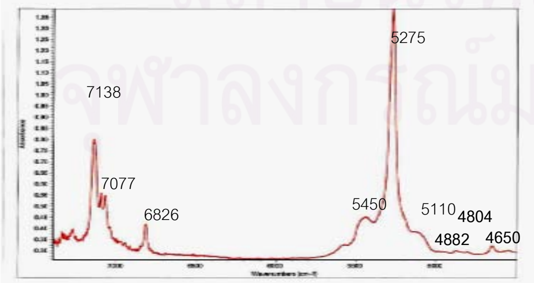	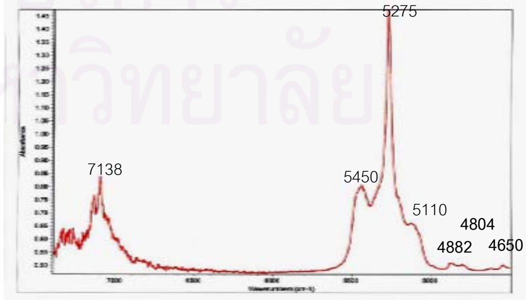

FTIR spectra of emerald samples from Colombia: *Type I H_2O dominant + II H_2O (Ib)*, continue

CO 26	CO 27
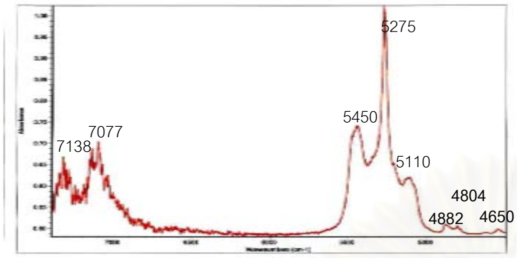	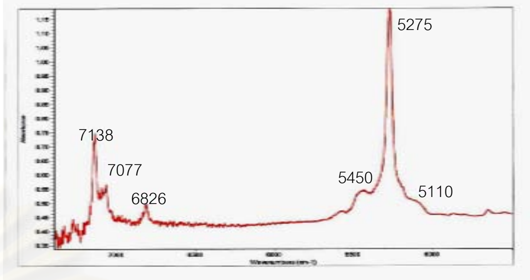

FTIR spectra of emerald samples from Santa Terezinha, Brazil: *Type II H_2O* dominat *(IIa)*

SAN 3	SAN 7
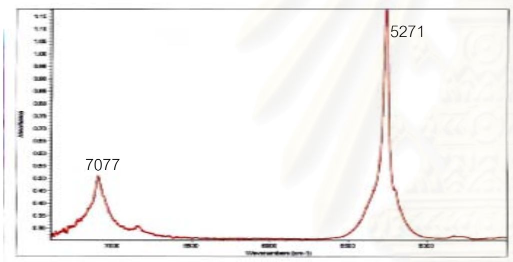	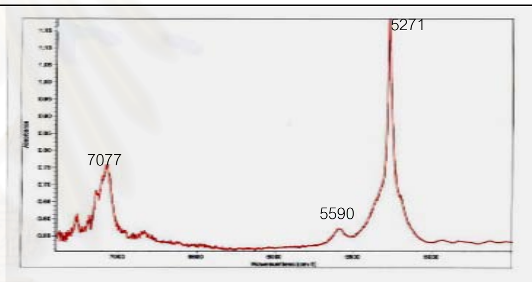
SAN 9	**SAN 10**
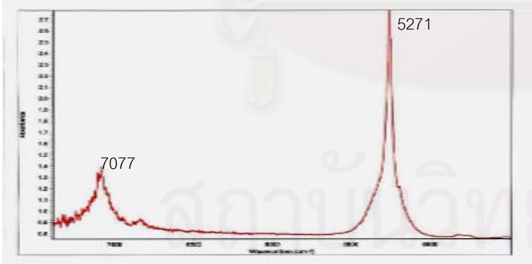	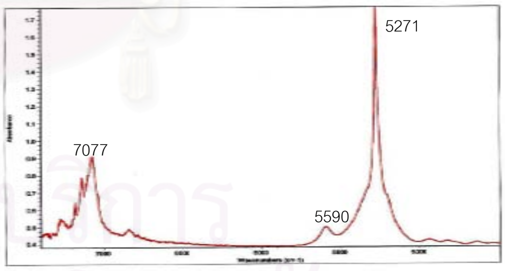

FTIR spectra of emerald samples from Madagascar: *Type I H_2O + II H_2O (IIb)*

MA 1

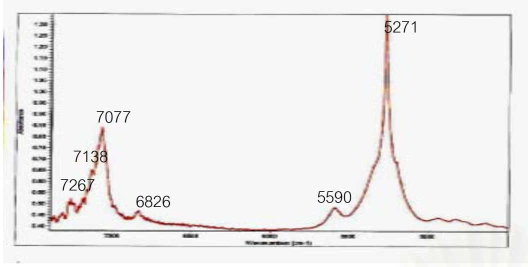

MA 3

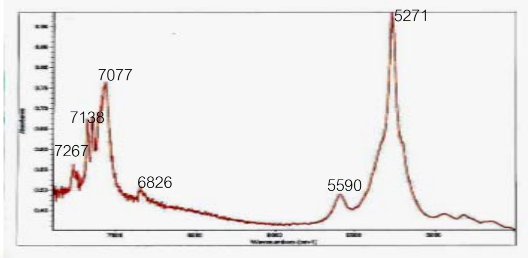

MA 9

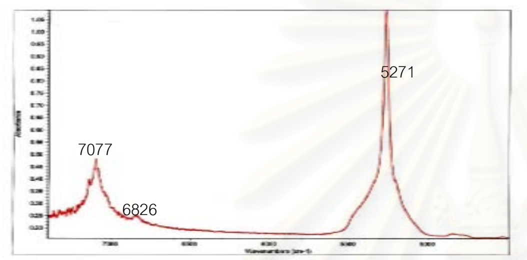

MA 15

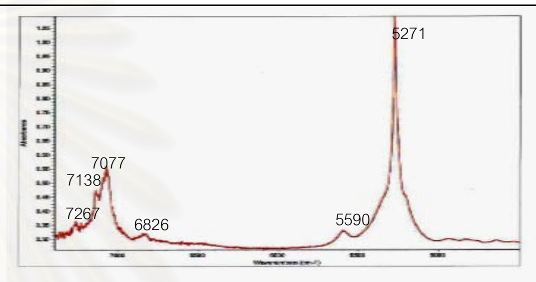

MA 17

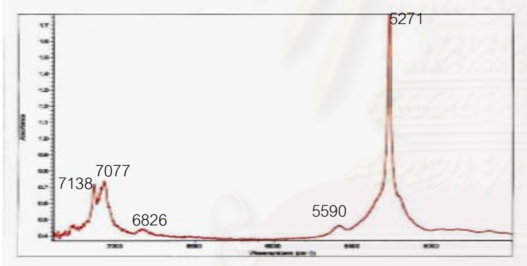

MA 18

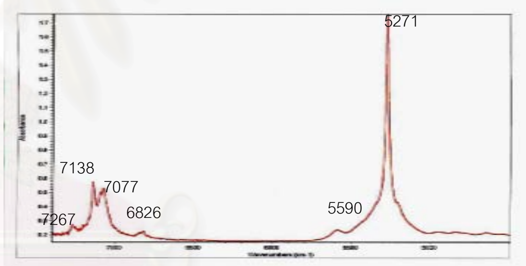

MA 21

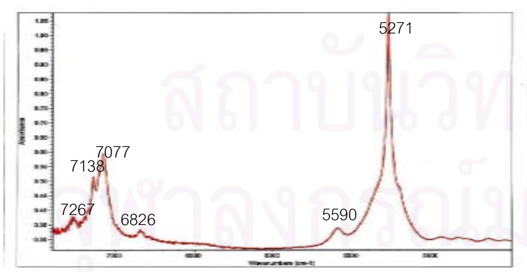

MA 23

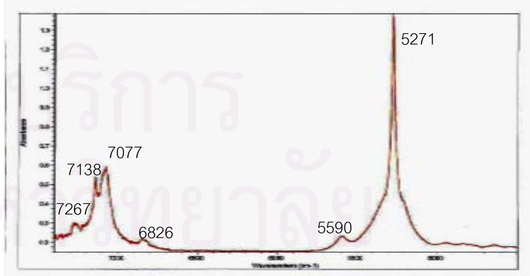

FTIR spectra of emerald samples from Madagascar: *Type I H_2O + II H_2O (IIb)*, continue

MA 24

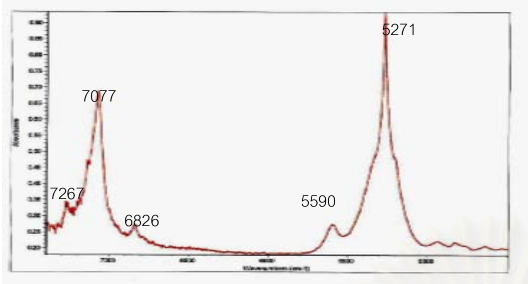

MA 26

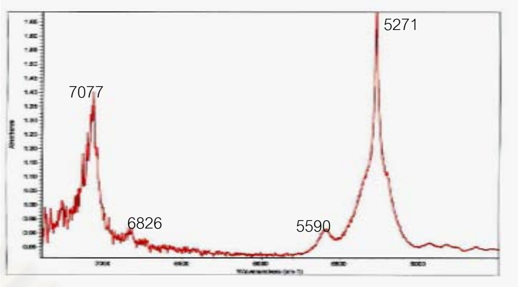

MA 27

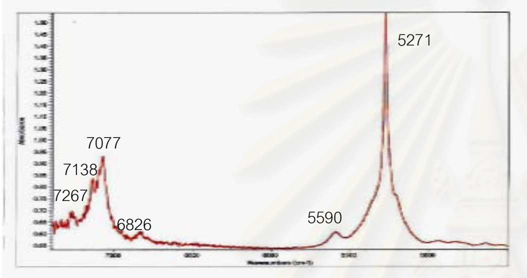

MA 28

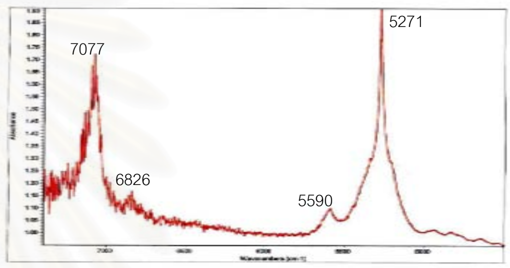

MA 29

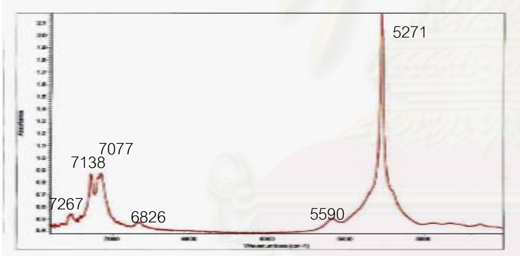

MA 30

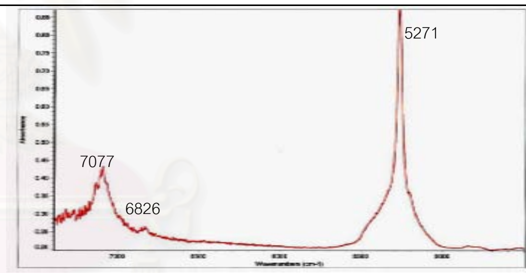

FTIR spectra of emerald samples from Zambia: *Type I H_2O + II H_2O (IIb)*

ZA 3

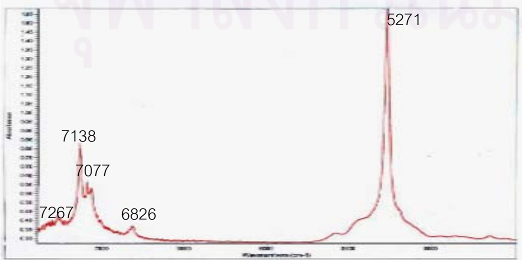

ZA 4

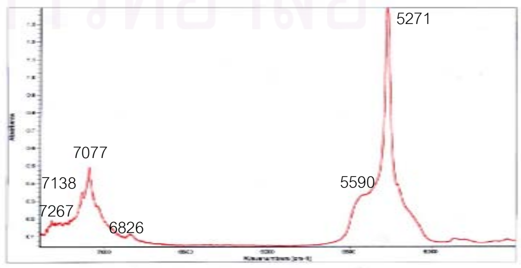

FTIR spectra of emerald samples from Zambia: *Type I H_2O + II H_2O (IIb), continue*

ZA 5

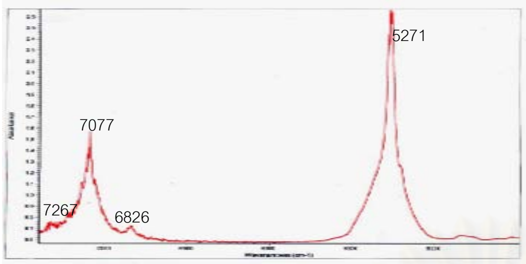

ZA 9

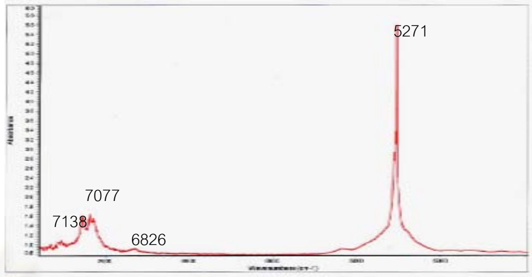

ZA 11

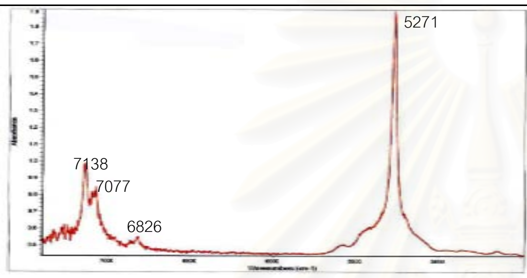

ZA 13

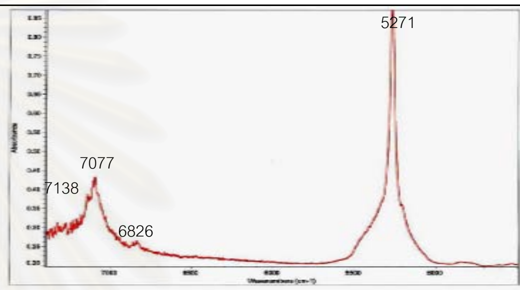

ZA 14

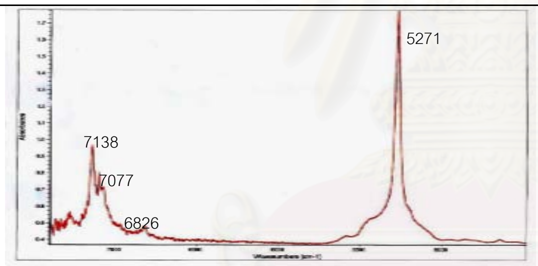

ZA 15

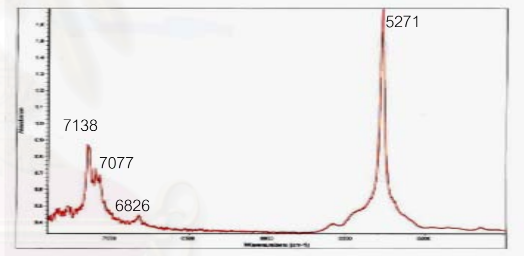

ZA 18

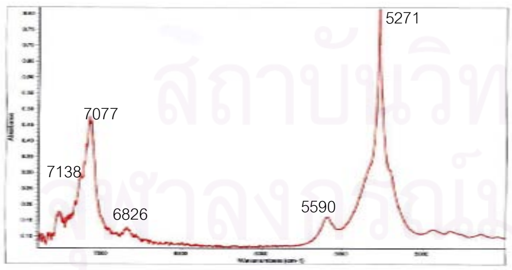

ZA 19

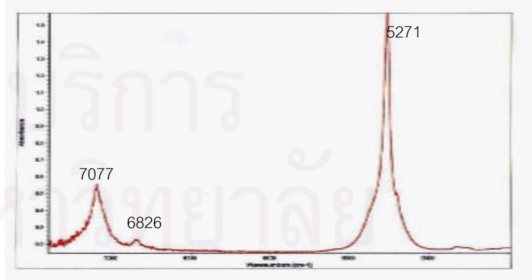

FTIR spectra of emerald samples from Zambia: *Type I H_2O + II H_2O (IIb), continue*

ZA 20	ZA 24
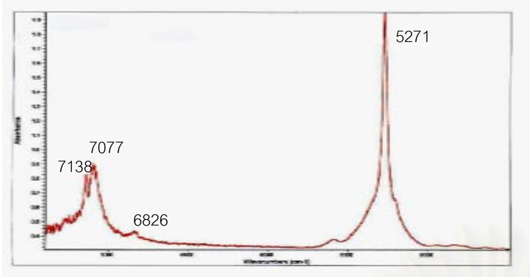	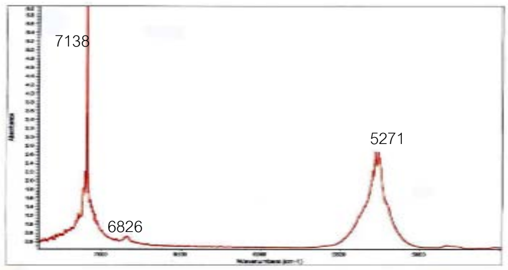
ZA 29	**ZA 30**
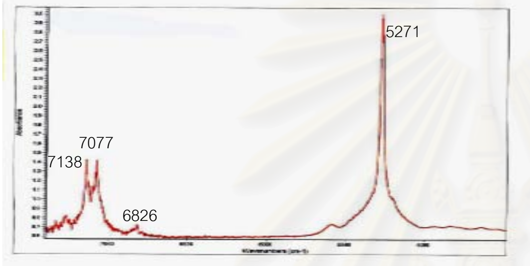	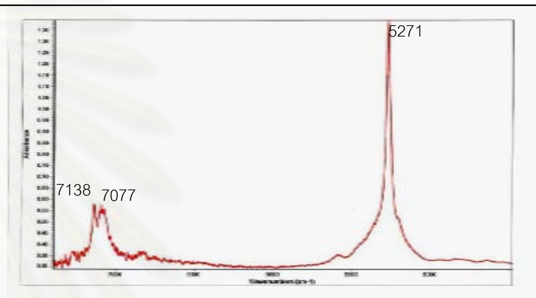

FTIR spectra of emerald samples from Carnaiba/Socoto, Brazil: *Type I H_2O + II H_2O (IIb)*

CAR 2	CAR 3
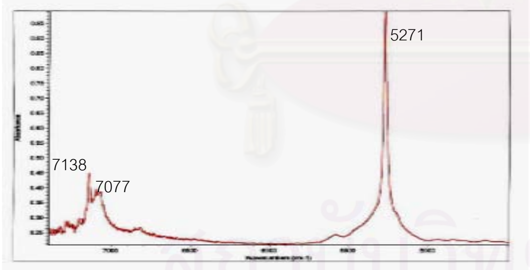	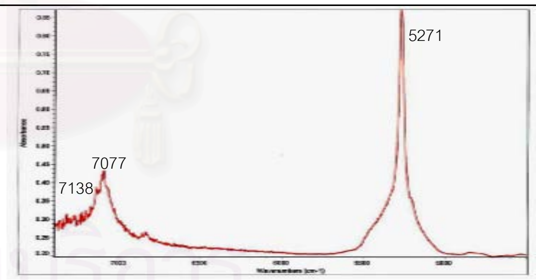
CAR 4	**CAR 8**
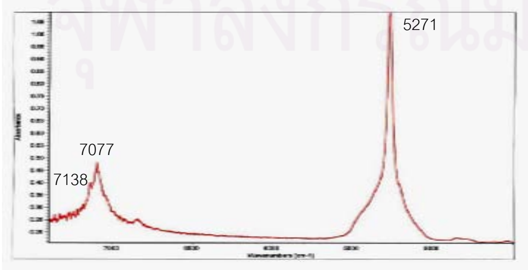	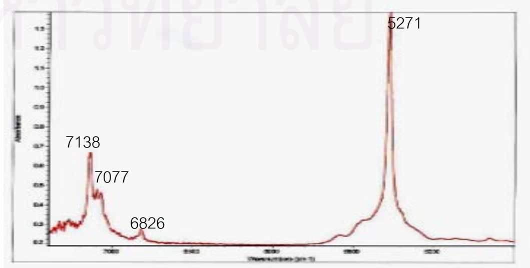

FTIR spectra of emerald samples from Carnaiba/Socoto, Brazil: *Type I* H_2O + *II* H_2O *(IIb)*, continue

CAR 9

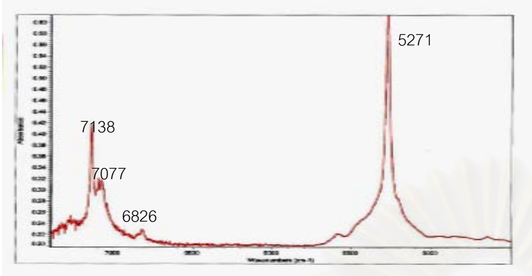

FTIR spectra of emerald samples from Itabira, Brazil: *Type I* H_2O + *II* H_2O *(IIb)*

ITA 1

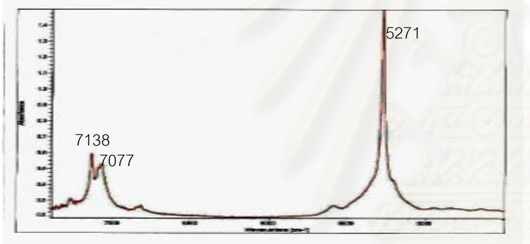

ITA 2

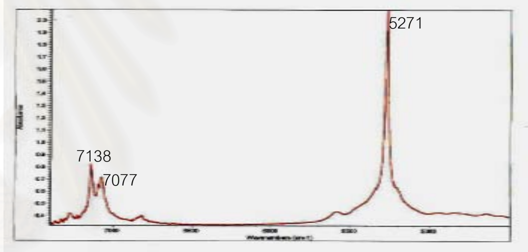

ITA 3

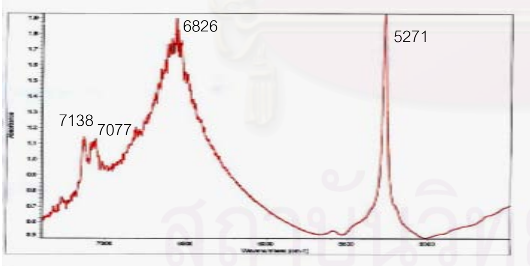

ITA 7

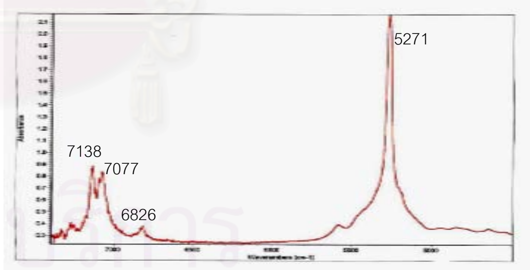

ITA 9

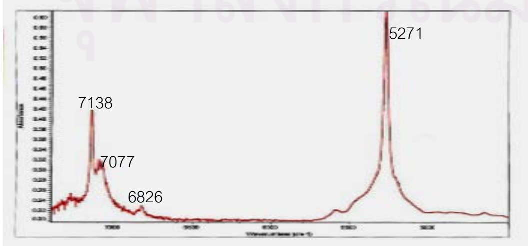

APPENDIX III

UV-Vis-NIR spectra of emerald samples from Nigeria, Colombia, Brazil, Madagascar and Zambia;

- 15 samples of Kaduna Plateau emeralds from Nigeria: NI3, NI4, NI5, NI11, NI12, NI14, NI15, NI17, NI10, NI20, NI23, NI24, NI25, NI28, NI30

- 12 samples of Cordillera Oriental emeralds from Colombia: CO1, CO2, CO4, CO6, CO8, CO11, CO13, CO18, CO20, CO22, CO26, CO27

- 4 samples of Santa Terezinha from Goais State, Brazil: SAN3, SAN7, SAN8, SAN10

- 14 samples of Manajary emeralds from Madagascar: MA1, MA3, MA9, MA15, MA17, MA18, MA21, MA23, MA24, MA26, MA27, MA28, MA30

- 14 samples of emeralds from Ndola Rural district: ZA3, ZA4, ZA5, ZA11, ZA12, ZA14, ZA15, ZA17, ZA20, ZA23, ZA24, ZA25, ZA28, ZA30

- 5 samples of Carnaiba/Socoto emeralds from Bahia State, Brazil: CAR2, CAR3, CAR4, CAR8, CAR9

- 5 samples of Itabira emeralds from Minas Gerias State, Brazil: ITA1, ITA2, ITA3, ITA7, ITA9

UV-Vis-NIR spectra of emerald samples from Nigeria (--- = O-ray, --- = E-ray)

NI 3

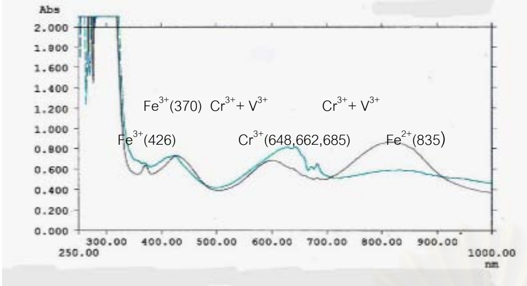

NI 4

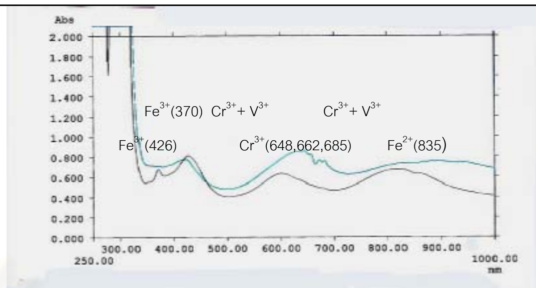

NI 5

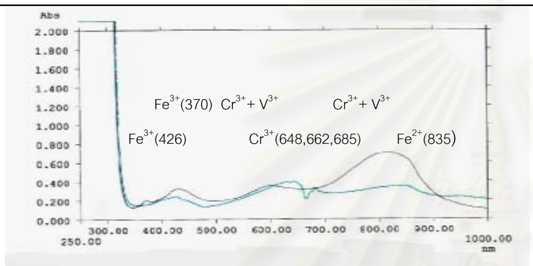

NI 11

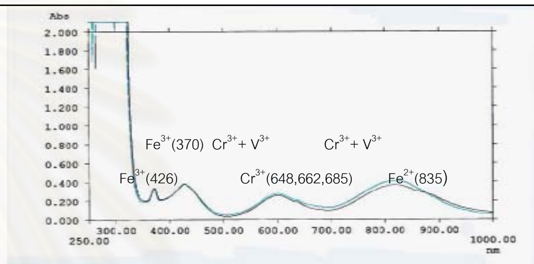

NI 12

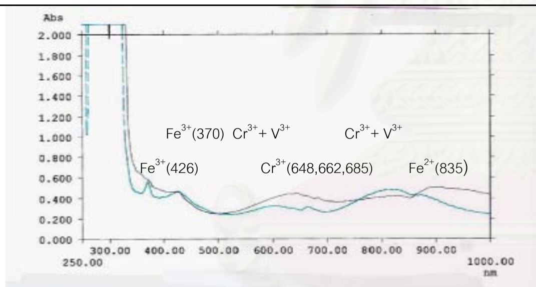

NI 14

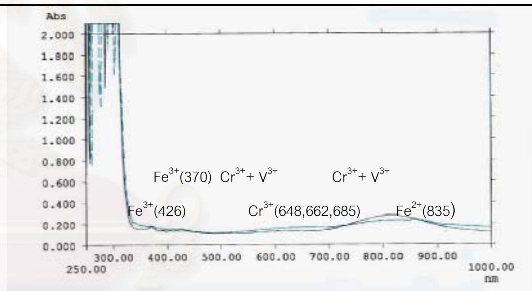

NI 15

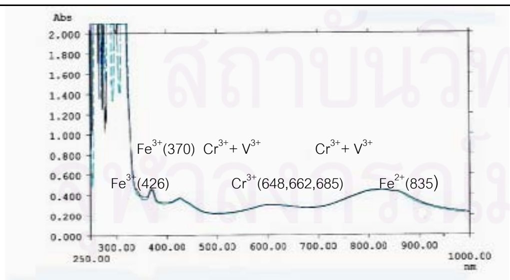

NI 17

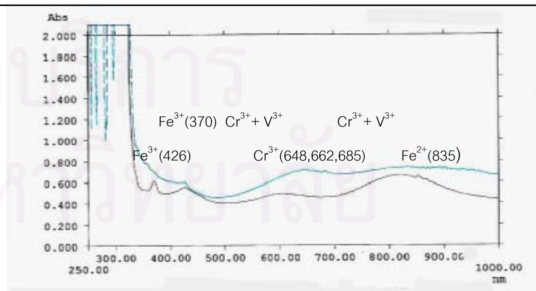

UV-Vis-NIR spectra of emerald samples from Nigeria (continue) (--- = O-ray, --- = E-ray)

NI 20

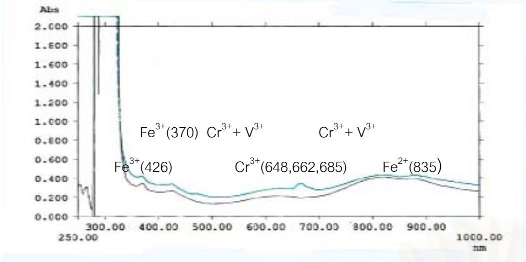

NI 23

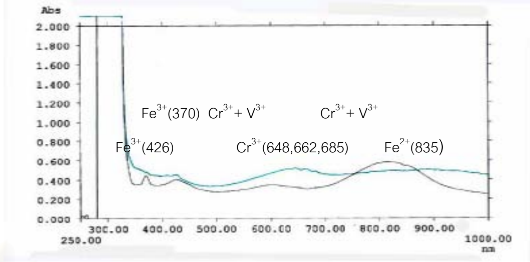

NI 24

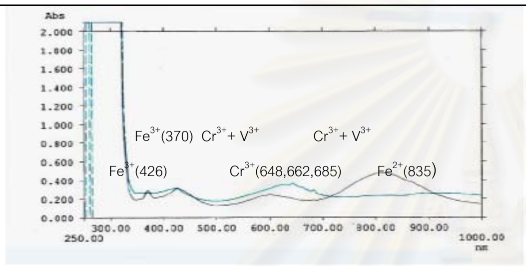

NI 25

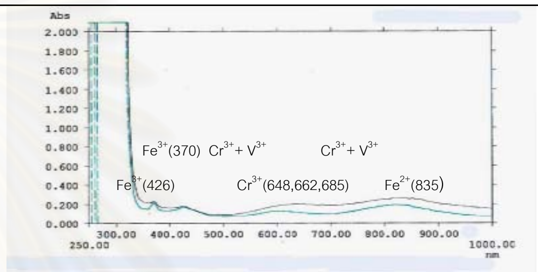

NI 28

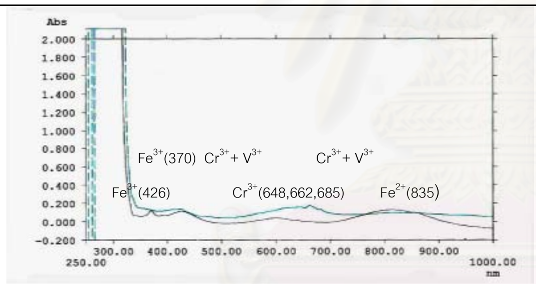

NI 30

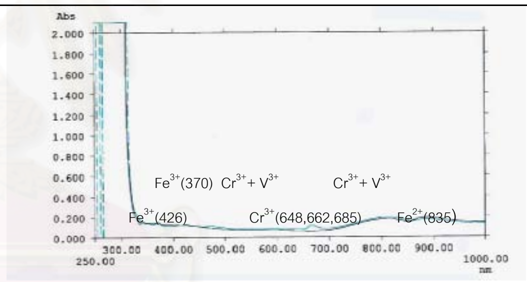

UV-Vis-NIR spectra of emerald samples from Colombia (--- = O-ray, --- = E-ray)

CO 1

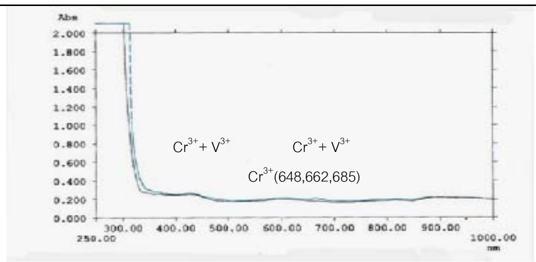

CO 2

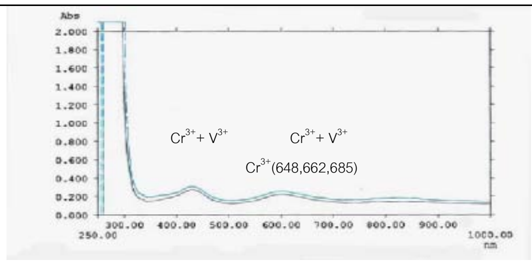

UV-Vis-NIR spectra of emerald samples from Colombia (continue) (--- = O-ray, --- = E-ray)

CO 4

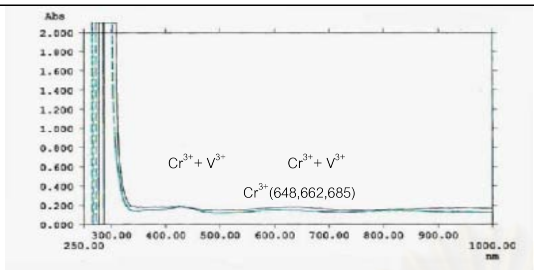

CO 6

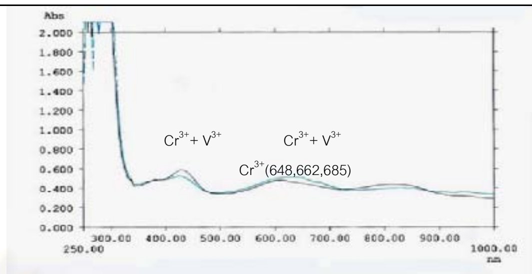

CO 8

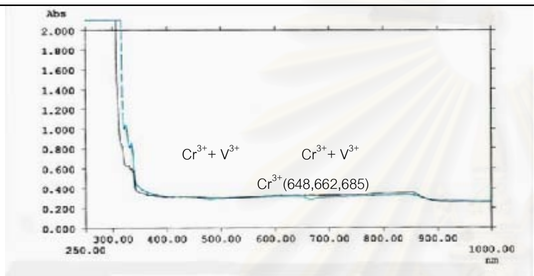

CO 11

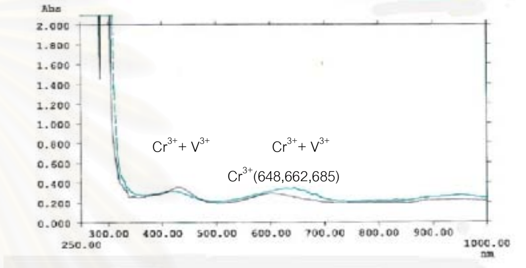

CO 13

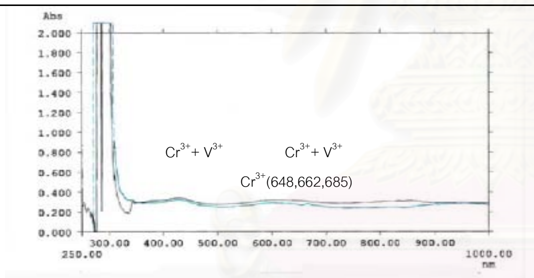

CO 18

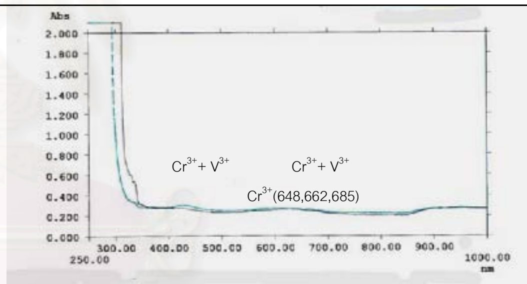

CO 20

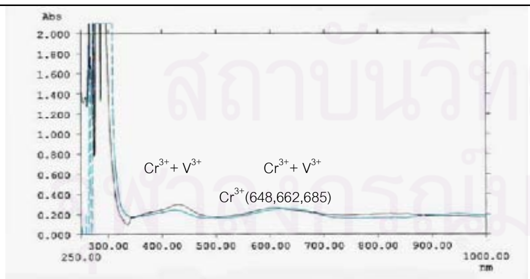

CO 22

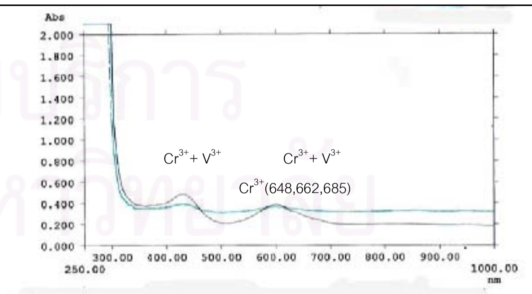

UV-Vis-NIR spectra of emerald samples from Colombia (continue) (--- = O-ray, --- = E-ray)

CO 26

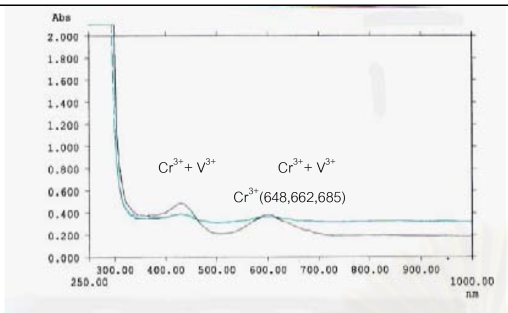

CO 27

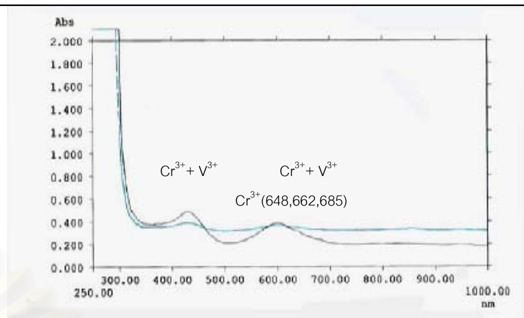

UV-Vis-NIR spectra of emerald samples from Santa Terezinha, Brazil (--- = O-ray, --- = E-ray)

SAN 3

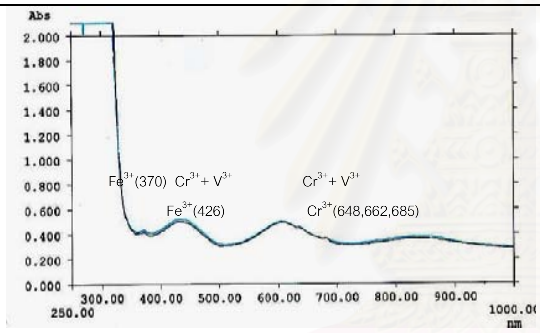

SAN 7

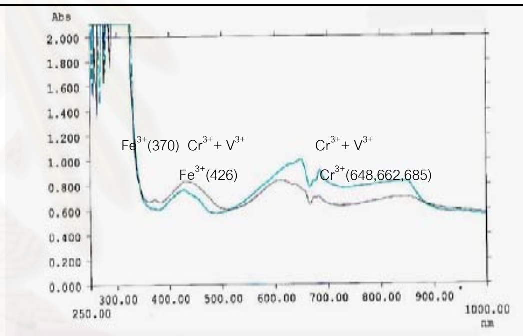

SAN 8

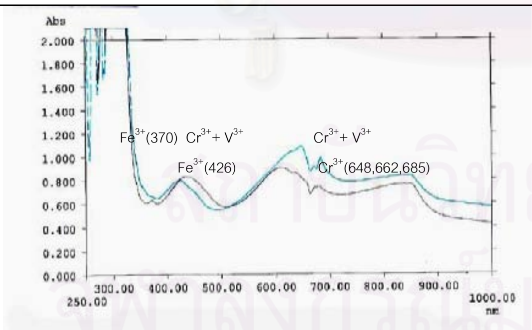

SAN 10

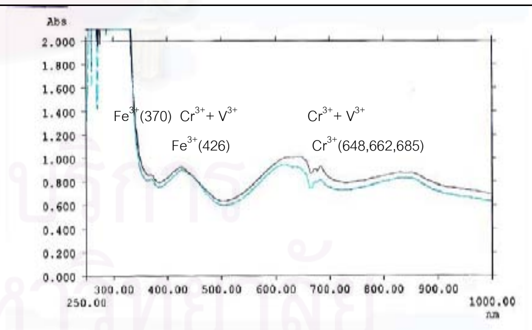

UV-Vis-NIR spectra of emerald samples from Madagascar (--- = O-ray, --- = E-ray)

MA 1

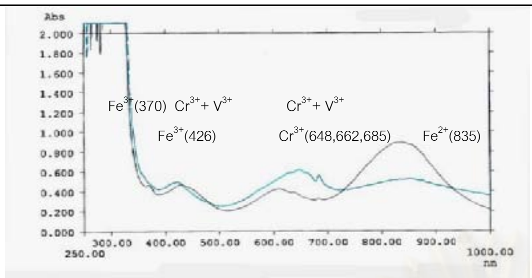

MA 3

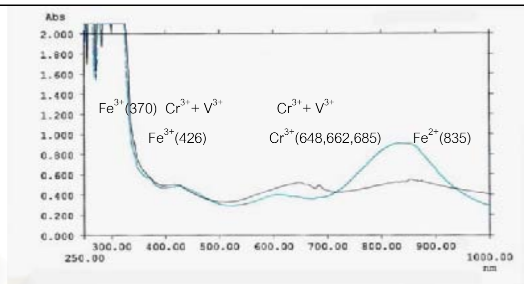

MA 9

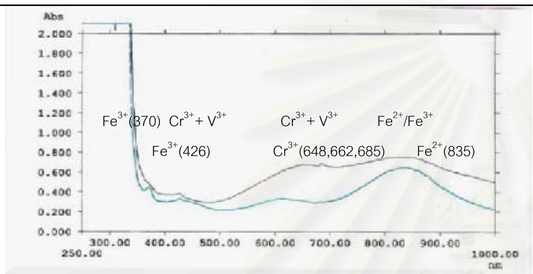

MA 15

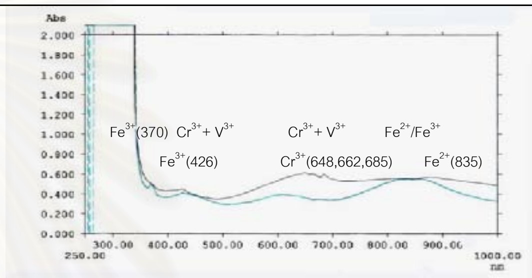

MA 17

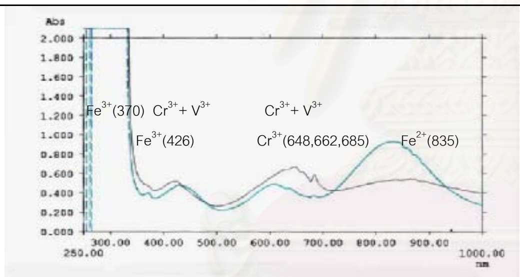

MA 18

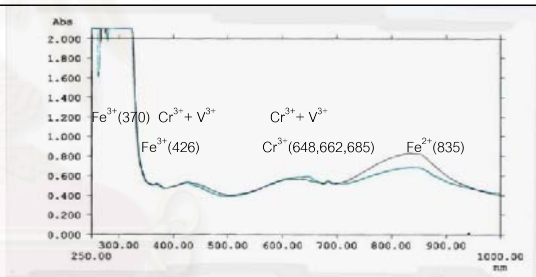

MA 21

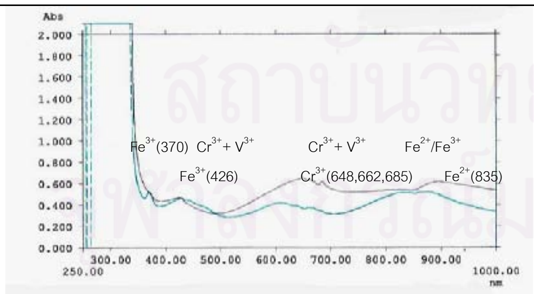

MA 23

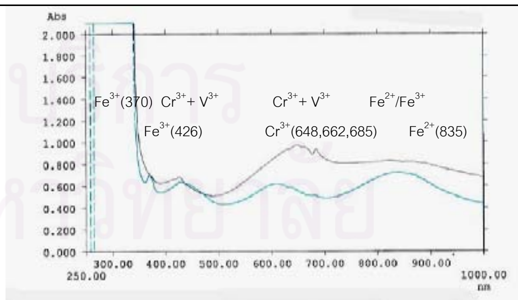

UV-Vis-NIR spectra of emerald samples from Madagascar (continue) (--- = O-ray, --- = E-ray)

MA 24

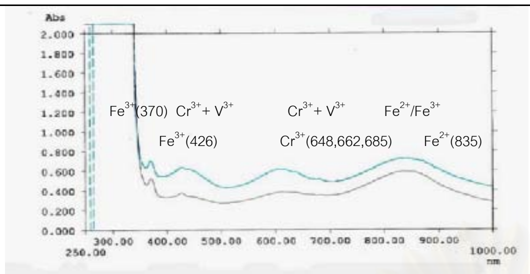

MA 26

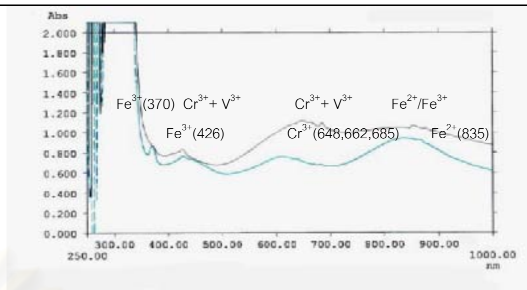

MA 27

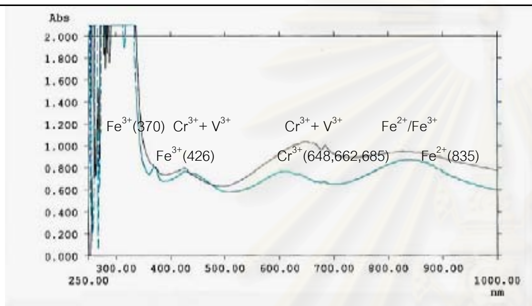

MA 28

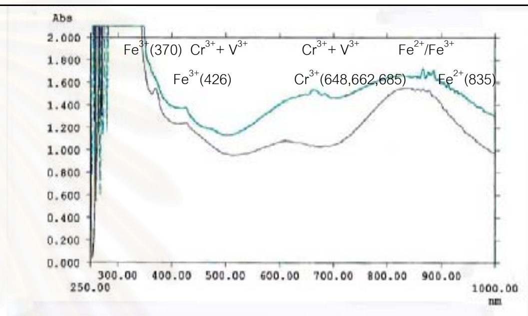

MA 29

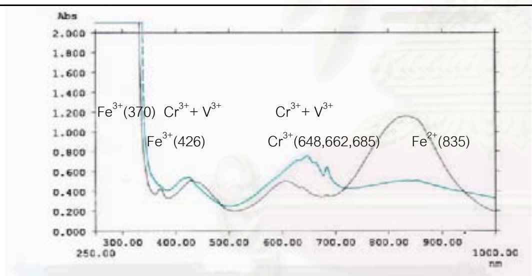

MA 30

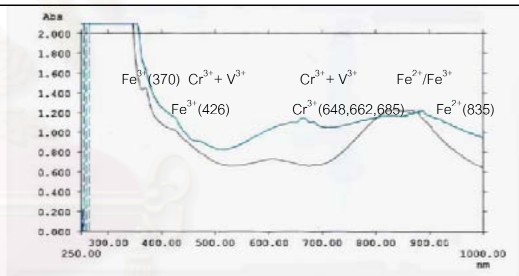

UV-Vis-NIR spectra of emerald samples from Zambia (--- = O-ray, --- = E-ray)

ZA 3

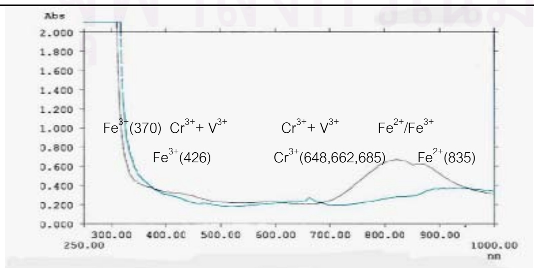

ZA 4

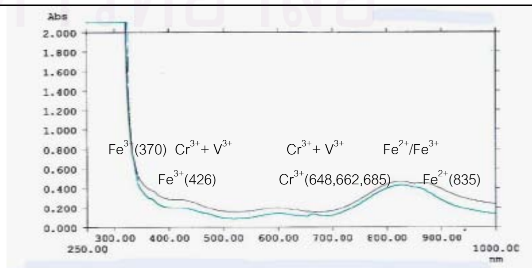

UV-Vis-NIR spectra of emerald samples from Zambia (continue) (--- = O-ray, --- = E-ray)

ZA 5

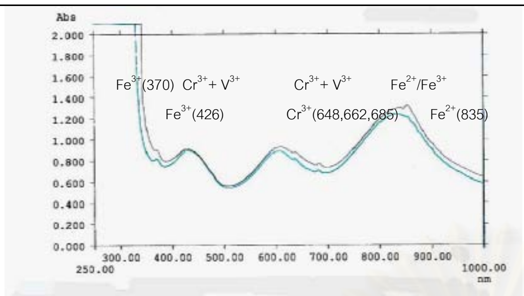

ZA 9

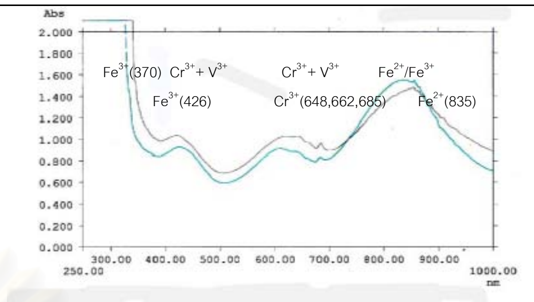

ZA 11

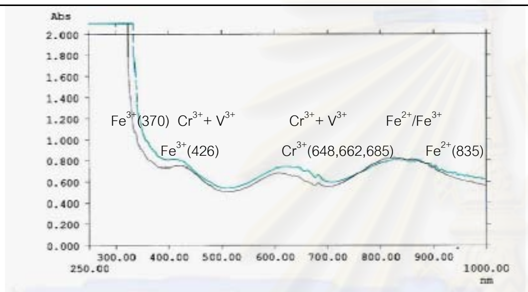

ZA 13

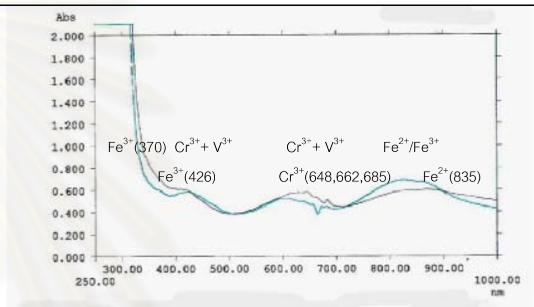

ZA 14

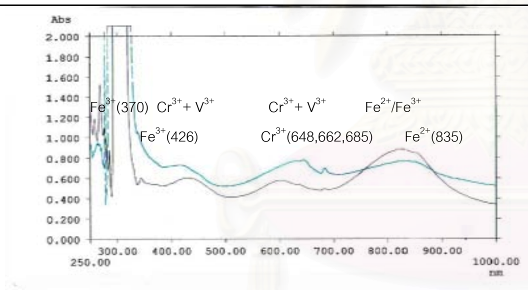

ZA 15

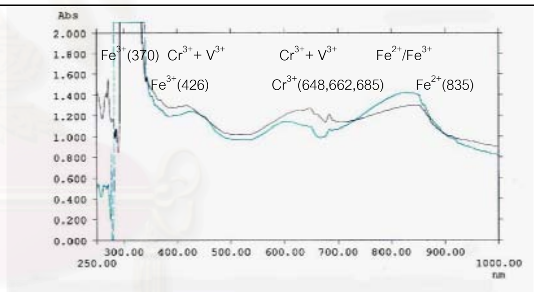

ZA 18

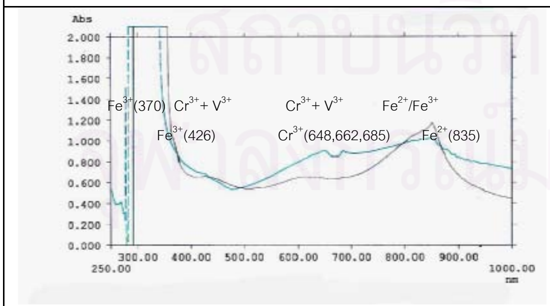

ZA 19

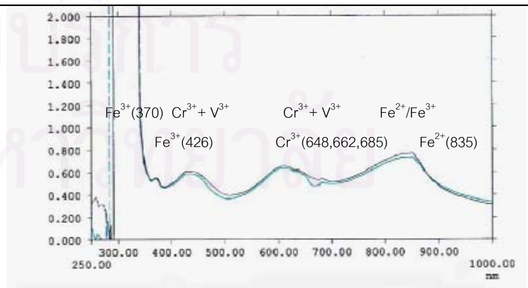

UV-Vis-NIR spectra of emerald samples from Zambia (continue) (--- = O-ray, --- = E-ray)

ZA 20

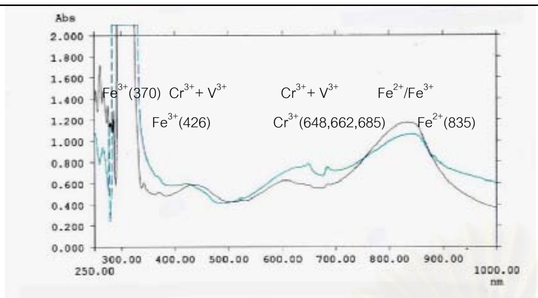

ZA 24

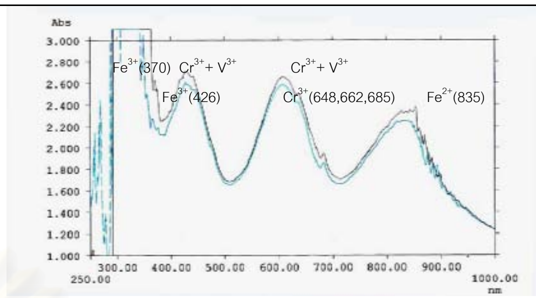

ZA 29

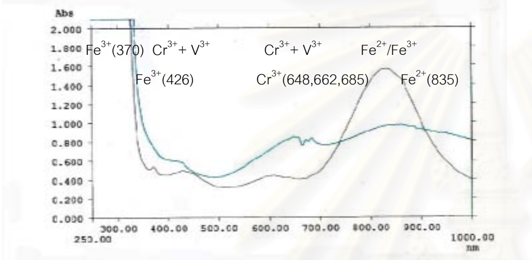

ZA 30

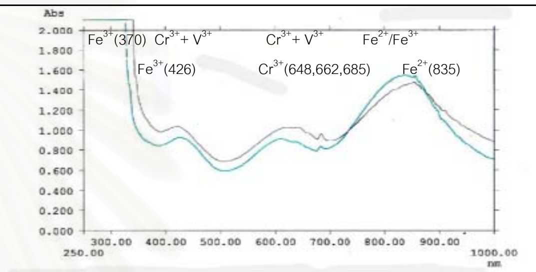

UV-Vis-NIR spectra of emerald samples from Carnaiba/Socoto, Brazil (--- = O-ray, --- = E-ray)

CAR 2

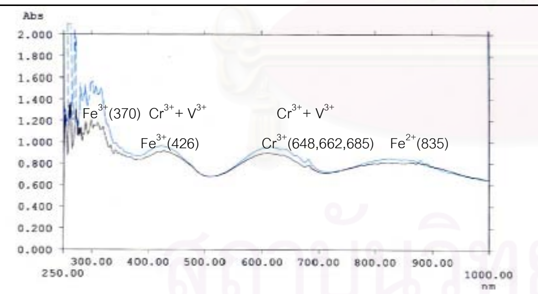

CAR 3

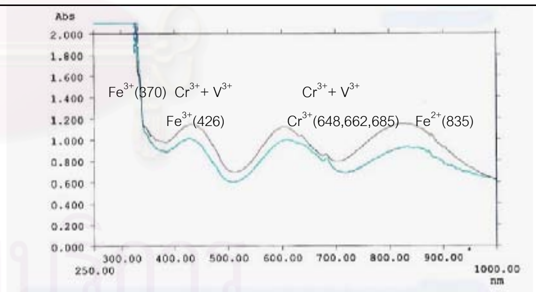

CAR 4

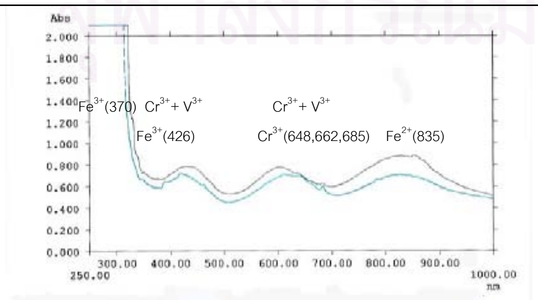

CAR 8

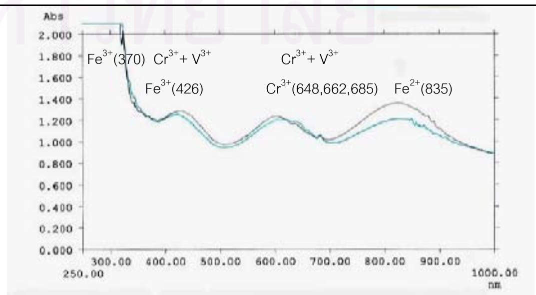

UV-Vis-NIR spectra of emerald samples from Carnaiba/Socoto, Brazil (continue) (--- = O-ray, --- = E-ray)

Car 9

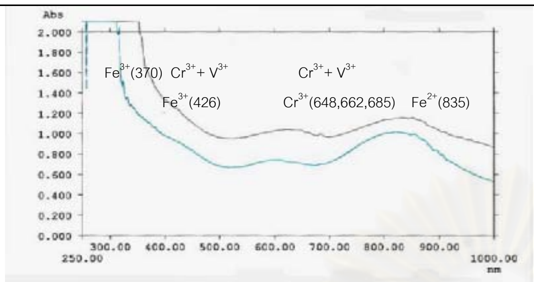

UV-Vis-NIR spectra of emerald samples from Itabira, Brazil (--- = O-ray, --- = E-ray)

ITA 1

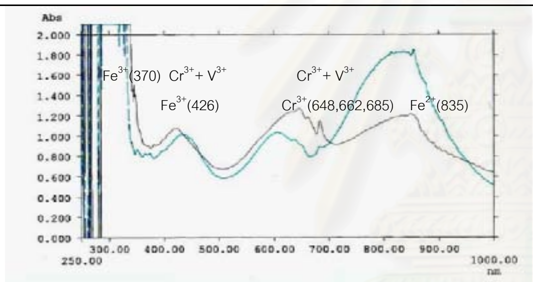

ITA 2

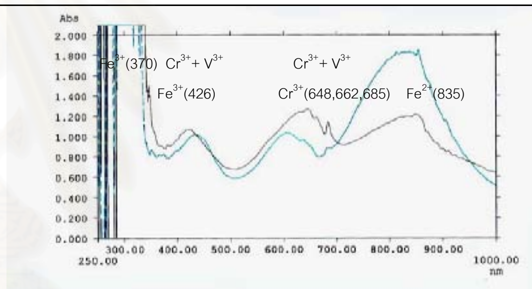

ITA 3

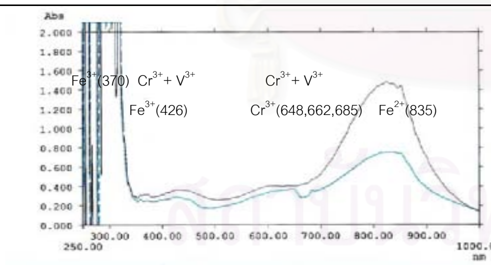

ITA 7

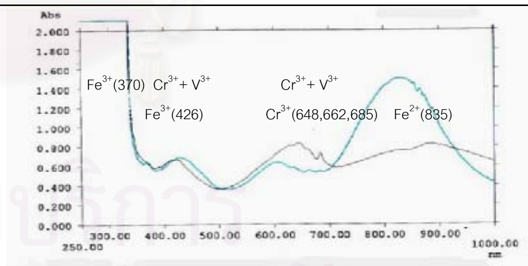

ITA 9

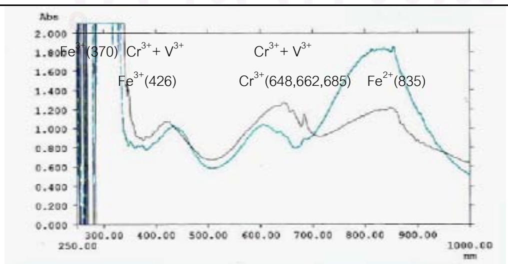

APPENDIX IV

Table IV.1 to IV.7: Chemical data show concentration (atom mole ppm) of 16 trace elements of emeralds from Nigeria (NI), Colombia (CO), Santa Terezinha (STA), Madagascar (MA), Zambia (ZA), Carnaiba/Socoto (CAR) and Itabira (ITA).

Table IV.1: Chemical data show concentration (atom mole ppm) of 16 elements of 4 samples of emerald from Nigeria (NI)

Cation (atom mole ppm)	**NI1-1**	**NI1-2**	**NI1-3**	**NI1-4**	**NI1-5**	X	SD
Li7	99.512	242.710	250.598	182.606	96.495	174.384	74.527
Be9	102401.687	104588.166	102766.068	102382.188	102584.013	102944.424	931.969
B11	46.415	30.991	48.368	37.576	41.011	40.872	6.990
Na23	504.844	951.278	863.929	736.591	446.199	700.568	220.143
Mg24	173.293	435.819	439.682	358.472	183.424	318.138	131.697
Al27	62268.134	62229.569	60594.090	60801.682	61733.851	61525.465	787.729
Si29	211614.368	207995.334	212289.853	211854.220	212111.468	211173.049	1794.750
P31	52.551	35.999	46.418	55.445	36.780	45.439	8.885
K39	13.025	227.106	88.727	9.167	84.673	84.540	88.230
Ca42	77.904	50.472	64.349	57.407	59.057	61.838	10.259
Ti47	1.592	5.579	5.219	4.207	1.398	3.599	1.987
V51	139.370	176.875	96.179	174.938	138.917	145.256	33.031
Cr53	102.059	158.963	97.858	103.962	64.588	105.486	33.929
Mn55	3.084	2.202	1.662	2.894	2.118	2.392	0.586
Fe57	1502.076	1868.891	1346.942	2238.597	1415.948	1674.491	374.121
Cs	0.083	0.046	0.057	0.048	0.059	0.059	0.015
Total (atom mole %)	37.900	37.900	37.900	37.900	37.900	37.900	

Table IV.1: Chemical data show concentration (atom mole ppm) of 16 elements of 4 samples of emerald from Nigeria (NI), continued

Cation (atom mole ppm)	NI11-1	NI11-2	NI11-3	NI11-4	NI11-5	NI11-6	X	SD
Li7	78.885	130.750	137.854	94.546	140.525	191.589	129.025	39.574
Be9	102143.296	103860.453	105145.114	104382.888	104292.981	0.000	86637.455	42455.301
B11	39.587	35.139	25.610	28.206	37.930	43.902	35.062	6.974
Na23	761.890	914.919	991.943	538.360	1089.299	1448.648	957.510	308.396
Mg24	132.703	295.356	296.915	131.221	312.144	409.589	262.988	109.949
Al27	61096.828	60695.143	61384.950	61505.609	60431.235	84304.897	64903.110	9513.593
Si29	212366.768	210152.170	207780.672	209896.302	209492.792	288798.271	223081.162	32228.202
P31	63.089	41.283	33.582	56.023	31.538	55.509	46.837	13.148
K39	9.522	6.367	94.639	6.959	108.061	8.458	39.001	48.494
Ca42	63.770	43.743	36.305	49.117	51.522	65.390	51.641	11.315
Ti47	0.709	11.158	9.305	1.732	13.201	7.221	7.221	5.062
V51	140.242	149.560	178.907	193.190	162.595	165.816	165.052	19.214
Cr53	51.944	61.203	117.373	194.602	61.935	46.357	88.902	57.712
Mn55	0.513	3.442	4.078	1.186	3.897	4.685	2.967	1.701
Fe57	2049.929	2599.274	2762.723	1920.028	2770.297	3448.942	2591.865	555.108
Cs	0.326	0.039	0.029	0.030	0.047	0.056	0.088	0.117
Total (atom mole %)	37.900	37.900	37.900	37.900	37.900	37.900	37.900	

Table IV.1: Chemical data show concentration (atom mole ppm) of 16 elements of 4 samples of emerald from Nigeria (NI), continued

Cation (atom mole ppm)	N116-1	NI16-2	NI16-3	NI16-4	NI16-5	NI16-6	X	SD
Li7	58.294	136.992	161.972	122.004	111.932	120.985	118.697	34.403
Be9	102804.832	104395.562	103875.632	104783.323	102665.523	0.000	86420.812	42345.785
B11	37.275	42.469	61.753	34.171	40.188	65.714	46.928	13.371
Na23	334.419	1321.975	1712.078	1217.548	1077.787	530.103	1032.318	514.127
Mg24	78.914	329.245	319.772	306.348	276.034	122.310	238.770	109.380
Al27	62274.107	59728.972	60360.475	60306.388	59801.830	83915.191	64397.827	9606.239
Si29	211483.603	209812.849	208837.236	208711.937	211815.502	291516.143	223696.212	33250.286
P31	67.243	48.132	50.684	36.898	64.161	73.300	56.736	13.741
K39	9.125	8.464	227.303	86.441	9.371	246.690	97.899	112.011
Ca42	71.805	65.880	51.332	43.462	67.633	104.703	67.469	21.187
Ti47	0.692	9.823	9.991	3.106	3.785	5.479	5.479	3.759
V51	150.741	139.488	164.315	173.583	200.154	130.970	159.875	25.158
Cr53	121.110	35.538	71.737	142.114	110.299	210.599	115.233	60.199
Mn55	0.637	4.449	19.734	4.152	4.685	0.512	5.695	7.134
Fe57	1502.870	2880.846	3039.112	3004.444	2716.779	1956.648	2516.783	636.389
Cs	4.334	39.316	36.875	24.080	34.335	5.207	24.024	15.793
Total (atom mole %)	37.900	37.900	37.900	37.900	37.900	37.900	37.900	

Table IV.1: Chemical data show concentration (atom mole ppm) of 16 elements of 4 samples of emerald from Nigeria (NI), continued

Cation (atom mole ppm)	**NI27-1**	**NI27-2**	**NI27-3**	**NI27-4**	**NI27-5**	X	SD
Li7	82.953	134.460	113.540	121.161	99.850	110.393	19.807
Be9	102330.540	101551.964	99409.115	105521.811	103209.232	102404.533	2239.969
B11	40.190	60.296	48.739	40.779	41.987	46.398	8.488
Na23	380.374	541.154	456.572	434.538	407.597	444.047	61.359
Mg24	164.959	273.709	239.306	211.133	200.677	217.957	40.982
Al27	62138.974	60839.649	61414.453	61413.931	62222.254	61605.852	575.479
Si29	212083.232	213605.903	215357.957	209240.697	210918.642	212241.286	2363.986
P31	48.562	63.307	62.813	62.830	51.619	57.826	7.147
K39	159.753	13.495	15.747	10.471	154.777	70.848	78.929
Ca42	64.970	91.454	101.718	68.287	69.527	79.191	16.374
Ti47	0.894	2.759	1.384	3.004	1.476	1.903	0.924
V51	97.206	85.525	104.634	126.329	126.520	108.043	18.110
Cr53	116.409	72.149	114.994	154.307	149.559	121.484	33.043
Mn55	1.051	1.968	1.879	2.425	1.598	1.784	0.506
Fe57	1283.492	1639.644	1542.015	1566.414	1330.626	1472.438	156.078
Cs	6.443	22.563	15.134	21.882	14.059	16.016	6.587
Total (atom mole %)	37.900	37.900	37.900	37.900	37.900	37.900	

Table IV.2: Chemical data show concentration (atom mole ppm) of 16 elements of 4 samples of emerald from Colombia (CO)

Cation (atom mole ppm)	**CO1-1**	**CO1-2**	**CO1-3**	**CO1-4**	**CO1-5**	X	SD
Li7	169.292	503.550	658.548	597.360	172.199	420.190	234.308
Be9	98781.447	98636.906	99116.161	99556.855	99325.014	99083.277	378.861
B11	45.085	48.324	40.303	36.189	44.598	42.900	4.713
Na23	2323.420	3290.579	3383.024	3331.025	3666.640	3198.938	511.129
Mg24	2349.702	3088.603	3102.313	3138.809	3801.663	3096.218	514.015
Al27	71102.210	72163.081	70465.441	71338.294	68825.747	70778.955	1249.647
Si29	203624.702	200758.973	201851.142	200633.108	202486.853	201870.956	1247.409
P31	99.249	70.322	76.420	75.833	63.915	77.148	13.346
K39	19.348	60.407	14.669	12.207	33.038	27.934	19.859
Ca42	175.151	129.889	123.791	101.268	102.227	126.465	30.048
Ti47	1.821	2.453	1.562	1.178	5.676	2.538	1.814
V51	135.235	79.188	51.086	51.935	135.760	90.641	42.480
Cr53	38.857	24.323	20.025	20.539	39.985	28.746	9.893
Mn55	0.604	0.460	0.430	0.352	0.601	0.489	0.111
Fe57	132.434	140.906	93.915	103.914	293.773	152.988	81.066
Cs	1.441	2.036	1.171	1.133	2.310	1.618	0.529
Total (atom mole %)	37.900	37.900	37.900	37.900	37.900	37.900	

Table IV.2: Chemical data show concentration (atom mole ppm) of 16 elements of 4 samples of emerald from Colombia (CO), continued

Cation (atom mole ppm)	**CO11-1**	**CO11-2**	**CO11-3**	**CO11-4**	**CO11-5**	X	SD
Li7	167.226	176.554	175.226	177.520	177.782	174.861	4.384
Be9	96089.071	96326.817	95541.980	95517.003	95702.181	95835.411	357.442
B11	62.637	41.522	49.141	62.900	59.550	55.150	9.451
Na23	1794.391	1959.909	1926.644	1918.958	1869.036	1893.788	64.377
Mg24	1809.037	1916.828	1881.326	1866.216	1826.493	1859.980	43.136
Al27	71140.006	73383.651	71807.122	72854.341	71933.061	72223.636	891.010
Si29	207552.796	204783.269	207251.332	206115.288	207031.091	206546.755	1122.405
P31	69.114	74.792	70.627	59.520	72.112	69.233	5.820
K39	21.385	48.830	20.856	145.185	38.350	54.921	51.828
Ca42	163.359	139.755	151.076	141.485	157.115	150.558	10.077
Ti47	1.000	1.115	0.963	1.393	1.028	1.100	0.173
V51	50.632	52.085	51.376	51.291	48.996	50.876	1.170
Cr53	27.596	28.862	26.972	27.796	27.231	27.691	0.728
Mn55	0.581	0.491	0.539	0.522	0.558	0.538	0.034
Fe57	50.168	64.435	43.703	59.489	54.286	54.416	8.046
Cs	1.003	1.083	1.118	1.093	1.130	1.085	0.050
Total (atom mole %)	37.900	37.900	37.900	37.900	37.900	37.900	

Table IV.2: Chemical data show concentration (atom mole ppm) of 16 elements of 4 samples of emerald from Colombia (CO), continued

Cation (atom mole ppm)	CO18-1	CO18-2	CO18-3	CO18-4	CO18-5	X	SD
Li7	81.472	96.107	82.869	87.891	82.873	86.242	6.032
Be9	98506.813	97824.564	96952.674	96178.075	96145.907	97121.607	1034.858
B11	55.626	54.661	55.663	77.790	66.268	62.002	10.027
Na23	2244.925	2632.193	2515.641	2445.275	2220.200	2411.647	176.801
Mg24	2404.154	2727.554	2687.376	2535.758	2336.980	2538.365	170.713
Al27	72056.890	70951.767	71465.005	71147.092	71928.257	71509.802	479.421
Si29	203230.388	204370.578	204616.356	206115.882	205580.949	204782.831	1120.464
P31	71.565	82.021	70.248	95.080	77.248	79.233	10.030
K39	17.029	19.527	283.029	22.604	250.885	118.615	135.908
Ca42	119.095	139.110	132.788	154.569	156.221	140.357	15.529
Ti47	0.791	0.990	0.993	1.001	1.210	0.997	0.148
V51	100.771	35.835	36.509	38.148	34.940	49.241	28.830
Cr53	23.253	14.324	32.474	30.486	36.045	27.316	8.634
Mn55	0.434	0.499	0.491	0.567	0.571	0.512	0.057
Fe57	85.174	49.406	67.080	68.891	80.629	70.236	13.936
Cs	1.619	0.865	0.803	0.889	0.818	0.999	0.349
Total (atom mole %)	37.900	37.900	37.900	37.900	37.900	37.900	

Table IV.2: Chemical data show concentration (atom mole ppm) of 16 elements of 4 samples of emerald from Colombia (CO), continued

Cation (atom mole ppm)	**CO22-1**	**CO22-2**	**CO22-3**	**CO22-4**	**CO22-5**	X	SD
Li7	72.947	68.219	52.826	84.244	79.570	71.561	12.136
Be9	98691.091	97867.837	98308.515	98329.143	97019.338	98043.185	642.449
B11	60.168	57.601	58.916	55.252	47.567	55.901	5.002
Na23	1560.177	2101.818	1408.971	2637.442	2525.046	2046.691	553.225
Mg24	1659.714	2173.565	1465.418	2792.807	2650.726	2148.446	585.983
Al27	71632.600	71088.406	72721.642	70062.248	70719.023	71244.784	1003.840
Si29	204869.644	205020.038	204635.570	204313.948	205017.010	204771.242	299.795
P31	74.249	59.651	84.847	61.273	49.564	65.917	13.748
K39	13.255	213.765	16.303	139.017	186.315	113.731	94.210
Ca42	100.782	123.028	126.100	110.692	105.405	113.201	11.003
Ti47	0.644	0.945	0.986	0.802	0.758	0.827	0.140
V51	106.964	100.655	52.516	154.004	272.199	137.268	83.559
Cr53	89.550	40.769	26.524	170.530	232.991	112.073	87.961
Mn55	0.410	4.448	0.458	0.412	0.403	1.226	1.801
Fe57	66.689	78.128	39.893	86.455	92.179	72.669	20.679
Cs	1.119	1.126	0.517	1.731	1.906	1.280	0.554
Total (atom mole %)	37.900	37.900	37.900	37.900	37.900	37.900	

Table IV.3: Chemical data show concentration (atom mole ppm) of 16 elements of 3 samples of emerald from Santa Tererzinha (STA)

Cation (atom mole ppm)	**STA1-1**	**STA1-2**	**STA1-3**	**STA1-4**	**STA1-5**	X	SD
Li7	372.522	290.938	442.189	423.523	276.700	361.174	75.247
Be9	95792.319	95770.684	96496.281	95973.092	95658.902	95938.256	331.671
B11	29.502	31.729	32.219	30.037	34.064	31.510	1.822
Na23	12332.536	12699.995	12209.993	12275.319	12460.427	12395.654	193.490
Mg24	12271.026	10980.741	11570.977	10764.340	11395.956	11396.608	584.748
Al27	53004.257	53555.184	53846.599	53898.545	53018.570	53464.631	433.963
Si29	201038.446	201090.182	200068.347	201272.276	201566.270	201007.104	563.944
P31	41.975	40.394	38.718	47.764	35.941	40.958	4.412
K39	115.114	217.141	126.981	99.863	301.116	172.043	85.403
Ca42	39.834	48.842	37.082	46.622	49.029	44.282	5.487
Ti47	2.479	1.637	1.710	1.593	1.711	1.826	0.368
V51	149.474	128.946	128.759	125.833	141.465	134.896	10.135
Cr53	1081.393	1548.352	1251.634	1339.897	1572.917	1358.839	206.502
Mn55	2.522	1.744	2.429	2.821	2.421	2.387	0.395
Fe57	2655.194	2528.801	2684.642	2635.890	2433.349	2587.575	104.366
Cs	71.408	64.690	61.441	62.584	51.162	62.257	7.306
Total (atom mole %)	37.900	37.900	37.900	37.900	37.900	37.900	

Table IV.3: Chemical data show concentration (atom mole ppm) of 16 elements of 3 samples of emerald from Santa Tererzinha (STA), continued

Cation (atom mole ppm)	**STA3-1**	**STA3-2**	**STA3-3**	**STA3-4**	**STA3-5**	X	SD
Li7	357.197	444.225	468.034	345.188	300.020	382.933	70.641
Be9	95829.623	95115.557	95728.633	92974.650	96418.002	95213.293	1333.964
B11	28.751	34.927	30.492	36.636	30.337	32.228	3.369
Na23	12626.457	12021.775	11353.517	11842.211	12400.685	12048.929	496.069
Mg24	12685.643	11438.450	10459.592	10626.233	12015.841	11445.152	936.283
Al27	53769.618	55056.119	54801.759	50754.319	52416.170	53359.597	1789.110
Si29	199755.732	200747.951	202571.602	202614.277	200652.843	201268.481	1269.612
P31	142.268	33.537	54.012	49.714	34.233	62.753	45.376
K39	108.337	360.476	89.503	128.720	146.505	166.708	110.414
Ca42	36.141	53.779	70.796	50.229	39.867	50.163	13.615
Ti47	1.266	3.670	1.008	6.168	1.927	2.808	2.146
V51	148.128	119.755	118.233	171.072	141.607	139.759	21.894
Cr53	804.230	976.672	835.955	4546.203	1891.071	1810.826	1592.808
Mn55	2.489	2.775	2.036	28.357	2.395	7.610	11.601
Fe57	2638.998	2535.381	2362.702	4749.855	2449.857	2947.359	1012.810
Cs	65.122	54.953	52.125	76.168	58.640	61.402	9.581
Total (atom mole %)	37.900	37.900	37.900	37.900	37.900	37.900	

Table IV.3: Chemical data show concentration (atom mole ppm) of 16 elements of 3 samples of emerald from Santa Tererzinha (STA), continued

Cation (atom mole ppm)	STA8-1	STA8-2	STA8-3	STA8-4	STA8-5	X	SD
Li7	566.158	479.261	464.767	475.361	506.094	498.328	40.862
Be9	96683.980	96573.034	95426.156	97152.893	97084.880	96584.189	693.765
B11	27.593	29.009	30.413	26.522	24.833	27.674	2.162
Na23	12026.382	12285.736	12217.432	12057.778	12087.023	12134.870	111.332
Mg24	10731.032	10927.886	13115.199	10959.693	12333.411	11613.444	1054.710
Al27	54687.154	51443.228	50592.640	53138.363	54410.552	52854.388	1800.569
Si29	200185.130	200879.366	198714.663	200276.287	197819.495	199574.988	1263.666
P31	52.815	46.272	44.040	44.755	34.432	44.463	6.594
K39	26.114	158.544	582.032	74.316	128.339	193.869	222.849
Ca42	50.800	47.988	47.661	47.951	507.461	140.372	205.213
Ti47	2.793	6.956	10.870	7.298	5.998	6.783	2.896
V51	113.193	124.067	104.621	124.033	116.953	116.573	8.159
Cr53	369.577	1812.969	3403.644	314.093	345.554	1249.167	1362.370
Mn55	5.201	6.342	15.167	6.125	5.930	7.753	4.167
Fe57	3381.192	4088.852	4164.595	4196.867	3500.987	3866.498	392.609
Cs	90.886	90.488	66.100	97.664	88.057	86.639	12.024
Total (atom mole %)	37.900	37.900	37.900	37.900	37.900	37.900	

Table IV.4: Chemical data show concentration (atom mole ppm) of 16 elements of 4 samples of emerald from Madagascar (MA)

Cation (atom mole ppm)	**MA4-1**	**MA4-2**	**MA4-3**	**MA4-4**	**MA4-5**	X	SD
Li7	306.189	279.212	274.793	270.299	286.097	283.318	14.052
Be9	98346.086	97479.314	97287.947	97074.075	96908.454	97419.175	561.233
B11	39.717	45.718	47.104	40.856	44.464	43.572	3.167
Na23	12813.076	12019.668	11572.061	11332.029	10948.325	11737.032	716.075
Mg24	12554.201	11964.081	11476.623	11167.049	10944.875	11621.366	646.651
Al27	47932.848	49257.077	49942.924	50009.722	49516.815	49331.877	841.120
Si29	203647.599	204469.024	205697.421	204861.117	204334.912	204602.015	752.826
P31	70.591	61.304	101.520	65.570	47.203	69.238	20.037
K39	35.712	538.081	157.851	1876.323	3718.391	1265.272	1553.881
Ca42	113.637	155.137	181.751	182.500	165.235	159.652	28.193
Ti47	1.924	1.850	2.729	2.244	1.483	2.046	0.468
V51	19.249	24.666	19.072	19.072	19.108	20.234	2.479
Cr53	327.832	531.181	368.302	343.092	317.498	377.581	87.968
Mn55	3.439	4.314	3.848	5.675	4.063	4.268	0.850
Fe57	2690.800	2141.572	1847.424	1732.942	1726.641	2027.876	407.028
Cs	97.100	27.802	18.629	17.435	16.435	35.480	34.743
Total (atom mole %)	37.900	37.900	37.900	37.900	37.900	37.900	

Table IV.4: Chemical data show concentration (atom mole ppm) of 16 elements of 4 samples of emerald from Madagascar (MA), continued

Cation (atom mole ppm)	**MA7-1**	**MA7-2**	**MA7-3**	**MA7-4**	**MA7-5**	X	SD
Li7	222.451	212.088	216.390	226.044	204.802	216.355	8.407
Be9	99121.173	98660.189	99672.639	99306.105	101071.843	99566.390	917.175
B11	33.334	25.747	29.350	34.517	30.361	30.662	3.463
Na23	9058.704	9117.858	8744.993	8684.632	8373.268	8795.891	302.619
Mg24	9798.712	9849.828	9770.047	9740.349	8810.465	9593.880	439.799
Al27	50239.551	50494.260	50963.684	50875.433	52810.551	51076.696	1012.371
Si29	206154.291	204614.717	203459.578	204463.166	202982.047	204334.760	1224.881
P31	53.051	37.591	42.136	44.920	40.652	43.670	5.873
K39	1749.949	3831.469	3985.324	3278.154	1966.797	2962.339	1044.344
Ca42	100.360	193.324	140.355	86.352	70.953	118.269	49.242
Ti47	2.548	3.056	2.646	2.462	1.829	2.508	0.443
V51	16.344	15.579	15.582	15.466	23.800	17.354	3.620
Cr53	202.881	200.741	202.007	201.624	379.893	237.429	79.643
Mn55	5.578	8.775	6.484	5.957	4.863	6.331	1.488
Fe57	2228.584	1723.624	1737.548	2023.083	2213.669	1985.302	246.284
Cs	12.489	11.154	11.236	11.736	14.208	12.165	1.260
Total (atom mole %)	37.900	37.900	37.900	37.900	37.900	37.900	

Table IV.4: Chemical data show concentration (atom mole ppm) of 16 elements of 4 samples of emerald from Madagascar (MA), continued

Cation (atom mole ppm)	MA8-1	MA8-2	MA8-3	MA8-4	MA8-5	MA8-6	X	SD
Li7	201.477	206.258	166.255	214.662	192.085	180.035	193.462	17.888
Be9	96161.628	96687.512	98064.822	96132.181	96778.897	97368.551	96865.598	743.479
B11	50.866	44.971	37.952	42.061	49.384	40.998	44.372	5.012
Na23	8926.603	8753.586	9529.442	8758.004	9259.157	8812.219	9006.502	318.480
Mg24	9351.422	9121.619	9384.474	9306.399	9679.098	9015.714	9309.788	230.478
Al27	50967.245	50947.373	51620.806	50665.461	51236.596	50416.003	50975.581	422.992
Si29	208435.706	208062.010	203243.747	208394.307	206381.515	206905.638	206903.821	1978.816
P31	55.344	46.690	39.981	43.826	57.956	51.818	49.269	6.949
K39	1563.958	2381.206	4148.972	2576.106	2343.650	3417.685	2738.596	909.968
Ca42	153.040	138.232	88.265	140.073	110.126	145.306	129.174	24.767
Ti47	1.994	2.732	2.927	2.415	2.617	2.537	2.537	0.318
V51	36.083	23.246	24.926	23.721	24.025	23.268	25.878	5.037
Cr53	690.443	378.769	412.460	386.571	388.922	385.154	440.387	123.045
Mn55	3.653	3.666	3.868	3.204	3.592	3.390	3.562	0.233
Fe57	2382.109	2183.408	2212.265	2291.976	2473.465	2213.969	2292.865	114.266
Cs	18.430	18.721	18.839	19.035	18.915	18.346	18.714	0.274
Total (atom mole %)	37.900	37.900	37.900	37.900	37.900	37.900	37.900	

Table IV.4: Chemical data show concentration (atom mole ppm) of 16 elements of 4 samples of emerald from Madagascar (MA), continued

Cation (atom mole ppm)	**MA18-1**	**MA18-2**	**MA18-3**	**MA18-4**	**MA18-5**	X	SD
Li7	142.659	134.484	132.726	122.490	132.546	132.981	7.181
Be9	99812.027	98878.459	99785.783	99206.859	99823.650	99501.356	434.746
B11	45.260	46.502	43.512	41.736	40.240	43.450	2.542
Na23	9343.799	9449.977	9720.916	10156.254	10377.115	9809.612	446.208
Mg24	9753.783	9640.966	9799.613	9729.144	9612.763	9707.254	78.258
Al27	51322.196	51149.291	51499.585	51053.527	50277.353	51060.390	469.716
Si29	204151.235	205377.994	204449.346	205380.369	205457.894	204963.368	615.252
P31	52.396	50.271	66.757	42.907	56.374	53.741	8.769
K39	2221.697	2140.120	1218.193	745.676	25.737	1270.284	933.893
Ca42	87.206	94.802	87.542	87.911	85.083	88.509	3.686
Ti47	2.024	2.356	2.161	2.762	2.353	2.331	0.279
V51	17.250	16.444	16.376	16.331	33.383	19.957	7.515
Cr53	302.244	295.665	284.965	281.827	604.189	353.778	140.224
Mn55	4.540	4.606	4.147	3.429	3.225	3.989	0.634
Fe57	1724.615	1701.278	1871.710	2110.175	2454.737	1972.503	314.910
Cs	17.069	16.784	16.668	18.604	13.358	16.497	1.919
Total (atom mole %)	37.900	37.900	37.900	37.900	37.900	37.900	

Table IV.5: Chemical data show concentration (atom mole ppm) of 16 elements of 4 samples of emerald from Zambia (ZA)

Cation (atom mole ppm)	**ZA5-1**	**ZA5-2**	**ZA5-3**	**ZA5-4**	**ZA5-5**	**ZA5-6**	**ZA5-7**	X	SD
Li7	1272.895	1358.055	1393.622	1458.974	1550.796	1536.183	1493.080	1437.658	101.206
Be9	100981.881	101616.554	101951.215	103558.789	103747.971	102344.072	100062.435	102037.559	1325.008
B11	37.791	31.277	28.889	27.984	32.317	31.899	44.762	33.560	5.857
Na23	10393.061	9913.001	9831.758	9241.594	9400.253	9598.382	9641.513	9717.080	377.437
Mg24	7580.443	7740.588	7672.924	7284.382	7322.253	7501.441	7442.613	7506.378	170.954
Al27	51528.975	51450.882	52308.792	51798.783	51220.196	51146.114	53586.262	51862.858	854.500
Si29	203524.793	203293.410	202259.998	202319.634	202408.013	203163.432	203116.865	202869.449	523.372
P31	49.735	45.039	36.830	36.768	32.150	30.149	51.125	40.257	8.393
K39	18.285	15.171	103.989	170.822	13.270	233.043	105.132	94.245	85.559
Ca42	63.902	56.405	47.882	44.873	35.434	42.129	54.638	49.323	9.639
Ti47	1.528	1.597	1.654	1.693	1.631	2.173	2.326	1.800	0.314
V51	37.547	36.106	34.419	30.129	33.999	31.203	29.383	33.255	3.094
Cr53	494.184	348.244	369.996	439.386	431.345	483.328	486.793	436.182	58.160
Mn55	10.578	13.450	12.844	10.516	9.530	9.815	11.250	11.140	1.489
Fe57	2867.228	2950.947	2820.662	2465.983	2627.872	2723.692	2757.188	2744.796	160.857
Cs	137.173	129.275	124.527	109.691	132.969	122.947	114.635	124.459	9.782
Total (atom mole %)	37.900	37.900	37.900	37.900	37.900	37.900	37.900	37.900	

Table IV.5: Chemical data show concentration (atom mole ppm) of 16 elements of 4 samples of emerald from Zambia (ZA),continued

Cation (atom mole ppm)	ZA6-1	ZA6-2	ZA6-3	ZA6-4	ZA6-5	X	SD
Li7	817.484	874.075	608.543	706.609	748.851	751.112	102.270
Be9	102808.310	103501.311	103392.663	102455.620	103025.405	103036.662	427.936
B11	30.045	34.194	30.560	32.919	27.611	31.066	2.572
Na23	5335.665	5561.589	6594.459	6599.968	5897.534	5997.843	582.530
Mg24	3268.549	3443.240	4115.265	4035.685	3488.730	3670.294	379.943
Al27	58875.734	59510.573	56871.861	57724.216	57922.206	58180.918	1029.550
Si29	206256.813	204534.070	204759.837	204572.721	205352.424	205095.173	727.294
P31	44.870	43.213	37.417	38.442	47.194	42.227	4.186
K39	12.632	35.912	127.340	271.063	9.744	91.338	111.267
Ca42	65.587	66.375	61.975	50.917	61.050	61.181	6.172
Ti47	1.233	1.679	1.915	1.696	1.559	1.616	0.250
V51	12.619	10.241	20.233	17.792	18.384	15.854	4.222
Cr53	26.175	24.308	115.623	117.556	101.701	77.073	47.714
Mn55	5.149	4.814	10.009	11.818	11.651	8.688	3.459
Fe57	1384.087	1299.904	2159.119	2279.826	2176.322	1859.852	475.916
Cs	55.048	54.501	93.182	83.153	109.635	79.104	24.139
Total (atom mole %)	37.900	37.900	37.900	37.900	37.900	37.900	

Table IV.5: Chemical data show concentration (atom mole ppm) of 16 elements of 4 samples of emerald from Zambia (ZA),continued

Cation (atom mole ppm)	**ZA23-1**	**ZA23-2**	**ZA23-3**	**ZA23-4**	**ZA23-5**	X	SD
Li7	969.211	864.430	758.366	812.559	838.949	848.703	77.993
Be9	102110.337	98804.341	98299.428	94075.104	101923.513	99042.544	3278.558
B11	39.140	53.270	48.504	40.378	36.370	43.532	7.072
Na23	11751.342	12244.261	12370.288	11569.765	12237.978	12034.727	351.538
Mg24	9796.776	9915.994	10389.938	9761.469	10302.387	10033.313	292.914
Al27	50666.284	49882.081	47170.797	47917.563	48086.268	48744.599	1464.665
Si29	199495.295	203597.714	204987.261	208937.683	201210.786	203645.748	3638.744
P31	50.786	88.364	49.208	55.626	29.136	54.624	21.407
K39	201.474	13.717	360.496	638.424	265.046	295.832	229.669
Ca42	78.427	111.735	123.556	294.159	91.982	139.972	87.937
Ti47	4.525	5.018	2.145	3.201	1.922	3.362	1.385
V51	47.692	24.885	58.075	44.527	48.838	44.803	12.223
Cr53	481.018	363.450	734.715	471.150	700.867	550.240	160.201
Mn55	6.129	5.272	6.602	6.068	3.619	5.538	1.174
Fe57	3240.529	2960.702	3552.308	4299.613	3147.771	3440.185	525.942
Cs	61.037	64.767	88.312	72.713	74.567	72.279	10.551
Total (atom mole %)	37.900	37.900	37.900	37.900	37.900	37.900	

Table IV.5: Chemical data show concentration (atom mole ppm) of 16 elements of 4 samples of emerald from Zambia (ZA),continued

Cation (atom mole ppm)	**ZA25-1**	**ZA25-2**	**ZA25-3**	**ZA25-4**	**ZA25-5**	X	SD
Li7	1063.070	1072.760	948.844	1141.393	851.300	1015.474	114.886
Be9	101745.794	100640.621	100394.517	101410.451	100212.682	100880.813	665.072
B11	43.651	40.215	41.065	32.903	39.377	39.442	3.991
Na23	10907.098	11326.656	11678.907	11541.305	11830.198	11456.833	358.820
Mg24	8835.792	8694.886	9025.814	9038.413	9230.264	8965.034	205.614
Al27	51421.354	51660.322	50307.511	50394.843	49646.814	50686.169	836.359
Si29	201165.215	202037.579	202768.528	201417.476	203184.819	202114.723	861.138
P31	33.541	51.765	36.125	39.844	23.882	37.031	10.135
K39	238.891	62.336	218.674	125.207	179.584	164.938	71.897
Ca42	63.553	56.989	60.899	56.508	56.821	58.954	3.135
Ti47	2.913	2.701	2.413	1.827	1.847	2.340	0.492
V51	32.851	31.510	35.179	34.890	35.493	33.985	1.727
Cr53	498.416	322.615	393.840	550.390	641.024	481.257	125.905
Mn55	5.940	7.096	2.786	5.008	2.259	4.618	2.059
Fe57	2850.609	2869.380	2965.684	3098.971	2978.254	2952.580	99.476
Cs	91.311	122.568	119.214	110.570	85.381	105.809	16.664
Total (atom mole %)	37.900	37.900	37.900	37.900	37.900	37.900	

Table IV.6: Chemical data show concentration (atom mole ppm) of 16 elements of 3 samples of emerald from Carnaiba/Socoto (CAR)

Cation (atom mole ppm)	**CAR1-1**	**CAR1-2**	**CAR1-3**	**CAR1-4**	**CAR1-5**	X	SD
Li7	1613.500	694.849	1025.150	917.975	1004.843	1051.263	340.494
Be9	97029.587	95926.947	97685.207	98255.261	97717.730	97322.946	893.193
B11	35.217	42.255	48.110	33.116	44.998	40.739	6.391
Na23	5579.208	8446.489	6159.109	5872.088	6608.561	6533.091	1135.062
Mg24	4294.344	7969.710	5319.766	5142.326	6035.334	5752.296	1385.803
Al27	69841.235	70180.468	69448.124	70405.629	67712.006	69517.492	1072.115
Si29	200013.482	195243.309	198936.995	198010.062	199210.203	198282.810	1843.651
P31	97.489	68.390	75.316	74.842	62.880	75.784	13.166
K39	19.005	58.747	14.457	12.047	32.504	27.352	19.251
Ca42	172.045	126.321	122.003	99.944	100.573	124.177	29.347
Ti47	1.789	2.386	1.539	1.162	5.584	2.492	1.785
V51	132.836	77.012	50.349	51.256	133.563	89.003	41.742
Cr53	38.168	23.655	19.736	20.270	39.338	28.233	9.729
Mn55	0.594	0.447	0.423	0.347	0.591	0.480	0.109
Fe57	130.085	137.034	92.559	102.555	289.020	150.251	79.752
Cs	1.416	1.980	1.154	1.118	2.273	1.588	0.515
Total (atom mole %)	37.900	37.900	37.900	37.900	37.900	37.900	

Table IV.6: Chemical data show concentration (atom mole ppm) of 16 elements of 3 samples of emerald from Carnaiba/Socoto (CAR), continue

Cation (atom mole ppm)	**CAR4-1**	**CAR4-2**	**CAR4-3**	**CAR4-4**	**CAR4-5**	X-	SD
Li7	1615.910	706.353	1009.385	921.842	995.941	1049.886	338.874
Be9	97174.486	97515.045	96182.961	98669.128	96852.030	97278.730	919.606
B11	35.269	42.955	47.371	33.255	44.599	40.690	6.118
Na23	5587.540	8586.348	6064.392	5896.823	6550.014	6537.023	1197.357
Mg24	4300.757	8101.651	5237.956	5163.986	5981.866	5757.243	1439.589
Al27	67995.369	59371.598	64946.155	65572.057	63694.173	64315.870	3175.937
Si29	200646.685	200994.946	203197.557	200213.766	202525.082	201515.607	1281.493
P31	52.480	46.730	42.823	39.424	37.184	43.728	6.078
K39	110.698	236.441	265.590	50.120	228.727	178.315	92.929
Ca42	71.409	112.935	127.297	55.986	63.605	86.246	31.804
Ti47	2.336	1.520	1.833	1.650	3.304	2.129	0.726
V51	12.607	34.806	16.340	27.792	17.842	21.877	9.152
Cr53	23.118	1443.055	636.020	1107.725	269.424	695.868	584.368
Mn55	4.024	6.848	4.036	4.223	4.519	4.730	1.201
Fe57	1049.446	1620.336	1129.805	1160.557	1375.483	1267.126	231.353
Cs	317.865	178.433	90.479	81.668	356.208	204.931	127.116
Total (atom mole %)	37.900	37.900	37.900	37.900	37.900	37.900	

Table IV.6: Chemical data show concentration (atom mole ppm) of 16 elements of 3 samples of emerald from Carnaiba/Socoto (CAR), continue

Cation (atom mole ppm)	CAR-7/1	CAR-7/2	CAR-7/3	CAR-7/4	CAR-7/5	X	SD
Li7	1834.589	1808.423	1722.180	1188.830	1066.577	1524.120	366.815
Be9	96535.208	95683.819	97597.689	97506.029	98528.345	97170.218	1090.026
B11	44.292	41.900	27.963	53.292	36.654	40.820	9.373
Na23	3993.347	3829.212	3816.417	5118.181	5851.088	4521.649	919.128
Mg24	2499.628	2816.517	2473.266	5658.375	4835.235	3656.604	1486.682
Al27	71547.572	70725.647	70920.355	67356.785	65616.478	69233.367	2599.606
Si29	201425.362	202595.316	201527.248	200086.618	200162.375	201159.384	1050.336
P31	44.090	41.173	42.640	32.629	46.726	41.452	5.341
K39	221.368	515.517	42.110	253.471	194.184	245.330	171.432
Ca42	90.893	68.518	70.156	58.636	47.592	67.159	16.044
Ti47	1.893	4.592	1.412	0.452	0.795	1.829	1.641
V51	2.927	3.093	3.051	10.471	14.343	6.777	5.319
Cr53	157.913	153.490	156.451	544.658	1591.636	520.829	621.814
Mn55	7.197	13.525	8.055	24.461	9.958	12.639	7.042
Fe57	507.853	619.197	510.869	979.915	863.538	696.274	214.620
Cs	85.868	80.061	80.139	127.198	134.477	101.548	26.963
Total (atom mole %)	37.900	37.900	37.900	37.900	37.900	37.900	

Table IV.7: Chemical data show concentration (atom mole ppm) of 16 elements of 2 samples of emerald from Itabira (ITA)

Cation (atom mole ppm)	ITA-2/1	ITA-2/2	ITA-2/3	ITA-2/14	ITA-2/5	ITA-2/6	X	SD
Li7	162.268	184.519	178.583	176.794	149.442	169.576	170.197	12.751
Be9	95356.447	94910.373	97633.572	97858.262	96733.991	97278.243	96628.481	1226.854
B11	39.304	41.685	31.641	28.562	38.207	35.037	35.739	4.959
Na23	7816.435	7061.787	7407.471	7373.765	7818.951	9282.649	7793.510	784.772
Mg24	8570.181	7898.246	7926.276	7908.192	8349.208	8940.457	8265.427	431.977
Al27	61359.009	62958.717	63661.214	63508.228	61651.935	60316.691	62242.632	1339.093
Si29	203752.609	204293.121	200480.286	200303.169	202163.160	200768.921	201960.211	1735.021
P31	44.722	48.615	46.125	53.905	49.349	41.677	47.399	4.222
K39	94.009	146.624	146.838	248.027	167.851	179.868	163.870	50.640
Ca42	62.361	115.685	117.996	201.778	69.270	102.049	111.523	49.994
Ti47	1.714	1.008	0.922	0.888	0.946	1.096	1.096	0.312
V51	32.481	15.945	15.673	15.636	30.629	34.205	24.095	9.210
Cr53	659.103	178.619	168.204	164.366	620.570	708.683	416.591	271.176
Mn55	1.483	1.549	1.682	1.789	1.420	1.584	1.584	0.134
Fe57	1039.327	1133.778	1174.102	1147.296	1146.156	1129.733	1128.399	46.316
Cs	8.546	9.731	9.415	9.344	8.916	10.032	9.331	0.538
Total (atom mole %)	37.900	37.900	37.900	37.900	37.900	37.900	37.900	

Table IV.7: Chemical data show concentration (atom mole ppm) of 16 elements of 2 samples of emerald from Itabira (ITA), continued

Cation (atom mole ppm)	ITA10-1	ITA10-2	ITA10-3	ITA10-4	ITA10-5	X	SD
Li7	146.547	152.505	150.512	133.465	169.107	150.427	12.807
Be9	94771.863	97606.045	97462.842	97366.051	97850.433	97011.447	1265.176
B11	26.767	34.739	32.596	29.230	27.636	30.194	3.378
Na23	6902.002	6735.486	6846.381	8412.311	6818.013	7142.839	712.197
Mg24	7383.058	6976.295	7099.061	7698.938	7232.152	7277.901	279.899
Al27	59928.475	63659.400	63813.994	60277.109	63339.078	62203.611	1929.352
Si29	207156.644	201717.091	201342.962	202140.902	201483.743	202768.268	2471.736
P31	48.397	48.129	40.270	46.049	43.060	45.181	3.479
K39	139.620	103.920	207.724	74.611	148.169	134.809	50.240
Ca42	65.428	163.750	214.402	69.057	161.131	134.753	65.197
Ti47	1.814	2.309	2.371	1.355	2.434	2.057	0.462
V51	29.680	12.748	12.618	35.070	12.572	20.537	10.973
Cr53	460.121	255.370	244.970	694.137	252.357	381.391	196.946
Mn55	3.911	2.432	2.712	3.323	2.701	3.016	0.597
Fe57	1921.855	1520.376	1517.318	2004.745	1448.182	1682.495	259.618
Cs	13.817	9.405	9.268	13.647	9.231	11.074	2.429
Total (atom mole %)	37.900	37.900	37.900	37.900	37.900	37.900	

BIOGRAPHY

Miss Thitintharee Pavaro was born in February 23, 1975, in Bangkok. She graduated with a bachelor degree in Gemology from the Department of Materials Science, Faculty of Science, Srinakharinwirot University in 1997. At present, she works as a gemologist at The Gem and Jewelry Institute of Thailand, and also studies in a Master Program in Earth Science at the Department of Geology, Chulalongkorn University.